CENTRE D'HYDROGÉOLOGIE
CENTRE OF HYDROGEOLOGY

UNIVERSITÉ DE NEUCHÂTEL
FACULTÉ DES SCIENCES
INSTITUT DE GÉOLOGIE

---

# CHARACTERISATION OF A CARBONATE AQUIFER FOR THE APPLICATION OF A REGIONAL DISCRETE CONTINUUM FLOW MODEL

(CASTELO DE VIDE CARBONATE AQUIFER - ALENTEJO, PORTUGAL)

Thesis presented to the Faculty of Sciences of the Neuchâtel University to fulfil the requirements for the title of Docteur ès Sciences

J. Paulo Monteiro
30th November 2001

M. Sc. In Applied Geology at the Sciences Faculty of Lisbon

Members of the thesis jury:

Prof. François Zwahlen, Thesis director, University of Neuchâtel (Switzerland)
Prof. Pierre Perrochet, member of the jury, University of Neuchâtel (Switzerland)
Prof. Luís Ribeiro, member of the jury, Technical University of Lisbon (Portugal)
Dr. Séverin Pistre, member of the jury, University of Montpellier II (France)

---

# IMPRIMATUR POUR LA THÈSE

Characterisation of a carbonate aquifer
for the application of a regional discrete
continuum flow model
(Castelo de vide carbonate aquifer -
Alentejo, Portugal)

de M. J. Paulo Monteiro

---

UNIVERSITÉ DE NEUCHÂTEL

FACULTÉ DES SCIENCES

La Faculté des sciences de l'Université de Neuchâtel sur le rapport des membres du jury,

Messieurs F. Zwahlen (directeur de thèse), P. Perrochet, L. Ribeiro (Portugal), S. Pistre (France)

autorise l'impression de la présente thèse.

Neuchâtel, le 7 décembre 2001

Le doyen:

F. Zwahlen

**ACKNOWLEDGEMENTS**

I am grateful to a large number of people and institutions that assisted the completion of this thesis during the last years. It is not possible for me to list by name all the Professors, colleagues (and friends) who contributed with encouragement and support for this work. I thank you all very much! And specially:

- Professor François Zwahlen, director of the Hydrogeology Centre of the Neuchâtel University and Thesis Director, by the acceptance of my dissertation theme and, above all, for encouraging me to stick to my priorities in the right sense, during the more difficult phases of this work.

- Professor Pierre Perrochet at Hydrogeology Centre of the Neuchâtel University for accepting to be part of the thesis jury and for giving me the opportunity to attend his short course in hydraulic and groundwater modelling, where I learned to look at the hydrogeologic problems in a much more systematic way.

- Professor Mário Lourenço Silva at the Departamento de Geologia da Universidade de Lisboa. Between 1996 and 1999 he guided the research project "Aplicação de Métodos Geoquímicos Isotópicos e Modelos de Escoamento ao Aquífero Carbonatado da Serra de S. Mamede – PEAM/SEL/557/95" granted by the Fundação para a Ciência e Tecnologia. Most of the experimental work supporting this thesis was performed during the execution of this project.

- Professor Laszlo Kiraly at the Centre of hydrogeology of the University of Neuchâtel for providing his finite element codes and several of the pre and post-processing modelling tools employed in this work. In addition to providing his computer programs, Professor Kiraly also helped me with ideas and advice in countless discussions we had during the last three years.

- Dr. Amelia Carvalho Dill (now at the Instituto Geológico e Mineiro) for the support during my long absences from Algarve University. During these periods she substituted me in lectures and provided precious support in obtain the license period spent to develop this work.

- Fabien Cornaton, now assistant at the Neuchâtel University, who gave me the opportunity to profit its special talent in deal with groundwater modelling problems. I was very lucky in work with him at the time he was implementing discrete continuum and double continuum flow models, which were the basis of its "Travail de Diplôme" presented in 1999 at Neuchâtel University.

- The help of Dr. Farid Achour (now at University of Alberta in Canada) was essential during my first periods at Neuchâtel University. Fortunately he was there finishing is Pos-Doc at the time I was starting this thesis. We passed many hours together discussing my work, as well as many other interesting hydrogeological problems. He also helped me countless times in solving informatic problems.

- Professor Martin Burkhard, at the Neuchâtel University for the revision of the sections of the text related to the description of the regional and local geological setting.

- Manuel Oliveira, my colleague working at the LNEC in Lisbon for providing his programs used for interpretation of pumping tests.

- Professor Luis Ribeiro at the Instituto Superior Técnico in Lisbon for the support in the development of the work, constructive criticism and also for the perspectives opened toward the continuity of the present research after the end of the thesis.

- Luis Nunes, , my colleague at Algarve University for many discussions about the objectives of the thesis and for the revision of some chapters of this text.

- Ellen Milnes, my colleague working at CHYN, which was brave and patient enough for the complete final revision of the text.

- Members of the jury for their evaluation of this work.

Many thanks also to Fundação Calouste Gulbenkian for the support materialised in a three-year scholarship and to Fundação para a Ciência e Tecnologia (former JNICT) for the financial support for this work during two research projects: (1) Aplicação de Métodos Geoquímicos Isotópicos e Modelos de Escoamento ao Aquífero Carbonatado da Serra de S. Mamede (project PEAM/SEL/557/95) and (2) Identification of mathematical models for prediction and control of karstic aquifer systems (Project 2/2.1/CTA/381/94).

**ABSTRACT**

The characterisation of carbonate aquifers in which diffuse and conduit flow overlap within the same flow domain at the different levels required to define quantitative flow models is a problem without a well-defined solution. Moreover, the kind of models that must be used to predict the spatial distribution and temporal evolution of state variables in such aquifers is also a controversial issue. Therefore, the present state-of-the-art in groundwater flow modelling does not provide standard methods allowing the solution of many common problems related to the management of groundwater resources in this particular kind of geologic environment. Under these conditions, the detailed investigation of any carbonate aquifer in which such hydraulic behaviour is detected provides an opportunity to increase our knowledge of the hydrodynamic parameters and the variables controlling flow in such systems.

The research work reported in the present thesis aims at such a characterisation of the Castelo de Vide carbonate aquifer (Alentejo, Portugal) at the levels required for the application of a regional discrete continuum flow model. The aim is to assess the possibilities and limitations of quantitatively simulating the observed regional flow pattern and the temporal variability of the state variables. Discrete continuum models allow the simulation of diffuse and conduit flow interacting in the same flow domain. Therefore, they provide a more adequate conceptual basis for the interpretation of flow processes usually present in carbonate aquifers than single continuum models currently used to simulate groundwater flow in porous media. Despite the existence of a theoretical framework allowing the application of finite element discrete continuum models to groundwater flow problems, such an approach is not currently used in applied hydrogeology due to: (1) the absence of standard software allowing the simultaneous use of 1-D, 2-D and 3-D finite elements in the same computational grid, (2) the lack of methods allowing the characterisation of the parameters controlling flow in aquifer systems where the predominant processes change from diffuse to conduit flow with change of scale. The absence of standard software allowing the implementation of discrete continuum models was overcome in the present thesis by the use of computer programs available at the Neuchâtel Hydrogeology Centre which had been developed in the course of karstic hydrogeological research during the last three decades. The application of this kind of model, as of any other distributed parameter model, is based on the treatment of information on geometry and water balance and on the spatial distribution and temporal evolution of the state variables, boundary conditions and hydraulic parameters of the flow domain to be investigated. The methods employed to characterise the Castelo de Vide carbonate aquifer at all these levels are described in the present dissertation. However special emphasis is made on the aspects related to the problems specifically associated with carbonate aquifers.

Prior to the use of the discrete continuum approach in the Castelo de Vide carbonate aquifer, different mathematical models were applied in order to determine the hydraulic parameters at different scales. At the well scale, hydraulic conductivity values were calculated by the interpretation of pumping tests using single continuum and double continuum analytical models. On the regional scale, equivalent hydraulic conductivity values were estimated separately for the three flow systems identified in the aquifer, using a single continuum analytical model, and for the entire aquifer system, using a single continuum numerical model. Parameters determined in pumping tests allowed an accurate simulation of the drawdown and recovery observed in wells as a response to pumping. At the same time, equivalent hydraulic conductivity values, determined at the aquifer scale, allowed a reliable steady-state description of the aquifer, compatible with the observed spatial distribution of hydraulic heads, and the long-term water balance, calculated with different methods. Therefore, it is possible to obtain reliable estimates of the hydraulic conductivity at both well and aquifer scales. However, the values obtained at these levels cannot be linked to define an overall representation of the aquifer. This limitation is related to the presence of a conduit network, which influences the parameter distributions and which cannot be captured by pumping tests or by methods allowing the determination of equivalent parameters at the aquifer scale. As the characterisation of the geometry and the hydraulic parameters of a conduit network is always fragmentary and incomplete, its role in the definition of the observed regional flow pattern in a carbonate aquifer is very difficult to establish.

Taking into account that the propagation of any perturbation affecting the hydraulic head must be almost instantaneous in the channel network, compared to the slow changes in hydraulic head occurring in a more or less fractured rock matrix, we propose that the detection of regional trends in the spatial distribution of hydraulic head gradients in carbonate aquifers probably reflects the efficiency of the conduit network, in establishing hydraulic connection between different parts of the aquifer. To test this hypothesis, three sectors were defined, with different degrees of hydraulic connectivity with the aquifer discharge areas in an initially defined “artificial conduit network” controlling flow at aquifer scale. This procedure showed remarkable positive results in the simulation of the aquifer hydraulic behaviour in both steady state and in transient simulations, using a 3-D regional discrete continuum model. As these results are well supported by both experimental and theoretical considerations, it is suggested that the regional analysis of hydraulic head gradients can be transformed into a useful tool for the interpretation of the role of conduit networks in the definition of the regional flow pattern of carbonate aquifers, including the particular case of karst aquifers.

**TABLE OF CONTENTS**

# Chapter 4

CONCEPTUAL FLOW MODEL AND ESTIMATION OF EQUIVALENT HYDRAULIC CONDUCTIVITY AT THE AQUIFER SCALE



# Chapter 5

HYDRAULIC PARAMETERS OF THE CARBONATE ROCKS

# Chapter 6

THREE DIMENSIONAL FLOW MODEL AT THE AQUIFER SCALE



# Chapter 7

GENERAL CONCLUSIONS AND FURTHER PERSPECTIVES

**LIST OF FIGURES**

Fig. 6.11 – Location of the segments of the conduit network presenting a conductive parameter similar to the hydraulic conductivity of the low permeability rock volumes. The dashed lines represent the general conduit network and the areas with changed parameters are marked in bold. Note that the 3-D conduit network is represented by a 2-D projection at the aquifer top.

Fig 6.12 – Relation between hydraulic head computed from measurements in observation points and simulated using the discrete continuum model, considering the existence groundwater flow controlled at the regional scale by sectors of an "artificial conduit network" with different degrees of connectivity with the aquifer discharge areas. Hydraulic conductivity is $10^{-6}$m/s for 3-D elements and the conductive parameter for 1-D elements is $10m^3/s$. Measured values are the average of observations between 1991 and 1999.

Fig. 6.13 – Top 2-D projection of the finite element mesh top showing the location of the 2-D cross-section AB, defined along the aquifer axis. The dashed lines represents the "artificial conduit network". The areas with changed parameters are marked in bold. Black arrows pointing to aquifer limits in the cross-section indicate the position of discharge areas. GWD – groundwater divides between Castelo de Vide and Escusa sectors. Equidistance of potential lines is 2.5m. Vertical exaggeration is 3 times.

Fig. 6.14 – 2-D vertical cross-sections of the 3-D model showing equipotentials and flux vectors. Cross-sections: C-D (1104m), equidistance of equipotentials-1.0m; E-F (645m) equidistance 0.2m; G-H (1007m) equidistance 0.2m; I-J (810m) equidistance 0.3m. Aquifer thickness is always approximately 200m. The arrow outside the aquifer limits in profile C-D shows the perturbation produced by the pumping well used for Castelo de Vide Water Supply, directly implanted in a conduit with a pumping rate of 15 l/s.

Fig. 6.15 – Relation between hydraulic head computed from measurements in observation points and simulated using the discrete continuum flow model, considering the existence groundwater flow controlled at the regional scale by sectors of an "artificial conduit network" with different degrees of connectivity with discharge areas. Hydraulic conductivity is $10^{-5}$m/s for 3-D elements and the conductive parameter for 1-D elements is $10m^3/s$. Measured values are the average of observations between 1991 and 1999.

Fig. 6.16 – Classification of pumping wells according Specific capacity ($C_s$), for drawdown registered after one hour of pumping.

Fig. 6.17 – Boxplots representing hydraulic head variability registered between 1991 and 1999. Dots marked in bold correspond to hydraulic head values calculated by the steady state simulation presented in section 6.5.1.2

Fig. 6.18 – Specific storage distribution for 3-D elements, used in the discrete continuum model for the variant with best results for an eight-month aquifer recession period. General value used in most of the aquifer corresponds to $10^{-3}$ $m^{-1}$. Value for shaded elements, in part of the Escusa sector, was assigned to $10^{-4}$ $m^{-1}$.

Fig. 6.19 – Hydraulic head values registered in the aquifer (solid lines) and calculated using the discrete continuum model (dashed lines) for the Castelo de Vide sector.

Fig. 6.20 – Hydraulic head values registered in the aquifer (solid lines) and calculated using the discrete continuum model (dashed lines) for the Escusa sector.

Fig. 6.21 – Hydraulic head values registered in the aquifer (solid lines) and calculated using the discrete continuum model (dashed lines) for the P. Espada sector.

Fig. 6.22 – Calculated water transference from the aquifer toward discharge areas during the simulated recession period. Sever River is represented by the dashed line. The solid line represents transferences toward crystalline rocks contacting the aquifer near the Castelo de Vide area.

Fig. 6.23 – Calculated water transference from the aquifer toward the crystalline rocks contacting the aquifer near the Castelo de Vide area during the simulated recession period.

Fig. 6.24 – Hydraulic head values registered in the aquifer (solid lines) and calculated using the discrete continuum model (dashed lines) for the Escusa sector.

**LIST OF TABLES**

Table 5.4 – Calculated hydraulic conductivity of fractured zones using the values of transmissivity calculated by the Boulton and Streltsova (1977) method. Sdt –Step drawdown test.

Table 6.1 – Water balance calculated by the discrete continuum model for the model variant in this section. Autogenic recharge corresponds to infiltration on the top of the aquifer. Allogenic recharge corresponds to infiltration originated from deposits covering the aquifer in Escusa sector (see figure 6.8 in section 6.4).

Table 6.2 – Length of the segments ($L_c$) where the conductive parameter for conduits was changed to $10^{-6}m^3/s$

Table 6.3 – Water balance calculated by the discrete continuum model for the model variant in the present section. Autogenic recharge corresponds to infiltration at the top of the aquifer. Allogenic recharge corresponds to infiltration originated from deposits covering the aquifer in Escusa sector (see figure 6.8 in section 6.4).

Table 6.4 – Conduit network density. NA – conduit network controlling flow at aquifer scale, used in the model variant presented in section 6.5.1.2; NB- conduit network used in the model variant presented in section 6.5.1.3, based in the definition of sectors in the conduit network.

Table 6.5 – Extractions in wells during a 5784 hours (241 days) emptying period of the aquifer corresponding to a drought period. Then stress periods were defined between February 1997 and October 1997. Pumping rates are values calculated by the multiplication of instantaneous pumping rates, in each well, by the average number of extraction hours. TPR – total pumping rate for each stress period; TPV – total pumped volume during each stress period. Total value of extractions during the entire period is $1.22\times10^6m^3$.

Table 6.6 – parameters used in the model for the more realistic transient simulation of the eight-month recession period.

# Chapter 1

GENERAL INTRODUCTION

---

Contents

## 1 – General Introduction

### 1.1 – General framework for the use of distributed parameters models in carbonate aquifers

Groundwater flow processes active in carbonate aquifers range from cases where diffusive phenomena are dominant to systems where regional flow pattern is mainly controlled by conduit flow at the aquifer scale. In the cases where diffuse flow is dominant, methods based on the single continuum approach can be used in order to predict the hydraulic behaviour of carbonate aquifers. The use of these models is actually a standard approach used to solve groundwater flow problems and it is generally accepted that they give reliable predictions when provided with adequate data about the porous flow domain geometry, boundary conditions and spatial distribution of controlling parameters. In the cases were flow processes are higly dominated by a well developed conduit network, alternative methods better adapted to handle these characteristics are needed in order to interpret and predict hydrodynamic parameters and state variables. It is generally accepted that, in the case of well-developed karst aquifers, the simplifications inherent to the use of single continuum flow models are excessive to allow the characterisation of features essential to an efficient simulation of these systems. The use of distributed parameters models in these cases is, by far, less common than in the cases where diffusive flow is dominant and is based on methods solving the partial differential equation characterising the flow domain as a double continuum or a discrete continuum media. Therefore, the selection of the models that can be used in carbonate aquifers requires the definition of a boundary between two arbitrary extremes: the mainly diffusive carbonate aquifers and the systems dominated by concentrated flow in karst channels. A possible approach to verify the possibilities to characterise a given carbonate aquifer as an equivalent single continuum consists on the interpretation of the aquifer global responses.

The interpretation of global responses, identified by the analysis of spring hydrographs is usually employed as a tool to make inferences about the structure and flow processes present in karst aquifers. These methods are based on the investigation of correlations in discharge-discharge and recharge-discharge temporal data sets and are the conceptual base of black box models, which are used to establish transfer functions. These functions are then used to predict the temporal variability of discharge in karstic springs. The use of methods based on global responses to define the level of similarity between a particular carbonate aquifer and an equivalent porous media, and thus to check the possibility to use single continuum models, is made by the identification of the "karstic character" of carbonate aquifers. The basis of this methods lies in the identification of the more or less pronounced presence of the typical hydraulic behaviour detected in springs draining well-developed karst aquifers. The classification is based in the determination of the "system memory", which is very short (less than a week) for very karstified aquifers and as long as 70 days for inertial systems. In the latter case it is admitted that single continuum models are utilisable.

The above described methods cannot however be generalised because it implies that temporal variability recorded in hydrographs of karst spring is representative of the aquifer global responses. Therefore, the applicability of such an approach is reserved for the cases when the aquifer outflow is associated to the presence of major individual springs. Taking into account the large set of natural conditions defining boundary conditions in aquifers there are many situations where principal outflow from carbonate aquifers takes place towards surface water bodies or towards adjacent hydrostratigraphic units. In the case of the Castelo de Vide aquifer both situations are present: the main discharge area is towards Sever river and, additionally, a second discharge area is towards the crystalline rocks contacting the NW limit of the carbonate aquifer.

Despite the underlying difficulty in defining the limit for the cases when concepts as the existence of a "representative elementary volume" can or cannot be defined, the single continuum approach has been widely used in recent years to simulate flow and solute transport problems in karst aquifers. For example, Larocque *et al*. (1999), Dassarges and Brouyère (1997) and Angelini and Dragoni (1996) presented studies where such an approach was applied. In contrary, Mangin (1997) considered that the state of the art in the development of deterministic flow models does not allow its use in karst aquifers. Between these extremes, Estrela and Sahuquillo (1997) and Pulido-Bosh & Padilla (1988) discuss methodologies based on the analysis of global responses using correlation, spectral analysis and deconvolution methods to determine whether a particular karst aquifer could be simulated adequately using a model based on the single continuum approach. As both the single continuum and discrete continuum approaches were used in the present work for the implementation of finite element models at the aquifer scale, this problem will be discussed with basis in experimental evidence. According to the obtained results, it can be shown that the starting point for a meaningful use of discrete continuum models is not there where the single continuum approach attains its applicability limits. Both approaches are worthwhile, depending on the objectives defined for model use.

### 1.2 – Double continuum and discrete continuum models

Despite of the existence of alternative modelling approaches to single continuum models, allowing a more realistic description of the flow processes present in carbonate aquifers, in which the regional flow pattern is strongly controlled by a conduit network, the use of these methods is not a common practice in applied hydrogeology. This is the case for both double continuum and discrete continuum approaches. There are three reasons for this: (1) unlike single continuum models, these methods are not implemented in public domain or in commercial computer programs; (2) there are no standard methods allowing the characterisation of the hydraulic parameters needed to implement this kind of models; (3) the conceptual framework of these methods has not yet become textbook material. Therefore, these approaches are still generally confined to research and academic applications.

The theoretical framework of the models allowing the description of flow domains where diffusive and fracture flow are simultaneously present started with double continuum models initially formulated by Barenblatt *et al.* (1960). Later more general models where developed allowing the simultaneous use of discrete and continuum subsystems in the same flow domain using numerical models (Kiraly, 1976a; 1976b). Actually the main use of double continuum models is related to the application of one-dimensional analytical solutions, describing radial flow to wells, allowing the determination of hydraulic parameters in pumping tests. Kazemi et al (1969), Warren and Root (1963), Mavor and Cinco (1979) and Moench (1984), are only a few of the references among a large number of benchmark contributions in this field.

On the other hand, discrete continuum models were often used in the last three decades in theoretical studies, aiming of the reliability assessment of methods based on the analysis of karst aquifers global responses. The approach used in these studies consists in the use of "artificial karst aquifers" where the variables to be inferred by the analysis of "artificial karstic spring hydrographs" are previously known in detail. Under these conditions it was possible to check the reliability of previsions provided by the methods based on the analysis of global responses. Examples of research in that field are provided in Kiraly and Morel (1976a), Kiraly and Morel (1976b), Kiraly *et al.* (1995), Eisenlohr (1995), Eisenlohr *et al.* (1997a), Eisenlohr *et al.* (1997b) and Cornaton (1999).

### 1.3 – Remarks about modelling approaches available to solve practical problems in karst aquifers

As referred to in the last two sections the kind of distributed parameters models used to simulate flow and transport problems in carbonate aquifers can be classified in three groups: (1) single continuum models; (2) double continuum models and (3) discrete continuum models. Among these, single continuum models are the more commonly used. On the other hand, despite the fact that discrete continuum models provide a more adequate conceptual basis to solve this class of problems, this kind of models is, by far, the less applied in practice.

As referred to by Barrett and Charbeneau (1996), in their literature review analysis of the approaches available to solve management problems at the aquifer scale in karstic systems, distributed parameter models are normally chosen to increase the accuracy of predictions and to achieve a higher degree of spatial resolution in Karst aquifers. However, despite the high degree of spatial resolution, difficulties in generating input data for single continuum models have limited its usefulness. On the other hand, the quoted author's remarked that models more adapted to the natural conditions prevailing in karst aquifers, as dual porosity distributed parameter models, have the advantage of being able to represent the fast transit and slow depletion often exhibited by karst aquifers. However, the cost of more than doubling the number of parameters required for calibration difficult even more the problems in generating input data existing when single continuum models are used. As consequence of these difficulties distributed parameters are not used to any great extent by regulatory agencies or other groups working in applied hydrogeology of karstic systems. In addition to the comments provided in this work it is interesting to remark that the possibility to use discrete continuum models is not even mentioned among the possibilities that one can choose as an alternative, when the needs related to the management of karst aquifers is the problem at hand.

Taking into account the above considerations it is not surprising that the mainly applications to solve practical problems in karst aquifers is not based in distributed parameters models. In fact, an overview of publications describing case studies in carbonate aquifers shows that most of the practical problems commonly related with water resources management are usually solved by the use of black box models or lumped parameter models.

## 1.4 – Objectives

Despite of the existence of a theoretical framework allowing the use of finite-element discrete continuum models to treat groundwater flow problems, a conspicuous lack of discussion exists regarding the application of that approach to "real carbonate aquifers". This is the reason why the characterisation of a carbonate aquifer at the levels required for the application of a discrete continuum flow model is the main objective of this thesis. Instead of approaching this subject in a theoretical framework, the discussion of the different aspects related to this problem will be based on a real case study: The Castelo de Vide carbonate aquifer.

The general objectives can be expressed as the search for the answer to two questions:

- Do the actual possibilities to investigate the characteristics of a particular carbonate aquifer allow the definition of a simplified symbolic representation of the system, compatible with the information needed to implement a discrete continuum model?

- Does the actual state of development of discrete continuum models allows the simulation of the hydraulic behaviour in carbonate aquifers, where conduit and diffuse flow are superimposed in the same flow domain?

In addition to these questions, essentially related to conceptual issues, some particular aspects related to water extraction in pumping wells need special attention. In fact the use of discrete continuum models is traditionally restrained to the analysis of theoretical problems in karst aquifers. However taking into account the defined objectives it must be considered that in many carbonate aquifers water extractions affects the natural water balance considerably. This is the case in the Castelo de Vide aquifer where, for some years, the total volume of abstractions from pumping wells is superior to the total recharge. Therefore, an additional challenge for this work consists in the evaluation of the impact of water use on the aquifer flow field. The problems arising from this aspect are related to the model calibration, which must be done taking into account the simulation of the system at the aquifer scale and, simultaneously, at the well scale. Some practical results were obtained in this field with respect to the classification of wells according to their hydraulic behaviour, depending on whether they were implanted in dissolution channels or within the low permeability rock volumes.

The application of discrete continuum models, as any other distributed parameters models, is based on the treatment of information at the levels of geometry, water balance, spatial distribution and temporal evolution of state variables, boundary conditions and hydraulic parameters of the flow domain to be investigated. The methods applied to characterise the Castelo de Vide Carbonate aquifer at all these levels are described in the present dissertation. Special emphasis is made on the aspects related to the problems specifically associated to carbonate aquifers.

The problems arising from the implementation of a discrete continuum model at the aquifer scale are mainly related to the absence of methods allowing the characterisation of hydraulic parameters in flow domains where processes change from diffuse to conduit flow with change in scale. Thus, prior to the use of the discrete continuum approach, different mathematical models were extensively applied in order to determine hydraulic parameters at different scales. At the well scale hydraulic conductivity values were calculated by the interpretation of pumping tests (using single continuum and double continuum analytical models). At the regional scale, equivalent hydraulic conductivity values were estimated separately for three flow systems identified in the aquifer (using a single continuum analytical model), and for the entire aquifer system, (using a single continuum numerical model).

Despite of the possibilities in obtaining reliable estimations of the hydraulic conductivity at the well and the aquifer scales, the values obtained at these levels cannot be linked in order to define a spatial distribution for this parameter allowing the simulation of the system at an intermediate level of scale. This limitation is related to the presence of a conduit network, which influence in parameters distribution cannot be captured by pumping tests or by methods allowing the determination of equivalent parameters determined at the aquifer scale. As the characterisation of the geometry and hydraulic parameters of a conduit network is always fragmentary and incomplete, its role in the definition of the observed regional flow pattern in a carbonate aquifer is very difficult to establish.

Taking into account that the propagation of any stress conditions affecting hydraulic head must take place almost instantaneously throughout the channel network, when compared with slow changes in hydraulic head occurring in a more or less fractured rock matrix, we suggest that the detection of regional trends in the spatial distribution of hydraulic head gradients can be related to the efficiency of the conduit network in establishing hydraulic connection between different parts of the aquifer. The definition of three sectors, with different degrees of hydraulic connectivity with the aquifer discharge areas, in an initially defined "artificial conduit network" controlling flow at the aquifer scale, with basis in that assumption, showed remarkable positive results in the simulation of the aquifer hydraulic behaviour in both steady state and transient

simulations of the aquifer system, using a 3-D regional discrete continuum model. As this results are well supported by both experimental results and theoretical considerations, we further suggest that the regional analysis of hydraulic head gradients can be generalised as an useful tool to interpret the role of conduit networks in carbonate aquifers, including the particular case of karst aquifers.

### 1.5 – Thesis structure

This thesis is organised in seven chapters including the actual general introduction. A general overview of the structure of this work will briefly be elaborated in the present section.

Chapter 2 presents the physical principles of the methods applied for the interpretation of pumping tests, the determination of equivalent hydraulic conductivity at the aquifer scale and simulation of groundwater flow at the regional scale. Some developments of these basic principles are presented in more detail later, at the time of the presentation of the techniques used to interpret pumping tests. A very general description of the "standard" finite element method is also presented in order to identify the steps where the discrete continuum approach, used in this work, differs from the finite element models commonly used to solve hydrogeological problems. A general framework is also discussed for the use of numerical models implemented at the aquifer scale, taking into account the relations between the model and the programs used to perform pre-processing and post-processing tasks.

Chapter 3 aims at the characterisation of the Castelo de Vide Carbonate aquifer at some levels required for the implementation of a regional flow model: definition of the system geometry, estimation of the recharge and discharge rates and interpretation of the relations of the aquifer with its surrounding environment. The aquifer geometry was defined by the interpretation of the regional and local geology. A long-term water balance was established by estimation of evapotranspiration and recharge using several different methods. A detailed registry of pumping rates in wells was also established in order to quantify the impact of extractions in the global water balance. The characterisation of state variables is also presented with respect to spatial distribution and time variability of hydraulic head and spring hydrographs. Emptying periods of the aquifer were also characterised by the analysis of recession curves in hydrographs using the Maillet equation. The obtained results allow the discussion of some aspects related to the inferences that usually are made using this method about diagnosis of the karstic character of carbonate aquifers and infiltration processes.

In chapter 4 a conceptual flow model is proposed with basis in the interpretation of the aquifer geometry, long-term water balance and boundary conditions. The characterisation of the aquifer at these levels, expressed in a "synthetic conceptual flow model", allows the formulation of a problem, in which the unknown variable is the equivalent hydraulic conductivity at the regional scale. This problem was solved by two methods: (1) using a cross-sectional finite element model single continuum describing the entire aquifer as a single continuum and (2) using an analytical model based on the Dupuit-Forcheimer theory, describing flow in an unconfined system, bounded by a free surface in equilibrium with uniform recharge. The final sections in this chapter are devoted to the interpretation of identified relations between the established conceptual flow model and the hydrochemical trends identified in the aquifer.

Chapter 5 focuses mainly on the characterisation of hydraulic parameters in carbonate rocks at the well scale. A review of methods for interpretation of pumping tests using the double continuum approach is presented in order to discuss its range of applicability in carbonate aquifers. However, most of the parameters determined in pumping tests were based on the single continuum approach mainly due to limitations regarding experimental conditions. Experimental results showed that, despite the strong heterogeneity characterising carbonate rocks, pumping tests allow reliable previsions of the hydraulic behaviour of wells in carbonate rocks. However, it is also shown that the values obtained for hydraulic parameters cannot be generalised (distribute parameters at the aquifer scale). The evaluation of expected orders of magnitude for parameters characterising karstic channels, entirely based on theoretical considerations, is also presented in this chapter.

Chapter 6 is devoted to the discussion of the aspects related to the implementation of a 3-D finite-element model defined at aquifer scale using the discrete continuum approach. A method used to identify sectors in the "real conduit network", by the detection of positive "regional anomalies in hydraulic head gradients" is described in detail. Thus, in addition to be used to assess the coherence of information obtained using other techniques, the implemented discrete continuum model was used itself as a tool contributing for the characterisation of the system. The steps for model calibration are described in detail as well as the results of some steady state and transient simulations.

Finally, in chapter 7 the general conclusions are presented and some additional considerations are made about the perspectives for the future development of this work.

# Chapter 2

PHYSICAL PRINCIPLES AND GENERAL FRAMEWORK OF REGIONAL FLOW MODELLING

---

Contents

## 2.1 – Introduction

The physical principles in the basis of the methods employed for interpretation of pumping tests, determination of equivalent hydraulic conductivity at aquifer scale and groundwater flow simulation at regional scale are presented in this chapter. Some developments of these basic principles will be discussed in more detail in chapter 5, at the time of the presentation of the techniques used to interpret pumping tests. A very general description of the "standard" finite element method is also presented in order to identify the steps where the discrete continuum approach, used in this work, differs from the finite element models commonly used to solve hydrogeological problems. The final section of the this chapter present a general framework for the use of numerical models implemented at aquifer scale, taking into account the relations between the model and the programs used to perform pre-processing and post-processing tasks.

## 2.2 – Physical principles of the methods used

The more explicit form of the partial-differential equation describing three-dimensional transient flow of groundwater of constant density through saturated porous media is based on Darcy's law, expressing the momentum conservation coupled with an equation of continuity that describes the conservation of fluid mass (Freeze and Cherry, 1979):

$$\frac{\partial}{\partial x}\left(K_{xx}\frac{\partial h}{\partial x}\right)+\frac{\partial}{\partial y}\left(K_{yy}\frac{\partial h}{\partial y}\right)+\frac{\partial}{\partial z}\left(K_{zz}\frac{\partial h}{\partial z}\right)+Q=S_s\frac{\partial h}{\partial t} \tag{2.1}$$

where:

- $K_{xx}$, $K_{yy}$ and $K_{zz}$ are values of hydraulic conductivity [$LT^{-1}$] along the *x, y* and *z* Cartesian axes, which are assumed to be parallel to the major axes of hydraulic conductivity, $h$ is the hydraulic head [$L$], $Q$ is a volumetric flux per unit volume [$L^3T^{-1}L^{-3}$], representing sources and/ or sinks and $S_s$ is the specific storage [$L^{-1}$].

Hydraulic conductivity is expressed by:

$$K=\frac{\rho g k}{\mu} \tag{2.2}$$

where $\rho$ is the density of water [$ML^{-3}$]; $g$ is the acceleration due to gravity [$LT^{-2}$]; $k$ is the intrinsic or geometric permeability [$L^2$] and $\mu$ is the dynamic viscosity [$ML^{-1}T^{-1}$];

The hydraulic head [$L$] corresponds to the fluid potential neglecting the kinetic energy of the fluid and is expressed as the sum of the elevation of the point of measurement or elevation head $z$ [$L$] and the pressure head $p$ [$ML^{-1}T^{-2}$] and is defined as:

$$h=\left(\frac{p}{\rho g}\right)+z \tag{2.3}$$

Specific storage [$L^{-1}$] is defined as:

$$S_s=\rho g(\alpha+n\beta) \tag{2.4}$$

were $\alpha$ is the compressibility of the geologic media [$LT^2M^{-1}$], $n$ is the effective porosity (dimensionless) and $\beta$ is the water compressibility [$LT^2M^{-1}$].

Equation 2.1 is often expressed in a more compact form using the gradient and divergence operators:

$$S_s\frac{\partial h}{\partial t}+div\left(-[\mathrm{K}]\,\overrightarrow{grad\,h}\right)=Q \tag{2.5}$$

In steady state conditions the variables are time-independent. In this case the equation 2.5 is reduced to equation 2.6:

$$div\left(-[\mathrm{K}]\overrightarrow{grad\ h}\right)=Q \tag{2.6}$$

**2.3 – Numerical model**

The controlling differential equation describing groundwater flow can be solved for particular boundary conditions by the finite element method, which is a particularly well-suited approach for integrating partial differential equations over space and thus to simulate flow and transport phenomena in flow domains with complex geometry. The single continuum 2-D cross-sectional flow model presented in Chapter 4, and the discrete continuum 3-D groundwater flow model presented in Chapter 6 were designed using this method. The use of finite element models is actually a standard approach to solve problems in hydrogeology and is described in textbooks as Huyakorn and Pinder (1983), de Marsily (1986), Kinzelbach (1986), Wang and Anderson (1982) and Bear and Verruijt (1987).

**2.3.1 – Standard finite element method**

The finite element method is implemented in several commercial and public domain codes to solve hydrogeologic problems. The most employed method to assemble the element matrix is the Galerkin method. The principles of this method will be described in a very general way, considering only the necessary aspects needed to identify the steps where the standard finite element formulation differs from the scheme employed to formulate the discrete continuum approach used in this work, defined by Kiraly (1979).

The flow domain is divided into discrete elements, each of them characterised by its shape, hydraulic conductivity and specific storage. Equation 2.6 is presented in the form:

$$L(h)=0 \tag{2.7}$$

Where $L$ is a differential operator and $h$ is the dependent variable (hydraulic head).

A trial solution $\hat{h}$ for the unknown variable is defined as function of a set of quadratic or linear polynomial functions, expressed by the Equation (2.8).

$$\hat{h}\approx\sum_{j=1}^{n}N_j h_j \tag{2.8}$$

where $h_j$ are the unknown nodal values, $N_j$ are the interpolation (or basis) functions and $n$ is the total number of nodes defining the elements in a mesh representing the geometry of the flow domain.

When $h$ is substituted by $\hat{h}$ in equation 2.8 an approximate solution is defined. Therefore residuals $r$, defined by equation (2.9) will occur:

$$r=L(\hat{h})\neq 0 \tag{2.9}$$

To minimize the residual over the entire flow domain an integral equation is written to ensure that the basis functions satisfies the partial differential equation of flow. This is accomplished by defining a weighted integral of $r$ over the elements of the flow domain and then setting this integral equal zero. As consequence of this the weighted integral will be zero over the entire flow domain $V$ an thus over the entire set of $n$ weighting functions ($W_i$):

$$\int_V W_i L\left(\sum_j N_j h_j\right)dV=0 \qquad \text{for } i=1,2,\ldots,n \tag{2.10}$$

Thus the method of weighted residuals seeks to determine the unknown $h_j$ in such a way that the error is minimised in the flow domain $V$. In the Galerkin method the employed interpolation (or basis) functions and weighted residual functions are the same ($N_i = W_j$). After the definition of these functions (usually linear or quadratic polynomials) the

values of $\hat{h}$ calculated by equation 2.8 are combined with equation 2.10 to provide a set of simultaneous equations where the unknown variable $\hat{h}$ is defined for each of the *n* nodes of the finite element mesh (equation 2.11):

$$[\mathbf{A}] \cdot \{\hat{h}\} = \{f\} \tag{2.11}$$

Where [**A**] is the global stiffness matrix and $\{\hat{h}\}$ is the vector of unknown variables and $\{f\}$ is the source term.

Once the values of all elements are combined, including prescribed boundary conditions, the resulting set of simultaneous linear algebraic equations is solved using different solution algorithms. Different direct and iterative solvers based in matrix solution techniques are available to solve the resulting assembled algebraic equations.

The basis functions employed as interpolation and weighting functions are mapped using local coordinates, which define 1-D, 2-D (triangular or quadrilateral elements) or 3-D (tetrahedral, triangular prisms or hexahedral elements). Each archetypal element has a regular shape in local coordinates. The elements are linear, if there are nodes only in the corners and quadratic when an additional node exists in the mid-side of an edge. In the first case only a linear interpolation of the nodal values can be performed. For quadratic elements a quadratic interpolation is possible for the nodal values. Therefore, one of the essential operations to be performed in order to obtain the solution of the defined problem, consists in relating the equations obtained in the local space with the global space, representing the "real shape" of the flow domain, and hence based on finite elements of arbitrary shape.

Therefore , the integral calculation (as in equation 2.10) is generally performed on the local coordinates system, according for a mapping relation between the local ($\xi$, $\eta$, $\zeta$), and global ($x$, $y$, $z$) coordinates. That relation applies to the gradients as follows:

$$\begin{pmatrix} \frac{\partial N_j}{\partial x} \\ \frac{\partial N_j}{\partial y} \\ \frac{\partial N_j}{\partial z} \end{pmatrix} = [J]^{-1} \begin{pmatrix} \frac{\partial N_j}{\partial \xi} \\ \frac{\partial N_j}{\partial \eta} \\ \frac{\partial N_j}{\partial \zeta} \end{pmatrix} \tag{2.12}$$

$$[J] = \begin{pmatrix} \frac{\partial x}{\partial \xi} & \frac{\partial y}{\partial \xi} & \frac{\partial z}{\partial \xi} \\ \frac{\partial x}{\partial \eta} & \frac{\partial y}{\partial \eta} & \frac{\partial z}{\partial \eta} \\ \frac{\partial x}{\partial \zeta} & \frac{\partial y}{\partial \zeta} & \frac{\partial z}{\partial \zeta} \end{pmatrix} \tag{2.13}$$

where [*J*] is the Jacobian of the change of coordinates between the local and global space. Uniqueness of the transformation is assured if the element is not excessively deformed in the global space.

The transformation between the local and global space using the standard finite element technique works well when the number of local coordinates is the same as the number of Cartesian global coordinates (for example 3-D elements in a 3-D global space or 2-D elements in a 2-D global space). However when 1-D or 2-D elements are mapped into a 3-D global space, the number of local coordinates will be less than the number of global coordinates. Under these circumstances, the Jacobi matrix will no longer be an invertible square matrix and the relation expressed in equations 2.12 and 2.13 cannot be used to relate gradients between the local and global space.

The discrete continuum approach used in this work is based on the Galerkin method but a different technique is used to perform the transformation between the local and global space, allowing the simultaneous use of 1-D and 2-D elements in a 3-D finite element mesh.

### 2.3.2 – The discrete continuum modelling approach

The method proposed by Kiraly (1979) overcomes the impossibility, found in the standard finite element method; it performs the transformation between local and global coordinates when 1-D and 2-D finite elements are embedded in a 3-D global space.

The simultaneous use of 1-D and 2-D and elements in a 3-D space are based on the representation of gradients in curvilinear coordinates. In addition to the transformation between the local and global space employed in the standard finite element method, represented by equations 2.12 and 2.13, the mapping of 1-D and 2-D and elements in a 3-D space require the computation of covariant base vectors and the contravariant metric tensor. This method could be applied in the finite element method each time an inversion of the Jacobi matrix is needed with the same results of the standard method, when only 3-D elements are present in the finite element mesh (Kiraly, 1979; Perrochet, 1995). Therefore, the adoption of this technique allows the design of more adequate models for structures of complex geometry as fractured or karstic aquifers.

In the present case the used elements are 1-D segments with 3 nodes, 2-D elements with 8 nodes and 3-D hexahedral elements with 20 nodes. These elements are represented in local coordinates as straight segments, squares and cubes, which corners are located at points $\xi = \pm 1$, $\eta = \pm 1$, $\zeta = \pm 1$ (figure 2.1).

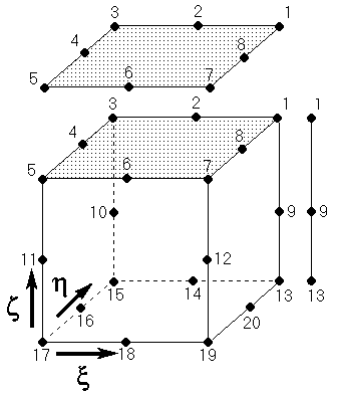


Fig. 2.1 – Type of archetypal quadratic elements used in this work represented in local space: 1-D elements with 3 nodes; 2-D quadrilateral elements with 8 nodes and 3-D hexahedral elements with 20 nodes. In the global space the elements may undergo deformations in order to approximate the geometry of the flow domain.

The computer codes FEN1 and FEN2 employed in the present work make use of these features and allow the simulation of steady state and transient flow problems, respectively, using the discrete continuum approach. These computer programs are the actual enhanced versions of the code FEM301 described in detail in Kiraly (1985).

The programs FEN1 and FEN2 solve equations 2.6 and 2.5. Therefore the computations performed from the assemblage of 1-D "pipe" elements, 2-D "fault elements" and 3-D "block elements" is done assuming that Darcy's law is valid in all these cases, the flow domain is fully saturated and water density is constant. As will be showed later, piezometric observations in the Castelo de Vide aquifer revealed fluctuations of the equipotential surface very small compared to the total thickness of the aquifer. Therefore, the role of the processes developed in the unsaturated zone is restricted to a very thin layer, only few meters below the ground surface. Under these conditions simulations considering the existence of a fully saturated flow domain will not introduce important errors in the model. As water is only slightly compressible in the range of the observed temperatures, the simulations based on a constant water density are also realistic. On the other hand, the use of Darcy's law in 1-D elements is probably an oversimplification of the reality, that can lead to errors impossible to assess. In cases where flow is turbulent the specific discharge for a given gradient will be overestimated. Despite the fact that the calculation of the Reynolds number can be used to evaluate the conditions corresponding to the validity domain of Darcy's law, no means are available to validate these conditions in the used model.

In the prevailing natural conditions usually present in carbonate aquifers conduit flow is very often turbulent. Therefore, as will be show in chapter 5 (section 5.5), and later in chapter 6, the parameters assigned to characterise the "artificial conduit network" introduced in the discrete continuum model lead to a quite unrealistic representation of the dissolution channels present in the "real conduit network". In fact the parameters used to characterise these conduits correspond to equivalent parameters of pipes with circular cross-section with only 8 cm in diameter. This is in contradiction with the presence of conduits with metric dimensions often encountered in all the aquifer sectors. However, taking into account

the role of the conduits in the definition of the regional flow pattern observed in the aquifer, this is the only way to use the program FEN in order to simulate flow at the aquifer scale in real conditions. It must be emphasized that this is the major drawback associated to the modelling technique employed in this work.

In the present case study the model was designed using 1-D elements to simulate the role of the higher order dissolution conduits that control flow at regional scale; 2-D elements to simulate diffuse discharge at the top of the aquifer and 3-D elements to simulate the low permeability rock volumes containing lower order fractures or channels.

Despite the drawbacks related to the validity limits of Darcy's law, particularly in the 1-D channels, the designed model allows a more realistic description of the aquifer than what can be obtained by standard models based on a model describing the media as a single equivalent continuum. Unlike a model based on the discrete continuum model, the equivalent continuum approach alone cannot be used to: (1) simulate the effect of regionally developed karstic networks in the regional flow pattern; (2) analyse the propagation of the potentials throughout the aquifer in function of different proportions of concentrated recharge/ diffuse recharge and (3) analyse the discharge volumes in outflow areas as response of the ratio between concentrated recharge and diffuse recharge.

The simultaneous use of 1-D, 2-D and 3-D elements in a 3-D finite element mesh presents practical limits. In order to keep the results realistic, the hydraulic gradients perpendicular to 1-D or 2-D elements must be negligible. One of the ways to avoid excessive curvatures in the vicinity of 1-D or 2-D elements consists in separating these elements by two, or preferably more, slices of 3-D elements in the finite element mesh.

**2.4 – General framework of the modelling process**

The partial differential equations controlling flow (equations 2.5 and 2.6) are commonly used to solve hydrogeological problems. Generally, these equations appear as one component of a boundary-value problem (Freeze and Cherry, 1979). According to these authors, the complete definition of a transient boundary-value problem for subsurface flow requires the knowledge of: (1) the size and shape of the region of flow; (2) the equation of flow within the region; (3) the boundary conditions around the boundaries; (4) the initial conditions in the region; (5) the spatial distribution of the hydrogeologic parameters that control the flow, and (6) a mathematical method of solution. If the boundary-value problem is established for a steady state system, requirement (4) is removed.

Methods used to solve boundary-value problems are often analytical. For example, the methods used to interpret pumping tests throughout chapter 5 are based on one-dimensional radial analytical solutions of equation 2.6 expressed in radial coordinates. However the complexity of many problems at the level of the domain's boundaries, heterogeneity, nonlinearity, irregular source functions, etc., make the derivation of analytical solutions impossible. Therefore many problems are solved using numerical methods instead of analytical solutions. One example of a numerical method used to solve hydrogeological problems is the finite element method, briefly described in the last two sections.

In the cases where numerical methods are used, the solutions are calculated with computer programs. The steps usually required to the use of a numerical model in hydrogeology can be schematically described in five steps as follows (Gable *et al.*, 1996): (1) Geologic Data is gathered and stored as computer accessible files; (2) A geological framework is defined. This geologic framework represents the geometry of the flow domain with coordinate point data and material assignments for these points representing complex geologic features and material attributes; (3) Generation of a 1-D, 2-D or 3-D discretized finite element mesh (also named computational grid) that maintains the integrity of the original data; (4) The computational model uses the mesh for solving differential equations representing the physics of a problem, in this case the Darcy's law coupled with the continuity equation; (5) finally, during the performance assessment phase (model calibration) results are evaluated by comparing the model predictions with field data. Finally, alternative ways to characterise the problem are defined in order to improve the obtained solutions. These steps are summarised in figure 2.2.

The five steps evolved in the implementation of a flow model defined above are based on the use of programs that can be grouped in three categories, pre-processing tools, the numerical model itself, and post-processing tools.

The pre-processing tools are computer programs used to manage geo-referenced information in order to translate the geological data on computer files that express the system geometry, boundary conditions and material characteristics (as hydraulic parameters). These files must be generated in a format compatible with the input files used by the model. An essential pre-processing tool is the mesh generator, which is used to construct a finite element mesh that maintains the integrity of the original data.

The numerical model assembles the linear algebraic equations corresponding to the problem defined in the spatial flow domain represented by the finite element mesh by a procedure as the finite element method described in Section 2.3.1. In addition to that task, a solver, based on different mathematical techniques for solving matrix equations, is used to calculate the solution of the defined problem. The major computational efforts of the modelling process are related to the number of calculations performed by the solver. Therefore, the degree of discretization of the mesh will condition the possibility of finding a solution for the problem because computers have a limit for the size of matrixes that can be stored and solved. There are two basic kinds of solvers: (1) solvers based on direct methods, which provide an exact solution, except for computer round off errors. The main disadvantage of direct solvers is that computers have a limited capacity to store the matrices or solve the system in a reasonable time, when the number of nodes is large and (2) solvers based on iterative methods, which use avoids the need for storing large matrices. Usually iterative solvers are much faster than direct solvers for large systems. However the efficiency of iterative methods depends on an initial estimation of the solution and on relaxation and acceleration factors being problem dependent. In practice the best solver to use depend on the problem to be treated. Many common flow and transport models provide a set of different direct and iterative solvers that can be used depending on the particular difficulties associated to a particular problem. The solver embedded in the numerical codes FEN1 and FEN2 codes is the frontal solution method (Irons, 1970), which is a direct solver based on the improvement of the Gauss elimination procedure, which is more efficient for large 3-D problems than the original Gauss method (Kiraly, 1985).

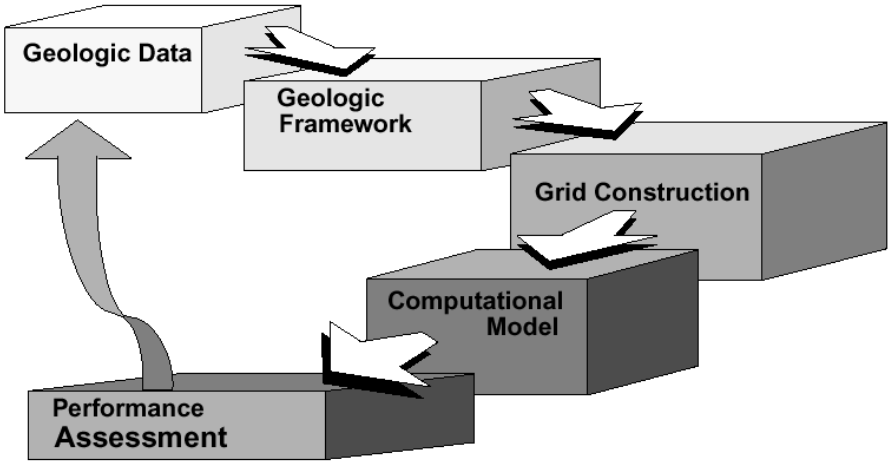


Fig. 2.2 – Steps needed to implement a hydrogeologic numerical model (*in* Gable et al., 1996).

The post-processing tools are computer programs used for verification and visualisation of the results generated by the models. These tools are used to plot calculated and observed state variables in global representations of the aquifer or in selected regions or points of the flow domain. These programs are used to illustrate the model results but also to assess the quality of the obtained results. Therefore post-processing tools are mainly graphic programs, which are essential to use for model calibration. Most of the modern models available as free-domain or commercial codes have a large set of available pre-processing and post-processing tools that are far more sophisticated than the numerical model itself.

The construction of a 3-D regional flow models as the one presented in Chapter 6, using the discrete continuum approach, poses additional difficulties in pursuing the general framework illustrated in Figure 2.2. This is because the currently available finite elements mesh generators, pre-processing and post-processing graphical tools are designed to cope with the standard finite element method based on the single continuum approach. Therefore, these standard tools can only deal with 1-D, 2-D and 3-D elements alone and not with all of them simultaneously. On the other hand, as discussed in section 2.3.2 the discrete continuum approach is based on the use of 3-D elements to simulate the low permeability rock volumes containing lower order fractures or channels, 1-D elements to simulate the role of the higher order dissolution conduits controlling flow at regional scale and 2-D elements used to simulate diffuse discharge at the top of the aquifer.

One of the essential tasks that must be performed in order to allow the use of the discrete continuum approach in current applied hydrogeology projects consists in the development of pre-processing and post-processing tools adapted to the particular needs of this method. Only to give a figure of the meaning of these aspects a complex geometry using a modern mesh generator for a single continuum model could be a task for a couple of days. On the other hand, a finite element mesh for a discrete continuum model, as the one used in Chapter 6 of the present work, takes weeks of hard and cumbersome work.

# Chapter 3

CHARACTERISATION OF THE CASE STUDY

---

Contents

### 3.1 – Introduction

The preliminary steps needed to implement a regional flow model for the Castelo de Vide carbonate aquifer require the definition of the system geometry, estimating recharge and discharge rates, assigning boundary conditions and defining a distribution for the hydraulic parameters at aquifer scale. The first three of these topics will be treated in the present chapter. The definition of the hydraulic parameters at the aquifer scale and at the well scale will be treated, respectively in chapters 4 and 5.

### 3.2 - Geological setting

The interpretation of the geology and structure of the studied area is presented in order to define the geometry of the Castelo de Vide carbonate aquifer and its contact areas with other lithologies. The coupled analysis of the geology and geomorphology of the region contributes also to the qualitative delimitation of discharge areas, recharge areas and zones where water transference between the aquifer and surface waters bodies or adjacent hydrostratigraphic units take place.

#### 3.2.1 – The carbonate aquifer in the regional context

The Devonian carbonate rocks supporting the aquifer under study, constitutes the nucleus of a complex syncline with Ordovician and Silurian flanks known in literature as "Castelo de Vide Syncline". The Castelo de Vide syncline is located along the southern limit of the Central-Iberian Zone. This zone is characterised by the presence of broad antiforms of pre-Ordovician sequences and narrow synforms which display younger sequences (Ordovician, Silurian and Devonian). The transgressive Ordovician Quartzites (Ribeiro, 1990) constitute a markhorizon of an Arenig age.

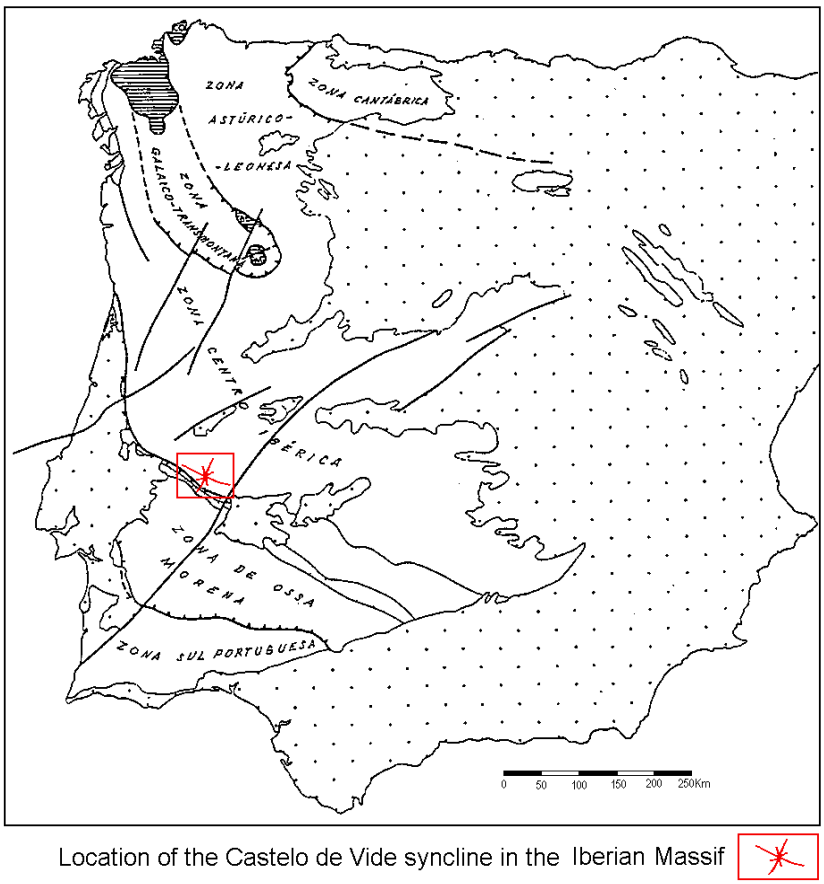


Fig. 3.1 – Location of the Castelo de Vide syncline in the context of the pre-Mesozoic geology of Iberia. Adapted from Ribeiro *et al.* 1979.

From the tectonic point of view the Central-Iberian zone is regarded as the axial domain in the Iberian Variscan Fold belt. The paleogeographic features that characterise the Central-Iberian Zone, when compared with the surrounding zones, concern mainly the pre-Ordovician sequences. The widespread Armorican quartzite (Arenig) unconformably overlies the "slate and greywacke complex" of Late Precambrian to Cambrian age, deformed during the Sardic deformation phase.

In Amêndoa, Buçaco, S. Pedro, Alcudia, and other areas of the Central-Iberian Zone in Portugal and Spain, narrow synclines similar to the Castelo de Vide Syncline are present; the Ordovician-Silurian and sometimes Devonian sequences are always surrounded by the pre-Ordovician sequences, usually referred to as "slate and greywacke complex". A general discussion of the geology and structure of the Central-Iberian Zone is provided in Ribeiro *et al.* (1979), and Ribeiro (1990).

It is interesting to note that some of the general aspects, regarding the local hydrogeological conditions in many of the synclines of the Central-Iberian Zone (namely the occurrence of similar patterns for the distribution of aquifers and water quality in the Ordovician quartzites) are closely related to the fold structure of this range.

### 3.2.2 – Local geology of the Castelo de Vide Syncline

The Castelo de Vide Syncline is a periclinal structure with an axis oriented in NW-SE direction. The length of the structure along its axis is about 40 km; the maximum width perpendicular to the axis is about 10km. The contact of the syncline with the surrounding rocks is marked by Ordovician quartzites (Arenig). Towards NE these quartzites are in direct contact with the Hercinian Nisa granites whereas toward SW they overly the Pre-Hercinian Portalegre Granites. Locally, rocks of the "slate and greywacke complex" are present beneath the NE limit of the Arenig quartzites (figure 3.2).

The fact that the Castelo de Vide Syncline is not completely surrounded by the sequences of the "slate and greywacke complex" is related to the granitic intrusions that denote the southern contact of the Central-Iberian Zone with the neighbour Ossa-Morena Zone. The sedimentation of the Paleozoic sequences within the Castelo de Vide Syncline are younger than the Portalegre granite but older than the intrusion of the Nisa Granite. This can easily be seen in figure 3.2; arkoses below the Ordovician Quartzites mark the transgression of the early Ordovician rocks over the Portalegre Granites. On the other hand, the NE limits of the syncline with the Nisa granites is an intrusive contact, associated with hornfels and marked by contact metamorphism related to the intrusion of these granites.

The geology and structure of the Castelo de Vide Syncline was described by Teixeira (1981), Gonçalves *et al.* (1978), Perdigão & Fernandes (1976), Fernandes et al. (1973); Perdigão (1972), Perdigão (1967a), Perdigão (1967b) and Silva & Camarinhas (1961). The cited references are mainly related to the lithology, petrography, paleontology and stratigraphy of the Castelo de Vide Syncline.

The only available geological 1:50000 map from the Portugal Geological Survey was not accurate enough to pursue the present studies. A detailed geological survey of the area where the carbonate rocks occur was done with a 1:25000 basemap. The geology of the Castelo de Vide Syncline is shown in figure 3.2. The general basis was adapted from Fernandes et al. (1973) and Perdigão & Fernandes (1976). The geometry of the carbonate rocks was assessed during field surveys performed in the area.

The stratigraphy of the carbonate formation is not completely defined due to the absence of fossils and the lack of studies allowing its absolute dating. The different authors quoted above suggest different ages, always in the Middle Devonian.

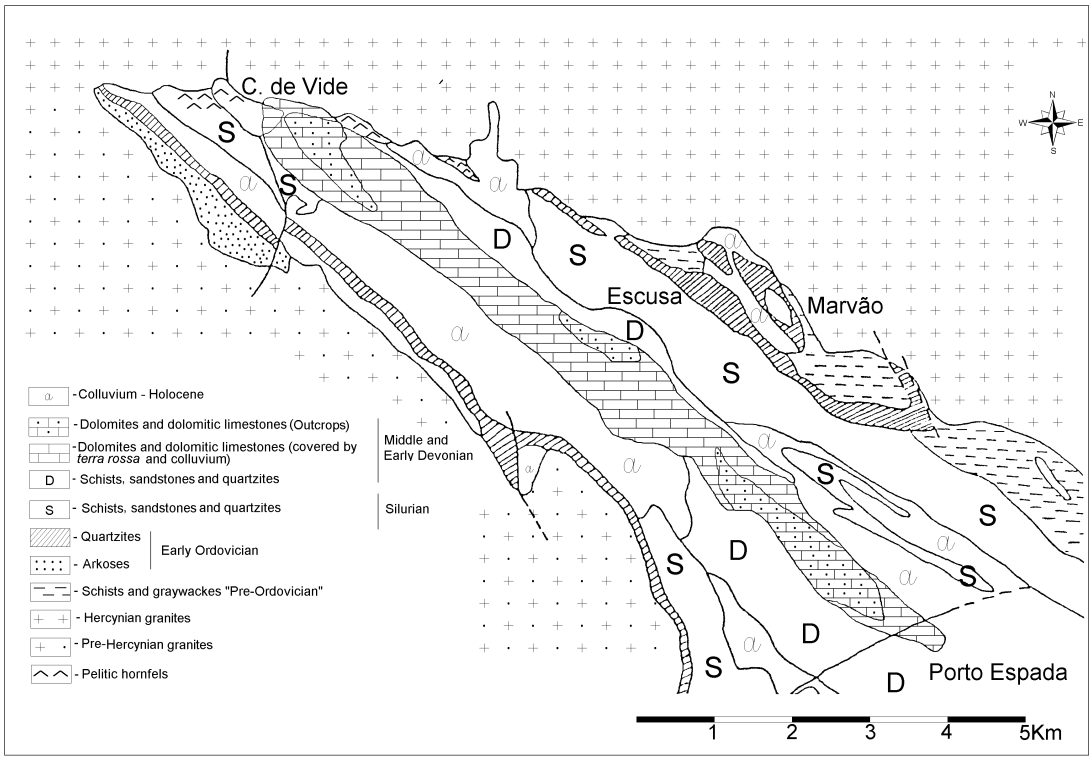


Fig. 3.2 – Local Geology and Structure of the Castelo de Vide syncline.

The carbonate rocks are predominantly dolomites as shown by the mineralogical and geochemical characterisation presented by Silva and Camarinhas (1961). Dolomite is the dominant mineral (82.75 to 93.64%) of the rock volume. The ratio MgO/ CaO ratio determined from chemical analysis is between 1/ 1.50 to 1/ 1.86. The carbonate rocks are relatively homogeneous by both mineralogical and chemical criteria and are classified as dolostones. The microscopic grain-size analysis shows that the grain dimensions are between 30 and 340μ. The most abundant class is between 31 and 36μ. Dissolution features of both calcite and dolomite were observed in all samples together with micro fractures affecting the rock matrix at a microscopic scale.

The effects of active karstic processes at field scale are responsible for the presence of lapiaz, swallow holes, sinking streams, flowing from the neighbouring low permeability schists, and frequent collapse of the roof of shallow dissolution cavities affecting the land surface. In some cases damage to constructions was reported. A cave accessible to human explorers having a geometry which is not well defined is present in the SE area of figure 3.2.

The wells drilled during the experimental work as well as the available technical reports describing the characteristics of boreholes in carbonate rocks showed that the inferior limit of the formation was never attained. The maximum depth drilled up to now is 139m. According to the analysis of the syncline structure the thickness of the carbonate formation must be about 200m. The area corresponding to the limits presented in the map of the figure 3.2 is of 7.9km$^2$. In some other areas of the Castelo de Vide syncline carbonate rocks exist at the top of the Paleozoic structures. However they are not in hydraulic connection with the studied area.

The carbonate formation is covered in most of its extension by *terra rossa* and colluvium deposits resulting, respectively, from the weathering of the carbonate rocks and from the mechanical weathering of the surrounding crystalline rocks (predominantly fragments of the Ordovician quartzites). The areas where the carbonate rocks are exposed in outcrops are distinguished from the covered zones in figure 3.2. In the previously available geologic maps of the region these outcrops were the only referenced areas reporting the presence of the carbonate formation.

### 3.3 – General distribution of the aquifers in the Castelo de Vide Syncline

As referred to in the last section, the Ordovician quartzites are the flanks of the Castelo de Vide syncline and are in contact toward NE and SW, respectively, with the Nisa and Portalegre and Granites. These rocks are present in two divergent branches starting from a point located about 2.5 Km to W from the Castelo de Vide town. A group of few wells screened in this aquifer supply a mineral water plant. The waters present a very low value for the total dissolved solids (always lower than 50mg/l) and present a calcium and sodium chloride hydrochemical facies. Locally, at the NW

extreme of the syncline, the quartzites are in contact with arkoses resulting from the weathering of the Portalegre granite. The recharge of this aquifer occurs, both directly across the narrow outcrops of quartzites and throughout the arkoses. The Ordovician quartzites are very fractured and a characterisation of their hydraulic parameters is presented in Oliveira (1993).

The Silurian and Devonian schists, sandstones and quartzites (where the schists are largely predominant) are in direct contact with the underlying Ordovician fractured aquifer. The limit between the Silurian and the Devonian rocks is transitional (occurring inside the same depositional sequence) and defined only on the basis of paleontologic criteria. In hydrogeological terms these rocks are of very low permeability and define simultaneously the confining layer of the Ordovician fractured aquifer and the "impermeable" substratum of the carbonate aquifer. These "impermeable" rocks have more than 200m of thickness. The carbonate rocks are the uppermost aquifer of the cited sequences. In geological terms they are the nucleus of the syncline and their position corresponds to the top of the Devonian sequences.

The hydrogeology of the carbonate aquifer was described in Monteiro (1992a, 1992b). The conceptual model for the aquifer defined in these studies is based on data collected for the general characterisation of the aquifer during two years. Prior to these references the only information about the hydrogeology of the carbonate rocks in that area corresponded to technical documents reporting the characteristics of wells. The data collected after these studies allowed its reinterpretation and showed that the general conclusions presented are compatible with the more recent observations. However the actual knowledge about the hydraulic properties of the aquifer regarding aspects as boundary conditions, hydraulic parameters and characterisation of the state variables evolution is now much more detailed.

The following discussion is based the quoted works and on some new interpretation of the available data. A very simplified schematic cross section showing the aquifers in the Castelo de Vide Aquifer is presented in figure 3.3.

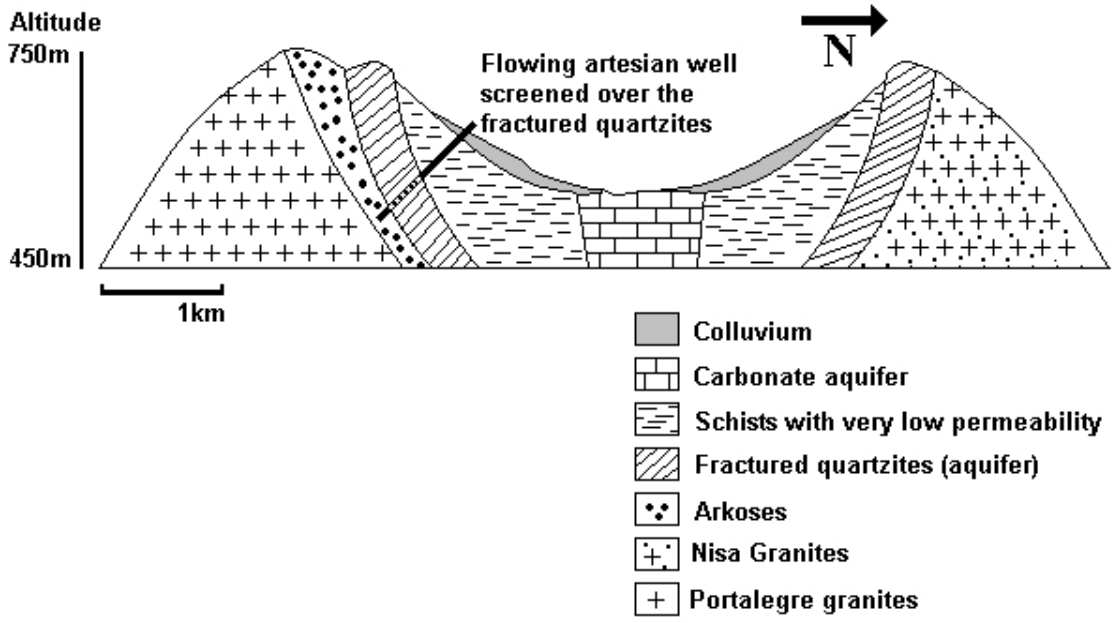


Fig. 3.3 – Schematic N-S cross-section of the aquifers present in the Castelo de Vide Syncline. Note that the scales are approximate and aspects as the thickness and depth of the formations are completely fictive.

The artesian well represented in figure 3.3, constructed for the water supply of the mineral water plant located in Castelo de Vide Town, provides a good insight in the role of the "impervious sequences" underlying the carbonate aquifer. The well was drilled with a dip of 45 degrees and the quartzite aquifer was found at a 100 meters depth. Later, at a depth of 205 meters the arkoses were met. The well was screened over the entire thickness of the Ordovician quartzites and isolated from the other sequences. The hydraulic head at the time of drilling was 15m above the ground level.

Another feature visible in the cross section of the figure 3.3 is that the carbonate aquifer is located in the bottom of a "U" shaped valley. This is particularly important for the control of the recharge processes which are enhanced by the presence of several swallow holes corresponding to points of concentrated recharge developed near the contact with the

schists. Another process acting at the level of the recharge in relation with the morphology of the area corresponds to lateral diffuse infiltration from the colluvium deposits that partially cover the carbonate aquifer near its lateral limits in some areas. However, due to the limited extension of these deposits, this process must be less general than the lateral concentrated infiltration. As will be shown later in section 4.3.3, these kinds of conditions were confirmed in the central area of the aquifer by indirect analysis of the distribution of the hydrochemical facies. It is possible that similar processes take place in the area to the SW of the Sever River. These processes of lateral recharge are frequent in karstic aquifers and are referred to as "allogenic drainage". A complete systematisation of the recharge processes active in the aquifer will be presented in section 3.4.3.

In the rare zones where the lithologies in contact with the carbonate rocks are at lower altitudes, the water transference is towards the adjacent hydrostratigraphic units. These conditions occur only at the NW extreme of the aquifer. In figure 3.4 a shaded relief map of the Castelo de Vide syncline shows the distribution of altitude in the area of the carbonate aquifer. The carbonate rocks are at the bottom of the valley and they usually are at lower altitudes than the neighbouring formations.

As observed in figure 3.4 evident signs of linear erosion provoked by streams are visible in the low permeability lithologies surrounding the carbonate rocks. Because of the general distribution of the altitudes inside the limits of the syncline, the stream network converges towards the carbonate aquifer. The observation of these morphologic features was interpreted, in the previously available 1:25000 scale basemap from Instituto Geográfico de Exército (IGEOE), to define the stream network presented in this figure. Despite the good results in the area outside the limits of the carbonate aquifer, the stream network underlying the carbonate formation was misinterpreted. The valley at the centre of the syncline was mapped as a river floodplain, which simply doesn't exist. In fact, a careful field survey shows that the temporary streams converging to the carbonate rocks are present. However, when they are active, during precipitation events, the water infiltrates when the limits of the aquifer are met. This is true for the entire stream network present in the area except for the Sever River, having a discharge which increases in the part of its course over the carbonate aquifer. This is because the bed of the Sever River is the main area of discharge of the aquifer as will be shown by the analysis of piezometric maps in section 3.5.

The conclusion of these observations is crucial to the interpretation of the water balance at aquifer scale: the drainage density (linear length of the streams/ area) over the carbonate aquifer is almost zero. In practical terms, infiltration in the ascribed conditions equals the average depth of precipitation minus the evapotranspiration. Yet, the runoff generated laterally in the low permeability slopes surrounding the aquifer constitutes an additional source of recharge.

In figure 3.5 the digital terrain model is shown again, with the real stream network. Another important feature of the system is now visible: the NW limits of the aquifer, where the streams diverge from the limits of the carbonate rocks, correspond to a zone where water transferences takes place from the carbonate aquifer toward the adjacent lithologies. In this area the carbonate rocks are in contact with granites and tectonized hornfels, having a higher permeability than the schists limiting the aquifer in almost its entire extension.

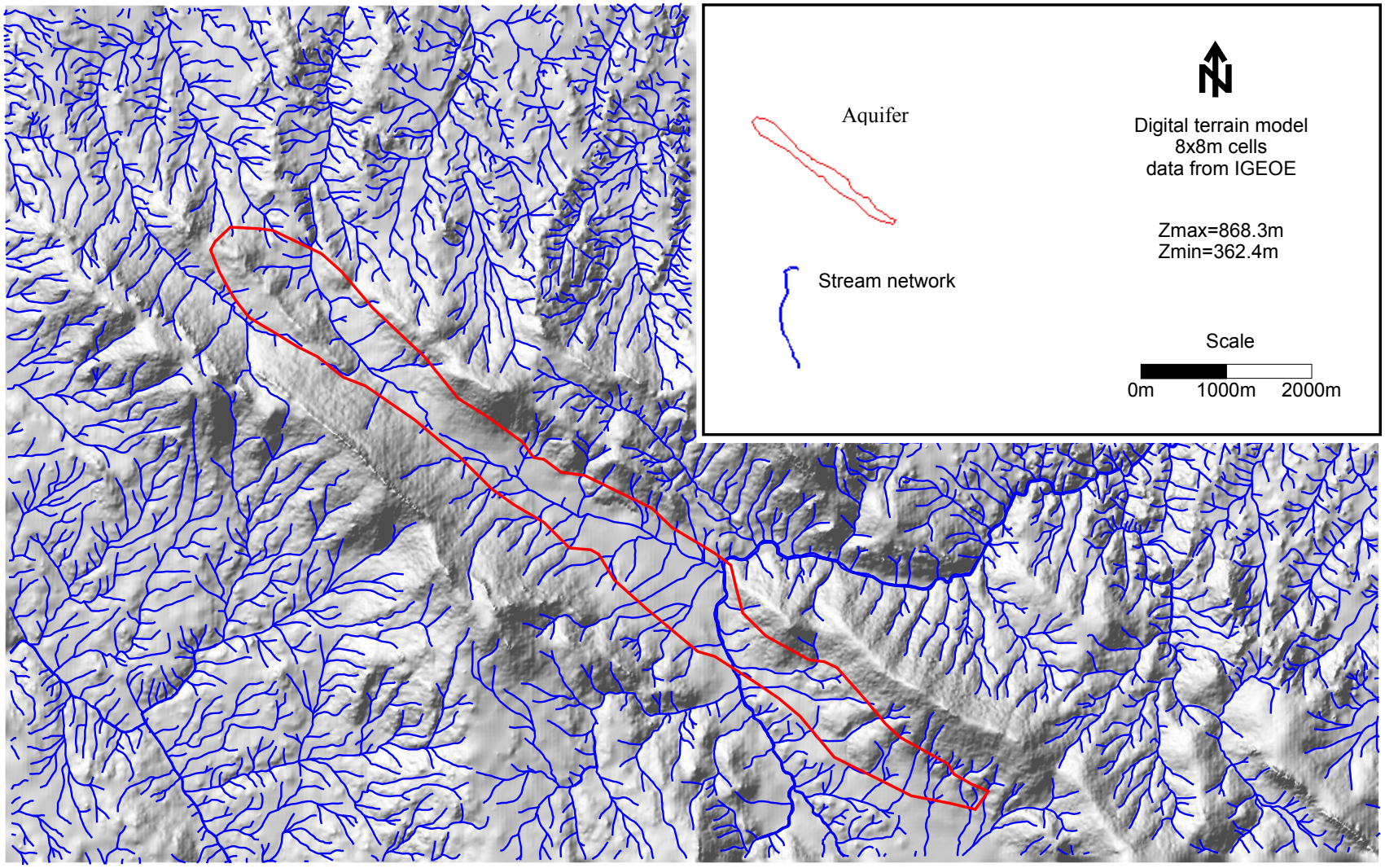


Fig. 3.4 – Digital terrain model showing the morphology of the study area. The carbonate aquifer limits and stream network are also represented.

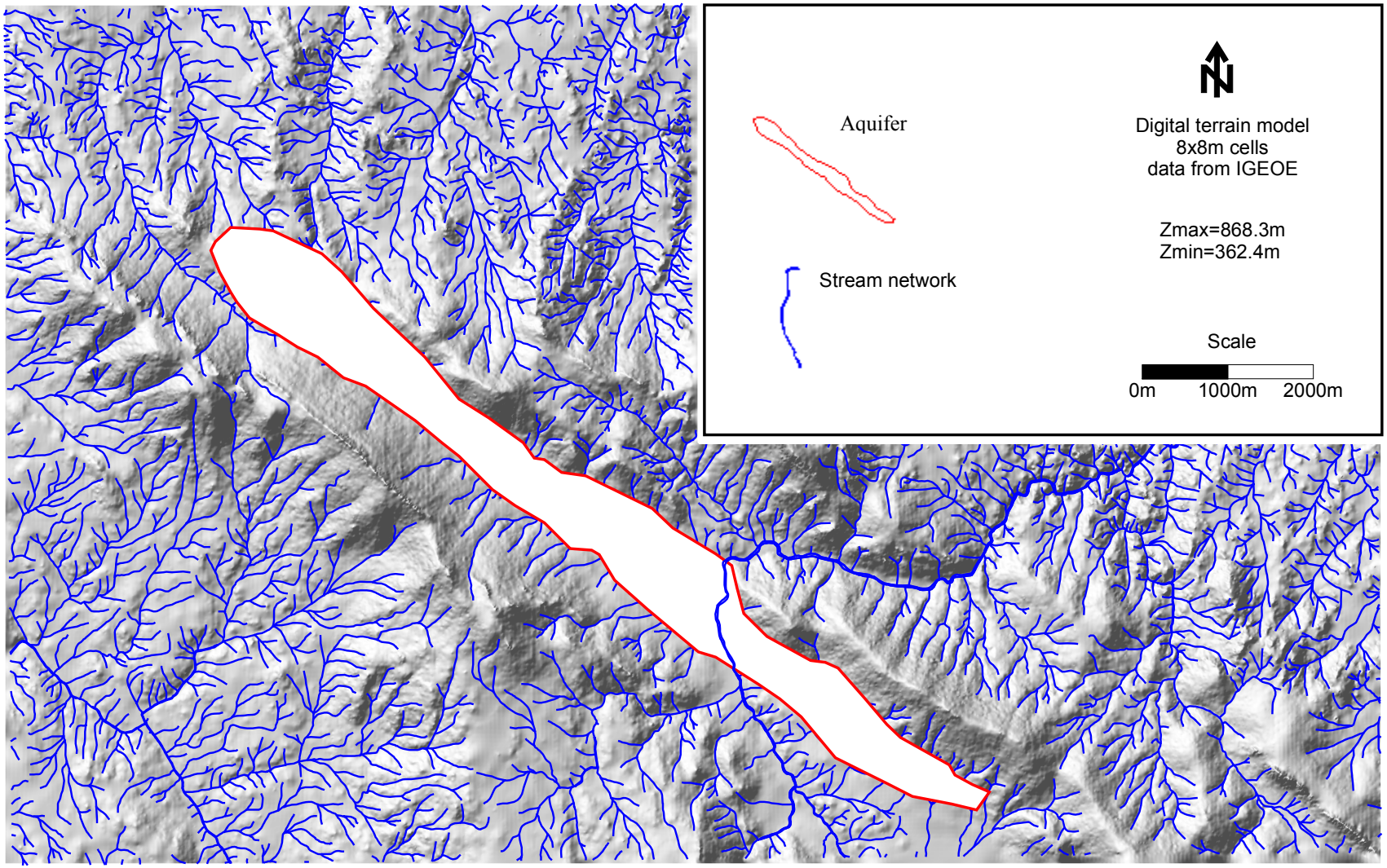


Fig. 3.5 – Digital terrain model showing the morphology of the study area. The stream network in the area of the carbonate aquifer, except for the Sever River, was eliminated (compare with figure 3.4).

### 3.4 – Estimation of water balance

The precipitation in the area of the Castelo de Vide syncline is strongly influenced by orographic effects. The highest altitude in Portugal to the south of the Tagus River (1025 m) is attained in a point located few kilometres to SE of the area mapped in figure 3.2. The study area is located in the Alentejo Region with a total surface of 26,350 km$^2$, where more than 87 percent of the altitude is between 0 m and 300 m.

The treatment of the basic data needed for the mass balance calculations presented in the sections 3.4.1 to 3.4.4 is presented in Monteiro (1993). The climatic raw data was submitted to well-established methods developed to assess the quality of precipitation data and estimating missing values. The employed methods include the evaluation of the data consistence (double mass analysis) and random tests of series sequences. The available precipitation and temperature data was used to establish the mass balance calculations. The Thornthwaite, Coutagne and Turc methods were used to calculate Evapotranspiration. The estimation of recharge was calculated using the Kessler (1965) and chloride balance method (Custódio and Llamas, 1976; Appelo and Postma, 1996). These techniques were extensively applied in the southern area of Portugal and showed a good adaptation of the particular climatic conditions of the region (Silva 1998, Almeida 1985).

#### 3.4.1 – Precipitation and temperature

The water balance of the carbonate aquifer was calculated using mass balance calculations, based on precipitation and temperature data. Due to the impossibility to determine these values by direct measures at aquifer scale; most of the methods employed for mass balance analysis are derived from experiments and observations rather than theory. Despite the results obtained by several empirical methods show consistency with point values experimentally determined over numerous worldwide studies, the water balance calculations must be done by different methods in order to validate the estimations (Custódio and Llamas, 1976).

Table 3.1 shows the precipitation gauge network available in the vicinity of the Castelo de Vide Syncline. The limits of the polygon limited by the observation points correspond to a surface of 816.3 km$^2$. An additional precipitation gauge not presented in Table 3.1 exists in the central area of the aquifer. However, that observation point (Escusa gauge) was recently installed and the data registry is not long enough to use it in the long-term data budget calculations. However, as that gauge is located inside the limits of the aquifer the corresponding data set is very useful to interpret the responses of the state variables of the aquifer monitored during the fieldwork performed in the last years.

| Gauge | Ref. | Lat. | Long. | Altitude (m) | Drainage basin | Available data |
|---|---|---|---|---|---|---|
| Castelo de Vide | CV | 39º 25' | 07º 27' | 540 | Tejo/Sever | P |
| Marvão | MA | 39º 24' | 07º 23' | 865 | Tejo/Sever | P e T |
| Beirã | BE | 39º 27' | 07º 22' | 75 | Tejo/Sever | P |
| Portalegre | PO | 39º 17' | 07º 25' | 596 | Tejo/Sorraia | P e T |
| Vale de Peso | VP | 39º 21' | 07º 39' | 596 | Tejo/Sorraia | P |
| Alter do Chão | AC | 39º 12' | 07º 39' | 270 | Tejo/Sorraia | P |
| Alpalhão | AP | 39º 25' | 07º 37' | 220 | Tejo/Sorraia | P |
| Póvoa e Meadas | PM | 39º 31' | 07º 31' | 338 | Tejo/Nisa | P |
| Nisa | NI | 39º 31' | 07º 38' | 300 | Tejo/Nisa | P |
| S. Julião | SJ | 39º 19' | 07º 18' | 530 | Guadiana/Xévora | P |
| Alegrete | AL | 39º 14' | 07º 19' | 458 | Guadina/Caia | P |

Table 3.1 – Meteorological survey network in the Castelo de Vide Syncline area. Kind of available data - Precipitation and Temperature.

The values of mean annual precipitation for the 1960/61-1989/90 period for each of the precipitation gauges is presented in table 3.2. Table 3.3 show the registry of the monthly temperatures averaged over the same 30 year period.

The isohyetal method permited the interpretation of orographic effects and allowed the definition of a more realistic precipitation pattern than could be obtained from the point values determined in the precipitation gauge network alone. The average depth of precipitation for the 1960/61-1989/90 period calculated using this method is 807mm for the 816.3km$^2$ area where the precipitation gauges are located. For the more restricted 7.9km$^2$ area corresponding to the carbonate aquifer the estimated value for the average depth of precipitation is 904mm. The isohyetal map in figure 3.6 shows the spatial distribution determined for precipitation values. In the same period, the mean average temperature determined from the Marvão gauge, located at a distance of about one kilometre from the central area of the aquifer, is 12.9 °C.

| Ref. | Average | Max | Min | Amplitude | Standard Deviation |
|---|---|---|---|---|---|
| BE | 672.3 | 960.4 | 350.5 | 609.9 | 187.5 |
| AC | 677.3 | 973.8 | 426.9 | 546.9 | 180.5 |
| NI | 712.4 | 1007.5 | 348.1 | 659.4 | 189.7 |
| PM | 724.5 | 1081.4 | 440.5 | 640.9 | 181.6 |
| AP | 776.4 | 1089.5 | 441.5 | 648.0 | 195.1 |
| VP | 786.9 | 1191.4 | 411.0 | 780.4 | 220.8 |
| CV | 836.2 | 1307.8 | 458.0 | 849.8 | 231.1 |
| PO | 889.2 | 1296.7 | 500.5 | 796.2 | 228.2 |
| AL | 910.3 | 1590.0 | 518.0 | 1072.0 | 258.0 |
| MA | 911.6 | 1467.1 | 270.2 | 1196.9 | 319.3 |
| SJ | 1120.5 | 1610.1 | 691.8 | 918.3 | 284.9 |

Table 3.2 – Some statistic parameters calculated from the mean annual precipitation values for the 1960/61-1989-/90 period.

| Ref. | Oct | Nov | Dec | Jan | Feb | Mar | Apr | May | Jun | Jul | Aug | Sep | Annual mean |
|---|---|---|---|---|---|---|---|---|---|---|---|---|---|
| MA | 14.3 | 8.8 | 6.5 | 5.6 | 6.4 | 8.2 | 9.8 | 13.4 | 17.9 | 22.1 | 22.2 | 19.5 | 12.9 |
| PO | 15.9 | 12.0 | 9.0 | 8.8 | 9.1 | 10.8 | 12.3 | 15.6 | 19.9 | 24.0 | 23.5 | 21.4 | 15.2 |

Table 3.3 – Values of the average monthly temperatures for the 1960/61-1989/90 period.

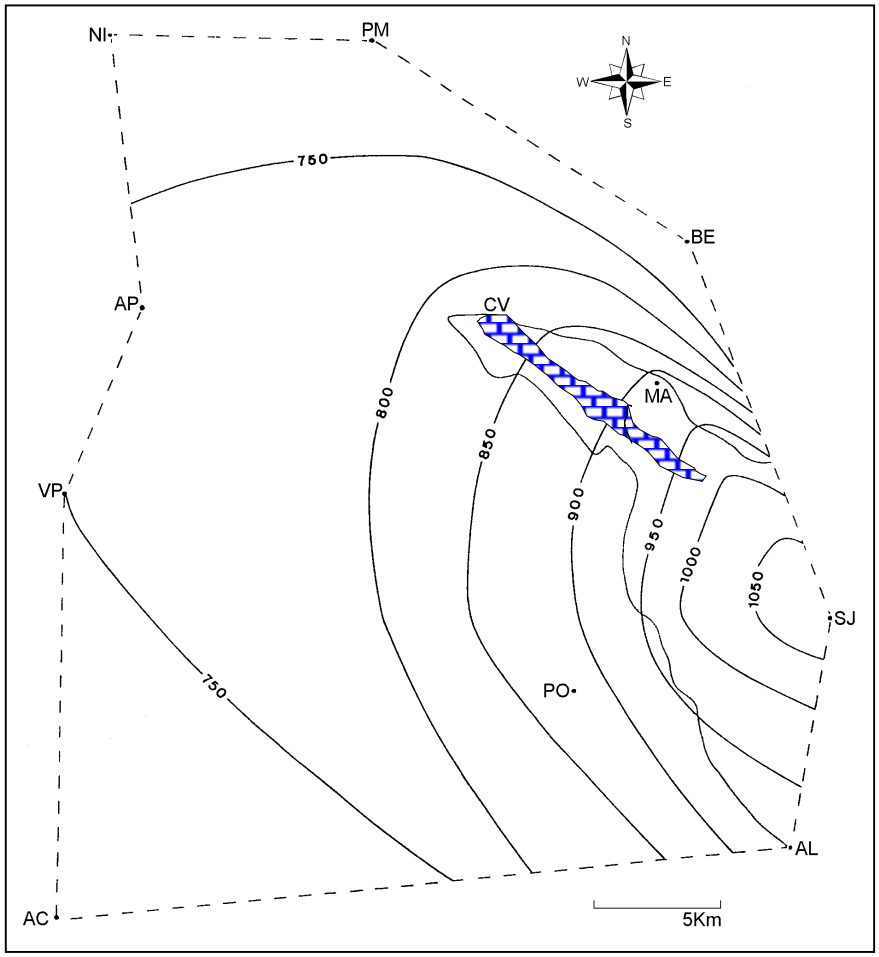


Fig. 3.6 – Isohyetal map drawn from the mean annual precipitation values for the 1960/61-1989/90 period in the Castelo de Vide syncline and surrounding area. The limits of the carbonate aquifer are shown inside the limits of the Syncline.

The mass balance calculations allowing the estimation of evapotranspiration and recharge are based on mean annual precipitation averaged over 30 years of data registries. The evolution in time of the precipitation values, illustrated in figure 3.7, shows that average values have a very general meaning in the climatic conditions prevailing in the study area.

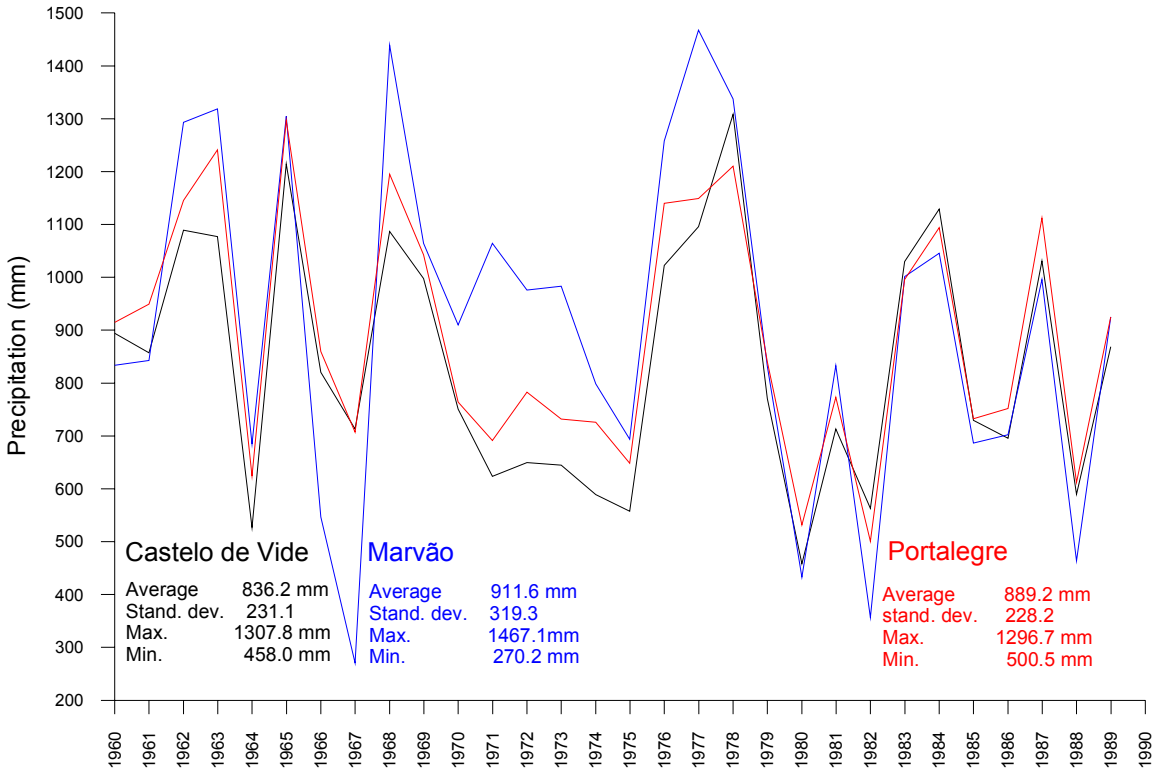

Fig. 3.7 – Precipitation in the gauges nearest the carbonate aquifer between 1960 and 1990.

The impact of the recharge events in the evolution of the aquifer state variables consists in responses detectable in very short periods. As usual in aquifers where concentrated flow in conduits is present, the responses of the system are clearly identified at a daily time scale or even at the scale of shorter storm events. These responses are fluctuations superimposed to the lower amplitude variability reflecting responses of the annual climatic conditions illustrated in figure 3.7.

### 3.4.2 – Evapotranspiration

The evapotranspiration values calculated by the methods of Thornthwaite, Coutagne and Turc, using the temperature and precipitation data sets collected in the Portalegre and Marvão gauges are showed in table 3.4. The formulation of these methods is provided in Custódio and Llamas (1976), de Marsily (1986) and Linsley *et al*. (1975) among many other authors.

The calculated values using the Thornthwaite method correspond to the potential evapotranspiration, which is defined as the amount of water that would be removed from the land surface by evaporation and transpiration processes if sufficient water were available in the soil to meet the demand. The values presented in table 3.4 correspond to the actual evapotranspiration, which is the proportion of the potential evapotranspiration that is actually evapotranspired depending on the existing soil moisture supply. As the actual evapotranspiration depends on the unsaturated moisture storage properties of the soil, the conversion of potential evapotranspiration in values of actual evapotranspiration is carried out with a soil-moisture budget approach. This is done considering a given value for the field capacity, defined as the part of the moisture content of a soil that can be drained by gravity. The values of field capacity in table 3.4 correspond to the amount of precipitation (in millimetres) needed to a given soil, with a previously negligible water reserve; attain the moisture content (volume of water/ total volume of a soil sample) corresponding to the field capacity (F.C.).

| Ref. | Thornthwaite | | | Turc | Coutagne |
|---|---|---|---|---|---|
| | F.C. 75 mm | F.C. 100 mm | F.C. 150 mm | | |
| PO | 460.0 | 485.0 | 535.0 | 561.0 | 619.1 |
| MA | 435.5 | 460.6 | 510.6 | 504.7 | 591.9 |

Table 3.4 – Calculated values for actual evapotranspiration by different methods for the data registries of Portalegre and Marvão (1960/61-1989/90 period). F.C.-field capacity.

The values calculated by the Turc and Coutagne methods allow the direct calculation of the actual evapotranspiration. This is because the soil-moisture budget calculations are not needed in these cases and a single value is provided for the results of these methods. The temperature and precipitation data sets needed to calculate the value of 435mm for the actual evapotranspiration using data of the Marvão gauge are presented in table 3.5.

| Month | T (°C) | P (mm) | PE (mm) | AE (mm) | R (mm) |
|---|---|---|---|---|---|
| Oct | 14.3 | 101.5 | 58.5 | 58.5 | 0.0 |
| Nov | 8.8 | 111.0 | 25.5 | 25.5 | 53.5 |
| Dec | 6.5 | 109.4 | 17.0 | 17.0 | 92.4 |
| Jan | 5.6 | 140.2 | 14.4 | 14.4 | 125.8 |
| Feb | 6.4 | 131.4 | 15.4 | 15.4 | 116.0 |
| Mar | 8.2 | 87.1 | 29.6 | 29.6 | 57.5 |
| Apr | 9.8 | 67.7 | 39.1 | 39.1 | 28.6 |
| May | 13.4 | 49.3 | 69.0 | 69.0 | 0.0 |
| Jun | 17.9 | 46.1 | 99.4 | 99.4 | 0.0 |
| Jul | 22.1 | 6.3 | 138.1 | 8.3 | 0.0 |
| Aug | 22.2 | 8.7 | 129.8 | 8.7 | 0.0 |
| Sep | 19.5 | 50.6 | 92.8 | 50.6 | 0.0 |
| Σ | | 909.3 | 728.6 | 435.5 | 473.8 |

Table 3.5 - Actual evapotranspiration values (AE) and total runoff (R) obtained from the potential evapotranspiration (PE) values using the Thornthwaite method and a soil budget calculation. The value for field capacity is 75 mm. The water reserve in the soil is considered to be negligible at the begin of October. Values calculated for the 1960/61-1989/90 period.

In order to provide a first evaluation for the meaning of the calculated values for evapotranspiration it is important to remember that the drainage density (linear length of the streams/ land surface) in the area of the carbonate aquifer is almost zero (see section 3.3). In practice, as the Sever River is the only stream in the area of the carbonate rocks and constitutes the main discharge area of the aquifer, we can consider that all the precipitation that escapes to the evapotranspiration processes (total runoff) contributes directly to the recharge of the aquifer. As shown in table 3.5, the recharge period in the aquifer is usually comprised between November and April. However, the recharge period is often shorter, as in all the southern regions of Portugal, where severe water shortages occurred in last years.

The detailed discussion of the calculated values of evapotranspiration will be presented after the estimation of the recharge values calculated by the Kessler and chloride balance methods provided in the next three sections.

### 3.4.3 – Recharge

The existence of different origins for the recharge processes occurring in the aquifer was briefly outlined in section 3.3. A denomination for each of the four different processes, identified in the present case study, exist in karst terminology (Field, 1999):

- Autogenic diffuse recharge occurring when the water reaches the saturated zone by slow percolation trough a myriad of small voids in the carbonate rock matrix.

- Autogenic concentrated discharge occurring when the precipitation falling directly in the area of the carbonate aquifer accessing the saturated zone in a very short time by percolation through large fractures or vertical shafts directly connected with swallow holes.

- Allogenic diffuse recharge derived from subsurface runoff in deposits that cover the carbonate rocks and the neighbouring low permeability schists (interflow) and drains into the carbonate aquifer.

- Allogenic concentrated recharge derived from sinking streams flowing from the neighbouring low permeability schists toward the aquifer. These streams disappear underground by infiltration in to swallow holes when the limit of the carbonate aquifer is reached.

Before searching for a way to define the relative importance of each of these recharge origins a more basic question needs an answer: what is the fraction of the precipitation infiltrated that escapes from the evapotranspiration processes and reach the saturated zone of the aquifer? In fact this first problem can be less difficult in karst aquifers than in other kinds of media. In the more general case, only one fraction of the total water that escapes from the evapotranspiration processes will be infiltrated. The remaining water will generate the surface runoff and thus flow into the stream network. In the frequent cases where the density of the stream network tends to zero in carbonate aquifers (as in the present case study) a reliable value for evapotranspiration is sufficient to define the fraction of precipitation corresponding to recharge.

The only question dressed in the present section is the quantification of the fraction of the total precipitation that constitutes the recharge. In fact this is only the simplest part of the problem. Even if we consider that a reliable value for the fraction of the precipitation contributing to recharge can be determined an important question remains: the determination of the fraction of the total recharge that reaches the saturated zone as concentrated or as diffuse infiltration.

This aspect is crucial because the responses of the aquifer to recharge events (in terms of hydraulic head distribution and water output) can be so different, for the same total recharge and different concentrated-diffuse proportions, as they are for doubled (or halved) total values of recharge.

In fact, the characterisation of the recharge processes of the present case study needs information at almost three different levels:

- The definition of the fraction of the total precipitation that corresponds to recharge;
- The shape of the function that characterise the infiltration process;
- The fraction of diffuse and concentrated infiltration.

Kiraly *et al.* (1995) discussed the last two problems referred above for the case of well-developed karst aquifers. Among many other conclusions, this work shows that the typical hydraulic behaviour of such systems is intimately related to the occurrence of concentrated infiltration which is conditioned by the presence of an epikarst zone defined as a “skin” of more permeable carbonate rocks at shallow depth. The conclusions and remarks provided in this work are crucial for the definition of the recharge processes that will be simulated in the model defined for the present case study and will be discussed later. In fact, in addition to these aspect another difficult question must be answered to characterise the recharge processes: the determination of the relative importance of each sinkhole for the total value of concentrated recharge. However at this point, a practical aspect related to the proportion of diffuse and concentrated infiltration must be done in order to avoid a misinterpretation of the meaning of some aspects related to the quantification of evapotranspiration.

In the previous section 3.4.2 it was defined that a given value of precipitation is needed in order to fill the moisture content corresponding to the field capacity leading to the start of the recharge process. As the aquifer is covered in most of its area by underlying deposits, it can be supposed, at a first glance, that diffuse infiltration dominates recharge processes. However this is not true because a fraction of the water infiltrated across these deposits can later reach the saturated zone by concentrated pathways.

Figure 3.8 illustrates the process, by which some of the initially diffuse infiltration can be converted to concentrated infiltration during the recharge. This kind of process can explain the seeming contradictions when the hydraulic behaviour of a covered carbonate aquifer shows responses of state variables in response to storm events compatible with the presence of concentrated recharge. Conversely, infiltration apparently started as concentrated can be slowly infiltrated through the fractured rock matrix.

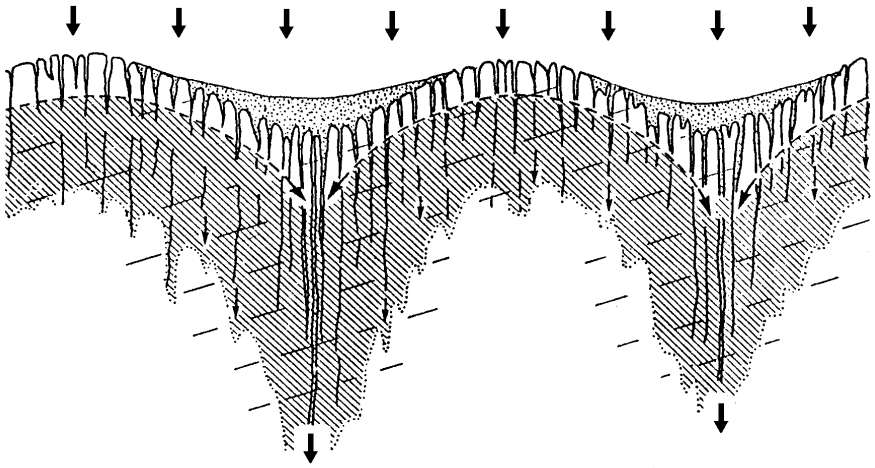

Fig. 3.8 – Diffuse infiltration converted to concentrated infiltration and concentrated infiltration converted to diffuse infiltration at shallow depth. Adapted from Williams, 1985 *in* Beck, 1988.

**3.4.3.1 – Kessler method**

The Kessler (1965) method was developed to estimate the recharge in a karstic region in Hungary where a careful validation of the obtained values was performed using experimental data. Later, this method was applied in different karstic aquifers in Mediterranean environments showing good correlation with values estimated using other mass balance calculations (Almeida, 1985). The method is based on the analysis of the distribution of precipitation in time rather than in the total values of annual precipitation. According to the results obtained by Kessler, the volume of the dynamical karstic water resources shows a better relation with the monthly distribution of the precipitation than with the simple annual precipitation values. That assumption explains the seeming contradictions when simultaneous temporal series of spring discharges and simple annual precipitations are compared.

The method is based on the definition of a "determinative precipitation rate" defined as the relation of the precipitation of the first four months of a given year to that of the total year, expressed in percentage. The determinative precipitation rate is corrected by a constant value ($k$) depending on the conditions of precipitation in the last four months of the previous year. The constant ($k$) can be obtained by determining the rate of the difference between the precipitation of the last four months (September-December) of the preceding year $P_{9\text{-}12}$ and the long-term average precipitation of the same four months $\bar{P}_{9\text{-}12}$. The value obtained is termed the "corrective precipitation rate" ($x$):

$$x = \frac{P_{9-12} - \bar{P}_{9-12}}{\bar{P}_{9-12}} \qquad 3.1$$

The relation of the corrective precipitation rate ($x$) to the correcting constant ($k$) is shown in table 3.6.

| Corrective precipitation rate (x) in percent | Values of the correcting constant (*k*) |
|---|---|
| 0-5 | 0 |
| 6-15 | 1 |
| 16-25 | 2 |
| 26-35 | 3 |
| 36-45 | 4 |
| 46-55 | 5 |
| 56-60 | 7 |
| 61-65 | 10 |
| 66-70 | 13 |
| >70 | 15 |

Table 3.6 – Values of the correcting constant (*k*) corresponding to the calculated values for the corrective precipitation rate (*x*).

The value of the correcting constant (*k*) is added or subtracted from the "determinative precipitation rate" according on the sign of the difference ($P_{9\text{-}12}$ - $\overline{P}_{9\text{-}12}$). Finally, the infiltration for a given year can be determined using the corrected values of the "determinative precipitation rate". The relation between the corrected determinative precipitation rate and infiltration is expressed by the graphic in figure 3.9.

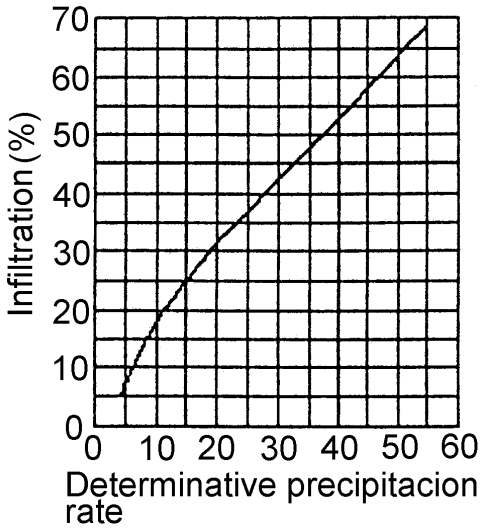


Fig. 3.9 – Curve representing the relationship between recharge and corrected determinative precipitation rate.

The calculated values for recharge, obtained by the Kessler (1965) method are presented in Table 3.7. The recharge and precipitation values for Castelo de Vide and Portalegre Gauges are plotted in the graphics of figures 3.10 and 3.11.

| Year | Castelo de Vide Recharge (%) | Portalegre Recharge (%) |
|---|---|---|
| 1960 | 63.8 | 64.7 |
| 1961 | 45.4 | 43.5 |
| 1962 | 64.5 | 66.6 |
| 1963 | 65.6 | 65.9 |
| 1964 | 86.3 | 87.8 |
| 1965 | 30.4 | 43.0 |
| 1966 | 83.6 | 81.2 |
| 1967 | 63.7 | 62.7 |
| 1968 | 55.6 | 53.1 |
| 1969 | 64.9 | 72.8 |
| 1970 | 66.5 | 69.6 |
| 1971 | 60.6 | 58.9 |
| 1972 | 50.8 | 46.9 |
| 1973 | 43.0 | 44.9 |
| 1974 | 65.4 | 72.9 |
| 1975 | 57.9 | 62.3 |
| 1976 | 39.1 | 38.5 |
| 1977 | 62.4 | 67.6 |
| 1978 | 55.5 | 56.4 |
| 1979 | 89.0 | 78.4 |
| 1980 | 63.1 | 63.5 |
| 1981 | 36.2 | 39.9 |
| 1982 | 45.8 | 55.1 |
| 1983 | 34.8 | 31.2 |
| 1984 | 53.1 | 51.6 |
| 1985 | 79.0 | 81.0 |
| 1986 | 67.4 | 63.6 |
| 1987 | 54.2 | 59.6 |
| 1988 | 58.2 | 54.8 |
| 1989 | 27.8 | 33.2 |

Table 3.7 – Recharge in percentage calculated by the Kessler (1965) method for the period 1960-1989.

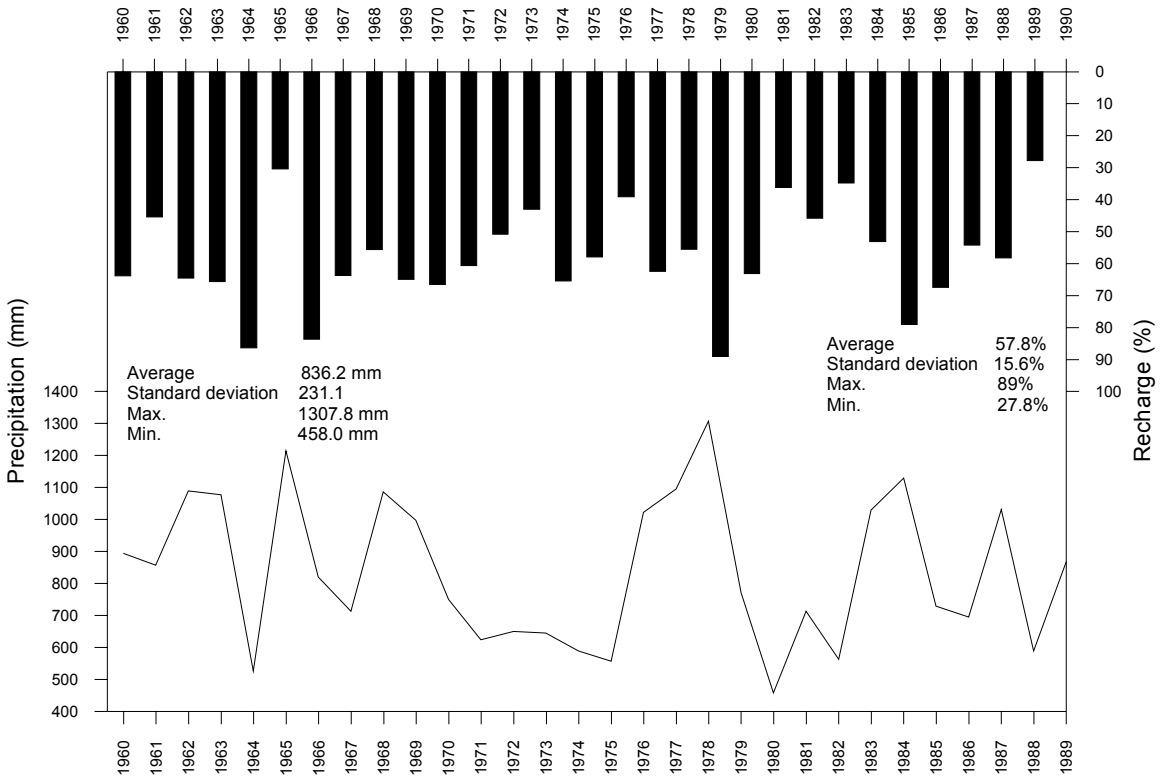


Fig. 3.10 – Recharge calculated applying the Kessler (1965) method using the precipitation values of the Castelo de Vide gauge.

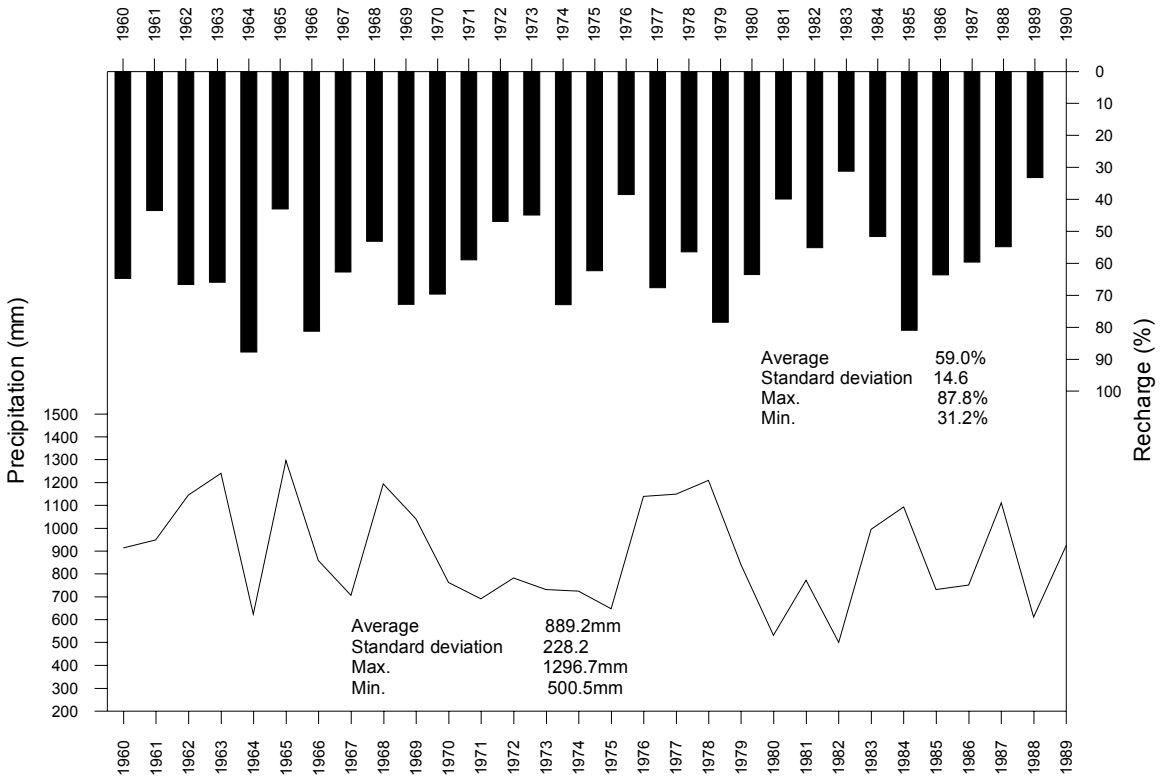


Fig. 3.11 – Recharge calculated applying the Kessler (1965) method using the precipitation values of the Portalegre gauge.

### 3.4.3.2 – Chloride balance

The method of the chloride Balance is quite simple and is widely applied to estimate recharge in carbonate aquifers. The method is based on the fact that the Chloride ion is relatively stable and, usually, it is not affected by chemical reactions during the infiltration process (Custódio and Llamas, 1976; Appelo and Postma, 1996). If we assume that the concentration of chloride ion in groundwater is the result of the increase of its concentration in infiltrated rainwater due to the evapotranspiration process the following expression can be used to estimate recharge:

$$inf = \frac{I}{P} \approx \frac{C_p}{C_i} \qquad 3.2$$

Where $I$ is the precipitation infiltrated, $P$ is the precipitation $C_p$ is the mean concentration of $Cl^-$ (ppm) in rainwater and $C_i$ is the mean concentration of $Cl^-$ (ppm) in groundwater.

Four rainwater samples collected in 1992 were analysed with the following results:

- 8/Jan – 5.7 ppm
- 12/Feb – 13.8 ppm
- 12/Jun – 4.26 ppm
- 15/Jun – 2.84 ppm

On 7th April 1992, 31 samples were collected in wells distributed over the carbonate aquifer. The mean $Cl^-$ concentration was determined for these samples leading to a value of 15.89 ppm. If we take that value and the average of the four samples for rainwater (6.65 ppm) we obtain a value of 41% for the infiltration.

It is very difficult to verify to what extent the simplifications evolved in this method are valid. For example, the irrigation in small farms in the central area of the aquifer contribute to a slight increase of chloride due the extraction-evapotranspiration-infiltration artificial cycles (and perhaps also by the use of fertilisers). In these cases, the infiltration using the chloride balance can lead to a underestimation of infiltration rates.

However we present the calculated values as an additional source of information for the evaluation of recharge. Only to give a figure of the coherence between the different methods we reference that, in the same year, the recharge value obtained by the Kessler (1965) corresponds to 32.4% using the data set available for the Castelo de Vide gauge.

### 3.4.4 - Coupled analysis of recharge and evapotranspiration

The calculation of the water budget presented throughout sections 3.4.1 to 3.4.2 provides a framework for the global evaluation of the water volume evolved in total runoff, evapotranspiration and recharge processes. As it is difficult to define the accuracy of each of these methods alone it is preferable to interpret the obtained values together and accept that the "real values" evolved in these transference processes must be comprised between the limits suggested by the different techniques.

The water budget defined by the actual evapotranspiration values calculated with the Turc and Coutagne methods correspond to the values obtained by the Thornthwaite method for excessively high values of field capacity (more than 150 mm). In fact, the first responses of hydraulic heads registered in piezometers at the start of the recharge period in different years show that the field capacity must be around one half of this value. That analysis is in agreement with the fact that the Turc and Coutagne methods tend to overestimate the real evapotranspiration values (Custódio and Llamas, 1976).

On the other hand if we take into account the total runoff values calculated by the Thornthwaite method by the soil-moisture budget approach, they must be close to the total recharge of the aquifer (because the surface runoff generated in the area of the carbonate rocks is zero). According to the values of actual evapotranspiration (table 3.4 in section 3.4.2), for a field capacity of 75mm, and an average depth of precipitation in the area of the aquifer of 904mm (section 3.4) the values for total runoff (and thus for recharge) for the 1960/61-1989/90 period are:

- (904.0-460.0) = 444.0 mm for the Portalegre gauge (49.1% of the precipitation);
- (904.0-468.5) = 468.5 mm for the Marvão gauge (51.8% of the precipitation).

The averages of the recharge values obtained in the same period using the Kessler (1965) method are of 59.0% and 57.8% for the Castelo de Vide and Portalegre gauges respectively. Therefore, the results obtained for the mass balance calculations using the Thornthwaite methods and recharge estimations obtained using the Kessler method allow the estimation of values varying within a range corresponding to about 10% of the total precipitation.

Based on the analysis of these values we admit that the long-term autogenic recharge for the aquifer is in the order of one half of the total precipitation occurring in the area of the aquifer. Using the Kessler method the values determined for recharge can vary from values of 30% to almost 90% of the precipitation. Such a high value as the maximum appointed must take into account the existence of cases where the water recharge in some years can include infiltration processes started in the previous year. Considering that the aquifer area is 7.9 $km^2$, and the average precipitation is 904 mm/ year and the long-term recharge is about 50% of the precipitation, the average annual recharge into the aquifer will be in the order of $3.6\times10^6$ $m^3$/ year.

The values calculated in this section are referred to a "long term" water balance for the aquifer based in data corresponding to the 1960/61-1989/90 period.

### 3.4.5 – Water use and global balance

The Castelo de Vide carbonate aquifer is the main source of water supply of the Castelo de Vide, Marvão and Portalegre Towns. Despite the fact that the aquifer area is only 7.9$Km^2$, the mainly granitic rocks present hundreds of square kilometres around cannot support wells productive enough to provide the water demands for these towns. For the Portalegre town the water exploited in wells with the inventory numbers 49 and 81 is conducted about 30km to the south of the aquifer. The wells used for public supply of these towns are listed in Table 3.8.

| Town | Inventory number of pumping wells | Start of exploitation | Average Pumping rates in the period 1990-98 (l/s) |
|---|---|---|---|
| Castelo de Vide | 8, 82 | 1957 | 15-25 |
| Portalegre | 49, 81 | 1959 | 30 |
| Marvão | 79, 80 | 1982 | 5 |

Table 3.8 – Wells in the Castelo de Vide Carbonate Aquifer used for public water supply.

As shown in Table 3.8 the withdrawals for Portalegre and Marvão towns are well described by a single average value for the last years. Despite the increase in pumping during summer, in these cases the difference in monthly averages is not important. In the case of Castelo de Vide, the data registries of extractions show that the pumping rates during summer increase enough to consider two different seasonal periods of exploitation: one, more intense, during summer (about 25 l/s) and another with smaller extraction volumes (about 15 l/s) during the rest of the year. These seasonal changes in extractions are probably related to the fact that this town is a tourist spot, having an increased demand during the last years.

In addition to the public water supply other wells are active today. These wells are mainly used for irrigation of food crops in the area of the carbonate rocks and are regularly active only during the dry months of the year.

Tens of large diameter wells used for irrigation in the past are nowadays abandoned and are used as observation points of the aquifer. Some of them are being pumped sporadically but the respective extraction volumes are negligible, when compared with the regularly used wells and with the global water balance.

A group of pumping wells, used in a mineral water plant, completes the description of water uses in the aquifer. The extraction volume of these wells is only $1.6\times10^3 m^3$/year. Therefore, this volume use is negligible compared with the global water balance.

The total extraction volume in the aquifer, taking into account the available data collected between 1996 and 1999 is 59.7 l/s ($1.88\times10^6 m^3$/ year). The average annual recharge into the aquifer, estimated in the last section based on the long-term water balance is 114.2 l/s ($3.6\times10^6$ $m^3$/ year). Under the present conditions of the aquifer water use the average annual ratio extractions/ recharge will be 52%. At a first glance, such value can lead to the conclusion that withdrawals from the aquifer are not in excess considering the average rate of replenishment indicated by estimated recharge values. However, taking into account the variability of precipitation in time it must be expected that in some years the recharge values will be inferior to the actual volumes of withdrawals. If the actual volume of pumping in wells ($1.88\times10^6 m^3$/ year) is compared with the recharge volumes estimated between 1960 and 1998 it can be seen that in 1981 and 1992 the withdrawals were superior to recharge (Table 3.9).

| Year | Precipitation (mm) | Recharge (percent of precipitation) | Recharge ($m^3$/year $\times 10^{-6}$) | Ratio Pumping/ recharge (%) | Year | Precipitation (mm) | Recharge (percent of precipitation) | Recharge ($m^3$/year $\times 10^{-6}$) | Ratio Pumping/ recharge (%) |
|---|---|---|---|---|---|---|---|---|---|
| 1960 | 1367.0 | 62.8 | 6.78 | 28 | 1980 | 523.9 | 62.1 | 2.57 | 73 |
| 1961 | 732.1 | 44.3 | 2.56 | 73 | 1981 | 628.7 | 36.2 | 1.80 | 105 |
| 1962 | 747.2 | 64.5 | 3.81 | 49 | 1982 | 604.5 | 45.8 | 2.19 | 86 |
| 1963 | 1373.1 | 65.6 | 7.12 | 26 | 1983 | 912.1 | 33.6 | 2.42 | 78 |
| 1964 | 667.1 | 85.4 | 4.50 | 42 | 1984 | 899.4 | 51.0 | 3.62 | 52 |
| 1965 | 887.2 | 30.4 | 2.13 | 88 | 1985 | 988.9 | 79.0 | 6.17 | 30 |
| 1966 | 1121.8 | 80.7 | 7.15 | 26 | 1986 | 586.2 | 67.4 | 3.12 | 60 |
| 1967 | 627.9 | 63.7 | 3.16 | 59 | 1987 | 944.9 | 53.1 | 3.96 | 47 |
| 1968 | 878.0 | 55.6 | 3.86 | 49 | 1988 | 876.4 | 58.2 | 4.03 | 47 |
| 1969 | 1054.9 | 64.9 | 5.41 | 35 | 1989 | 962.9 | 26.5 | 2.02 | 93 |
| 1970 | 838.0 | 66.5 | 4.40 | 43 | 1990 | 581.2 | 63.0 | 2.89 | 65 |
| 1971 | 668.0 | 57.4 | 3.03 | 62 | 1991 | 617.3 | 75.8 | 3.70 | 51 |
| 1972 | 824.7 | 50.8 | 3.31 | 57 | 1992 | 567.6 | 32.4 | 1.45 | 129 |
| 1973 | 608.3 | 43.0 | 2.07 | 91 | 1993 | 851.6 | 35.7 | 2.40 | 78 |
| 1974 | 525.1 | 65.4 | 2.71 | 69 | 1994 | 959.1 | 50.8 | 3.85 | 49 |
| 1975 | 621.7 | 57.9 | 2.84 | 66 | 1995 | 981.3 | 39.7 | 3.08 | 61 |
| 1976 | 829.8 | 39.1 | 2.56 | 73 | 1996 | 1234.8 | 75.0 | 7.32 | 26 |
| 1977 | 1087.1 | 61.4 | 5.27 | 36 | 1997 | 1288.5 | 27.6 | 2.81 | 67 |
| 1978 | 1230.3 | 54.4 | 5.29 | 36 | 1998 | 744.0 | 69.6 | 4.09 | 46 |
| 1979 | 1091.2 | 89.0 | 7.67 | 25 | | | | | |

Table 3.9 – Estimation of the ratio pumping/ recharge for the aquifer considering the average annual precipitation. Values of recharge were estimated using the Kessler method. The aquifer area is 7.9 $km^2$. Average values of extractions in the last years are about $1.88 \times 10^6 m^3$/ year. Precipitation data was collected in the Castelo de Vide gauge. Highlighted values correspond to years when recharge volumes were lower than withdrawals.

Even when considering that in some years withdrawals can be superior to recharge, it must be remarked that an "average hydrologic year" is enough to achieve recuperation of water levels to the usual values. In fact this is related to the fact that the carbonate aquifer is immersed in very low permeability lithologies and most of the aquifer thickness develop below the altitude of the discharge areas. In these natural conditions water storage is more efficient than in the cases where boundary conditions lead to continuous depletion of the aquifer during recession periods (see figure 3.12).

In addition to the above considered regime of withdrawals we report the recent construction of a new high capacity well in the Escusa sector of the aquifer (where tests showed that pumping rates of about 80 l/s are possible). This well was built to support the water use in a golf field and, as shown by the above-calculated budget, could be sufficient to lead to systematic withdrawals from the aquifer in excess of the average rate of replenishment.

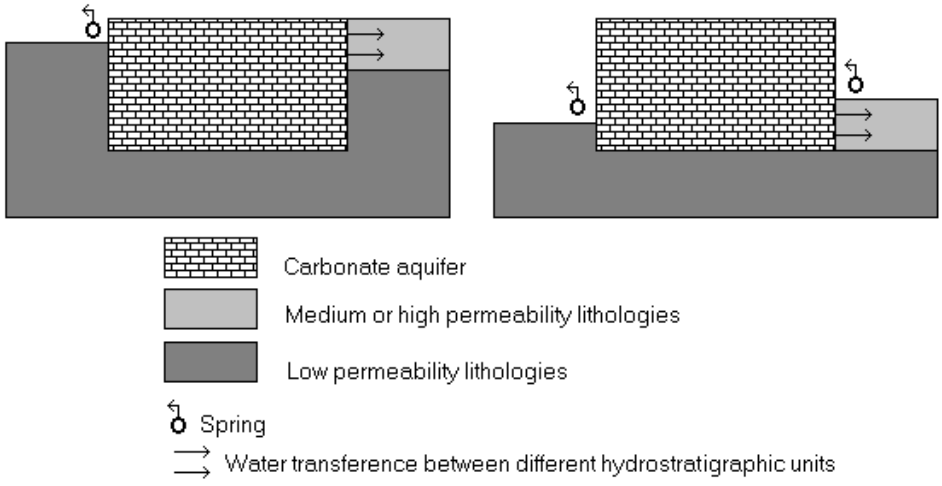


Fig. 3.12 – Example of boundary conditions leading to an efficient regularisation of water resources (left) and leading to important losses in water storage (right), depending on boundary conditions. The case of the Castelo de Vide aquifer corresponds to the situation illustrated at left.

### 3.5 – Interpretation of state variables

The available data for state variables in the aquifer correspond to piezometric observations and data registries for the discharges of some temporary springs. The Sever River is hydraulically connected with the aquifer and constitutes its main discharge area. The volume of water transference from the aquifer to the river is not quantified. This is a severe limitation for the analysis of the global responses of the aquifer (and for the quality assessment of the calculated water balance). The only way to determine the outflow throughout the riverbed consists in installing two gauges, monitoring the river discharge in two points immediately upstream and downstream of the carbonate aquifer limits. The difference between the determined values in these points corresponds to the aquifer discharge. Unfortunately, the available grants for the present work were not sufficient to acquire the equipment necessary to take such measures.

The collected registry of state variables is essential in two different phases of the present work: (1) for the qualitative interpretation of data allowing the definition of a conceptual flow model and (2) after the construction of a numerical flow model at regional scale (based on the conceptual flow model). Hydraulic head and discharges from the aquifer are the dependent variables calculated by the model. Therefore, the assessment of the quality of the simulations is performed by means of the analysis of the fit between the real state variables and the calculated ones.

#### 3.5.1 – Inventory of observation points

The 64 observation points presented in figure 3.13, within the aquifer limits and neighbouring area allowed the collection of water samples and/ or water level measurements. Among these wells 26 are small diameter drilled wells and 32 are dug wells with large diameter. For all these wells sporadic water level measurements are available from 1991 up to now. However, systematic collection of measurements was done only in 34 points for which altitudes where determined during a topographic survey. As these altitudes are referred to the Portuguese geodesic network, the determined values of hydraulic head will be expressed in meters above sea level.

The present inventory is not exhaustive. In addition to the points referenced in figure 3.13 some few wells exist but they are not accessible to observations. The inventory points outside the area of the carbonate rocks were very useful to improve the knowledge about the shape of the aquifer limits.

Despite the fact that the main discharge area of the aquifer corresponds to the Sever River, some secondary springs are present in the NW area of the carbonate rocks. The spring with the inventory number 58, located about 150m to E of the Sever River, is temporary and rarely active. This spring is an exception for the more general outflow pattern from the aquifer, which occurs mainly throughout the riverbed. When the transference from the aquifer to the river attains the highest values that spring is sometimes active. However, even in this case, the flow from the spring is discharged into the Sever River and its discharge can be computed in the total water transference from the aquifer to the river.

Systematic data of spring discharges is available for springs 5, 6, 51, 39 and 59. All of them are temporary and the discharges are always lower than 3 l/s. Spring 58 is also temporary and due to intense pumping in wells 49 and 81 it is rarely active today. However, some point values exist referencing a maximum discharge of 220 l/s.

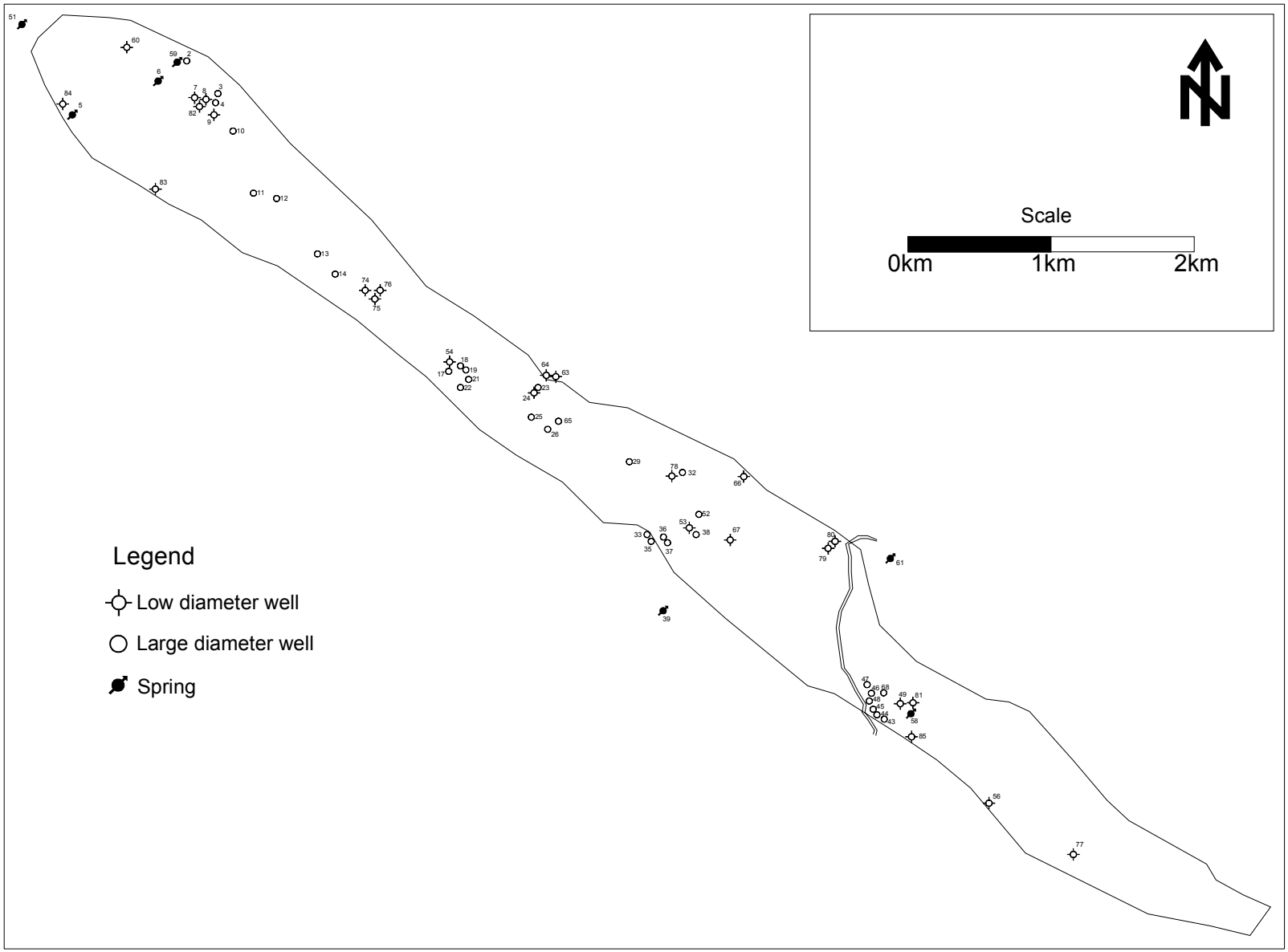


Fig. 3.13 – Inventory of observation points in the aquifer.

The position of the observation points in figure 3.13 are sometimes slightly displaced from its real position in order to keep the map readable at the presented scale. This is the case for the points around well 82 and for the wells and the spring located near the East margin of the Sever River.

### 3.5.2 – Remarks on the interpretation of piezometric data in aquifers with diffuse and conduit flow

Piezometric measurements can be used to build steady-state flow nets, which can be interpreted to provide information about groundwater flow directions, location of recharge and discharge areas and check the definition of boundary conditions. In fact, the construction of flow nets is one of the most powerful tools for the analysis of groundwater flow. Freeze and Cherry, 1979 provided a detailed description of the rules of interpreting flow nets as well as a careful definition of the limits associated with that approach.

Flow nets are two-dimensional representations of the considered flow domain. In such a representation the equipotentials (lines of equal hydraulic head) are assumed to be vertical along the entire thickness of the flow domain. Thus, the hydraulic head takes the same value along any vertical in the aquifer. This simplification fails even in homogeneous and isotropic flow domains, for example, near points located in the neighbourhood of pumping wells or along lines where streams are in hydraulic connection with aquifers. In very heterogeneous flow domains, as carbonate rocks, the interpretation of piezometric data is even more difficult because the hydraulic head shows a strong variation with depth even in natural flow conditions. Figure 3.14 shows a profile of hydraulic head determined at intervals of about three meters of depth during the drilling operations of boreholes 74 and 75. As shown in figure 3.14, the values of hydraulic head suffer important variations when fractured or karstified zones are met. It means that the evolution of potential is different when measured in intervals of the borehole corresponding to the rock matrix and karstified zones. Another interesting aspect resulting from the analysis of this figure is the fact that the hydraulic head is sometimes higher and sometimes lower in the dissolution channels than in the neighbouring rock matrix. As that measures where taken three days after a period of recharge they can give an idea about the complexity of the transient transference's between the rock matrix and dissolution channels associated to the propagation of the recharge inputs and subsequent emptying of the system.

During the field surveys a single value of water level was determined in each observation point. The determined water levels cannot be interpreted as representing a hydraulic head value assigned to a particular point in the aquifer (as if the piezometer was open in a single point). In most of the cases the wells are fully screened or screened at depths were more fractured or karstified zones are meet. Therefore, the hydraulic head values determined correspond to some value between the highest and the lower potential values along the considered vertical. For example, for well 75, the value of hydraulic head taken at the end of the drilling operations corresponds to 561.4 m. However, as shown in figure 3.14, hydraulic head vary between 553.3m and 562.8 along the vertical defined by the well.

One important aspect resulting from the analysis of information available in technical reports of well constructions is that, almost always, the water level in the boreholes rises to higher altitudes than what was previously encountered when saturated zone is attained. This is an indication that the aquifer behaves, in most of its area, as a confined system. On the other hand there is no evidence about the existence of preferential areas of recharge (except for points of concentrated recharge in swallow holes). The identification of areas where the carbonate rocks are exposed in outcrops, areas where the water levels are systematically higher in the aquifer and areas where streams sinking in the carbonate rocks could be considered as potential areas where recharge is more effective. However, the identification of wells with the described behaviour in these areas seems to show that recharge must occur in almost the hole area of the aquifer. In fact, as will be shown in chapter 4, as the oscillation in water levels in the aquifer is negligible when compared with the total saturated thickness, the hydraulic behaviour of the aquifer can be well described, at regional scale, with acceptable results baswd on both confined or unconfined conceptual flow models.

A set of interesting remarks about the interpretation of piezometric data in the case of well-developed karst aquifers is provided in Jeannin and Grasso (1997). As remarked in this paper, one of the basic rules to take into account is that the interpretation of piezometric data at local scale can lead to a wrong definition of the flow directions. Another remark provided in this paper is that the existence of transmissivity values for observation points is important because these values allow the identification of wells where the water level measures are mainly representative of the hydraulic head in dissolution voids or in the rock matrix. As will be shown in chapter 5, when time drawdown data available is not detailed enough to determine hydraulic parameters, the same results can be obtained using values of specific capacity. This is particularly important, not only to interpret piezometric data but also to define a classification of pumping wells in order to simulate its behaviour at local scale.

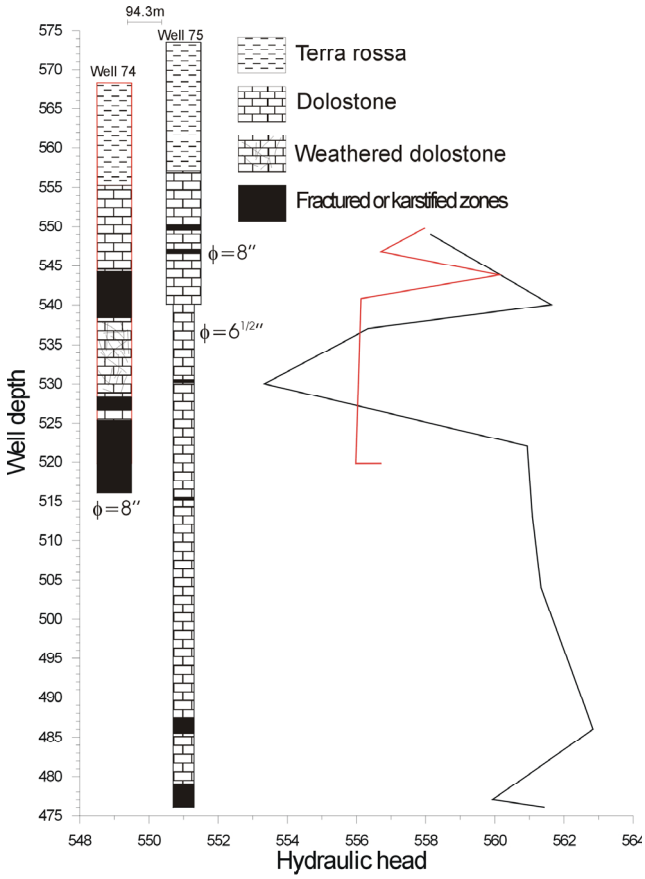


Fig. 3.14 – Hydraulic head plotted as function of depth in wells 74 and 75. Measures taken during the drilling operations on November 19 and 20, 1997, respectively, three days after the end of a 14 days recharge period.

### 3.5.2.1 – Analysis of the spatial distribution of piezometric data

As referred to in section 3.5.2, when diffuse flow and conduit flow are superimposed in a very complex pattern, the interpretation of piezometric observations at local scale must be performed carefully in order to avoid abusive conclusions or simply wrong interpretations. However, by using the determined point values of hydraulic head it is possible contour an approximate equipotential surface in order to define the prevailing flow directions at aquifer scale. In this case, instead of being used to draw well-defined flowpaths, the piezometric maps are employed as valuable tools to define the general directions of water transference between different aquifer sectors toward the discharge areas.

As the fluctuations of hydraulic head in the aquifer affect the flow conditions continuously, the general steady state regional flow pattern is better-defined analysing the average equipotential surfaces corresponding to extreme values of hydraulic head. The equipotentials presented in figure 3.15 were contoured from two different data sets. The first one corresponds to observations at the end of a period of severe drought affecting the region in 1992. The second corresponds to the measurements at the end of 1996 when the highest potentials where registered.

Figure 3.15 shows that three flow systems can be distinguished in the aquifer according to the general flow directions. In the central area of the aquifer towards NW of the Sever River a groundwater divides can be outlined. From this area two divergent flow systems can be defined: toward NW in direction to the Castelo de Vide town and toward SE, toward the Sever River. These flow systems will be referred thereafter, respectively, as Castelo de Vide and Escusa sectors. The third flow system corresponds to the entire area of the aquifer located to the SE of the Sever River. In this case the predominant flow direction is SE-NW, towards the Sever River. This last system will be named P. Espada sector and the flow direction defined by the equipotentials is only indicative due to the lack of observation points. However, the few data available for that area shows that the P. Espada and Escusa sectors share the same outflow area, which corresponds to a groundwater divides line defined by the Sever River. The same conclusion can be drawn on the basis of the hydrochemical trends identified in the aquifer discussed in Section 4.3.2.

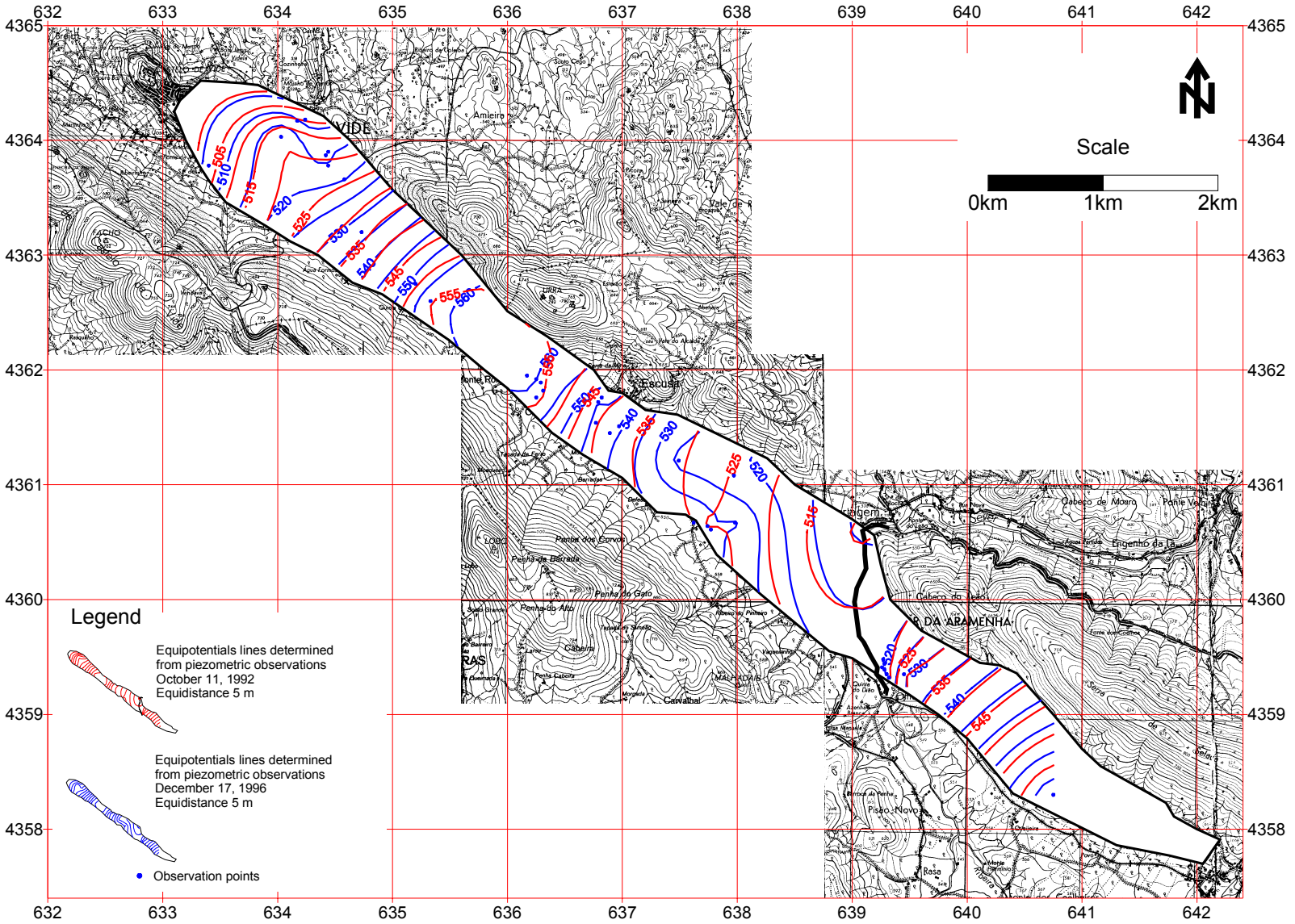


Fig.3.15 – Equipotential lines contoured from data collected when the lowest (October 1992) and highest (December 1996) values of hydraulic head were detected in the aquifer.

Under such conditions the flow from the P. Espada and Escusa sectors converge towards the same area. Therefore, the flux in that area is upwards and reaches the Sever River throughout its bed.

As shown by the spatial distribution of hydraulic head in both conditions of drought and high waters (fig. 3.15), the defined sectors are an acceptable basis for the interpretation of the long-term hydraulic behaviour of the aquifer at regional scale.

The basemap in figure 3.15 surrounding the area of the aquifer shows the morphology of the secondary discharge area of the aquifer near Castelo de Vide. The NW limit of the aquifer in that area shows two important differences regarding the general pattern of the aquifer limits: The "impermeable" Silurian and Devonian sequences are absent in part of that area and; the lithologies in contact with the aquifer are at lower altitudes than the aquifer itself. In that area, the water flowing from the Castelo de Vide Sector is discharged to adjacent lithologies and later to the small streams diverging from the NW aquifer limit. It must be remarked that the discharge of the temporary springs with inventory numbers 5, 6 and 59 is conditioned by threshold values for the capacity of the neighbour, relatively low permeable, lithologies to assimilate the outflow from the carbonate aquifer.

As the outflow in the NW area of the aquifer is done in the contact with low permeability lithologies, the residence time of the water in the Castelo de Vide Sector is longer than in the Escusa and P. Espada sectors. This is confirmed by hydrochemical evidence as showed in section 3.6.1.

**3.5.2.2 - Analysis of time variability of piezometric data**

As shown in the last section, the spatial distribution of hydraulic heads in the aquifer allows the definition of three different sectors according to the predominant flow directions toward discharge areas. In strictly technical terms that analysis corresponds to a steady state characterisation of the system and its only possible if the general configuration of the equipotential surface does not change with time. In practice this statement is respected if the high points in equipotential surface remain highest and the low points remain lowest during the seasonal fluctuations of hydraulic head. However, due to the simultaneous presence of diffuse and conduit flow, carbonate aquifers are often highly transient systems and thus the validity of conclusions derived from the spatial distribution of hydraulic head regarding the definition of general flow directions must me carefully checked.

Figure 3.16 provides a first evaluation of the temporal variability of hydraulic heads in the aquifer. For each of the 33 observation points the maximum, minimum median upper and lower quartiles of the registered hydraulic head values are represented in a sequence corresponding to the position of the points along the axis of the aquifer. The range of values for each observation point shows that gradient inversions are possible inside each of the defined sectors. In fact, this occurs mainly in the Escusa sector but can happen also in the other sectors. Figures 3.17, 3.18 and 3.19 show the fluctuations of hydraulic heads in the observation points between 24 September 1996 and 23 September 1998. These fluctuations are the result of the aquifer response to the annual climatic variability and to the effects induced by pumping wells.

Despite the fact that the observation point with the number 17 belongs to the Escusa sector it is also represented in the graphic of figure 3.17 where the observations points of the Castelo de Vide Sector are represented. This was done in order to show that the groundwater divides defining the boundary of these sectors is located somewhere between observation points 14 and 17. The interpretation of the boundary between Castelo de Vide and Escusa sectors was not easy to perform. The defined equipotential surfaces showing flow diverging from the central area of the aquifer toward Castelo de Vide and Toward the Sever River were identified in an area where no observation points were previously available. The wells with inventory numbers 74 and 75 where drilled in order to find some physical barrier or diminution in aquifer thickness justifying the highest potential values in that area. However, such features could not be identified. On the contrary, dissolution voids of metric dimensions were identified and the bottom of the aquifer was not reached because, as in other sectors of the aquifer, the losses in pressure of the drilling fluid in very karstified zones makes drilling impossible when a depth of around 100m is attained. As no other justification was found for the presence of that boundary the boundary between Castelo de Vide and Escusa aquifer sectors was interpreted as a groundwater divides, which position is defined by hydraulic factors as discussed in chapter 4

The observation of the temporal variability of hydraulic heads shows that despite the existence of gradient inversions the definition of sectors proposed in the previous section is still valid under transient conditions. More than that, the observation of figure 3.16 shows that the three sectors are also identifiable by different patterns in terms of temporal variability of hydraulic heads. In the Escusa sector the amplitude of hydraulic head is almost always wider than in the other sectors.

The available data registry characterising the time variability of piezometric data is mainly based on monthly observations. In such conditions the characterisation of the aquifer consists of the analysis of the seasonal fluctuations in hydraulic heads characterising the aquifer at the annual time scale. Climatic conditions in that region are characterised by a long period of the year without recharge (six months or more, as shown in section 3.4.2). Therefore, emptying periods of the aquifer are well characterised by monthly data. On the other hand, recharge episodes are characterised by infiltration processes that can be responsible for aquifer responses acting at a daily time scale. In such conditions monthly measures are not able to capture aquifer responses resulting from individual recharge events.

The available data sets are not exclusively collected monthly. Data collection for spring discharges and hydraulic head values determined in wells 32 and 67 were done on a weekly basis. In figures 3.20 and 3.21 the monthly and the weekly hydraulic head data sets, collected in observation points 32 and 67, are plotted simultaneously. That figure is very elucidative about the information lost when only monthly data is available. It must be remarked that the well 67 is sporadically exploited one day per week during about 6h. Sometimes the measures were taken during the extractions. The interference of these extractions is visible in figure 3.20. Dissolution channels are absent in these wells. Therefore, they are representative of changes in hydraulic head occurring in the low permeability rock volumes. In the cases where wells are drilled throughout dissolution channels, it must be expected that more important differences may found between monthly and weekly data registries. The more important conclusion regarding these data sets is the fact that during the emptying period of the aquifer a monthly data registry allows a very adequate characterisation of the hydraulic behaviour of the system.

Another aspect visible in the graphics showing the temporal variability of hydraulic head is the fact that the fluctuations of the equipotential surface are very small compared with the total thickness of the aquifer. This is a very important aspect because the role of the processes developed in the unsaturated zone is restricted to a very thin layer few meters below the ground surface. That feature allows very important simplifications when a flow model is defined to simulate flow in the aquifer.

The knowledge of the hydraulic head variation in time is also indispensable in order to quantify the volumes of water transference in the aquifer in different periods of the hydrologic cycle. As the distances between piezometers are known, it is possible to determine the hydraulic gradient $dh/dl$. Therefore, the specific discharge along sections of the aquifer can be calculated using the Darcy's law providing that hydraulic conductivity is known. As limit values of the order of magnitude of hydraulic parameters for individual dissolution channels and rock matrix can be known, it is possible to define zones of the aquifer with different degrees of connectivity with the discharge areas. The evolution of hydraulic heads presented in the present section is essential to perform such analysis. However, the discussion of the aspects related to the definition of the degree of connectivity of the sectors identified in the aquifer with discharge areas can be done only after the determination of hydraulic parameters, which will be discussed in chapters 4 and 5.

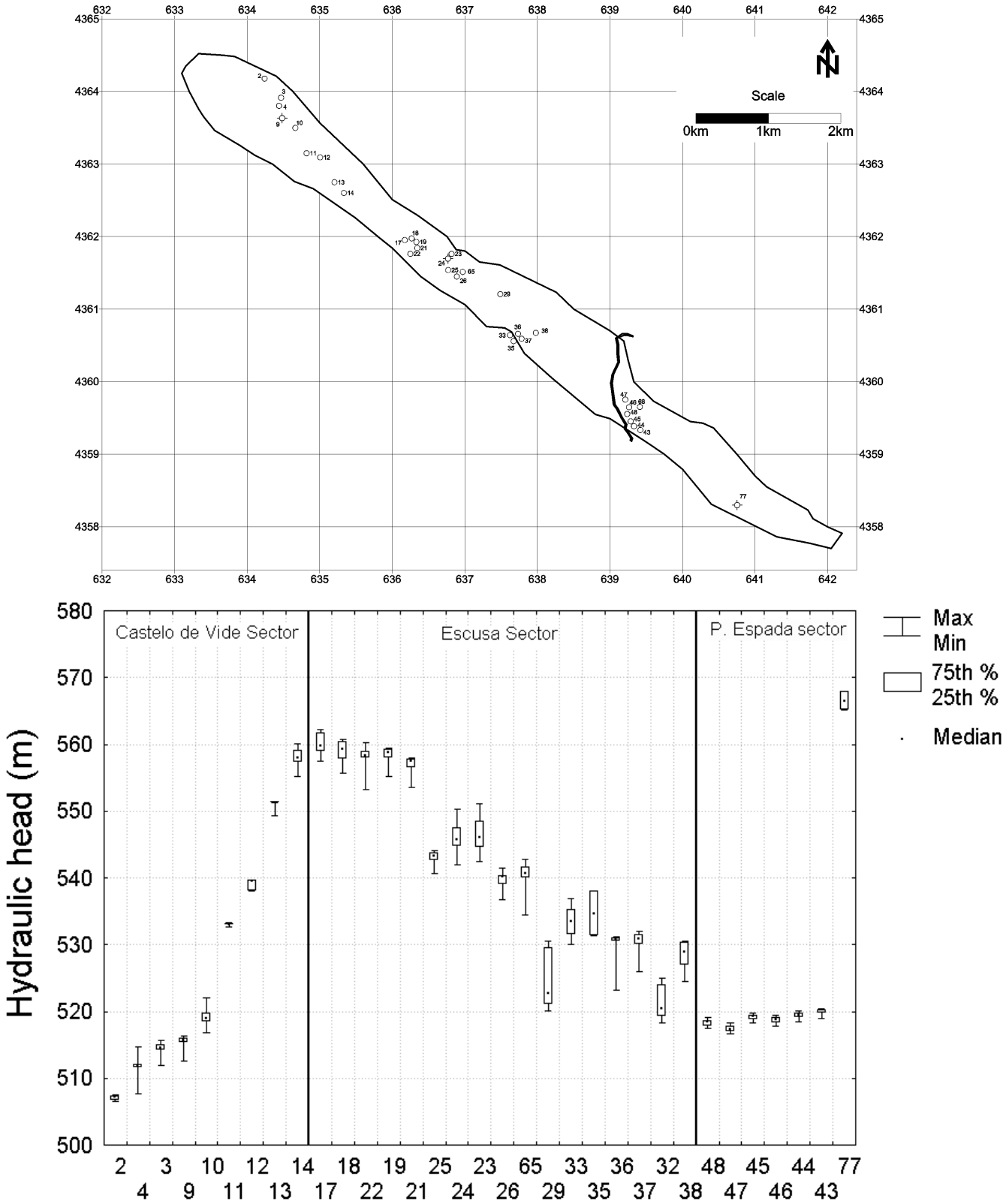


Fig. 3.16 – Box plots showing the range of variation, upper and lower quartiles and median of hydraulic head values registered between 1991 and 1999. The 33 observation points are represented along a line coinciding with the axis of the aquifer, between observation points 2 and 77. The points 33 and 35 are outside the limits of the aquifer and were drilled through the deposits covering the carbonate rocks and the adjacent "impermeable" lithologies. Note that the three sectors of the aquifer defined in the previous section are identified in the graphic. The position of the points is shown in the above map, geo referenced with a kilometric grid (UTM co-ordinates).

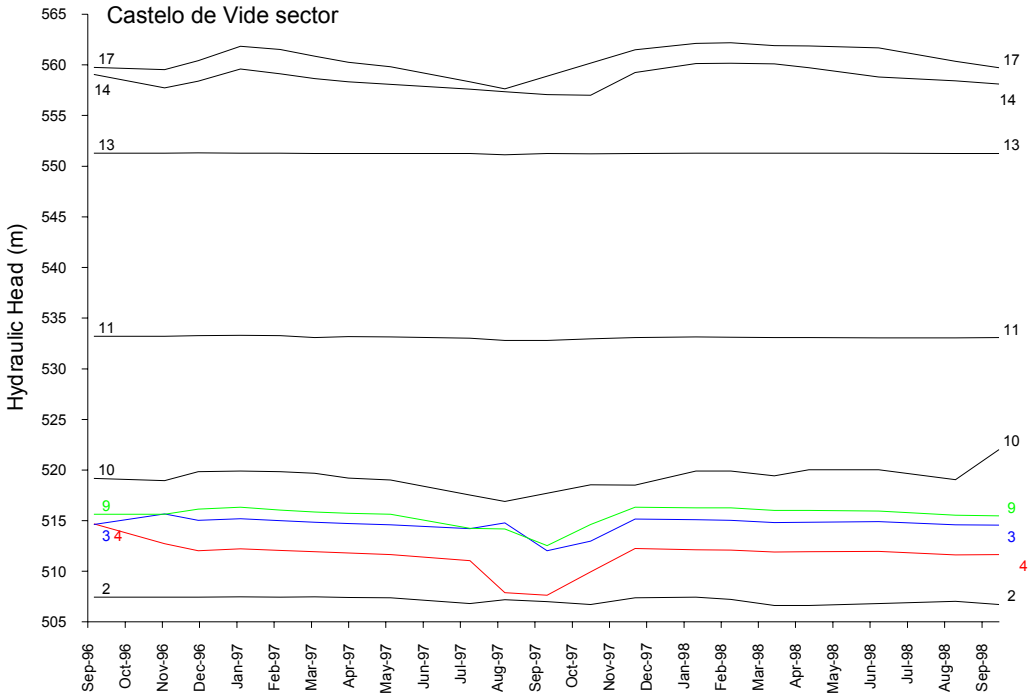


Fig. 3.17 - Temporal variability of hydraulic heads in the Castelo de Vide sector. Line labels correspond to identification of observation points mapped in figure 3.13.

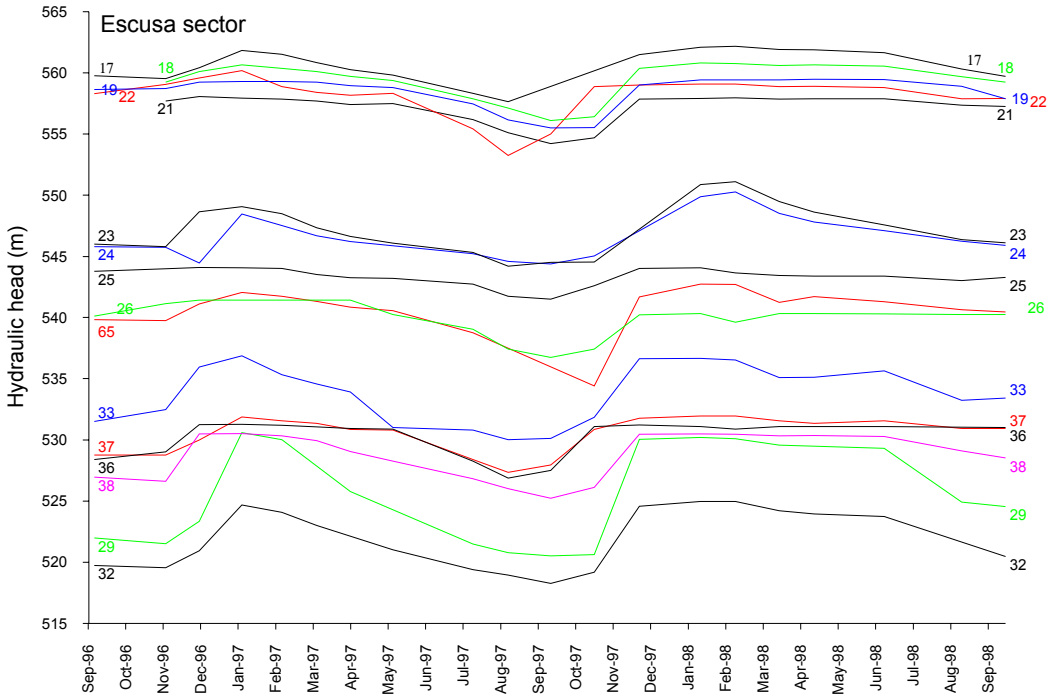


Fig. 3.18 - Temporal variability of hydraulic heads in the Escusa sector. Line labels correspond to identification of observation points mapped in figure 3.13.

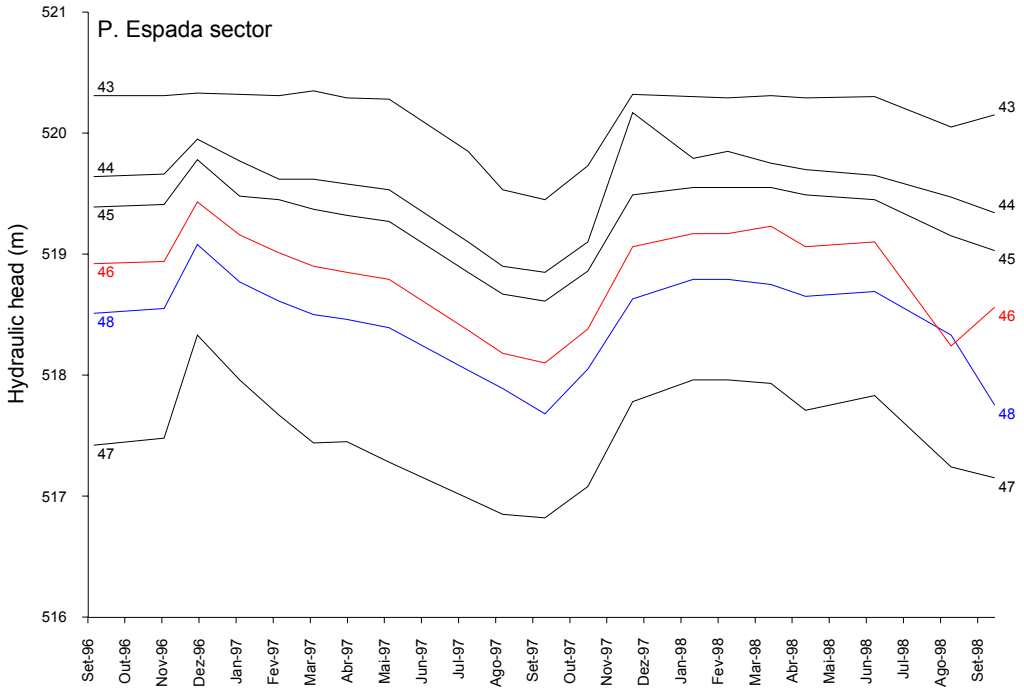


Fig. 3.19 – Temporal variability of hydraulic heads in the P. Espada Sector. Line labels correspond to identification of observation points mapped in figure 3.13.

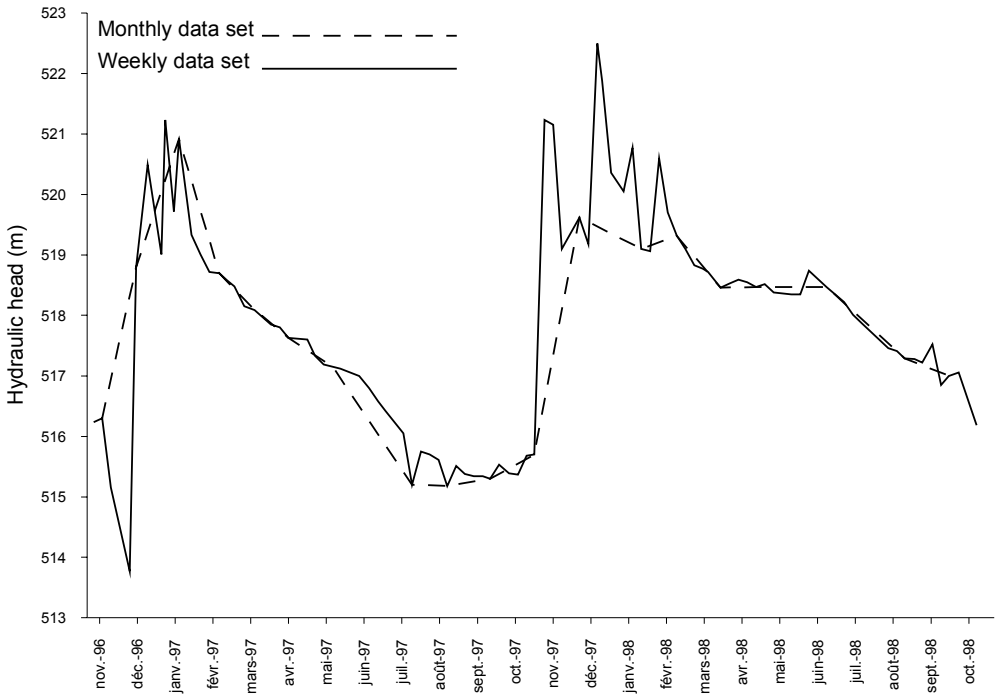


Fig. 3.20 – Comparison between weekly and monthly data sets for well 67.

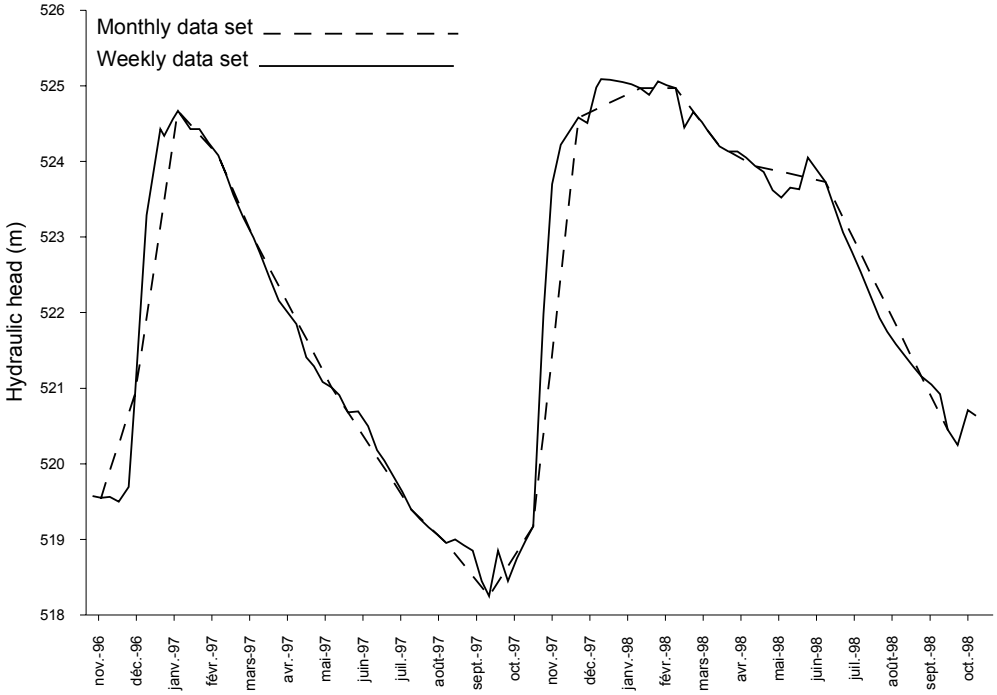

Fig. 3.21 – Comparison between weekly and monthly data sets for well 32.

### 3.5.3 – Spring hydrograph analysis

#### 3.5.3.1 – Remarks on the use of methods based on "global responses" to characterise karst aquifers

The hydrograph of a spring is the final result of the processes that govern the transformation of water inputs, in the spring drainage area, into the flow at the point of discharge. As the possibilities in characterising karst aquifer parameters are very limited, the interpretation of spring hydrographs is often applied as an indirect tool to make inferences about infiltration, groundwater flow processes and hydraulic parameter fields in karst aquifers (Kiraly and Morel, 1976b; Eisenlohr, 1995; Kresic, 1997; Kiraly, 1998).

A very extensive number of contributions are available on this topic. A detailed description of objectives and methods of several techniques allowing the interpretation of spring hydrographs is available in Eisenlohr (1995). These methods can be based on the analysis of the complete hydrograph or only in the interpretation of the outflow period corresponding to the emptying of the aquifer. The recession of a spring represents the emptying of the system and, during that period, the aquifer is in the stage of continuous outflow without disturbances caused by recent recharge events. Therefore, in that period inferences about groundwater flow, hydraulic parameters and infiltration processes can be done without the direct influence of infiltration on the hydrograph shape (Kresic, 1997).

The data needed to apply different methods depends on the aquifer characteristics. Very often the referenced data sets are collected daily or even hourly. After the analysis of the data specific to a given aquifer it is possible to take samples with lower frequency, if the detected responses are well characterised by measurements collected at wider time steps. Naturally the methods based on the analysis of the entire hydrograph require more detail in terms of data availability.

The methodologies applied for spring hydrograph analysis are conceived to characterise the aquifers "global response" and are well suited for the analysis of karstic systems where the outflow is mainly concentrated in karstic springs. The use of these methods is almost always based on the diagnosis of the hydraulic properties characterising karst aquifers. The presence of global responses in a very short time after recharge events followed by slow drainage of the low permeability rock volumes is the expected behaviour allowing the identification of the karstic character of a given aquifer. Such kind of transformation of water input in the spring discharge reflects the dichotomy of recharge, flow and outflow processes resulting from the coexistence of diffuse and conduit flow overlapped in a very complex transient pattern.

That way to define karst aquifer is so common that the definitions presented by most authors for karst aquifers include near always a reference of a karstic spring draining the system. It must be noted that implicitly such definitions are dependent of the boundary conditions characterising the aquifers and not only on the presence of a regional flow pattern controlled by dissolution channels. On the other hand it is not reasonable to deny that some carbonate aquifers, in which

concentrated points of discharge are absent, must be characterised by the same essential features responsible for the typical outflow pattern characterising the "global responses" of karst aquifers. This is the case, for example, when the outflow from a carbonate aquifer is towards adjacent hydrostratigraphic or surface water bodies. As shown before this is the case in the Castelo de Vide carbonate aquifer where the discharge takes place towards a river and towards adjacent low permeable lithologies.

The utility of the methods based on the "global response" analysis is unquestionable due the scarce data on hydraulic parameters that can be collected by direct methods in karst aquifers. However, in addition to dealing with the limitations inherent to the difficulties in interpreting "global responses" to characterise karst aquifers a basic requirement must be fulfilled in order to use such techniques: The existence of a quantifiable global response. A conspicuous absence of discussion about this topic in karst hydrogeology literature is responsible for the dependency of the "karst aquifer" definition from the identification of the typical behaviour of karst springs.

The intrinsic characteristics of karst aquifers are responsible for the duality of the infiltration, groundwater flow field and discharge processes (Kiraly, 1995). All these characteristics can be present without the existence of a concentrated point of discharge materialised as a karstic spring (as in the present case study).

The base for the quantitative treatment is the general form of Maillet (1905 *in* Milanovic, 1981) equation, which is used for fitting the recession curves of hydrographs. The general form of the Maillet equation is:

$$Q_t = Q_0 \cdot e^{-\alpha(t-t_0)} \qquad 3.3$$

Where:

$t$ – time [$T$]
$t_0$ – time representing the start of the aquifer water discharge [$T$]
$Q_0$ – spring discharge at instant $t_0$ [$L^3 \cdot T^{-1}$]
$Q_t$ – spring discharge at instant t [$L^3 \cdot T^{-1}$]
$e$ – base of natural logarithms
$\alpha$ - discharge coefficient [$T^{-1}$]

The coefficient $\alpha$ represents the rates of release of water and can be related to the hydraulic parameters of the aquifer. If the value of the discharge coefficient decreases the underground retardation increases (the recession curve has a low slope). When $\alpha$ is larger, the recession curve is steeper and the underground has a poor retardation capability.

The recession curves observed in karst aquifers are often characterised by several straight lines with different slopes, when the logarithm of discharge is represented as function of time. Each of these straight lines is therefore characterised by a different discharge coefficient. According to the relation between the $\alpha$ values and the hydraulic properties of the karst aquifers structure, a physical explanation for the values of the discharge coefficient $\alpha$ of the Maillet is generally accepted: The higher values, for example, of the order $10^{-2}$ indicate rapid drainage of karst channels. The milder and lower slopes of the recession curve ($\alpha$ of the order $10^{-3}$) represent slow drainage of micro fissures and small voids, representing the aquifer matrix porosity (Kresic, 1997). In that case the Maillet equation takes the form:

$$Q_t = \sum_{i=1}^{n} Q_{0_i} \cdot e^{-\alpha_i(\Delta t)} \qquad 3.4$$

In this case the recession period is characterised by the existence of $n$ different periods with constant slope, each of them corresponding to a $\Delta t$ period during the recession period. According to that interpretation the definition of the best-fit coefficients of an exponential function characterise different phases of the recession period of the hydrograph. Each of these coefficients is regarded as representing successive phases of emptying of different components of the aquifer between the high permeability dissolution channels and the low permeability rock volumes.

Using decimal logarithms and rearranging equation 3.3 the Maillet model takes the form:

$$\alpha = \frac{\log Q_0 - \log Q_t}{0.4343 \cdot \Delta t} \qquad 3.5$$

Using 3.5 the best-fit values of $\alpha$ for the successive phases of the recession period of the hydrograph can be easily determined using graphical methods.

It must be remarked that the interpretation of the successive values of $\alpha$ as representing the emptying of successive parts of the aquifer is not universally accepted. Another current interpretation of the different slopes is the presence of turbulent flow in conduits. Regarding the interpretation of the different periods of the recession period Kiraly (1976) showed that it is possible to produce a spring hydrograph with three recession coefficients by using a numerical discrete continuum model, where only two different sets of parameters are present. On the other hand, as the applied model simulations are entirely performed in laminar flow conditions the quoted author showed that the hypothesis based on the effects of the presence of turbulent flow are not necessarily valid. More recently the systematic test of different theoretical karst aquifers, using the same approach and testing other schemes for the analysis of the global responses of karst aquifers confirmed these conclusions (Eisenlohr *et al.* 1997a; 1997b).

Despite the controversial interpretations for the existence of different slopes in the recession period of hydrographs in karst springs, further developments of the Maillet equation are often applied in order to calculate hydraulic parameters of karst aquifers. Examples of the use of such techniques are provided in Milanovic (1981), or more recently in Baedke and Krothe (2001).

Another use of the Maillet equation in applied hydrogeology of karst aquifers is related to the quantification of the relative importance of concentrated rapid infiltration and diffuse slow infiltration. Accepting that the different origins of water can be distinguished by the separation of the recession period of the hydrograph, it is possible to estimate the water volumes previously stored in dissolution channels and in the low permeability rock volumes. The interpretation of these values simultaneously with the total volume of recharge (estimated, for example, by the methods presented throughout section 3.4.3) can be used to calculate the proportion of concentrated and diffuse infiltration. It must be remarked that despite the insight that such an approach provides the relative importance of concentrated and diffuse recharge in karst aquifers some limits must be defined for the reliability of the method. As suggested by Kiraly *et al*. (1995), during the periods of rapid concentrated infiltration the inversion of gradients between conduits and rock matrix induce water transference from the dissolution channels toward the low permeability rock volumes and thus the occurrence of negative values of base flow. Therefore, the volume of rapid recharge into the dissolution channels (epiflow) may be much greater than the spring discharge. The occurrence of such conditions will be responsible for an overestimation of the diffuse recharge because some of the rapid concentrated infiltration will feed the low permeability rock volumes and thus incorporate the fraction of the water volume computed as originated from diffuse infiltration.

The aspects presented in the above paragraphs are only few cases, among many others where the methods based on global responses provide contradictory inferences about the hydraulic behaviour of karst aquifers. An extensive analysis of the potential and limits of several methods based on the interpretation of "global responses" of karst aquifers is provided in Kiraly and Morel (1976b), Eisenlohr *et al*. (1997a) and Eisenlohr *et al.* (1997b). These works are based on the analysis of the global responses of simplified theoretical karst aquifers. Using that approach the verification of the inferences provided by the global responses can be compared with the characteristics of the model and thus it is possible to check the validity of the interpretation schemes.

**3.5.3.2 – Data interpretation**

The data collected during the present work consists of time-discharge series collected for five springs draining both the carbonate rocks and the lithologies surrounding the aquifer. The measures were taken between October 1996 and February of 1999 for springs with inventory numbers 5, 6, 59 and 39. For spring 51 and 58 the available data corresponds, respectively, to the period between April 97 - February 99 and June 84 - April 86. The data set for spring 58 consists of a historical registry corresponding to sporadic measurements of discharge collected by the Environmental Agency of Alentejo Region. All the other measures were collected weekly.

The springs 51 and 39 drain, respectively, the low permeability lithologies in contact with the NW limit of the carbonate aquifer and the deposits covering the "impermeable" lithologies surrounding the aquifer in most of its extension. All the other springs drain the carbonate aquifer. The positions of the springs are presented in figure 3.22.

As noted previously the main discharge area of the aquifer corresponds to the Sever River. The springs with inventory numbers 5, 6 and 59 are secondary points of discharge in the NW area of the carbonate rocks. The discharge in these springs is conditioned by threshold values for the capacity of the neighbour, relatively low permeable lithologies to assimilate the outflow from the carbonate aquifer. The altitude of these three springs can be observed in the cross-section presented in figure 3.23 This figure shows that, on the contrary of the more usual morphologic conditions, the altitude of the carbonate rocks is higher in that area than the surrounding lithologies.

The spring with the inventory number 58, located about 150m to E of the Sever River, is also temporary and rarely active. This spring is an exception for the more general outflow pattern from the aquifer, which occurs mainly throughout the riverbed. When the transference from the aquifer to the river attains its highest values that spring is sometimes activated. However, even in this case, the flow from the spring is discharged to the Sever River and its discharge can be computed in the total water transference from the aquifer to the river.

All the springs are temporary and the discharges are always lower than 3 l/s except for spring 58, which is also temporary. Thus, the total outflow volume in these springs, except for spring 58, is negligible when compared with the volume of the total water balance. Actually spring 58 is only active in response to the more important recharge episodes. However, the historic data set shows that the maximum discharge measured is 220 l/s. Global values of discharge in the main outflow area of the aquifer are not quantified. However, the existence of short periods with high contrasts in discharge values, observable in spring 58, show that the typical behaviour of karst aquifers must be present in the outflow pattern of the aquifer. Unfortunately the discharge of spring 58 are strongly affected by the pumping wells 49 and 81 which are submitted to intense pumping for water supply of the Portalegre town located about 20Km to the south of the aquifer. The same problem exists for spring 5, which is affected by pumping in well 84.

The hydrographs of the springs are shown in Figures 3.24 and 3.25. In order to illustrate the relationship between precipitation and spring discharge figure 3.24 shows also the daily precipitation values determined in the Escusa precipitation gauge.

According to the data collection periodicity the only approach possible to quantitatively interpret the spring hydrographs is the analysis of recession periods. On the other hand, in the described conditions, the analysis of spring hydrographs cannot be identified as a global response of the aquifer. As referred before, the quantification of aquifer discharge can be done only by collecting data for the Sever River discharge in two points located immediately upstream and downstream of the limits of the carbonate formation. The difference between both values can be used to characterise the carbonate aquifer by means of methods based on “global response” analysis. However, even if these datasets are made available the “global response” obtained in this way will reflect (according to the more optimistic expectations) two of the three aquifer sectors: the Escusa and Porto Espada sectors, which share Sever River as discharge area (Castelo de Vide is drained by a different discharge area). In a more pessimistic scenario, the use of water transference from the aquifer toward Sever River will be useful only to characterise parts of the Escusa and P. Espada sectors, because the part of the aquifer conduit network present in these sectors seems to be characterised by different degrees of connectivity with the river. The aspects related to the identification of the connectivity degree of different sectors of the conduit network with the aquifer discharge areas will be discussed in chapter 6 and is one of the central aspects discussed in this work.

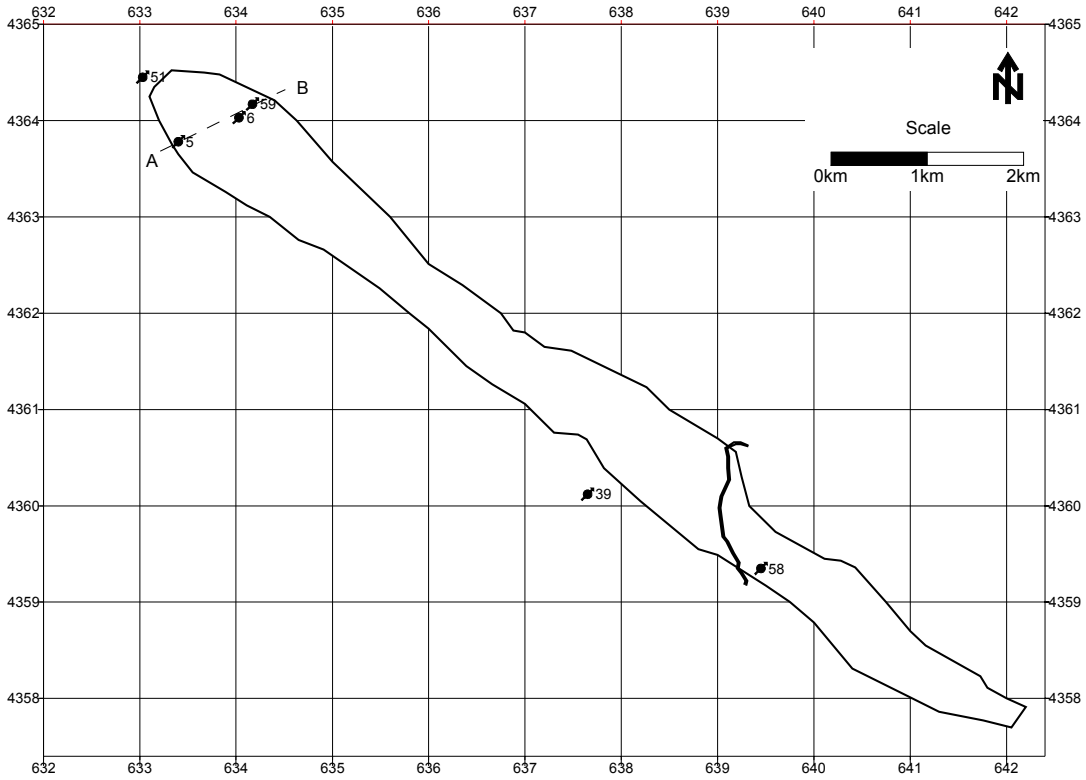


Fig. 3.22 – Location of springs with data registries.

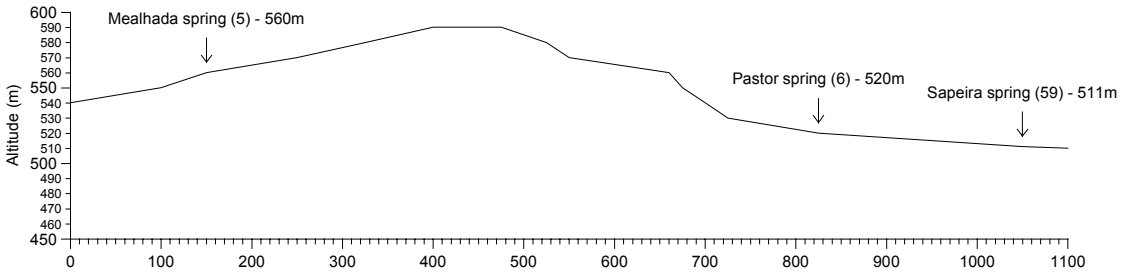


Fig. 3.23 – Cross-section showing the altitude distribution along a line through springs 5, 6 and 59. On the contrary of the usual morphologic conditions, in that area the carbonate rocks are present on higher altitudes than the adjacent lithologies. The position of the profile between points A and B is shown in figure 3.22.

Considering the limits of the presently available data it is interesting to compare the hydraulic behaviour of the secondary points of discharge draining the carbonate rocks with other temporary springs occurring in the vicinity of the aquifer draining other lithologies. As the climatic conditions are the same it is useful to analyse to what extent the transformation of water inputs, in the different spring's drainage area can be distinguished in the point of discharge depending on the type of lithologies where groundwater flows.

The recession hydrograph analysis for springs 6, 39, 51 and 59, using the Maillet equation is presented in figure 3.26. As the spring 5 is affected by the pumping well with the inventory number 84, the interpretation of recession periods is not possible. As remarked before, the same problem exists for spring 58, which is affected by pumping wells 49 and 81. In that case the discharge values were measured only sporadically and the recession analysis is also impossible. For these springs only a qualitative interpretation can be done.

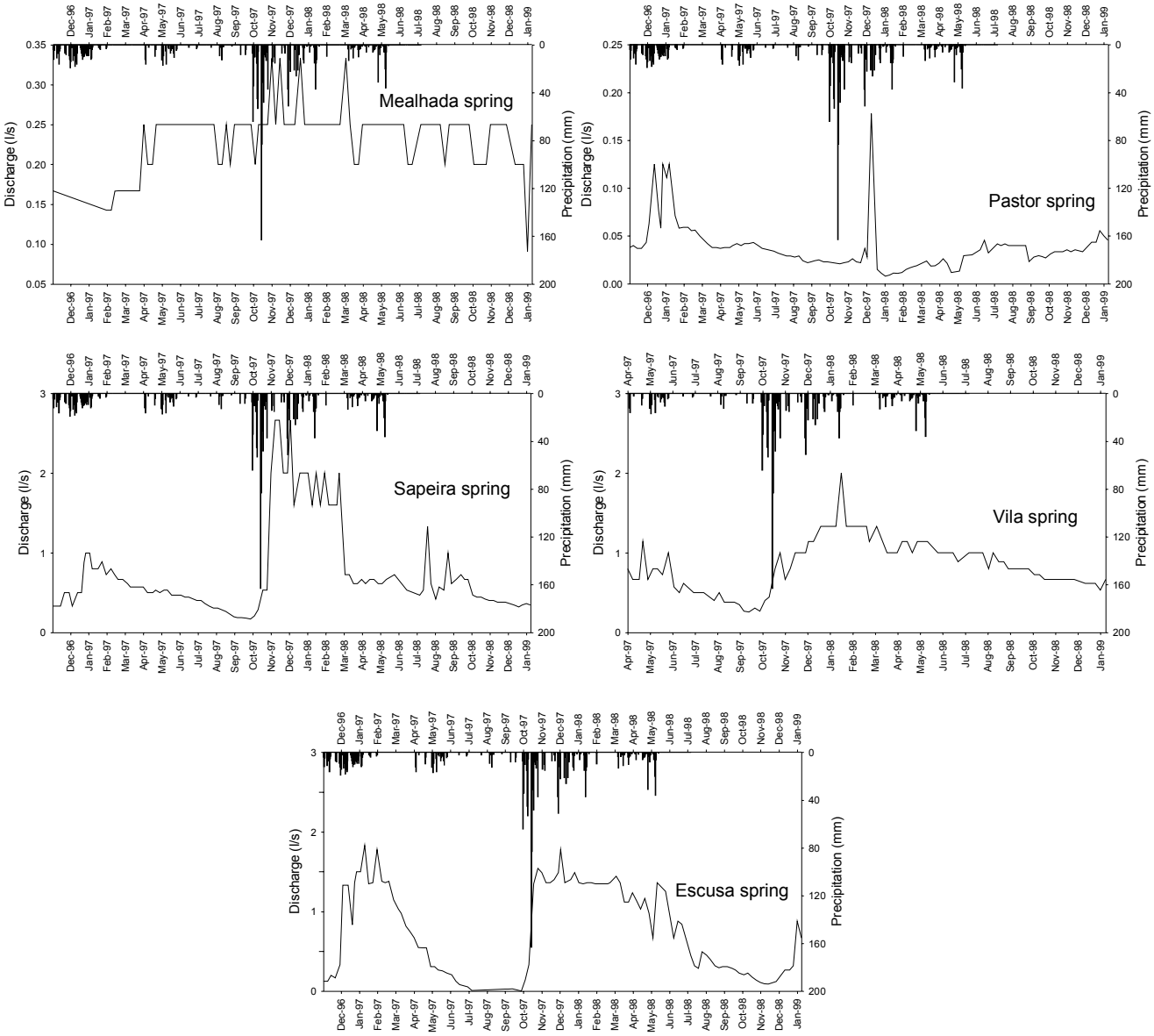


Fig. 3.24 – Discharge plotted as function of time for springs 5 (Mealhada), 6 (Pastor), 39 (Escusa), 51 (Vila) and 59 (Sapeira). The precipitation values of the Escusa precipitation gauge are also shown.

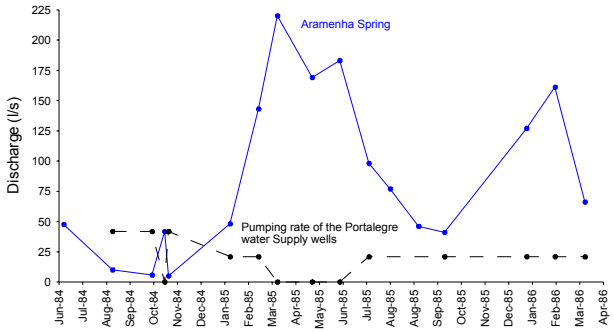


Fig. 3.25 – Discharge of springs 58 (Aramenha) and pumping rate of the Portalegre water supply wells plotted as function of time. As can be seen the pumping rate affects the spring discharge.

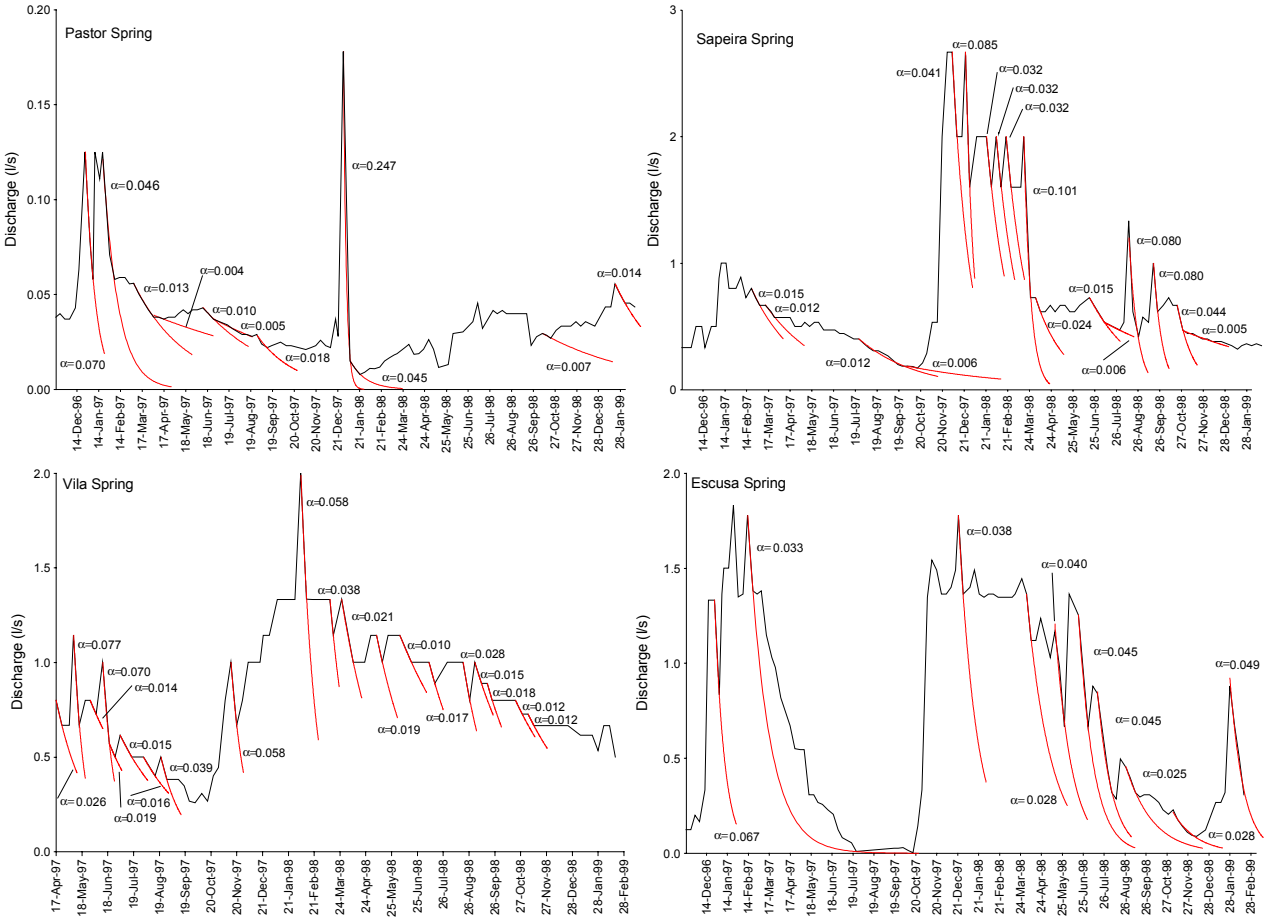


Fig. 3.26 – Discharge plotted as function of time for springs 6 (Pastor), 39 (Escusa), 51 (Vila) and 59 (Sapeira) and fit of different emptying periods of the aquifer with $\alpha$ values obtained using the Maillet exponential equation. Note that the two springs on top drain the carbonate aquifer and the lower two drain other units.

The results of the recession coefficients $\alpha$ for springs 6 and 59 are summarised in tables 3.10 and 3.11. These tables are not exhaustive in terms of representation of all the values calculated for recession coefficients shown in figure 3.26. In fact the tabulated values correspond only to situations in which the recession period allowed the detection of $\alpha$ values corresponding to different slopes during the emptying of the aquifer.

| Model Characteristics | Period 20/1 -17/4/97 | Period 12/6 -21/8/97 | Period 9/12 -12/9/97 |
|---|---|---|---|
| $Q_1$ (l/s) | 0.125 | - | 0.178 |
| $Q_2$ (l/s) | 0.056 | 0.043 | 0.015 |
| $Q_3$ (l/s) | 0.037 | 0.037 | - |
| $\alpha_1$ ($s^{-1}$) | 0.046 | - | 0.247 |
| $\alpha_2$ ($s^{-1}$) | 0.013 | 0.010 | 0.05 |
| $\alpha_3$ ($s^{-1}$) | 0.004 | 0.005 | - |

Table 3.10 – Recession coefficients α adapted to different periods of recession in Pastor Spring (6)

| Model Characteristics | Period 24/7 -14/8/97 | Period 16/3 -9/4/98 | Period 18/6 -31/7/98 | Period 15/10 -10/12/98 |
|---|---|---|---|---|
| $Q_1$ (l/s) | 0.400 | 2.000 | 0.727 | 0.667 |
| $Q_2$ (l/s) | 0.186 | 0.727 | 0.533 | 0.471 |
| $\alpha_1$ ($s^{-1}$) | 0.012 | 0.101 | 0.015 | 0.044 |
| $\alpha_2$ ($s^{-1}$) | 0.006 | 0.024 | 0.006 | 0.005 |

Table 3.11 – Recession coefficients α adapted to different periods of recession in Sapeira spring (59)

The results obtained for the recession coefficients found in springs draining the carbonate aquifer and adjacent lithologies allow the analysis of some interesting aspects as follows:

- None of the Vila or Escusa springs, which drain the lithologies surrounding the Castelo de Vide carbonate aquifer show any trend to present a decrease of slope in any of the registered recession periods (even during the longer periods without precipitation). In both cases the recession values are always comprised in the same order of magnitude. The determined values are always in the interval [$1.5\times10^{-2} \leq \alpha \leq 7.7\times10^{-2}$];

- The springs draining the carbonate rocks show successive periods of emptying characterised by a decrease of the recession coefficient $\alpha$. This is expected in carbonate aquifers but cannot be assigned to the emptying of different parts of the aquifer with different hydraulic properties. In fact the Pastor spring (inventory point number 6), which discharge is the lowest among all the present springs is the one where different recession coefficients are more distinguishable (the highest discharge ever registered in that spring is 0.178 l/s). In such conditions it cannot be expected that such hydraulic behaviour is derived from the emptying of parts of the aquifer characterised by hydraulic parameters differing by many orders of magnitude. On the other hand, taking into account the very low discharge values, it is also difficult to conceive that the observed behaviour of that spring should be explained by the existence of turbulent flow. It must be remarked that $\alpha$ values determined in the Pastor spring lie within three orders of magnitude. The registered values in that spring are comprised in the interval [$4.0\times10^{-3} \leq \alpha \leq 2.5\times10^{-1}$]. It is also interesting to remark that, as will be shown in Section 4.3, the Pastor spring is the only point of the aquifer where chemical equilibrium with respect to calcite and dolomite dissolution is present (in all the other points water is undersaturated with respect to these minerals). This is another reason to think that spring drains only the low permeability rock volumes.

- The Sapeira spring drains also the carbonate rocks and presents recession periods characterised by exponential curves with decreasing slopes. As in the Pastor Spring the $\alpha$ values vary within three orders of magnitude. However that kind of behaviour is less marked than in the case of the Pastor spring. On the other hand, the maximum values of discharge for that spring are higher and attain a maximum value of 2.67 l/s. In that case the interval of variation of the recession coefficient $\alpha$ is [$5.0\times10^{-3} \leq \alpha \leq 1.0\times10^{-1}$].

**3.5.3.3 – Comments on the interpretation of spring hydrographs as a tool to identify the hydraulic behaviour of karst aquifers**

The identification of the typical behaviour usually defined as resulting from the "global responses" of karst aquifers in secondary springs draining small areas of the aquifer under study seems to confirm the contradictions associated with the use of such methods as foreseen by Kiraly and Morel (1976b). Some of these contradictions were briefly discussed at the beginning of the section 3.5.3.1. As remarked before the available experimental results for the present study are very scarce. However the climatic conditions make the analysis of long recession periods possible. Therefore, it seems that the general conclusions drawn from the emptying of the aquifer are reliable.

It must be remarked that it is technically possible to use further developments of the Maillet equation in order to obtain information about hydraulic parameters and water budget in karst aquifers. Some examples are the methods applied in Kresic (1997), Jeannin and Grasso (1997), Milanovic (1991) and Baedke and Krothe (2001) to accomplish tasks as calculate the proportions of diffuse and concentrated discharge and determine values for transmissivity and specific yield. However, as shown by the present experimental results the risks in adopting the usually accepted interpretation for the presence of different slopes in recession periods can be very important.

In the actual case study the observed transformation of water input in the spring discharge draining the carbonate aquifer reflect the complexity of the transient flow processes resulting from the coexistence of diffuse and conduit flow overlapped in a very complex pattern. These processes are not necessarily related to particular conditions conditioning the existence of large karst springs. Therefore, the establishment of cause effect relations between the aquifer structure at regional scale (or the determination of the proportion of diffuse and concentrated infiltration) by the interpretation of hydrographs of large springs seems to be impossible.

As remarked before in this section, the definitions of karst aquifer available in the literature are always dependent on the presence of "karst springs" which hydraulic behaviour characterise the global response of the aquifer. However, facing the interpretation of the experimental results discussed above it seems that such definitions are not general enough to include all the situations where the difficulties inherent to the interpretation of groundwater flow problems in the aquifers defined as "karstic aquifers" are present. One of the unfortunate consequences of this is the fact that many times the "global responses" are used to detect the "karstic" or "non karstic" character of particular aquifers. Such classification is applied, for example, to decide if a regional flow model for a carbonate aquifer can be well characterised as a single continuum equivalent media. In the present case study, for example the absence of an evident "global response" typical of karst aquifers could encourage the use of such models in order to simulate flow at regional

scale. However, it will be shown later in this work that such a decision can only provide very limited previsions of the aquifer hydraulic behaviour.

The absence of well defined concentrated discharge areas easily identifiable (as karst springs) makes difficult the identification of the particular problems encountered in characterising aquifers where diffuse flow is present but the regional flow pattern is controlled by the presence of dissolution channels. Therefore, the use of methodologies based on the "global response" methods, which depend on the existence of particular boundary conditions (related to the existence of well-defined karst springs), need to be substituted by methods allowing the identification of the dichotomy of the recharge and flow processes.

In our opinion instead of focusing on the usual features characterising karst aquifers, based on the identification of hydraulic responses associated to particular boundary conditions (the existence of a karst spring) a more general definition should be used in order to encompass more general situations. Taking into account the fact that the essential flow processes acting in karst aquifers are present in the present case study (duality of the infiltration processes, duality of the groundwater flow field and duality of the discharge conditions), simultaneously with the absence of a well identified global response (due the inexistence of boundary conditions leading to the existence of a karst spring) a more general definition is required in order to characterize the Castelo de Vide carbonate aquifer as a karst aquifer. Such a definition could be based in the existence of a fractured porous media where flow at the regional (or even aquifer) scale is controlled by a dissolution conduit network leading to the presence of diffuse and concentrated infiltration, low flow velocities in the fractured volumes and high flow velocities in a conduit network. In fact the current definition of karst aquifers is based in the variability of state variables (global responses) and particular boundary conditions (leading to the existence of springs draining the entire flow domain), instead to be based in the intrinsic hydraulic properties, which are in the basis of the presence of those characteristics in some carbonate aquifers.

# Chapter 4

CONCEPTUAL FLOW MODEL AND ESTIMATION OF EQUIVALENT HYDRAULIC CONDUCTIVITY AT THE AQUIFER SCALE

---

Contents



# Chapter 4

---

There are very few physical parameters that take on values over 13 orders of magnitude. In practical terms, this property implies that an order-of-magnitude knowledge of hydraulic conductivity can be very useful. Conversely, the third decimal place in a reported conductivity value probably has little significance.

*Freeze & Cherry (1979)*

## 4.1 – Introduction

In the previous Chapter a global characterisation of the aquifer was presented. The aspects discussed regard the definition of the system geometry, water balance and boundary conditions. These aspects are necessary but not sufficient to compile all the information needed to build a groundwater flow model with quantitative predictive capabilities of the state variables, because hydraulic parameters, characterising the entire flow domain, must also be defined in order to accomplish the quantitative characterisation of the aquifer.

The expression "conceptual flow model" lacks a precise sense. Different authors provide different kinds of information when characterising a conceptual flow model conceived to solve a particular problem. For example, Mercer and Faust (1980) consider that the definition of a conceptual model is the first step in developing a groundwater flow model and consists of determining cause-effect relationships that express how the system operates. As the determination of point values of hydraulic parameters using pumping tests will be treated later in Chapter 5, it can be argued that it is not yet possible to propose a "complete conceptual flow model", which must include also a first guess for parameters. However the information presented up to now about the aquifer expressed in a "synthetic conceptual flow model" allows the definition of a problem, which unknown variable is the equivalent hydraulic conductivity characterising the steady state description of the system at regional scale. The formulation of this problem will be done with based on the interpretation of the transversal cross-section in figure 4.1 representing aquifer hydraulic behaviour.

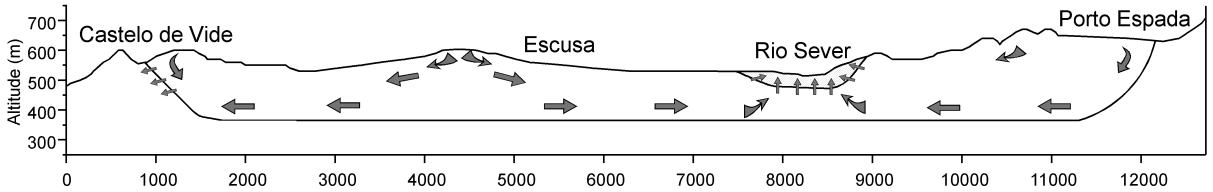


Fig. 4.1 – Schematic cross-section showing the predominant flow directions and discharge areas of the Castelo de Vide carbonate aquifer. The distances along the axis are given in meters. The biggest arrows represent the predominant flow directions. The small arrows, crossing the aquifer boundaries represent the position of discharge areas.

The three sectors as well as the discharge areas identified in section 3.5.2.1 are represented in figure 4.1. In the Castelo de Vide and the Escusa sectors, respectively, flow diverges from the groundwater divides located near Escusa toward Castelo de Vide and toward the Sever River (Rio Sever). In the P. Espada sector the predominant flow is toward the Sever River. Therefore, the flow from the P. Espada and Escusa sectors contributes to the major discharge area of the aquifer, which is throughout the riverbed. Near Castelo de Vide discharge is towards the low permeability lithologies in contact with the carbonate aquifer in that area. The remaining area of contact of the aquifer with adjacent lithologies is done with "impermeable" series and thus no more outflow areas are considered.

The analysis of the defined conceptual flow model shows that the existence of the Escusa and P. Espada sectors is independent of hydraulic conductivity values. According to the altitude of the recharge areas, the position of the river and the absence of other discharge areas in these sectors no other general flow pattern can be conceived if hydraulic conductivity is considered as homogeneous. On the other hand, the groundwater divides boundary between the Castelo de Vide and Escusa sectors depends not only on the boundary conditions but also on the hydraulic conductivity and recharge values. This is because according the variation of these values the groundwater divides will be displaced toward the area of the river or toward the area of Castelo de Vide. At the beginning of the present work, different origins for the existence of the boundary between the Escusa and Castelo de Vide Sectors were analysed. The more obvious explanations to the presence of that boundary where the presence of some hydraulic barrier or the presence of an area of the aquifer with a thickness inferior to the adjacent sectors. As no observation points were previously available in that area two wells were drilled in order to clarify the nature of this boundary. The characteristics of these wells showed that any of these features is apparently in the origin of the presence of that boundary (see Figure 3.13 in section 3.5.2). Therefore, the analysis of the problem was shifted to the analysis of the flow pattern in the aquifer at regional scale.

The average annual recharge for aquifer long-term water balance is known with a reasonable precision and is about 450mm/year (section 3.4.4). As shown in section 3.5.2.2, the position of the groundwater divides lies somewhere between the wells with the inventory numbers 14 and 17. Considering that hydraulic head values in the discharge areas are also well-known, the conceptual flow model can be expressed in terms of a steady state flow problem, for which only one unknown variable exists: the hydraulic conductivity.

The problem formulated in the last paragraph can be solved using a numerical flow model. The solution provides a homogeneous equivalent hydraulic conductivity value allowing a steady state characterisation of the flow domain at

regional scale, accommodating the long-term mass balance of the aquifer and, simultaneously, the presence of the identified sectors expressed in the conceptual flow model presented in figure 4.1.

### 4.2 – Calculation of equivalent hydraulic conductivity as unknown variable of a boundary-value problem

As referred in section 2.4 there are 5 types aspects evolved in a hydrogeologic boundary-value problem (Freeze and Cherry, 1979): (1) the size and shape of the region of flow, (2) the equation of flow within the region, (3) the boundary conditions around the region, (4) the initial conditions of the region, (5) the spatial distribution of the hydrogeologic parameters that control the flow, and (6) a mathematical method of solution. If the boundary value problem is for a steady-state system, requirement (4) is removed.

As showed in last Chapter a detailed characterisation of the aquifer regarding these aspects is available, except for the distribution of parameters. In these conditions, taking into account the characteristics of the proposed conceptual flow model, the partial differential equation controlling groundwater flow (equation 2.6 in Chapter 2) can be solved with hydraulic conductivity as unknown variable (Monteiro, 2001).

#### 4.2.1 – Numerical solution

The solution of this problem was found using a cross-sectional steady state numerical flow model, which aggregate the knowledge about the aquifer regarding the system geometry, spatial piezometric patterns and definition of discharge areas. The steps needed to build the numerical model as well as its analogies with the conceptual flow model and the obtained results are summarised in figure 4.2.

The first step in building the numerical model was the definition of the geometry of the flow domain. As the aquifer is limited in near all its extension by "impermeable lithologies" the lower and lateral limits are represented by horizontal and vertical no-flow boundaries. The only exception corresponds of the top 50m of the vertical line representing the aquifer boundary near Castelo de Vide corresponding to the secondary outflow area of the aquifer. The dimension of these boundaries corresponds to the aquifer thickness (which is about 200m). Considering that the distance between the ground surface and water level in the aquifer is always very short (less than 25m) the top of the aquifer was defined by a profile corresponding to the shape of the ground surface slightly smoothed.

Figure 4.2 shows also a finite element mesh generated with basis in the defined geometry. At a first glance the discretisation of that mesh with 5887 nodes and 3099 quadratic triangular elements seems excessive for a so simple problem. However the short vertical dimension of the model with respect to the horizontal one and the reproduction of the ground surface shape difficult the generation of a coarser mesh. In fact the number of nodes in a vertical of the aquifer rarely exceed 18 nodes.

The calibration of the equivalent hydraulic conductivity was done starting by the definition of the boundary conditions with basis in the knowledge about the spatial pattern and temporal variability of hydraulic head in the aquifer. In practice this corresponds to the average altitude of the discharge areas of the aquifer, which are very close (515.0m for the Sever River and 515.5m for the contact of the Castelo de Vide area of the aquifer with the adjacent lithologies). The physical meaning of these values is less straightforward in the case of the Castelo de Vide discharge area than in the river region. This is because it is not possible to define in a precise way the geometry of the discharge area present in the hidden surface constituting the contact between the carbonate rocks and adjacent lithologies in Castelo de Vide region. As can be seen the in figure 3.15 (section 3.5.2.2) hydraulic head values in the aquifer near its limits in the Castelo de Vide area vary between 507m and 523m. The essential question arising about the characteristics of that discharge area is the impossibility in defining to what deep the water is transferred, from the aquifer to the adjacent fractured rocks. In the defined model it was considered that the discharge area is between the ground surface and 50m beneath the ground level.

The simulated water balance is controlled by a uniformly distributed 450mm/year recharge at top of the aquifer corresponding to the average infiltration estimated in section 3.4.5 with basis in the long-term water balance. After this the hydraulic conductivity was successively changed until the position of the groundwater divides, limiting the Castelo de Vide and Escusa sectors, occupies its correct position, which was previously known with basis in the piezometric observations. The value of hydraulic conductivity allowing the placement of the groundwater divides in the position showed in figure 4.2 is of $7.0\times10^{-4}$m/s. Using that value the discharge toward Sever River is about 3 times highest than the discharge in the Castelo de Vide area toward the adjacent lithologies.

After the described calibration the recharge values were changed between 100mm/year and 900mm/year values. This was done in order to check if the estimated maxim and minimum values of recharge for the long-term water balance are compatible with the observed position of the groundwater divides. In all the cases the limit between the Castelo de Vide and Escusa sectors is located between wells 14 and 17, there is, between the limits of its "real position" determined with basis in the available values of hydraulic head.

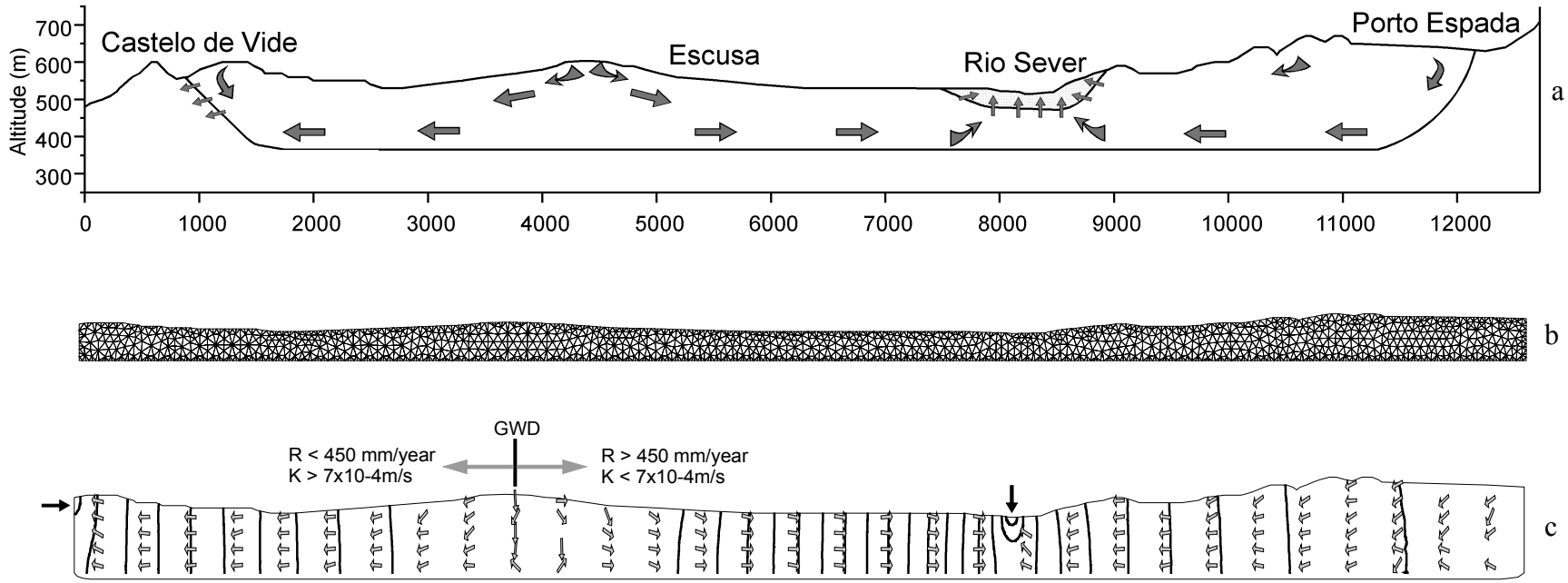


Fig. 4.2 - Calculation of equivalent hydraulic conductivity as unknown variable of a boundary value problem using a cross sectional steady state finite element flow model. The qualitative scheme at the top (a) represents the conceptual flow model defined based on geomorphology, spatial and temporal piezometric patterns and location of discharge areas. The finite element mesh (b) was generated based on the geometry of the conceptual flow model considering that the average thickness of the aquifer is about 200m. As the distance between the ground surface and water table in the aquifer is always very small (less than 25m) the top of the aquifer is represented by the geometry of the ground, just slightly smoothed. The lateral limits and the bottom of the aquifer are no-flow boundaries except for the top 50m of the vertical line representing the aquifer boundary near Castelo de Vide, which corresponds to the secondary outflow area of the aquifer. The mesh has the same vertical and horizontal scales and has 5887 nodes defining 3099 triangular quadratic elements. The cross-section (c) at the bottom of the figure has a two times vertical exageration and represents the computed solution. The simulation represents a 450mm/year homogeneous recharge at the top of the aquifer, which corresponds to the average infiltration estimated in section 3.4.5 for the aquifer with basis in the long-term water balance. The discharge areas of the aquifer were simulated by specified values of head. The black arrows pointing to the aquifer limits show the localisation of the discharge areas where the head values were specified. The line GWD represents the groundwater divides, which is the moving boundary between the C. Vide and Escusa sectors. As shown by the equipotentials (equidistance is 0.07m) and flux vectors, the GWD is in the position defined in the conceptual flow model based on the spatial and temporal distribution of hydraulic heads. That position of the GWD is obtained when a homogeneous value of $7.0\times10^{-4}$m/s is defined over the entire flow domain. The arrows starting at the horizontal line positioned above the GWD represent the displacement of the boundary between Castelo de Vide and Escusa sectors, according the change of recharge (R) and hydraulic conductivity (K) values.

### 4.2.2 – Analytical solution

The solution of the problem summarised in figure 4.2 can be also approached using the Dupuit-Forcheimer theory describing flow in an unconfined system bounded by a free surface. The use of this solution evolves two assumptions: (1) flowlines are assumed to be horizontal and equipotentials vertical and (2) the hydraulic gradient is assumed to be equal to the slope of the free surface and to be invariant with depth. In addition to these conditions it is considered that the free surface is in equilibrium with an uniform recharge value. The analytical solution for this classical problem is:

$$h(x) = \sqrt{h_0^2 + \frac{i}{K}(L^2 - x^2)} \qquad 3.6$$

Where $h_0$ is the outflow boundary, $h$(x) is the elevation of the free surface above the base of the flow system at a given distance from the outflow boundary, $k$ is hydraulic conductivity and $i$ is the value of an uniform infiltration feeding the system. These variables are identified in figure 4.3.

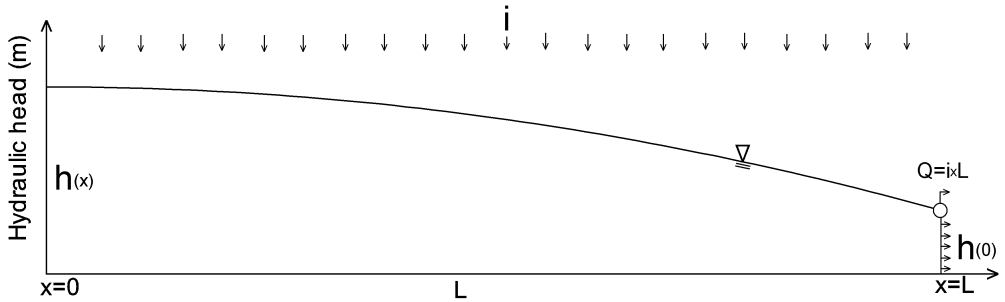


Fig. 4.3 – Diagram representing the variables evolved in the analytical solution defined in equation 3.6. Adapted from Perrochet (2000).

Considering the geometry of the system presented in figure 4.1 and the same data allowing the definition of the numerical solution presented in the previous section, it is possible to formulate a problem for each individual sector of the aquifer where hydraulic conductivity is the unknown variable. The obtained values of K are expressed in table 4.1.

| Aquifer sector | Hydraulic conductivity $k$ (m/s) |
|---|---|
| Castelo de Vide | $2.1\times10^{-4}$ |
| Escusa | $1.5\times10^{-4}$ |
| P. Espada | $2.9\times10^{-4}$ |

Table 4.1 – Hydraulic conductivity values calculated for the aquifer sectors using equation 3.6.

As can be seen in table 4.1 the calculated values are very similar to the value characterising the entire aquifer obtained using the cross sectional numerical model. In this case the calculated hydraulic conductivity was $7.0\times10^{-4}$m/s.

### 4.2.3 – Remarks on the obtained results

The hydraulic conductivity values calculated in the two last sections are compatible with a steady state description of the aquifer at regional scale in terms of the existence of the defined sectors and in terms of the long-term water budget. The presented formulation to calculate hydraulic conductivity circumvent the need of knowing values quantifying the outflow volumes in the discharge areas of the aquifer.

The hydraulic conductivity values were calculated by means of two distinct theoretical conceptions for the interpretation of the aquifer hydraulic behaviour. In both cases the known variables were the flow domain geometry and average hydraulic head values in discharge areas. The first solution is based on a numerical flow model where hydraulic conductivity is independent of hydraulic head and thus considering that the aquifer behaves as a confined aquifer. The second, calculated by means of an analytical solution, is based on a description of the aquifer considering the existence of a water table bounded by a free surface, having shape defined by the equilibrium between infiltration and hydraulic parameters characterising each of the aquifer sectors.

The calculated values must be regarded as an equivalent hydraulic conductivity characterising the entire flow domain. A complete equivalence between the real heterogeneous medium and the idealised one is impossible. The relation between the calculated equivalent hydraulic conductivity and the real values of this parameter in the real heterogeneous media is therefore defined, in a limited sense, according to certain criteria that must be equal for both media (Renard and de Marsily, 1996). In the present case the used criteria is based on flow equivalence and, additionally on the definition of the global flow pattern of the aquifer.

The calculated values of hydraulic head using both methods cannot be used in any other context than the characterisation of the aquifer global steady state flow pattern at regional scale. The description of the aquifer behaviour under specific stress conditions, different from the average recharge values will not be possible without a characterisation of a parameter distribution taking the flow domain heterogeneity into account.

However, the obtained solutions allow the analysis of some crucial basic questions. These questions shall be answered before the decisions needed to build a more sophisticated model allowing the analysis of more complex problems, related to the parameters distribution in a flow domain where transient and diffuse flow are overlapped in a very complex pattern. First of all it is possible to confirm the possible existence of the aquifer sectors proposed for the defined conceptual flow model. These sectors are present in an "artificial flow domain", similar to the real aquifer in terms of geometry, location of discharge areas and average water balance. Moreover, the global flow pattern can be described by different solutions based on a confined or unconfined description of the system.

As the general flow pattern can be described by such an artificial system it can be supposed that the boundary conditions are essentially correct and the reproduction of the observed state variables will be theoretically possible providing that a correct parameter distribution is defined.

In the next chapter point values of hydraulic conductivity will be calculated by the interpretation of pumping tests. As will be shown the employed methods to interpret these tests allow the estimation of hydraulic conductivity values characterising the fractured carbonate rock matrix and the unfractured rock matrix in some cases where wells were drilled without intercepting important fractures. For the dissolution channels present in the carbonated rocks it is only possible to determine orders of magnitude for hydraulic conductivity in a simplified theoretical framework.

As the hydraulic conductivity values depend on the presence of heterogeneities, having a structure varying at different scales it is worth trying to characterise the dependency of the determined values with the scale of flow processes. It is expected that the change in hydraulic parameters varies across different scales depending on the structure of each particular carbonate aquifer system.

The hydraulic conductivity values determined in the last two sections will be compared with values characterising the flow domain at the well scale. Parameters obtained in pumping characterise hydraulic parameters at a scale, which superior and inferior limits correspond roughly to the aquifer thickness and to few meters.

### 4.3 – Indirect role of hydrochemistry in the definition of the conceptual flow model

A brief characterisation of the hydrogeochemical processes identified in the aquifer will be discussed in the present section. The establishment of spatial relations between the identified aquifer sectors and hydrochemical processes can be worth in two senses. Not only the spatial trends of water composition can be better understood based on the interpretation of hydraulic behaviour of the aquifer but also the identification of active hydrochemical processes can help to validate the hydrodynamic conceptual flow model established for the aquifer.

#### 4.3.1 – Available data and predominant processes affecting water composition

Groundwater undergoes geochemical evolution as it moves throughout flow systems. Therefore, it is possible to investigate to what extent the defined aquifer sectors, identified with basis in geomorphology, spatial and temporal piezometric patterns and definition of discharge areas contribute for the distribution of identified hydrochemical trends (Freeze and Cherry, 1979; Appelo and Postma, 1996).

In addition to the data collected regarding the hydraulic characterisation of the aquifer the field surveys conducted during the experimental work included the collection of water samples, which were analysed for the determination of major ions ($HCO_3^-$, $SO_4^{2-}$, $Cl^-$, $NO_3^-$, $Na^+$, $K^+$, $Ca^{2+}$ and $Mg^{2+}$), $SiO_2$ and $CO_2$ concentrations. In some samples $F^-$ concentration was also determined. The calculations of chemical equilibrium evolving values of free ions and complexes concentrations controlling the dissolution of carbonate mineral processes are strongly dependent on the accuracy of pH and temperature measurements. Therefore, at the time of sample collection for chemical analysis in the field some physic and chemical parameters were measured *in situ* (pH, electrical conductivity and temperature). In all the chemical analysis employed for interpretation of water hydrochemistry charge-balance errors are less than 5%.

Values for the $\delta^{18}O$ and $\delta^{2}H$ ratios were also determined for the oxygen and hydrogen environmental stable isotopes in collected samples. The samples for isotopic analysis where collected in July 1995, June 1996, April 1997 and November 1997. The treatment and interpretation of the available hydrochemical and isotopic data is presented in Monteiro and Silva (1994) Monteiro *et al*. (1997) and Silva and Monteiro (1999). Here we present only the aspects allowing the definition of the identified relationships between the aquifer hydraulic behaviour and hydrochemical trends.

The available data corresponds to samples collected in September 1991, April 1992, November 1996 and January 1997, both in drought periods and after recharge events. The oscillations in water composition are dependent of the period of data collection according the evolution of the annual phase of the hydrological cycle. In order to illustrate the range of variation in water chemistry tables 4.2 and 4.3 show some statistical parameters characterising water composition in September 1991, after a emptying period of the aquifer and in January 1997, after a recharge period.

| | T | pH | EC | CO2 | TH | $HCO_3^-$ | $SO4_2^-$ | $Cl^-$ | $NO_3^-$ | $F^-$ | $SiO_2$ | $Na^+$ | $K^+$ | $Ca^{2+}$ | $Mg^{2+}$ |
|---|---|---|---|---|---|---|---|---|---|---|---|---|---|---|---|
| x | 15.9 | 7.30 | 300 | 13.4 | 156.5 | 156.7 | 4.4 | 13.9 | 30.5 | - | 8.8 | 5.5 | 0.9 | 34.0 | 17.7 |
| Md | 15.3 | 7.30 | 279 | 10.8 | 146 | 148 | 3.1 | 14.2 | 31.0 | - | 8.2 | 5.3 | 0.9 | 31.2 | 17.5 |
| σ | 1.95 | 0.33 | 106.15 | 6.94 | 66.86 | 74.29 | 4.4 | 2.92 | 8.91 | - | 5.3 | 1.7 | 0.5 | 11.6 | 9.8 |
| σ/x | 12.3 | 4.50 | 35.4 | 52.0 | 42.7 | 47.4 | 101.2 | 21.0 | 29.2 | - | 60.8 | 31.3 | 53.9 | 34.2 | 56.0 |
| M | 21.8 | 7.73 | 560 | 28.4 | 330 | 356 | 19.7 | 20.6 | 45.9 | - | 28.2 | 10.2 | 1.9 | 64.8 | 40.8 |
| M | 13.2 | 6.57 | 161 | 6.6 | 68 | 49.0 | 0.4 | 9.9 | 9.3 | - | 2.9 | 3.0 | 0.3 | 16.0 | 3.9 |

Table 4.2 - Statistic parameters obtained from the hydrochemical data collected in September 23, 1991. T - temperature (ºC), EC - electrical conductivity (µS/cm), TH - total hardness (ppm of $CO_3Ca$), ions – ppm. x – mean, Md - median, σ - standard deviation, σ/x – variance (%), M – maxim m – minim. Total number of samples is 22.

| | T | pH | EC | $CO_2$ | TH | $HCO_3^-$ | $SO4_2^-$ | $Cl^-$ | $NO_3^-$ | $F^-$ | $SiO_2$ | $Na^+$ | $K^+$ | $Ca^{2+}$ | $Mg^{2+}$ |
|---|---|---|---|---|---|---|---|---|---|---|---|---|---|---|---|
| $\bar{x}$ | 13.7 | 6.76 | 296.6 | 17.6 | 173.8 | 146.9 | 6.8 | 11.4 | 14.0 | 0.35 | 6.1 | 5.69 | 1.2 | 32.4 | 22.6 |
| Md | 13.7 | 6.80 | 299.0 | 16.4 | 162.0 | 132.4 | 5.66 | 11.1 | 12.3 | 0.22 | 6.3 | 5.05 | 0.8 | 31.2 | 22.2 |
| σ | 1.37 | 0.45 | 115.8 | 11.6 | 74.0 | 88.3 | 4.58 | 3.7 | 8.1 | 0.46 | 2.5 | 2.24 | 1.0 | 15.4 | 93.8 |
| σ/x | 10.0 | 6.66 | 39.1 | 65.6 | 43.2 | 60.1 | 67.2 | 32.6 | 57.5 | 131.9 | 40.4 | 39.4 | 83.6 | 47.5 | 42.9 |
| M | 16.2 | 7.42 | 528.0 | 46.6 | 330.0 | 345.3 | 19.2 | 22.1 | 33.2 | 1.83 | 10.4 | 12.9 | 3.9 | 68.0 | 42.3 |
| m | 11.5 | 5.70 | 119.0 | 3.4 | 76.0 | 19.0 | 0.69 | 5.5 | 1.1 | 0.03 | 2.1 | 3.0 | 0.2 | 4.8 | 9.2 |

Table 4.3 -Statistic parameters obtained from the hydrochemical data obtained in January 26, 1997. T - temperature (ºC), EC - electrical conductivity (µS/cm), TH - total hardness (ppm of $CO_3Ca$), ions – ppm. $\bar{x}$ – mean, Md - median, σ - standard deviation, σ/x – variance (%), M – maxim m – minim. Total number of samples is 25.

After the analysis of samples the obtained data was submitted to aqueous speciation performed using the program HIDSPEC (Carvalho and Almeida 1989). Aqueous speciation evolves the calculations of the mass balance equations, valence states, activity of water, and ionic strength in order to calculate the free-ion and complexes concentrations in aqueous solutions. After the characterisation of the distribution of aqueous species the program HIDSPEC allows also the calculation of the saturation index values for 55 minerals, including Calcite and Dolomite.

The interpretation of the results show that the predominant hydrochemical processes affecting water composition in the carbonate aquifer are the dissolution of carbonates rocks minerals, mainly dolomite and accessory calcite. In all the collected water samples the correlation coefficient between water electrical conductivity and the concentration of the species, which presence is controlled by reactions evolving water and carbonate minerals, is always higher than 0.9. This is verified in all the sampling periods for the concentration of $HCO_3^-$, $Ca^{2+}$ and $Mg^{2+}$ species and hardness. As usual in carbonate aquifers the pH values of the analysed waters are usually between 7 and 8. However, as showed in table 4.3, after recharge periods, pH values are lower. This can be directly related to the increase in $CO_2$ during infiltration.

In addition to the natural phenomena controlling the water quality the agricultural uses of the soil covering the aquifer affect slightly the water quality. As the agricultural irrigation of food crops is not intensive the effects in water chemistry are not enough to compromise severely water quality, which still drinkable according the European quality standards.

Tables 4.4 and 4.5 show the coefficient correlation values calculated between the different dissolved species. These values show that the species resulting from carbonate dissolution present high correlation values. At the same time, correlation is also found between $SO_4^{2-}$, $Cl^-$, $NO_3^-$, $Na^+$ and $K^+$ ions. The existence of identifiable correlation between these species is probably related to the slight influence of agriculture in the deposits covering the aquifer in water quality.

| | EC | TH | $HCO_3^-$ | $SO4_2^-$ | $Cl^-$ | $NO_3^-$ | $SiO_2$ | $Na^+$ | $K^+$ | $Ca^{2+}$ | $Mg^{2+}$ |
|---|---|---|---|---|---|---|---|---|---|---|---|
| EC | 1 | | | | | | | | | | |
| TH | 0.9939 | 1 | | | | | | | | | |
| $HCO_3^-$ | 0.9554 | 0.9732 | 1 | | | | | | | | |
| $SO4_2^-$ | -0.0461 | -0.1070 | -0.19 | 1 | | | | | | | |
| $Cl^-$ | 0.1911 | 0.1212 | -0.0739 | 0.4138 | 1 | | | | | | |
| $NO_3^-$ | 0.291 | 0.2801 | 0.2139 | -0.2609 | 0.0459 | 1 | | | | | |
| $SiO_2$ | 0.032 | -0.0047 | 0.078 | -0.1397 | -0.0563 | -0.3542 | 1 | | | | |
| $Na^+$ | 0.092 | 0.0073 | -0.0879 | 0.2651 | 0.6960 | -0.1782 | 0.6191 | 1 | | | |
| $K^+$ | -0.0324 | -0.1098 | -0.2036 | 0.5464 | 0.5353 | -0.0882 | 0.2608 | 0.6149 | 1 | | |
| $Ca^{2+}$ | 0.9482 | 0.9530 | 0.9618 | -0.1040 | 0.0445 | 0.1321 | 0.1781 | 0.0799 | -0.0752 | 1 | |
| $Mg^{2+}$ | 0.9691 | 0.9760 | 0.9252 | -0.1035 | 0.1682 | 0.3705 | -0.1361 | -0.0466 | -0.1293 | 0.8642 | 1 |

Table 4.4 - Correlation matrix calculated from samples collected in September 23, 1991. The correlation coefficients where calculated with basis in variables values expressed in the follow units: EC - electrical conductivity (µS/cm), TH - total hardness (epm of $CO_3Ca$), ions – epm. Total number of samples is 22.

| | EC | TH | $HCO_3^-$ | $SO4_2^-$ | $Cl^-$ | $NO_3^-$ | $F^-$ | $SiO_2$ | $Na^+$ | $K^+$ | $Ca^{2+}$ | $Mg^{2+}$ |
|---|---|---|---|---|---|---|---|---|---|---|---|---|
| EC | 1 | | | | | | | | | | | |
| TH | 0.9702 | 1 | | | | | | | | | | |
| $HCO_3^-$ | 0.9376 | 0.9651 | 1 | | | | | | | | | |
| $SO4_2^-$ | 0.1465 | 0.1068 | -0.0565 | 1 | | | | | | | | |
| $Cl^-$ | 0.1336 | -0.0173 | -0.1437 | 0.5607 | 1 | | | | | | | |
| $NO_3^-$ | -0.0226 | -0.1628 | -0.3192 | 0.6413 | 0.8992 | 1 | | | | | | |
| $F^-$ | -0.3403 | -0.4118 | -0.3565 | -0.2333 | 0.001 | -0.0206 | 1 | | | | | |
| $SiO_2$ | 0.3858 | 0.4113 | 0.3676 | 0.0405 | -0.0383 | -0.0995 | -0.2253 | 1 | | | | |
| $Na^+$ | 0.0781 | -0.0694 | -0.1702 | 0.3066 | 0.8116 | 0.7617 | -0.1504 | -0.2322 | 1 | | | |
| $K^+$ | -0.0152 | -0.1652 | -0.3033 | 0.4888 | 0.6803 | 0.6816 | 0.0719 | -0.016 | 0.6299 | 1 | | |
| $Ca^{2+}$ | 0.947 | 0.9556 | 0.9467 | 0.0359 | -0.0738 | -0.1985 | -0.3491 | 0.3181 | -0.0756 | -0.1574 | 1 | |
| $Mg^{2+}$ | 0.9123 | 0.9595 | 0.9039 | 0.1633 | 0.0373 | -0.1179 | -0.4284 | 0.4663 | -0.0618 | -0.1626 | 0.834 | 1 |

Table 4.5 - Correlation matrix calculated from samples collected in January 26, 1997. The correlation coefficients where calculated with basis in variables values expressed in the follow units: EC - electrical conductivity (µS/cm), TH - total hardness (epm of $CO_3Ca$), ions – epm. Number of samples is 25.

The dissolution of calcite, $CaCO_3$, and dolomite, $CaMg(CO_3)_2$, is controlled by different chemical and physical conditions. For example, the contact with an abundant supply of $CO_2(g)$ strongly enhances the water capacity in dissolve these minerals. Temperature values have an unusual influence in hydrochemical terms, as the dissolution of these minerals tends to be more effective at lower temperatures because $CO_2$ solubility decreases with increase in temperature. The processes controlling carbonate dissolution in natural waters will not be presented here. A detailed description of these processes can be consulted, for example, in Freeze and Cherry (1979) or Appelo (1993), among many other hydrochemistry textbooks.

The most remarkable hydrochemical feature characterising the hydrochemistry of the aquifer is the fact that, near always, including the severe periods of drought affecting the aquifer, water is undersaturated with respect to calcite and dolomite. This kind of hydrochemical behaviour is not rare and is one of the most enigmatic disequilibrium conditions in carbonate aquifers (Freeze and Cherry, 1979). According these authors, laboratory rates of calcite dissolution indicates that equilibrium should be attained in a matter of hours or days. However, in field conditions, weeks or even months of residence time can be necessary for dissolution to proceed to equilibrium with respect to calcite and dolomite.

One possibility to explain the seeming contradictions of the presence of undersaturated waters in aquifers where calcite and dolomite are the main minerals could be the circulation of water in dissolution channels or throughout short local flowpaths along fractures or bedding planes (Freeze and Cherry, 1979). In these conditions a decrease of the surface of contact area between water and rock could difficult the evolution of water chemistry in the sense of equilibrium conditions predicted theoretically.

In addition to calcite and dolomite dissolution and influence of agriculture in water quality, another identified natural process affecting water composition is ion exchange phenomena. The interpretation of available data suggests that calcium in water can be exchanged with sodium present in clay minerals, which is an additional possible explication for the undersaturation of water with respect to calcite and dolomite.

It must be remarked that the only sampling point where water was found to be supersaturated wit respect to calcite and dolomite corresponds to the spring with the inventory number 6 (sample collected in September 1991). In other dates the samples collected in that point are slightly unsaturated but always nearest from equilibrium than samples collected in other inventory points. In that spring the typical diminution in the slope characterising the recession periods of the hydrograph spring are better distinguished than in the other springs present in the studied area (see section 3.5.3.2). At

the time of interpretation of spring hydrographs was remarked that the different slopes observed during different recession periods in that spring cannot be related to the emptying of parts of the aquifer with very different hydraulic properties. In fact, the very low values of discharge suggest that spring number 6 must drain mainly the low permeability carbonate rock volumes. The fact that spring tends to show an equilibrium state nearest from equilibrium or even supersaturation with respect to calcite and dolomite dissolution contributes also for that interpretation. This is one more aspect making difficult the acceptance of the schemes regarding the diagnostic of the features characterising karst aquifers with basis in the typical behaviour of spring hydrographs in carbonate rocks (see section 3.5.3.3).

In the well with inventory number 8 water was also found to be in equilibrium with respect to calcite and very slightly unsaturated with respect to dolomite in September 1991. For all the other samples, in all analysed periods, the remaining waters are undersaturated. However, invariably, the samples collected in the Castelo de Vide sector are nearest of equilibrium conditions than the waters collected in the rest of the aquifer.

### 4.3.2 – Spatial trends of hydrochemical processes and regional flow patterns

As remarked before, the analysis of the saturation index values calculated in waters collected in the aquifer show that the Castelo de Vide sector tends to show a less accentuated trend to undersaturation with respect to calcite and dolomite than waters collected in the other two aquifer sectors. At the same time, the total dissolved solids of samples taken in the Castelo de Vide sector are characterised by the highest values in the aquifer. This is reflected by the electrical conductivity values of water in this sector, which average values are about 100 µS/cm highest than the values registered in the Escusa and P. Espada sectors. The highest values of total dissolved solids in the aquifer are registered in the spring with the inventory number 6 (at the same point where water samples are nearest of chemical equilibrium with respect to calcite and dolomite dissolution). The values of electrical conductivity measured in the waters drained by that spring range between 519µS/cm and 560µS/cm. That spring is located in the Castelo de Vide sector where the electrical conductivity values are usually around 300µS/cm.

In the Escusa and P. Espada sectors of the aquifer electrical conductivity values are around 200µS/cm and are often below this value. Simultaneously, the undersaturation of water with respect to calcite and dolomite in theses sectors is more accentuated than in the Castelo de Vide sector

The described trends in the spatial distribution of electrical conductivity and saturation indexes to respect calcite and dolomite are related to the regional flow pattern defined in the conceptual flow model defined at the start of the present Chapter. Moreover, the control of the observed hydraulic behaviour of the aquifer in the identified hydrochemical trend is very probably related to the time residence of water in the aquifer, which must be longer in the Castelo de Vide sector than in the Escusa and P. Espada ones. This is because the secondary outflow region controlling the flow pattern in the NW area of the aquifer near Castelo de Vide is toward relatively low permeable lithologies, which have a limited capacity to assimilate the transference's from the carbonate rocks. On the other hand, the flow toward the bed of the Sever River is more effective and thus the residence time of water flowing from the Escusa and P. Espada sectors must be shorter. In these conditions these sectors present less mineralised waters and thus, lower values for the saturation index with respect to calcite and dolomite.

Another hydrochemical trend identified in the aquifer is related to the values for the $\delta^{18}O$ ratio. According with the notation $\delta$, lower values of $\delta^{18}O$ represent a depletion of the $^{18}O$ heaviest isotope in relation with the lighter isotope $^{16}O$. That notation is used because the used standard analytical methods (mass spectrometry) allow more accurate determinations of the relative concentration of values with respect to a standard sample than the determination of absolute values for the concentration of each isotope. The use of the Standard Mean Ocean Water is universally adopted to express the relative concentration of both isotopes in water samples (Payne, 1983).

Precipitation falling at higher elevations is more depleted than that falling at lower elevations. The fact that a change in isotopic composition in precipitation with altitude ranging from -0.16‰ to –0.7‰ in $\delta^{18}O$ for a 100m increase in altitude is known to occur in a world-wide basis. A frequent value found is 0.2 ‰/100m (Eriksson, 1983; Payne, 1983; Quijano and Dray, 1983). This effect of altitude in isotopic composition of precipitation is particularly efficient in areas with marked orographic precipitation (as occurs in the studied area).

That property is of particular utility in diverse hydrologic applications, namely in the identification of groundwater origin in aquifers characterised by the existence of recharge areas with different altitudes. That altitude effect was detected in the Castelo de Vide Aquifer where determined values of $\delta^{18}O$ show that in the P. Espada sector water is depleted about 0.3‰ in $^{18}O$ with respect to the Castelo de Vide and Escusa sectors (Monteiro *et al*. 1997). That changes in values of $\delta^{18}O$ are related to the fact that average altitude in the P. Espada sector of the aquifer is around 650m, and about 520 to 550m in Castelo de Vide and Escusa sectors.

The identified trends of hydrochemical processes identified at regional scale, allowing an indirect confirmation of the defined conceptual flow model for the aquifer are summarised in figure 4.4.

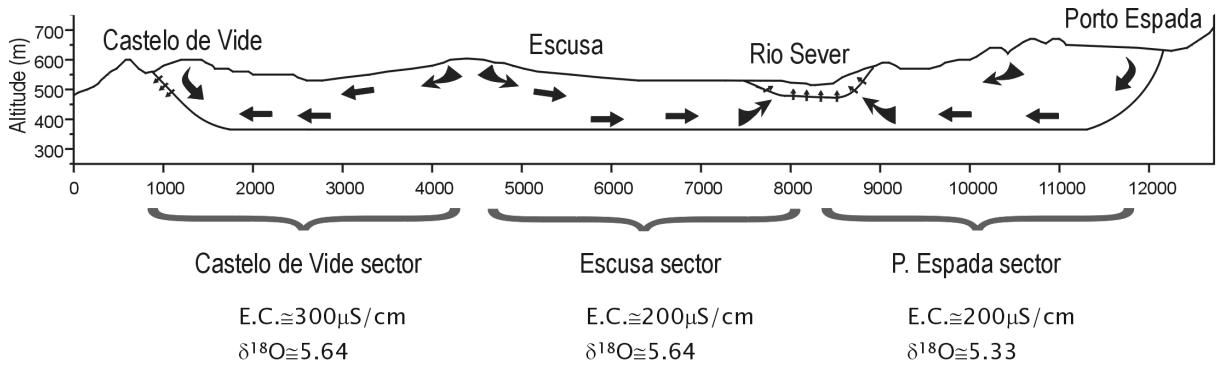


Figure 4.4 – Hydrochemical trends identified in the aquifer and aquifer sectors defined in section 3.6. In the Castelo de Vide sector the residence time of water is longer due the low permeability of the lithologies receiving outflow from carbonate rocks in the secondary discharge area of the aquifer near Castelo de Vide. Therefore, the amount of total dissolved solids in water is more important than in the other aquifer sectors because the chemical processes of carbonate dissolution are closest to equilibrium. This is reflected by the highest values of electrical conductivity in the Castelo de Vide sector. Due to the rapid outflows toward Sever River (Rio Sever) residence times are shorter in the Escusa and P. Espada sectors. In these sectors, the water is more undersaturated with respect to the dissolution of carbonate minerals than in Castelo de Vide sector, thus lower electrical conductivities characterise the waters in the sectors drained by the river. As the elevation of the recharge area in the P. Espada sector is about 100m higher than in the other sectors; a depletion in $^{18}O$ is observed allowing to distinguish the isotopic composition of water in this sector.

### 4.3.3 – Influence of allogenic recharge in hydrochemical facies

As usual in carbonate rocks, the predominant composition of waters in the Castelo de Vide carbonate aquifer corresponds to a bicarbonate calcic hydrochemical facies. This is the result of the fact that carbonate minerals dissolution is the predominant process controlling water composition. As dolomite is the predominant mineral in the aquifer some of the samples present bicarbonate calcic and magnesic, or even bicarbonate magnesic hydrochemical facies.

However, in some cases, mainly after recharge events, some analysed water samples present a shift toward a composition corresponding to a calcium and sodium chloride hydrochemical facies. Such kind of waters is not expected in carbonate aquifers and thus some explanation must be found to justify the existence of that trend. Some water samples collected in the deposits covering the very low permeability lithologies surrounding the carbonate aquifer are characterised by low values of total dissolved solids and a calcium and sodium chloride hydrochemical facies. These deposits are mainly coarse detritic rocks originated by weathering of the Ordovician quartzites in the flanks of the Castelo de Vide syncline. Figure 4.5 shows a transversal cross-section showing the geometrical relations between these deposits, the carbonate aquifer and the surrounding "impermeable" lithologies and the projection of the water composition in the carbonate aquifer in piper diagrams for the samples collected in September 1991 and January 1997. As showed in that figure a visible shift of the typical hydrochemical facies common in carbonate aquifers is visible toward the calcium and sodium chloride hydrochemical facies characterising waters in the deposits covering the aquifer near its limits. At the same time, the Piper diagrams show that the composition of the waters with intermediate composition can be interpreted as originating from a mixture between calcic and/or magnesic water type with calcium and sodium chloride water type.

As the waters with intermediate water types were usually collected in inventory points near the aquifer limits that results are interpreted as result of the mixture of waters originated from allogenic recharge processes that were identified by direct observation in the field as described in section 3.4.3.

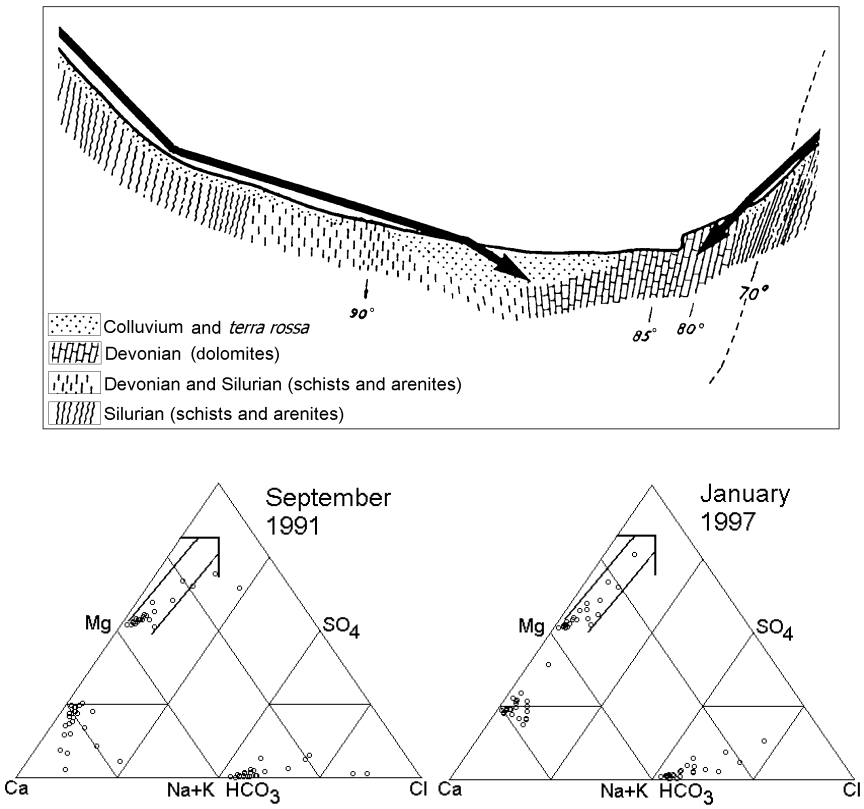


Fig. 4.5 – Piper diagram showing a shift of the hydrochemical facies from a bicarbonate calcic and/ or magnesic water type in the carbonate rocks to a calcium and sodium chloride water type near the limit of the carbonate aquifer. The transversal cross-section at the top of the figure shows the geometrical relations between these deposits, the carbonate aquifer and the surrounding "impermeable" lithologies as well as the allogenic recharge processes (black arrows) responsible for the hydrochemical trends represented by the arrows in the piper diagrams.

In section 3.4.3 different processes of water input where identified in the aquifer. In addition to autogenic diffuse recharge and autogenic concentrated recharge, occurring as result of infiltration of precipitation that falls directly under the carbonate aquifer two additional origins for water input in the aquifer where identified:

- Allogenic diffuse recharge derived from subsurface runoff in deposits that cover the carbonate rocks and the neighbouring low permeability schists (interflow) and drains into the carbonate aquifer.

- Allogenic concentrated recharge derived from sinking streams flowing from the neighbouring low permeability schists toward the aquifer. These streams disappear underground by infiltration in swallow holes when the limit of the carbonate aquifer is reached.

These processes of lateral recharge are present because sloppy terrains where infiltration is reduced surround the carbonate rocks and are responsible for the identified mixture of waters near the carbonate aquifer limits. These hydrochemical processes constitutes an additional possible cause for the general state of water undersaturation, with respect to calcite and dolomite dissolution.

**4.4 – Additional remarks on the identified hydrochemical processes**

As remarked in the previous sections the most remarkable hydrochemical characteristic of waters in the carbonate aquifer consists in the general state of undersaturation with respect to dissolution of calcite and dolomite. Three different possible causes for this were discussed: (1) the low residence time of water in the aquifer, which seems be confirmed by the presence of waters nearest the equilibrium state in the Castelo de Vide sector; (2) the presence of conduit flow diminishing the water-rock surface contact, and thus making difficult the rock-water interaction and (3) the

process of lateral recharge originated from adjacent areas where carbonate minerals are absent and thus waters are strongly undersaturated.

All these origins for the observed state of undersaturation are conceivable. However it is difficult to determine to what extent each of them contributes to the observed water composition.

# Chapter 5

HYDRAULIC PARAMETERS OF THE CARBONATE ROCKS

---

Contents



In nature the hydraulic system in an aquifer is in balance; the discharge is equal to the recharge and the water table or other piezometric surface is more or less fixed in position. Discharge by wells is a new discharge superimposed on the previous system. Before a new equilibrium can be established water levels must fall throughout the aquifer to an extent sufficient to reduce the natural discharge or increase the recharge by an amount equal to the amount discharged by the well. Until this new equilibrium is established water must be withdrawn from storage in the aquifer and conversely the new equilibrium cannot be established until an amount of water is withdrawn from storage by the well sufficient to depress the piezometric surface enough to change the recharge or natural discharge the proper amount. The depression of the piezometric surface is called the cone of depression.

Charles V. Theis, 1938 (*in* Fetter, 1994)

## 5.1 – Introduction

Hydraulic conductivity values characterising the Castelo de Vide carbonate aquifer at regional scale were calculated in Chapter 4. These values range from $1.5\times10^{-4}$ m/s to $7.0\times10^{-4}$m/s. As will be shown in the present chapter, hydraulic conductivity determined at well scale with pumping tests take on values over 4 orders of magnitude, ranging from $2.5\times10^{-6}$ m/s to $1.3\times10^{-3}$ m/s. Therefore the hydraulic conductivity determined at regional scale is near the highest values determined from the interpretation of pumping tests. These values reflect the change of hydraulic conductivity values with scale. This scale effect is particularly marked in flow domains where diffuse and conduit flow is overlapped in a complex flow pattern. The changes in hydraulic conductivity values with scale, foresee by Kiraly (1975), are closely related to the shape and dimension of different kind of voids developed in that kind of rocks and is expressed in figure 5.1.

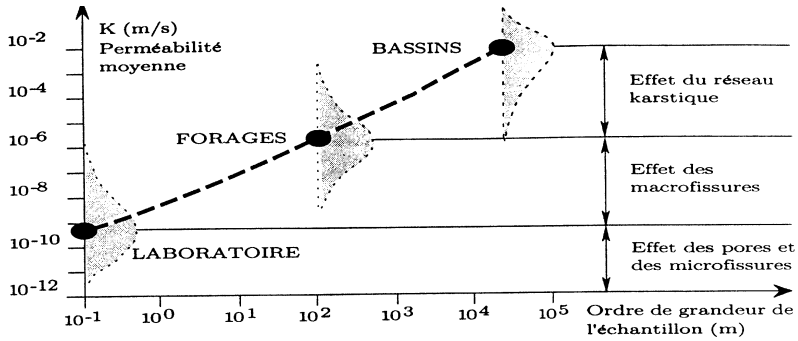


Figure 5.1– Scale effect in karst aquifers hydraulic conductivity. Adapted from Kiraly (1975).

Depending on their spatial extent three scales can be defined: the rock matrix, the local and the regional scales. At the lower extreme of the scale, porosity and hydraulic conductivity, depend on the existence of intercrystalline voids, moldic voids and microfractures, with dimensions ranging from sub-micrometers to millimetres. The volume of these voids tends to change according to the dominant active geologic processes. In some cases the porosity tends to be enhanced due to the dissolution of calcite and dolomite, the dominant minerals in carbonate rocks. In some other cases the hydraulic conductivity and porosity may be reduced due to calcite precipitation and cementation. This is identified as laboratory (or rock matrix) scale and is associated to the analysis of samples with few $Cm^3$ in dimension.

At an intermediate scale (local or well scale) the parameters are related to structures with dimensions varying from few meters to few hundred meters. In many cases that scale is in the order of the aquifer thickness. At this scale the hydraulic parameters depend on the distribution and connectivity of the voids in rock matrix and on the existence of fractures. Despite the fact that the fractures are not randomly distributed in space, many methods conceived for the determination of hydraulic parameters in double porosity media are based in methods assuming the presence of a fracture network that break the rock mass into blocks of equal dimension.

Tectonics affects the genesis and the evolution of voids over all scales, but at local scale the aperture, orientation and density of fractures are crucial factors in the distribution of parameters. Local scale can also be defined as "well scale". The productivity of wells in carbonate rocks is highly dependent on the presence of fractures and on the presence of karstic channels crossed by the borehole or in its vicinity. As karstic networks can be developed along kilometre wide scales and show hierarchical structure, they cannot be simulated as a regularly distributed network of channels. This limits the applicability of conventional double porosity models and led to the analysis of carbonate aquifers heterogeneity at regional scale.

At regional, or even at aquifer scale, we find a more or less developed network of dissolution channels. In well-developed karst aquifers these structures can control the flow pattern in the entire flow domain. In other cases more or less independent branches of channels are observed in different sectors of an aquifer system. Another important difference between the fracture network at well scale and karstic channels at regional scale is the fact the former are characterised by a configuration where one of the dimensions in space (aperture) is much smaller than the other two ones. In the case of karstic channels that rule cannot be generalised as their shapes vary from among a large set of geometries.

By taking into account these levels of heterogeneity, karst aquifers can be schematised as a high conductivity channel network embedded in a low-permeable fractured rock matrix (Kiraly, 1975). Since the nature of water flow and storage processes is different in the three types of voids, the efficiency of a mathematical model to simulate flow in such systems depend on its ability to deal with the processes, that develop at the scale of the problem under consideration. As the

scale of the problem increases the complexity of the problem increases also. For example, if a flow problem is to be treated at the regional scale, the corresponding model must provide a unified conceptual framework accommodating the processes acting at lower scales.

As result of the "scale dependent heterogeneity", the values of hydraulic parameters allowing an adequate description of a specific flow domain change depending on whether they are obtained in tests performed using cores extracted in boreholes (with few $cm^3$), in pumping tests (performed in wells with dimensions ranging from tens to few hundred meters) or using numerical models at regional scale (defined over areas from few to hundreds of km2). In practice, the occurrence of such conditions restrain dramatically the possibilities in distribute spatially the parameters obtained with tests characterising the rock matrix or well scales over a regional flow model.

Taking into account the general different levels of spatial variability referred above, the determination of hydraulic parameters cannot be done at all the required levels of scale by using a single investigation technique. As a different degree of accuracy (difficult to quantify) is inherent to each method to deal with the problem at different scales, this is an additional source of uncertainty affecting the global characterisation of parameters.

The values obtained from the interpretation of pumping tests can be regarded as point measures of hydraulic parameters at local or well scale. The interpretation of pumping tests in carbonate rocks using a conceptual model considering the flow domain as a fractured porous media allow the evaluation of parameters at well scale separately for the fracture and rock matrix sub-systems. Despite the very limited practical results obtained when the parameters resulting from the interpretation of pumping tests are distributed over the entire area of an aquifer, we will outline briefly the theoretical principles of these methods. Further, we will present a discussion about the order of magnitude of the parameters characterizing the dissolution channels present in the aquifer, entirely based in theoretical considerations. This is done in order to provide a general framework for the analysis of the difficulties in establish a coherent linkage between the punctual values for parameters determined at well scale and the distribution of parameters allowing the interpretation of flow at regional scale using numerical models.

### 5.2 – Interpretation of pumping tests using the single continuum and the double continuum approaches

The theoretical basis of the existing techniques for interpretation of pumping tests can be divided in two different approaches: methods considering the flow domain as a single continuum porous media and methods allowing the determination of parameters for both, fractures and rock matrix, in fractured porous media. The concept of "double porosity" often found in literature are reserved for the methods developed for flow and transport problems observed in fractured rocks where the role of the rock matrix is considered as an active part of the domain under study. In that sense, this approach can be distinguished from techniques related to the flow analysis in fractured media, where the rock matrix, surrounded by fractures, contain no void space, and is considered as an inert volume of the system without active interference in the process.

At a first glance, taking into account the properties of carbonated rocks, a better performance for double continuum methods could be expected for the characterization of hydraulic parameters. But, in several cases, a best fit of experimental data is obtained in practice when the methods based in the single continuum approach are used to interpret pumping tests performed in carbonate aquifers (including well developed karst aquifers). The apparent contradiction of these experimental results is also observed in the present case study. The interpretation of the available data will be used to show the possibility to conciliate the results obtained by both methods.

The sequence of procedures applied for the interpretation of time-drawdown data collected in the field will be made using the single continuum approach as a starting point. As will be shown this strategy can lead to a sequential analysis of data that starts with these methods, leading to the selection of the cases were the use of double continuum models is possible. In the cases where the data registry allow the use of double continuum methods, the determination of parameters can be done separately for rock matrix and fractures. At the end of the procedure a conclusion may be drawn: depending on the data available both methods are useful in order to obtain basic information about hydraulic parameters of the aquifer.

#### 5.2.1 - Theoretical principles

Here we provide only a very general overview of the theoretical principles of the methods available for the interpretation of pumping tests in double porosity media. A complete presentation of these principles is complex and a discussion of the subject is beyond the objectives for the present work. For a detailed description of these concepts we refer to the works of Almeida and Oliveira (1990), Almeida et al. (1992) and Oliveira, (1993). The program AQFIS developed by these authors allows the generation of theoretical, curves for 34 different double porosity models. That

program was used to generate the theoretical curves presented in this chapter and to perform the interpretation of pumping tests.

In general terms, if the controlling differential equation for flow in fissures is assumed to be described by the groundwater diffusion equation, with a source term to account for contributions from the rock matrix (see equation 2.1 in section in section 2.1 for details about variables), one can rewrite the problem, in terms of two interdependent subsystems:

For the fissures,

$$K_f \nabla^2 h_f = S_f \frac{\partial h_f}{\partial t} + q_\alpha \qquad 5.1$$

and similarly, for the rock matrix:

$$K_b \nabla^2 h_b = S_b \frac{\partial h_b}{\partial t} - q_\alpha \qquad 5.2$$

Where the subscript *b* refers to the matrix rock and the subscript *f* to the fissure system.

The simplest way to define the interaction between both continua in a double porosity system is to define that the left-hand side of equation 5.2 is zero. The practical meaning of that assumption is that the spatial variation of hydraulic head in rock matrix is negligible and thus the divergence of flow in the blocks is ignored. The pseudo-steady state flow from blocks to fractures is based on that simplification and yet in the assumption of the motion of fluid from blocks to fissures as response of the difference in average hydraulic head between fissures and rock matrix:

$$q_\alpha = -\alpha K_b (h_b - h_f) \qquad 5.3$$

The physical meaning of the parameter $\alpha$ is difficult to establish. A useful way to understand the impact of the changes in $\alpha$ is the analysis of the prediction of the drawdown in a well implanted in a double porosity media. When a well start pumping in such media, a rapid loss in hydraulic head is registered in the fractures. This is because near all the water released by the aquifer during the start of the pumping test comes from the fractures. During that first period the experimental data fits a Theis type curve which parameters characterise the fractures system. After that period, the water flow from the rock matrix to the fractures increases (as response to loss in head in fractures) and the drawdown in the pumping well is lower than the predicted for the Theis type curve characterizing the fractures system. This second period of the pumping test cannot be described by means of a single continuum model. At a later time, equilibrium is attained for the contributions of water from the fractures and rock matrix. At this point the time drawdown curve fits a second Theis type curve, which characterise the global parameters of the entire flow domain affected by the interference provoked by the pumping test. The typical behaviour of wells in double porosity model is schematically represented in Figure 5.2. The first Theis type curve is defined by the equation (Oliveira, 1993):

$$h_0 - h(r,t) = \frac{Q}{4\pi T_f} w(u_1); \qquad u_1 = \frac{r^2 S_f}{4 T_f t_1} \qquad 5.4a;b$$

And the second:

$$h_0 - h(r,t) = \frac{Q}{4\pi T_f} w(u_2); \qquad u_2 = \frac{r^2 S_t}{4 T_f t_2} \qquad 5.5a;b$$

Where $h_0$-$h$ is the drawdown referred to the radial distance $r$ from the pumping well at an instant $t$. $Q$ is the well discharge. The term "transmissivity" refers to the product of hydraulic conductivity and aquifer thickness. As the total transmissivity of the aquifer $T_f$ equals the transmissivity of the fractures, the second Theis type curve corresponds to a displacement of the first one along the time axis. The amount time of displacement of the curve depends in the storage coefficients (or storativity) characterising the system of blocks $S_b$ and the system of fractures $S_f$. The storage coefficient of the blocks system $S_b$ can be determined from the difference $S_t$-$S_f$ , where $S_t$ is the total storativity of the flow domain (Almeida and Oliveira, 1990).

The solution provided by Kazemi *et al*. (1969) for one-dimensional radial flow toward a well as response to pumping is one of the techniques for interpretation of pumping tests based in the above simplifications. The typical type curves obtained using that method are presented in Figure 5.2. In this figure the earlier dashed curve is a Theis type curve, which defines the hydraulic properties of the fracture system alone. The second dashed curve in the same figure is a Theis type curve characterizing the hydraulic properties of the entire media. After the point, where the type curves defined by Kazemi converge to the late solution of the Theis Solution, the entire flow domain behaves as a single continuum media. After this point, the total transmissivity equals the transmissivity of the fractures and the total storage coefficient ($S_t$) equals the sum of $S_b$ and $S_f$.

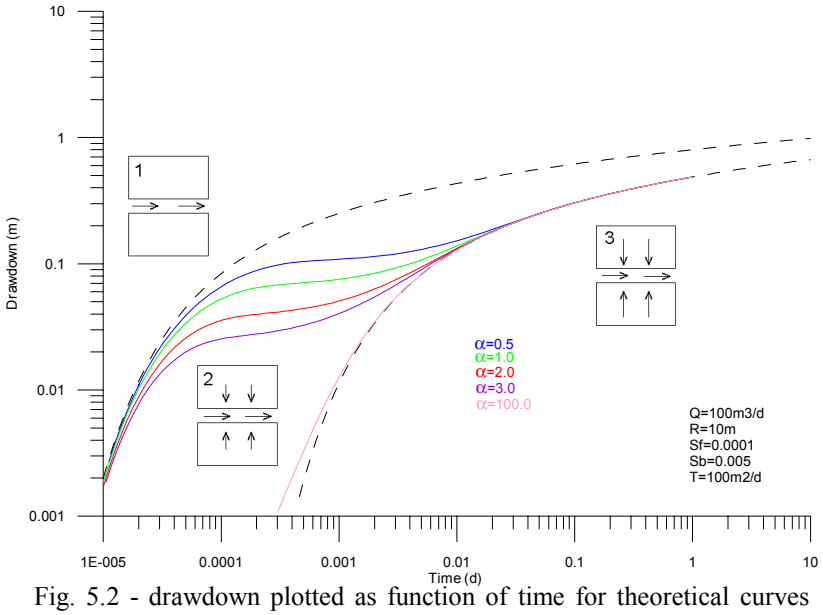


Fig. 5.2 - drawdown plotted as function of time for theoretical curves obtained by a pseudo-steady state block-to-fissure flow model, Kazemi (1969). Q – pumping rate; r – radial distance from pumping well to the piezometer; T –transmissivity of the aquifer.

A possible definition of a relation between α values and the intrinsic properties of the double porosity media can be made establishing geometric relations evolving the dimensions of regular blocks and fractures. For example α can be defined as the inverse of the product between the average half thickness ($b_b$) of a matrix block and aquifer thickness ($b$) and has the dimension of inverse area [$L^{-2}$] (Oliveira, 1993). According to this interpretation of the parameter α, the behaviour of the curves are to be interpreted as follows: As the values of α increase the drawdown decreases for a given time and thus the double porosity model fits the second Theis type curve in a shorter time. After enough α increase, the solution of the double porosity model converge to the second Theis type curve showed in Figure 5.2 and thus for the original Theis solution for a single continuum porous media.

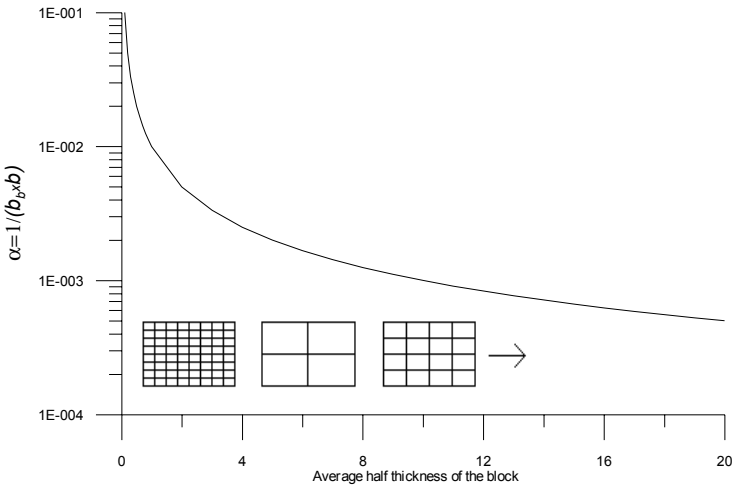


Fig. 5.3 – Values of the parameter α plotted in function of the half thickness of the average matrix block in meters (aquifer thickness 100m).

This can be easily visualised if we imagine the evolution of the double porosity media as the average block half thickness increases, and thus $\alpha$ decreases (Figure 5.3). For smallest values of $b_b$, the surface contact between the blocks and fractures is larger and the transference of water from block to fractures is more efficient. At the point where the blocks are small enough the system behave as a single continuum media.

More sophisticated solutions consider the divergence in blocks and include the pseudo-steady state models as a particular case. In the cases where flow from the block to the fissures has a profound influence on the drawdown in the fissure system, neglecting the divergence in blocks (zero in left-hand side of equation 5.2) is not justifiable. The work of Moench (1984) provides the unification of the pseudo-steady state and transient double porosity models using a fracture skin parameter. If the value of that parameter, introduced in a transient flow model, is large enough the surface of the matrix blocks present a low hydraulic conductivity and thus, most of the change in hydraulic head within a block occurs across the fracture skin. Consequently, changes in the gradients of hydraulic head within the block become small, thus justifying the assumption in the pseudo-steady state flow model that the divergence of flow in the block is negligible. In figure 5.5 theoretical curves built with the model presented by Moench (1984) are shown for different values of the fracture skin parameter.

In the transient models the time drawdown curves differ from those obtained from pseudo-steady state models in the first period of the pumping tests and during the time of transition from the earlier to the late Theis type curves. For these models an hypothetical geometry of the blocks can be related to the hydraulic conductivity of the rock matrix by the parameter $\phi\,[T^{-1}]$ defined as follows (Oliveira 1993):

$$\phi = \frac{K_b b}{b_b^{\,2}} \qquad 5.6$$

Where $K_b$ is the matrix hydraulic conductivity, $b$ is the aquifer thickness and $b_b$ is the average half thickness of the blocks. As the variables in the right hand of equation 5.6 cannot be determined separately in pumping tests, the parameter $\phi$ is very useful for the interpretation of the results obtained by double porosity transient models.

The existence of fractures and blocks overlapped in space without a definition of an explicit geometry is only possible when the pseudo-transient models are used. In the transient models the geometry of fissures must be assumed and correspond to simplified regular fracture systems that break the rock mass into blocks of equal dimensions. Different geometries are assumed as basis for the transient models but in practice, the obtained solutions are very similar or even equivalent. The geometries assumed are based in a pattern defined by groups of cubes, spheres or infinite slabs. Some of the idealised geometries to describe fractured porous media are presented in Figure 5.4.

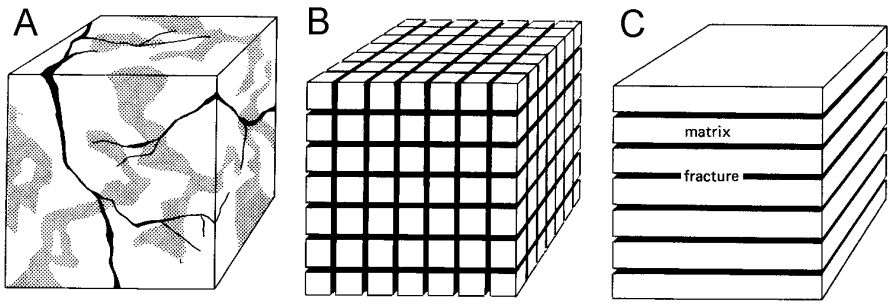


Fig. 5.4 - Idealised three-dimensional fracture systems (B and C) of a natural fractured porous media (a). Adapted from Kruseman and de Ridder (1990).

As the third period of time drawdown curves predicted by double porosity models correspond to a single Theis type curve characterizing both, matrix and fractures sub-systems, a good strategy to analyse experimental data sets consist in starting the interpretation of the tests using the Theis model. If a good agreement with that model is obtained after a given instant $t$ and the earlier period of the test cannot be predicted considering the single continuum approach, then it is possible to use the double porosity models in order to determine the parameters for both sub-systems (Almeida and Oliveira, 1990).

In Practice, the earlier period predicted by the double porosity models allowing the determination of the hydraulic properties of fractures can be detected only if a detailed time drawdown data set is available for a short period after the start of the pumping test. Consequently, the registry of data allowing the determination of parameters for the fractures is very difficult in practice. Because the double porosity models converge for the Theis solution after a short period of time, very often the only determined parameters are the ones characterizing the entire flow domain as a single continuum media.

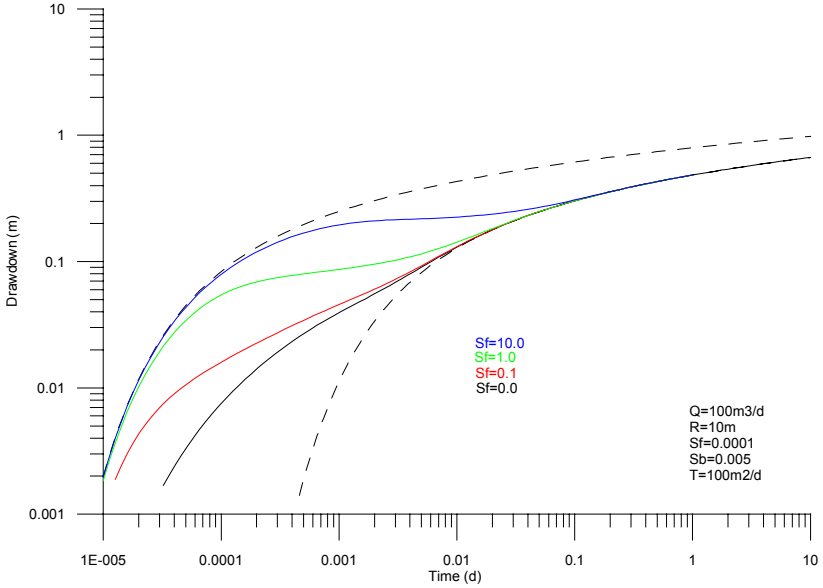


Fig.5.5 – Drawdown plotted as function of time for theoretical curves obtained by a transient block-to-fissure flow model, Moench (1984). Q- pumping rate; r – radial distance from pumping well to the piezometer; T – transmissivity.

### 5.2.2 – Analysis of incomplete time drawdown data sets

Some of the time drawdown data sets available in the present case study were obtained from technical reports, which were produced at the time of the construction of wells. In many cases the available data is not detailed enough for the use of the techniques based in theoretical type curves matching experimental time drawdown records. In such cases the media is treated as a single continuum flow domain and simplified methods based in the Theis method were applied. The pumping tests performed during the construction of boreholes are often limited to the time needed to detect a sensible decrease of drawdown with time. The available information in those cases consists in a value (or few values) for the pumping rate and the drawdown attained in an instant *t*. In such cases a simplified method to determine transmissivity was used: the Ogden Method (1965) described in Almeida (1985). This method is based in a very useful transformation of the Theis method. Taking the equation 5.4 a,b or 5.5 a,b and ignoring the subscripts referred to the matrix or block sub-systems we obtain the original formulation for the Theis model:

$$h_0 - h(r,t) = \frac{Q}{4\pi T} w(u); \qquad u = \frac{r^2 S}{4Tt} \qquad 5.7a,b$$

The well function, which argument is *u*, is defined by the exponential integral. Values for that function are tabulated in most hydrogeology textbooks. For example Freeze and Cherry (1979):

$$w(u) = \int_u^{\infty} \frac{e^{-u} d_u}{u} \qquad 5.8$$

If we express 5.7 a and 5.7 b in terms of $T$ the following expression is obtained:

$$T = \frac{Q}{4\pi(h-h_0)} \cdot w(u) = \frac{Sr^2}{4tu} \qquad 5.9$$

and thus:

$$u \cdot w(u) = \frac{\pi r^2 S(h-h_0)}{Q \cdot t} \qquad 5.10$$

As the values of $u \cdot w(u)$ can be determined from the tables for well function expression 5.10 and 5.7 b can be used in order to obtain a value of $T$ if an estimate of $S$ is provided. A value of $S$=$10^{-4}$ was used considering that the aquifer behaves as a confined system. It can be showed that even for a rough estimate of $S$, the errors in $T$ are not important (Almeida, 1985).

### 5.3 – Interpretation of experimental results

#### 5.3.1 – Characterization of the media as a single continuum

The interpretation of pumping tests was done starting by the use of the Theis model. As remarked in Section 5.2 the parameters determined when this method is applied characterise the entire flow domain affected by the test as a single continuum.

Figures 5.7, 5.8 and 5.9 shows the analysis of time drawdown data for wells 8, 56, 75, 83 and 84 using the Theis method. The data sets available for wells 7, 9, 49, 79, 78, 80, 81 and 82 were insufficient to interpret the tests by fitting experimental data with theoretical curves. The parameters in these cases were determined by the Ogden (1965) method. The determined values for the parameters and some characteristics of the wells are summarised in table 5.1 were the entries are sorted in crescent order of hydraulic conductivity values.

| Well Number | Pumping rate (l/s) | Transmissivity ($m^2$/d) | Well depth (m) | Hydraulic Conductivity (m/s×$10^4$) | Method |
|---|---|---|---|---|---|
| 84 | 0.80 | 5.50 | 25.00 | 0.025 | Theis |
| 9 | 2.00 | 13.30 | 60.30 | 0.026 | Ogden |
| 83 | Sdt | 32.20 | 29.00 | 0.129 | Theis |
| 75 | 5.00 | 120.70 | 97.50 | 0.143 | Theis |
| 82 | 9.60 | 142.90 | 47.20 | 0.350 | Ogden |
| 79 | 27.80 | 156.25 | 43.50 | 0.416 | Ogden |
| 80 | 13.90 | 125.00 | 33.00 | 0.438 | Ogden |
| 7 | 7.00 | 250.00 | 46.10 | 0.628 | Ogden |
| 56 | Sdt | 965.60 | 98.75 | 1.132 | Theis |
| 8 | 15.00 | 592.00 | 51.00 | 1.344 | Theis |
| 78 | 2.50 | 357.10 | 16.00 | 2.583 | Ogden |
| 81 | 55.20 | 1626.50 | 35.10 | 5.363 | Ogden |
| 49 | 92.00 | 4050.00 | 35.20 | 13.317 | Ogden |

Table 5.1 – Calculated transmissivity and hydraulic conductivity using the Theis (1945) and Ogden (1965) methods. Hydraulic conductivity calculated using well depth. Sdt –Step drawdown test.

Despite the fact that the number of values is not enough to make a reliable statistic analysis of the data, it is interesting to take a look at the histogram of hydraulic conductivity values in Figure 5.6. These values are distributed over four orders of magnitude. Moreover near 50% of the calculated values fall between $10^{-5}$ and $10^{-4}$ m/s. These values were determined in wells where the carbonate rocks are weathered and fractured. Generally, larger values correspond to the cases where dissolution channels were identified. The lower values, encountered in wells 84 and 9, correspond to

boreholes drilled without interception of important fractures or dissolution channels. According the available data, at least three boreholes were drilled in the aquifer with values of conductivity lower than the minimum registered in table 5.1. These cases correspond to boreholes classified as unproductive wells and not submitted to pumping tests in order to reduce the costs of the drilling programs. Unfortunately this is a usual procedure, which limit the characterization of the hydraulic properties of aquifers. Very probably values of conductivity lower than $10^{-6}$ m/s were identified in pumping tests if time drawdown data sets were available for boreholes drilled and considered unproductive by the economical point of view.

The spatial variability of hydraulic conductivity leads to the question of how to compose local permeability values in order to obtain an average permeability to assign to the mesh elements. As remarked by de Marsily (1986), whatever the spatial correlation and distribution function of conductivity and whatever the number of dimensions of the space, for uniform flow (parallel flow lines) the average conductivity always ranges between the harmonic mean and the arithmetic mean of the local conductivities. If we take the hydraulic conductivity values determined from the pumping tests the following average values are obtained (Figure 5.6).

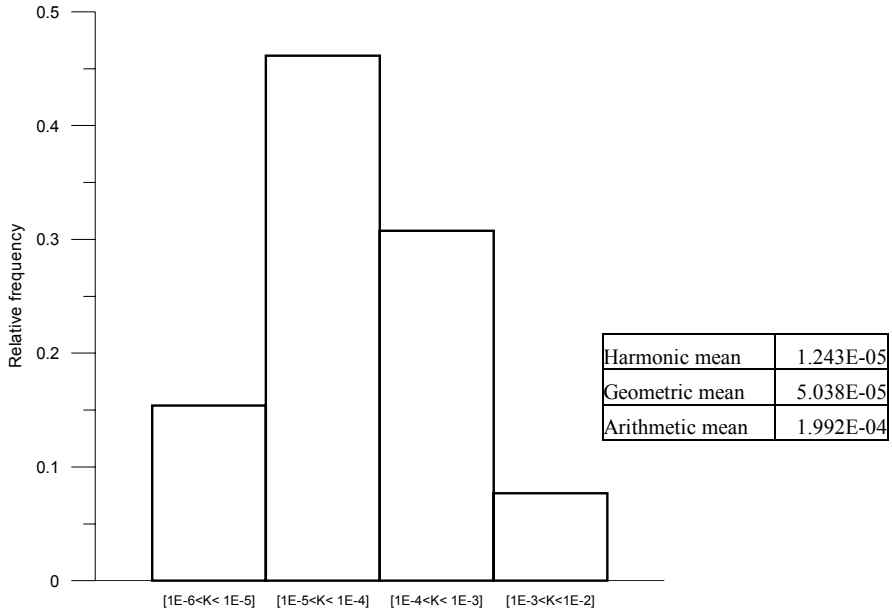


Fig. 5.6 – Histogram and average values for hydraulic conductivity (m/s) calculated by the interpretation of pumping tests.

In addition to transmissivity ($T$), a 2-D parameter that can be translated into hydraulic conductivity ($K$), which is a 3-D parameter, pumping tests provide also values of storage coefficient $S$ (or storativity). Storage coefficient is a 2-D (dimensionless) parameter defined as the volume of water that an aquifer releases from storage per unit surface area of aquifer per unit decline in the component of hydraulic head normal to that surface (Freeze and Cherry 1979). Storage coefficient values can be also translated in terms of specific storage $Ss$, [$L^{-1}$], a 3-D parameter, defined by equation 2.4 in chapter 2, by the relation $S$=$Ss \cdot b$, where $b$ refers to aquifer thickness.

Unfortunately, unlike transmissivity, storage coefficient values determined in single well tests are not reliable. It is not infrequent that $S$ values provided in this kind of tests are without physical meaning, because of the storage of the well itself. Despite this we present values obtained for storage coefficient and specific storage obtained in the cases where the Theis method was used to interpret pumping tests (table 5.2).

| Well | Pumping rate (l/s) | Storavity (*S*) (dimensionless) | Well depth (m) | Specific storage (Ss) (1/m) | Method |
|---|---|---|---|---|---|
| 84 | 0.8 | 0.00013 | 25 | 5.20E-06 | Theis |
| 83 | Sdt | 0.56 | 29 | 1.93E-02 | Theis |
| 75 | 5 | 0.015 | 97.5 | 1.54E-04 | Theis |
| 56 | Sdt | 15.76 | 98.75 | 1.60E-01 | Theis |
| 8 | 15 | 2.48 | 51 | 4.86E-02 | Theis |

Table 5.2 – Storage coefficient and specific storage values obtained from interpretation of pumping tests using the Theis method.

As can be seen in table 5.2 values for storativity calculated for wells 56 and 8 are excessive to be considered physically consistent. However, it is tempting to consider these values in global terms, which tend to point for the existence of high storativity in the aquifer.

The values obtained by pumping tests characterizing the flow domain as a single continuum describe the parameters of the rock matrix and fractures, i.e. two of the three levels of scale heterogeneity defined for carbonated rocks. However, some of the wells are affected by the presence of dissolution channels, crossed by the borehole or in its vicinity and thus the determined parameters are exclusively related to the hydraulic properties of the rock matrix and fractures.

As we will see later, these values are the basis for the characterization of the block conductivity characterizing the fractured rock matrix in regional numerical models, conceived to analyse flow at regional scale. By another hand the values determined in pumping tests are not enough to define a regional distribution of parameters allowing the characterisation of parameters at the aquifer scale.

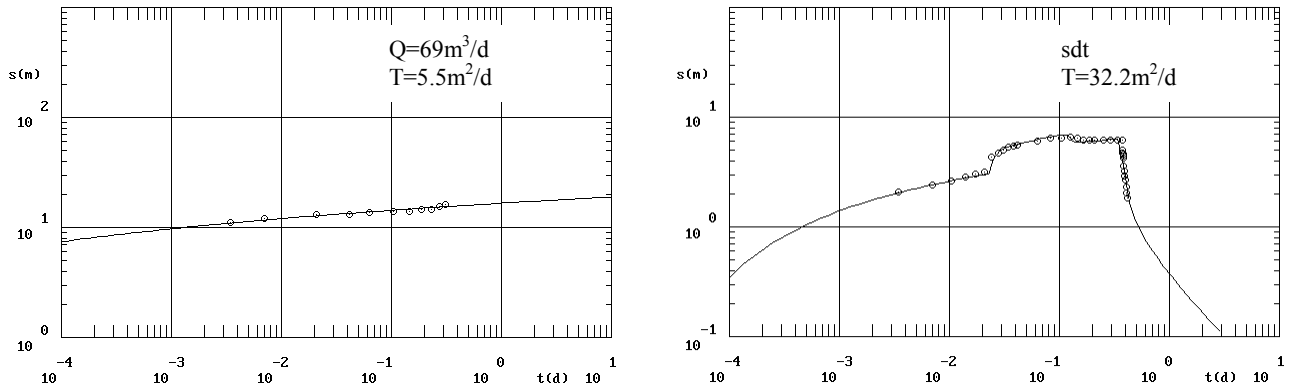


Fig. 5.7 – Drawdown plotted as a function of time and match to the Theis type curve for wells 84 (left) and 83 (right). Sdt-step drawdown test.

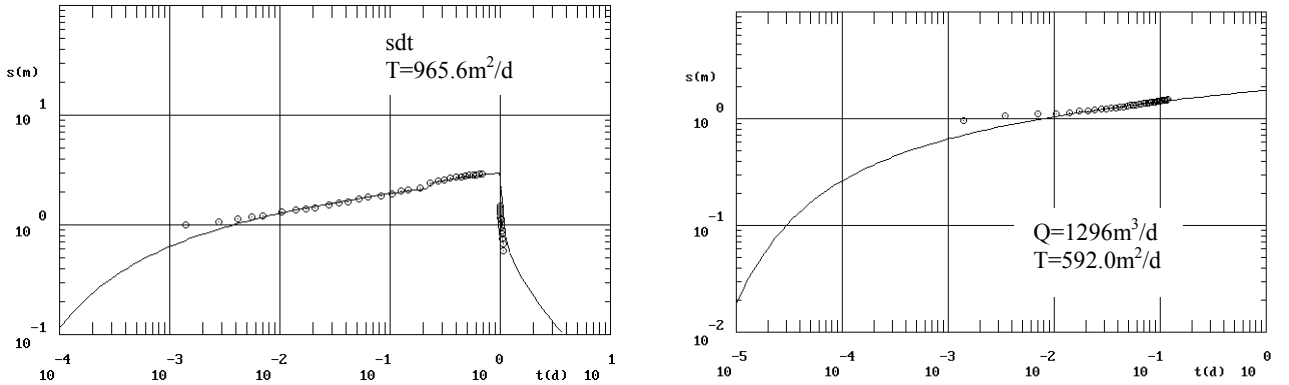


Fig. 5.8 – Drawdown plotted as a function of time and match to the Theis type curve for wells 56 (left) and 8 (right). Sdt - step drawdown test.

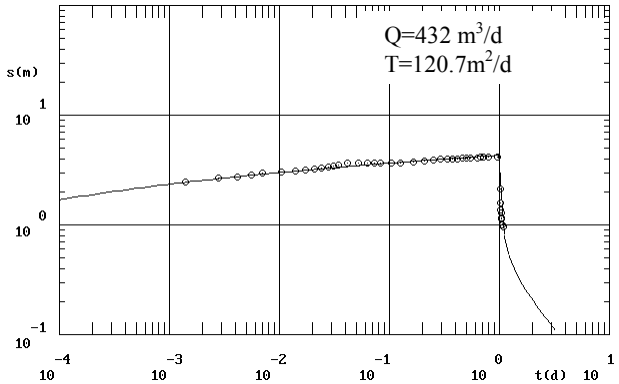


Fig. 5.9 – Drawdown plotted as a function of time and match to the Theis type curve for well 75.

### 5.3.2 – Characterization of the media as a double continuum

When a good agreement with the Theis model is detected after a given instant $t$ and the earlier period of the test cannot be predicted considering the single continuum approach, then double porosity models can be applied in order to try the determination of the parameters for both sub-systems of rock matrix and fractures separately. The results of the application of the Theis method presented through figures 5.7, 5.8 and 5.9 show that the typical well behaviour predicted by double porosity models in response to pumping was detected in wells 8 and 56.

Figure 5.10 shows the theoretical curves for the Boulton and Streltsova (1977) transient model and for the Kazemi (1969) pseudo-steady state model fitting the experimental data collected in the pumping test performed in well 8. The results show that both models could be used in order to obtain a good description for the well behaviour. However, if the objective of pumping tests is related to the characterisation of hydraulic parameters for both sub-systems of blocks and fractures, a deepest analysis of the problem is possible using models considering transient flow from block to fissures. For example, adjusting the Kazemi's pseudo-steady state model for time drawdown data collected in well 8 can be done considering a value of 5 $m^{-2}$ for $\alpha$. Using the expression $\alpha=1/(b_b.b)$, the value for $b_b$ will be 0.013m. It means that we are considering an average dimension for the blocks of 2.6 cm. It is not reasonable accept such value for the average dimension of the rock matrix blocks. That value can be calculated using the incorrect assumption that aquifer thickness $b$ equals the well depth. If a more realistic value for $b$, comprised between 150 and 200m were used an even smallest value for $b_b$ will be obtained. These results clearly show the difficulties in characterise the intrinsic properties of fractured porous media using pseudo-steady state double porosity models. Despite the gain in reliability in the description of well behaviour when compared with the results obtained when the media is characterised as a single continuum, the use of determined parameters in any other context is very difficult.

If the interpretation of the data set obtained for well 8 is done using the Boulton and Streltsova (1977) method, the calculated average block dimension is 10m. In that case the calculated value for the matrix transmissivity ($45m^2/d$) can be used to obtain a rough estimate for the hydraulic conductivity of the matrix ($K_b$) using the well depth. The obtained value is $1.02\times10^{-5}$ m/s.

For well 56 (figure 5.11) the obtained value for the hydraulic conductivity of the matrix, using the method of Boulton and Streltsova (1977) is $5.27\times10^{-6}$ m/s. This value was calculated again using the obtained value for matrix transmissivity and the well depth. In this case the average block dimension is 4m.

For both wells 8 and 56, the calculated values of hydraulic conductivity fall in the range of the higher values expected for rock matrix and, simultaneously in the range of the lowest values expected at well scale. If the values of block transmissivity are considered as representative of the entire vertical of the aquifer at the point where the pumping tests were performed (which is about 200m), we obtain a value of $2.6\times10^{-6}$ m/s for $K_b$ for both wells 8 and 56. That assumption means that we act as if the productivity of wells was not enhanced if they were drilled over the entire aquifer thickness. That value is remarkably near of the value obtained for wells 9 and 84 using the Theis method. Both wells 9 and 84 were drilled without intercept any fracture or visible void. These results show that the obtained values for the transmissivity of rock matrix using single continuum and double continuum methods can be interpreted in a coherent framework.

The values obtained in both wells 8 and 56 characterizing the wells as a double continuum media are summarised in table 5.3.

| Well Number | Pumping Rate (l/s) | Transmissivity of the fractures ($m^2/d$) | Transmissivity of the blocks ($m^2/d$) | Well Depth (m) | Hydraulic Conductivity of the matrix ($m/s\times10^6$) | Average dimension Of the blocks (m) |
|---|---|---|---|---|---|---|
| 8 | 15.00 | 592.00 | 45.00 | 51.00 | 10.21 | 10 |
| 56 | Sdt | 965.60 | 45.00 | 98.75 | 5.27 | 4 |

Table 5.3 – Hydraulic conductivity of rock matrix and block dimensions calculated using the Boulton and Streltsova (1977) method. Sdt - step drawdown test.

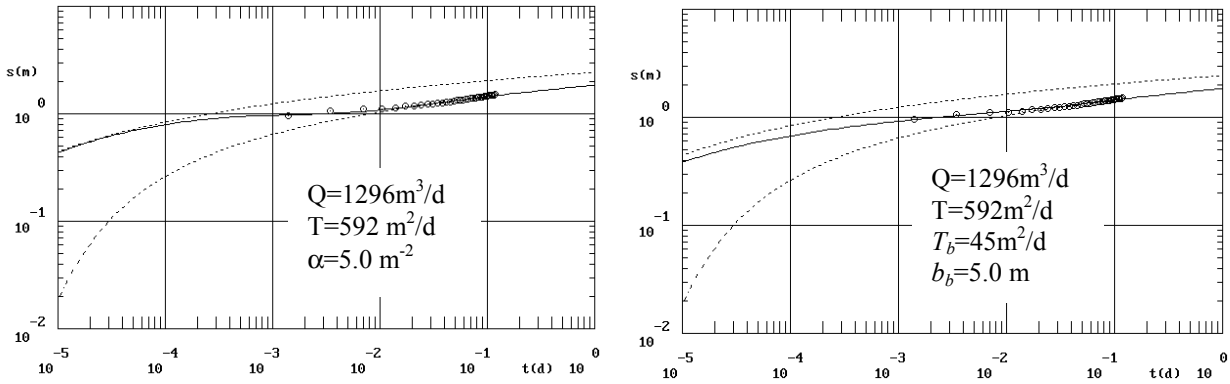


Fig. 5.10 – Drawdown plotted as a function of time and match to the Kazemi (1969) pseudo-steady state model (left) and Boulton and Streltsova (1977) transient model (right) for well 8.

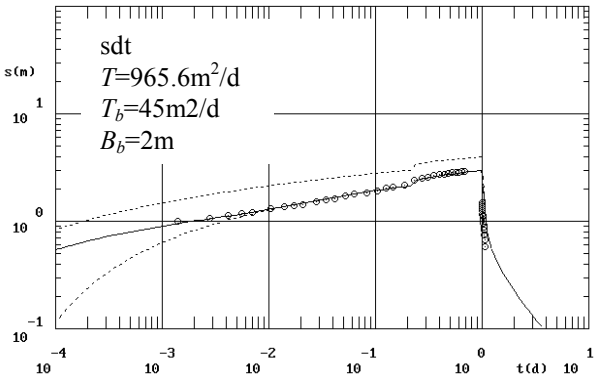


Fig. 5.11 – Drawdown plotted as a function of time and match to the Boulton and Streltsova (1977) model for well 56. Sdt –Step drawdown test.

**5.3.2.1 –Translation of fracture transmissivity values in hydraulic conductivity values in fractured porous media**

In the previous section the transmissivity values for the carbonate rock matrix obtained in pumping tests using single continuum and double continuum approaches were translated in hydraulic conductivity values. The results obtained by both methods are very similar. The point values calculated in boreholes where no important fractures or dissolution voids were identified are within the order of magnitude determined for the rock matrix using double continuum methods.

By another hand, when double continuum models are used, the parameters can be determined separately for the fractures contributing for flow toward the well. The analysis of the time drawdown data in response to pumping shows that the presence of fractures enhances considerably the productivity of wells in carbonated rocks. This is reflected in the contrast of transmissivity encountered between the values calculated for rock matrix and fractures when the double continuum models are employed. However, the translation of transmissivity values for fractures in values of hydraulic conductivity is more difficult and less objective than the same operation for the characterisation of the rock matrix hydraulic conductivity. This is related to the difficulties in define a precise meaning for the parameter “transmissivity of the fractures”. The values of transmissivity make available using double porosity methods does not characterise individual fractures but the group of fractures affected by the pumping well. That fact circumvents the difficulties in characterise the fractures individually. By another hand, the translation of fracture transmissivity values in hydraulic conductivity for a group of fractures, as needed for a three-dimensional flow analysis, cannot be done in a straightforward way.

In carbonate rocks the productivity of wells is typically related to zones where the density of fractures is higher or where dissolution channels are encountered during the drilling operations. Until such zones are encountered the well productivity is low and the values of parameters determined from pumping tests are of the order of magnitude of the values characterizing the rock matrix. In the cases where fractures are present and affect the hydraulic behaviour of the

wells, and thus double porosity models can be applied, the values of transmissivity determined are referred to a fractured zone. In practice, it is very difficult to define a test interval for the productive fractures and translate the values of transmissivity in values of hydraulic conductivity. If a borehole is drilled through a fracture zone and a pumping test is conducted, the sum $L$ of the apertures of the intercepted fractures can be used to determine the value of hydraulic conductivity by the expression $K_f=T_f/L$. If a fractured zone is identified during the drilling operations and the estimate of the sum of apertures corresponds to the double of is real dimension the calculated value of hydraulic conductivity will be halved. Usually the technical information about boreholes, available in technical reports, includes the identification of the fractured zones encountered during the drilling operations. By another hand, the existence of data about aperture of individual fractures is rare because the destructive methods actually employed in most of the cases are not compatible with the detailed characterization of the fracture aperture. In such conditions the determination of hydraulic conductivity of fractures is a subjective operation and can lead only to approximate values.

In the case of wells 8 and 56 we can use the reported values for the length of the fractured zones crossed by the boreholes in order to estimate the values of hydraulic conductivity (Table 5.4).

| Well Number | Pumping Rate (l/s) | Transmissivity of the fractures ($m^2/d$) | Transmissivity of the blocks ($m^2/d$) | Sum of the length of fractured zones (m) | Hydraulic Conductivity of the fractures ($m/s \times 10^4$) |
|---|---|---|---|---|---|
| 8 | 15.00 | 592.00 | 45.00 | 15.30 | 4.48 |
| 56 | Sdt | 965.60 | 45.00 | 11.60 | 9.63 |

Table 5.4 – Calculated hydraulic conductivity of fractured zones using the values of transmissivity calculated by the Boulton and Streltsova (1977) method. Sdt –Step drawdown test.

The values of hydraulic conductivity presented in Table 5.4 characterising fractures are certainly underestimated because the reported fractured areas have a dimension superior at the sum of the aperture of the existing fractures. Anyway, the analysis of the values presented in Tables 5.3 and 5.4 show that the calculated values for the hydraulic conductivity of fractures are about two orders of magnitude higher than the values calculated for the rock matrix. As showed in last sections, the values of hydraulic conductivity obtained for the rock matrix alone and for both matrix and fractures subsystems (characterised simultaneously as a single continuum media) are more reliable than the conductivity values calculated for the fractures alone. This is one of the reasons because the fractured rock matrix of carbonate rocks can be introduced in a regional flow model as a single continuum media, accommodating two of the three scales of heterogeneity presented at the start of the present chapter: the matrix and the well scales. It is important to remark that the description of the aquifer at these two levels of heterogeneity is a important part of the problem but is not enough for a global characterisation of the parameters allowing the correct simulation of the aquifer. As referred before, taking into account the levels of heterogeneity present in carbonate aquifers, the efficiency of a mathematical model to simulate flow in such systems depend on its ability to deal with the processes developed at different scales. Therefore, a model conceived to simulate flow at aquifer scale must include not only the heterogeneity's present at laboratory and well scales but also the influence of the dissolution channels present at regional scale. The problem in characterise that level of heterogeneity is the more difficult because actually no methods exits allowing the characterisation of the influence of the dissolution channels in the parameters distribution at regional scale.

Despite the impossibility in define the conduits parameters characterising the conduit network using direct methods it is possible to use a continuum discrete numerical model, defined at regional scale, in order to test some hypothesis about the role of the dissolution channels. However, before to define the method to do this, it is important to have some reference values expected for the structures introduced in the model simulating the channels network. The discussion of these values will be done, after the presentation of some remarks about the reliability of the employed methods to interpret pumping tests.

### 5.4 – Remarks about the reliability of parameters obtained in pumping tests

The employed methods to interpret pumping tests are analytical solutions of the equations 5.1 and 5.2 for the double continuum approach or of equation 2.1 (in chapter 2) for the single continuum approach. In addition of the limitations inherent to the simplifications assumed in order to obtain the analytical solutions (presented in section 5.2.1) some additional remarks must be done about practical problems related to experimental conditions:

- One of the simplifications assumed when dealing with the methodologies applied is that the well depth corresponds to the aquifer thickness. This is not true in any of the boreholes, which depth is, in many cases, far from attaining the base of the aquifer.

- The separation of hydraulic parameters for matrix and fractures needs detailed data in a very short period during the first instants of pumping. Many times, the accuracy of the methods employed to obtain the drawdown registry does not allow the collection of such detailed data.

- The data collected in the present case study correspond to "single well tests". Under these conditions the determined values for storage coefficient must be considered with precaution. In this kind of tests, transmissivity values are much more reliable than storativity values. Unfortunately in the cases where observation points were available in the vicinity of extraction wells, the perturbation induced in the aquifer was not enough to affect the potential at the distance required to produce drawdown in that points.

The above limitations related to the experimental conditions are very common. The last one is not so frequent in porous media. However, very often in carbonate rocks the drawdown does not affect piezometers located at very short distances from the pumping wells. Unfortunately it was true in all the tests performed in the present case study, despite the numerous cases where the tested wells are located near observation points. The location of the wells where the pumping tests were performed is showed in Figure 5.12.

Despite the limits in reliability ascribed for pumping tests, the analysis of the presented results show the possibilities in obtain reliable point values for hydraulic parameters characterising the rock matrix and the fractured rock matrix. The determination of these values using techniques for the interpretation of pumping tests, based in the single continuum and in the double continuum approaches, shows that the values obtained in both cases led to coherent interpretations. However, the characterisation of the parameters of the fractures system alone, which is theoretically possible using double continuum models, is more difficult and, in practice, the calculated values are only rough approximations. Therefore, considering the need in obtain parameters characterising the fractured rock matrix in order to simulate flow at regional scale it is preferable to characterise the heterogeneity at the rock matrix scale and at well scale using a single value, characterising both subsystems as a single continuum.

Despite the limits of double continuum methods in characterise the parameters of fractures, it is important to remark that these methods allow a high degree of accuracy in the prevision of the hydraulic behaviour of wells in carbonate rocks. This is true not only for the analysis of drawdown in wells pumping at a constant discharge rate but also for complex situations as variable pumping rates and well recovery after the end of a given pumping period. All these situations where analysed in real situations and it was showed that double continuum methods are a reliable tool to support the correct management of wells in carbonated rocks.

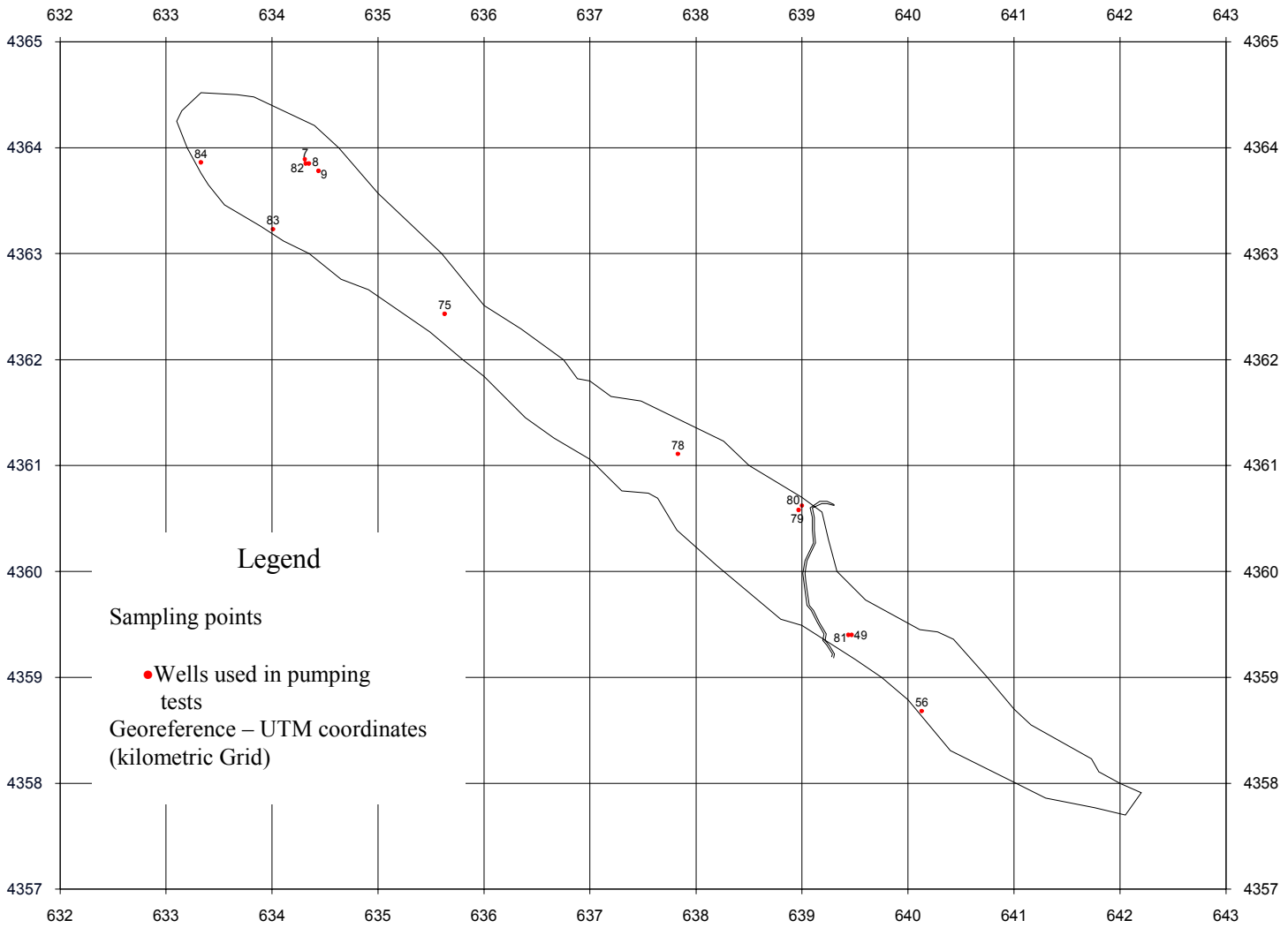


Fig. 5.12 – Location of wells used for pumping tests, limits of the aquifer system and location of Sever River.

**5.5 – Theoretical considerations about hydraulic parameters of conduits**

The more difficult step when modelling carbonated aquifers at regional scale is to define a distribution of parameters, which is affected by the presence of dissolution channels controlling the flow pattern at kilometre scale. In this case, the parameters obtained in pumping tests cannot capture the distribution of parameters related to the presence of heterogeneities developed at regional scale where the dominant processes change from matrix flow or fracture flow to preferential flow across dissolution channels.

The values of hydraulic parameters controlling flow in saturated dissolution channels cannot be easily calculated by direct experimental methods. If channels of circular section are considered as a hypothetical geometry for the dissolution voids developed at regional scale, the Darcy and Poiseuille laws can be applied to approximate the order of the magnitude for the parameters characterizing the karstic conduits. These laws express the specific discharge as function of loss in head and an analogy can be established in order to characterise the parameters of dissolution channels as follows.

In a tube of length $l$ and radius $r$ submitted to different pressures in extremities, the discharge Q is calculated by:

$$Q = 2\pi \int_0^r u\, v(u)\, du \qquad 5.11$$

where $v$ ($u$) is the velocity distribution in a vertical cross section.

The average velocity (or specific discharge) $v$ of the particles is expressed by:

$$v = \frac{q}{A} \qquad 5.12$$

where $A=\pi r^2$ is the area of the tube perpendicular to the flow direction.

Using the Poiseuille law, the average velocity of particles is calculated by:

$$v = \frac{r^2}{8} \cdot \frac{\Delta p}{\mu l} \qquad 5.13$$

where $\mu$ is the water dynamic viscosity [$M \cdot L^{-1} \cdot T^{-1}$],and $\Delta p$ is the pressure decrease over the distance $l$.

Thus the flow rate $Q$ can be expressed for an area $A$ perpendicular to the flow direction by:

$$Q = \frac{r^2}{8} \cdot \frac{\rho g}{\mu} \cdot \frac{\Delta h}{l} \cdot A \qquad 5.14$$

where $\rho$ is the water density [$M \cdot L^{-3}$], $g$ is the acceleration of gravity [$L \cdot T^{-2}$].

The terms in equation 5.14 can be directly related to the Darcy law by:

$$Q = k \frac{\rho g}{\mu} \cdot \frac{\Delta h}{l} A \qquad 5.15$$

where $k=r^2/8$ is the intrinsic permeability.

Taking this into account the conductive term $T_d$ [$L^3 . T^{-1}$] for a conduit with circular section becomes:

$$T_d = \pi r^2 \frac{r^2}{8} \cdot \frac{\rho g}{\mu} \qquad 5.16$$

The validity of that analogy can be done only for conditions corresponding to laminar flow. The limits of that condition can be identified with the Reynolds number $R_e$, a dimensionless number that express the ratio of inertial to viscous forces evolved in flow (Freeze and Cherry, 1979; Bear and Verruijt, 1987):

$$R_e = \frac{\rho v D}{\mu} \qquad 5.17$$

were $D$ is some representative microscopic length characterising the rock matrix (as average diameter of soil particles). The direct proportionality between flow rate and loss in head of Darcy and Poiseuille laws is valid as long as the Reynolds number does not exceed some values between 1 and 10 and thus the flow is laminar.

The storativity $S_d$ of a circular channel can be defined for a given diameter considering the concept of specific storage $S_s$ expressed by equation 2.4 introduced in Section 2.1:

$$S_s = \rho g(\alpha + n\beta)$$

were $\beta$ is the fluid compressibility $[L \cdot T^2 \cdot M^{-1}]$.

For the particular case of a circular channel, eliminating the aquifer compressibility $\alpha$ and considering that the porosity $n$ takes a value of 1, the storativity $S_d$ $[L]$ is defined as:

$$S_d = \rho g \beta \pi r^2 \qquad 5.18$$

In Figure 5.13 the values of conductivity and storativity for channels calculated with the expressions 5.16 and 5.18 are showed as function of diameter.

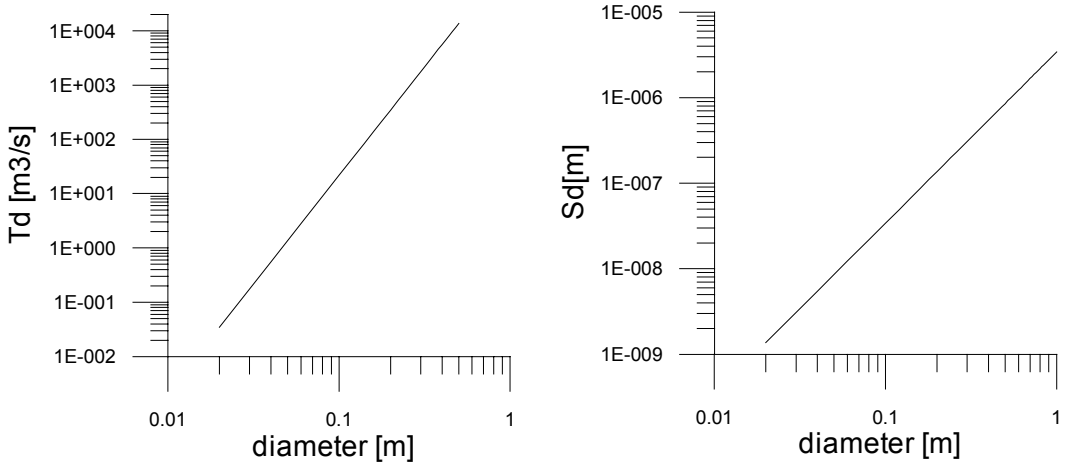


Fig. 5.13 – Conductivity and storativity of conduits defined as function of diameter for channels with circular section.

According the above theoretical considerations it must be remarked that both storativity and conductivity parameters for conduits are function of diameter. Thus, despite the references across this work regarding storativity and conductivity of the dissolution channels hydraulic properties it must be considered that these parameters are not independent of each other. The relation $T_d/S_d = r^2/(8\mu\beta) \approx 2.5 \times 10^{11}\ r^2$ that can be established using equations 5.16 and 5.18 show that both parameters could be considered as correlated by $r^2$.

**5.6 – Analysis of the regional distribution of hydraulic head gradients as a tool to interpret the role of conduit networks in the definition of the flow pattern of carbonate aquifers**

The presence of dissolution channels with metric dimensions in the saturated zone was often reported in all Castelo de Vide aquifer sectors. As flow in conduits with such dimensions is turbulent under the hydraulic head gradients observed in natural conditions and the programs used for flow simulation at the aquifer scale can only simulate laminar flow in the channels, the diameter of conduits with parameters equivalent to the ones characterising the "artificial conduit network" used for flow simulations in chapter 6 is only of few centimetres. Otherwise, if metric values were used to define equivalent parameters of conduits in the "artificial conduit network", simultaneously with flow simulation in laminar conditions, the calculated water transferences would be superior to the real ones by many orders of magnitude.

Anyway, it must be considered that a strong contrast exists between hydraulic conductivity of carbonate rocks and the conductive parameter characterising conduits. The difference in the order of magnitude for these parameters in both subsystems is in the order of 6 to 9 (or more) orders of magnitude. Therefore it is reasonable to accept that the propagation of any excitation affecting hydraulic head must be almost instantaneous in the channel network, when compared with slow changes in hydraulic head occurring in a more or less fractured rock matrix. In these conditions, the eventual presence of a well-developed conduit network, controlling flow at aquifer scale, will be responsible for a general flow pattern characterised by the existence of a smooth equipotential surface with a gentle slope toward the aquifer discharge areas. This is one of the conclusions presented by Kiraly *et al.* (1995, p. 203) from the analysis of a synthetic karst aquifer were conduits are well connected throughout the entire flow domain. It must be remarked that such homogenisation of potentials in the horizontal direction is entirely compatible with the presence of strong contrasts in hydraulic head along any vertical line in the aquifer, when conduits are present. It is well known that such hydraulic behaviour does not reflect the observations in real carbonate aquifers were diffusive and conduit flow exists. If it is true that strong changes in hydraulic head are always identified in real carbonate aquifers along the vertical direction, it is also true that a "rather gentle groundwater table" cannot be observed in real systems. That difference between the synthetic karst aquifer presented in Kiraly *et al.* (1995) and the hydraulic behaviour detected in the Castelo de Vide aquifer is possibly related to the presence, in the real system, of deficient hydraulic continuity of the conduits between discharge and recharge areas that are not considered in the theoretical syncline.

Taking into account that the propagation of any excitation affecting hydraulic head must be almost instantaneous in the channel network, when compared with slow changes in hydraulic head occurring in a more or less fractured rock matrix, we propose that the detection of regional trends in the spatial distribution of hydraulic head gradients in carbonate aquifers can be related to the efficiency of the conduit network in establish hydraulic connection between different parts of the aquifer. The interpretation of spatial distribution and temporal variability of hydraulic head at regional scale in the Castelo de Vide carbonate aquifer is a useful way to discuss this problem in a real context (figure 5.14).

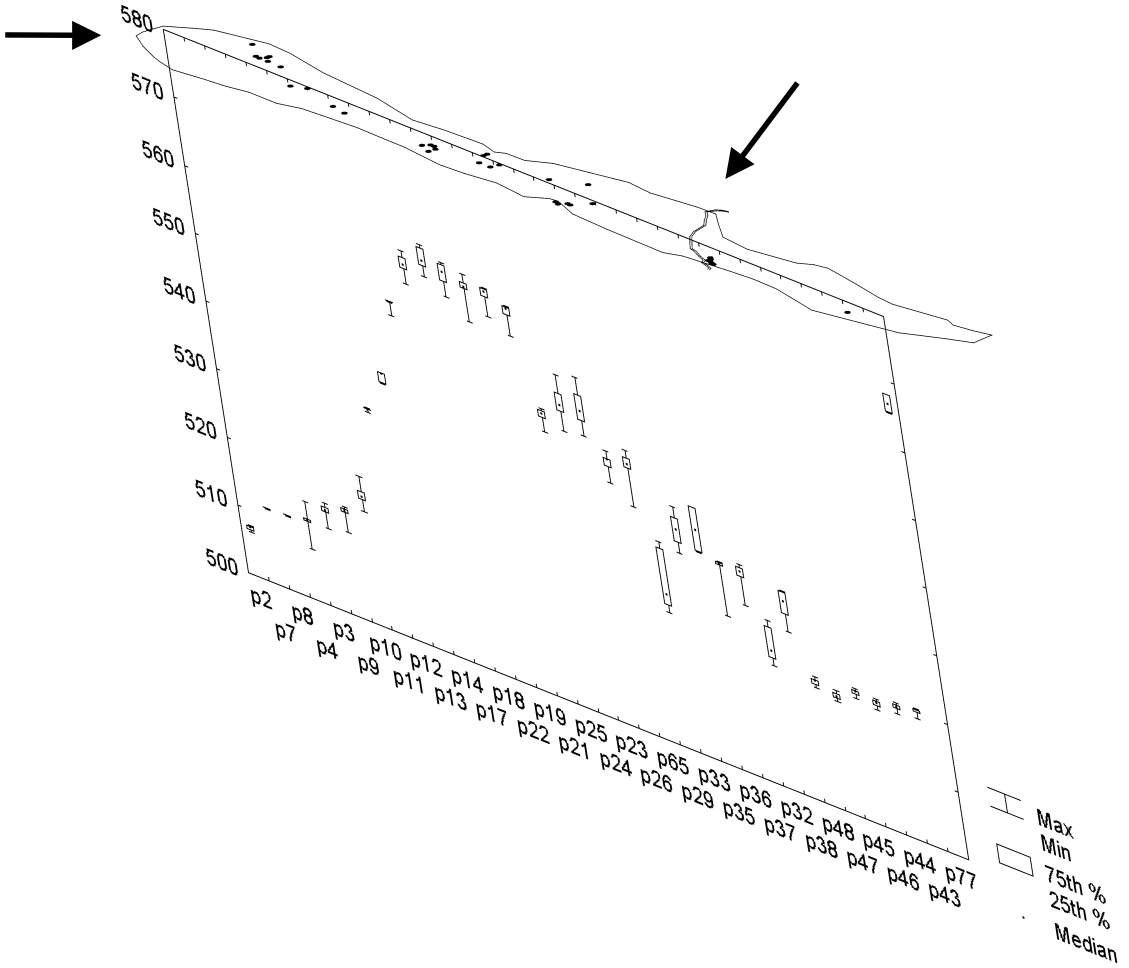


Fig. 5.14 – Spatial distribution and temporal variability of hydraulic head in the Castelo de Vide Carbonate aquifer. Aquifer discharge areas are represented by black arrows.

Dissolution voids with metric dimensions were often reported at the time of wells drillings in all the aquifer sectors. Moreover, the highest values in hydraulic head detected in the aquifer were determined from measures taken in observation points located between wells 11 and 17 in figure 5.14. Large dissolution voids where identified in some of these wells. This is the case for wells 74 and 75, which location can be seen in figure 3.12 (section 3.5.1). The dimension of dissolution voids intercepted by these wells can be seen in figure 3.13 (section 3.5.2). Boxplot graphics for hydraulic values cannot be presented for wells 74 and 75 in figure 5.14, because they were drilled recently and no systematic measures exist for these points. If we analyse simultaneously:

- The observed hydraulic head in wells between observation points 11 and 17.

- The presence of conduits with metric dimensions in the saturated zone often encountered in that area of the aquifer

- The outflow volumes in the aquifer discharge areas

It can be easily shown that the dissolution channels identified in that area cannot be part of a conduit network controlling flow at aquifer scale. In other words, these conduits are responsible for the control of flow pattern in some parts of the aquifer with different degrees of connectivity between them. Therefore the general conduit network must be composed by independent or semi independent sectors.

The identification of these conditions is very important because an analysis of the systems at these levels (order of magnitude of conduit parameters, spatial distribution in hydraulic gradients and global water balance) allow the establishment of limits for the hypothesis that can be conceived about the role of the conduit network in controlling the flow pattern at aquifer scale.

The definition of limits for the connectivity degree of a given conduit network, present in a given aquifer sector, is not necessarily based on the assumption of spatial discontinuity of dissolutions channels. Factors as changes in diameter and filling of dissolution channels can induce losses in head important enough to justify the existence of regions of a conduit network (with active circulation in the saturated zone) with deficient connectivity with the aquifer discharge areas. According the analysis of the conditions prevailing in the areas where systematic increase of hydraulic head were identified in the Castelo de Vide aquifer, some factors that could be in the origin of deficient hydraulic connection between different sectors of the conduit network are the occurrence of clay minerals filling channels, or important changes in shape and diameter of conduits. These features could induce losses in hydraulic head important enough to justify the existence of deficient hydraulic connectivity within spatially continuous dissolution voids. For example, the situation illustrated in diagram D in figure 5.15 was often identified in wells drilled in the vicinity of the groundwater divides between Castelo de Vide and Escusa aquifer sectors.

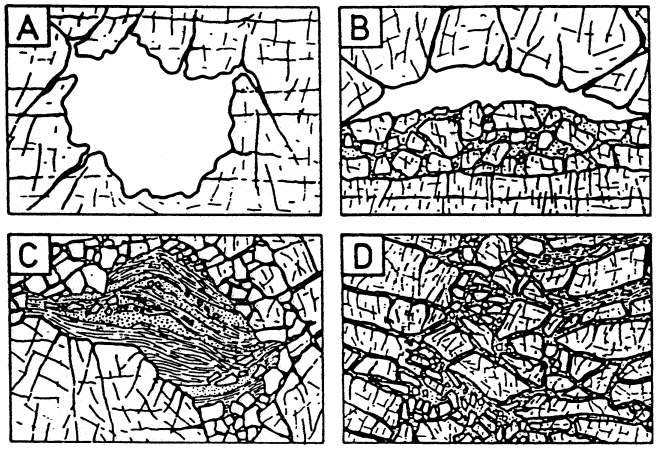

Fig. 5.15 – Types of filling of karst channels. A – open karst channels; B – karst channels partly filled with breccia zones; C - karst channels filled with fine-grained sediments; C – breccia zones. Adapted from Adamczyk *et al.* 1988.

These aspects are very important in the definition of some restrictions about the role of the conduit network in the definition of the global flow pattern in the aquifer. As will be shown in the next chapter the aspects discussed in the present section were essential at the time of the definition of an "artificial conduit network" that must be defined in order to implement a discrete continuum model at aquifer scale.

## 5.7 – Problems related to the linkage of parameters characterising hydraulic conductivity at the well and at the regional scales

At the same time we have an equivalent hydraulic conductivity value characterising the aquifer at regional scale (determined in Chapter 4) there are also point values for hydraulic conductivity resulting from the interpretation of pumping tests presented in previous sections of the present chapter. These values, characterising the aquifer at different levels of scale, are presented together in figure 5.16. The values determined in pumping tests are distributed over four orders of magnitude as showed in the histogram in that figure. The representation of these values in crescent order (graphic at left in figure 5.16) shows that only few of the highest values determined at well scale are near the value determined at aquifer scale (represented by the dashed line in the same graphic). These results reflect the change of hydraulic conductivity values with scale, often encountered when diffuse and conduit flow are present in the same flow domain.

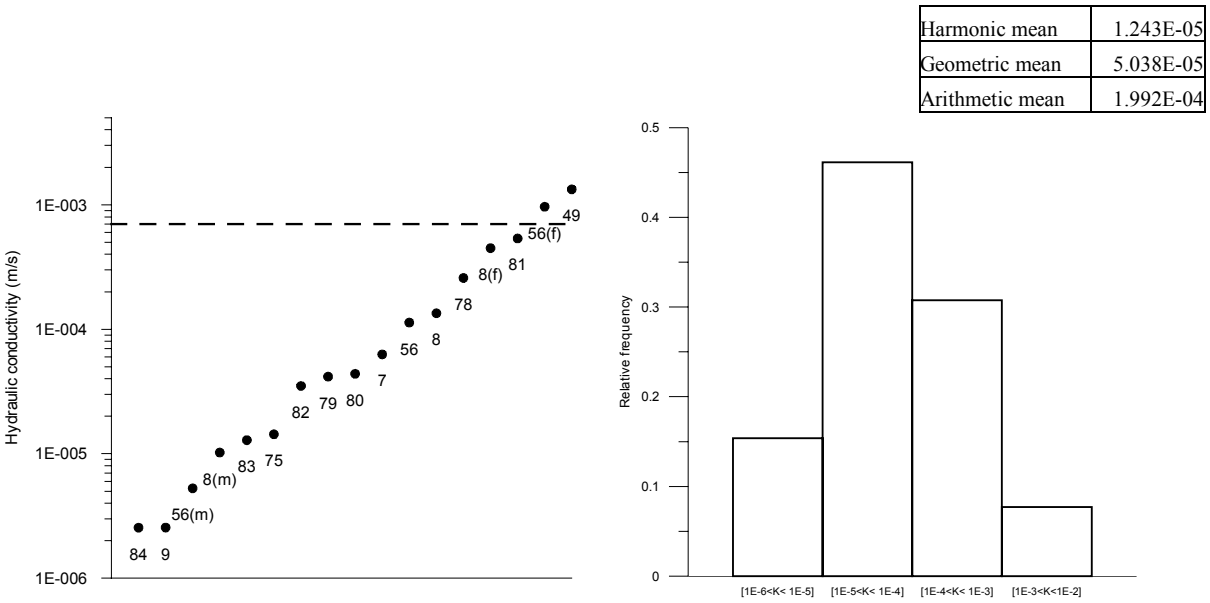


Fig. 5.16 – Hydraulic conductivity values calculated from the interpretation of pumping tests and equivalent hydraulic conductivity determined at aquifer scale. In the graphic at left the points identified by the suffix (m) and (f) correspond to values determined for the rock matrix and fractures, respectively, when double porosity models were applied to interpret pumping tests. The dashed line in this graphic is at the position of the calculated value of hydraulic conductivity characterising the aquifer at regional scale (see section 4.2 in chapter 4), which corresponds to $7.0\times10^{-4}$m/s. This graphic shows very clearly the scale effect affecting the values of this parameter. Note that the values are displaced along the *x* axis only to make the figure readable. The histogram and average values at right illustrate very well the inefficacy of arithmetic mean in characterise hydraulic conductivity values in strongly heterogeneous media.

In this cases upscaling of hydraulic conductivity is even more difficult than in the case of porous media where groundwater flow models are usually implemented using the single continuum approach. The reason why the upscaling techniques developed to define a regional distribution of hydraulic parameters in heterogeneous porous media cannot be used in flow domains where diffuse and conduit flow are present in the same flow domain can be illustrated by the analysis of the hydraulic behaviour often encountered in wells drilled throughout carbonate aquifers. In order to discuss this aspect we will anticipate some results obtained with the regional discrete continuum model presented later in this work. This will be done by the analysis of drawdown produced by pumping wells, in different conditions, simulated in one of the variants of the 3-D regional continuum discrete model, which results are discussed in chapter 6.

If we analyse the parameters obtained from pumping tests in wells drilled across the rock matrix without interception of important dissolution channels (as illustrated in the equipotentials at right in figure 5.17). The values determined in these conditions are often in agreement with values resulting from laboratory experiments characterising hydraulic conductivity at rock matrix scale.

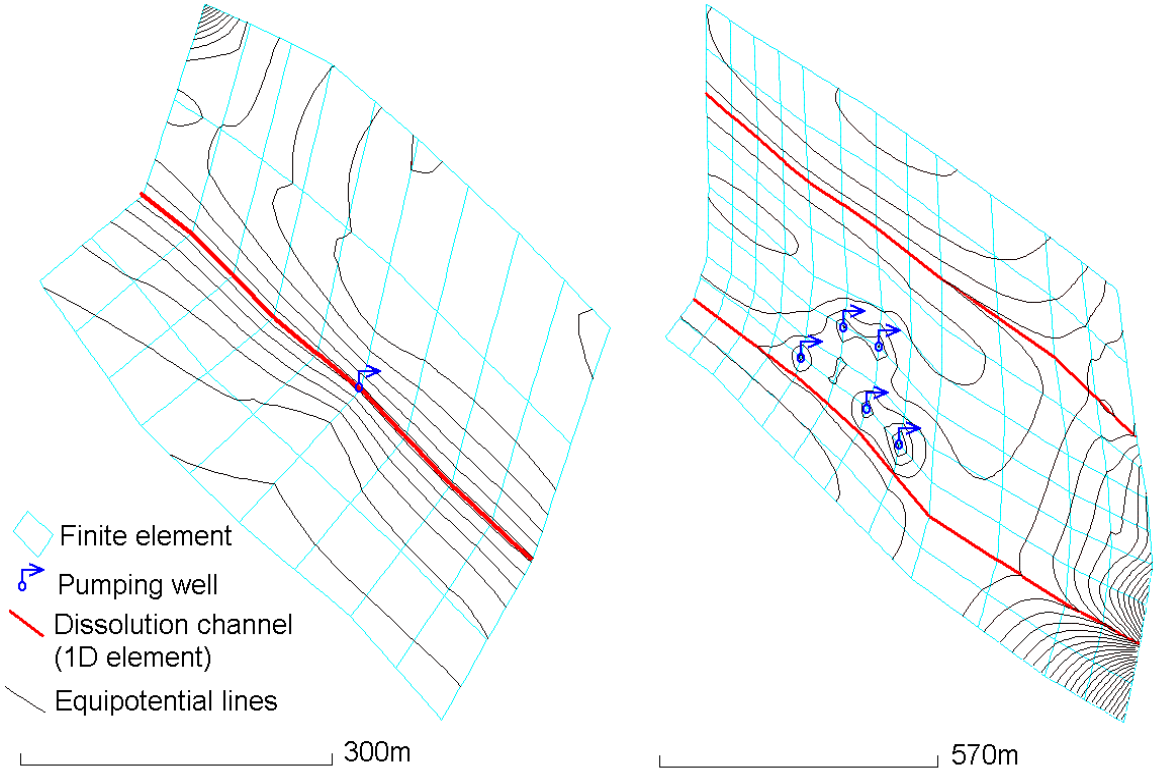


Fig 5.17 – Drawdown produced by pumping wells in carbonate aquifers simulated using a continuum-discrete model.

– left, well pumping in a high hydraulic conductivity 1-D element surrounded by low hydraulic conductivity 3-D elements. The pumping rate is 15 l/s and the equidistance of the isolines 2m;

– right, group of five wells located in low hydraulic conductivity 3-D elements near high hydraulic conductivity 1-D elements. The pumping rates of the wells vary between 0.25 and 0.5 l/s. Isolines equidistance is 0.7m.

Both situations where extracted from the same transient model corresponding to a simulation of a irrigation period in 1997. The quadrilateral polygons are horizontal plane projection of 3-D quadratic elements with 20 nodes in the top surface of the model. Lines marked in bold are 1-D elements with high hydraulic conductivity located at variable depth under the surface of the model (there are two slices of 3-D elements between the 1-D elements and the top surface of the model showed in the figures). The hydraulic conductivity values are: k=10 m/s, for 1-D elements and $k=10^{-6}$m/s for the surrounding low hydraulic conductivity 3D elements (see chapter 6 for further details).

In the situation illustrated by the equipotentials on the left hand in figure 5.17, when pumping tests are performed in wells crossing dissolution channels a transmissivity value (usually very high) is obtained. However this value cannot give any information about how the structure crossed by the well affect the parameters distribution at the conduit network scale. In practice the dissolution void can affect the parameters distribution only in the well vicinity (at local scale) or be part of a channel controlling the existence of conduit flow at the scale of the entire aquifer. In these conditions, since the pumping tests wells are interference tests it cannot be expected that they capture parameters which distribution is defined by structures which dimension is superior at the scale where the interference is produced. The practical meaning of these limitations of pumping test is the definition of a limit for the applicability of the respective determined parameters, which corresponds roughly to the aquifer thickness.

# Chapter 6

THREE DIMENSIONAL FLOW MODEL AT THE AQUIFER SCALE

---

Contents

## 6.1 – Introduction

All the aspects discussed in the previous chapters are related to the characterisation of the Castelo de Vide carbonate aquifer on the different levels required to implement a discrete continuum flow model. Despite the inherent uncertainty associated to the methods applied in order to characterise the system geometry, to estimate recharge and discharge rates and to assign boundary conditions (chapter 3), we assume that the actual knowledge on these levels allows an acceptable description of real conditions present in the real system. However it must also be assumed that the present knowledge of spatial parameter distributions at the regional scale does not allow the definition of a discrete continuum model able to deal with a global representation of the aquifer. The main source of uncertainty is related to the lack of knowledge of the role of the existing conduit network in the aquifer, with respect to the definition of the regional flow pattern.

Different mathematical models were extensively applied throughout this work in order to determine hydraulic parameters at the aquifer and at the well scales. In chapter 4 equivalent hydraulic conductivity values were estimated separately for three flow systems identified in the aquifer (using a single continuum analytical model) and for the entire aquifer system (using a single continuum finite element model). In chapter 5 hydraulic conductivity values were calculated by the interpretation of pumping tests (using single continuum and double continuum analytical models).

Despite the possibilities to obtain reliable estimations of hydraulic conductivity at the well and at the aquifer scales these values cannot be used to define a representation of the aquifer at an intermediate scale. That limitation is related to the presence of a conduit network, which as an influence on parameters distribution that cannot be captured by pumping tests or by methods allowing the determination of equivalent parameters determined at the aquifer scale. As the characterisation of geometry and hydraulic parameters of a conduit network is always fragmentary and incomplete, its role in the definition of the observed regional flow pattern in a carbonate aquifer is very difficult to establish. In the present case study we propose that the analysis of trends in hydraulic head gradients in the aquifer, allow the definition of some restrictions regarding the role of the conduit network in the definition of the regional flow pattern. These restrictions can be introduced in to an “artificial conduit network” in a discrete continuum model in order to approximate the role of the “real conduit network” and thus to contribute to the respective calibration.

## 6.2 – Method for the definition of an “artificial conduit network” in a discrete continuum model

The characterisation of geometry and hydraulic parameters of a conduit network present in a given carbonate aquifer cannot be done by direct methods. However, as discussed in section 5.6, the analysis of spatial distribution of hydraulic head gradients could contribute to interpret the role of conduit flow in the definition of the regional flow pattern in carbonate aquifers.

In the present case study an “artificial conduit network” was defined on the basis of the definition of sectors, composed by interconnected branches, with different degrees of connectivity with the discharge areas. These conduits were defined without any pretension to describe the real geometry of the real conduit network. The structure was defined using indicators allowing the identification of points or areas where some basic features of the real conduit network can be inferred by both: (1) punctual direct observations and (2) analysis of the hydraulic behaviour of the system. Therefore, the similarities between the “artificial conduit network”, defined in this way, and the “real conduit network” present in the aquifer are essentially related to hydraulic properties and not to the respective geometries. However it is important to remark that some geometric properties are also respected. A geometric feature that can be accurately reproduced in the model is the position of the swallow holes where concentrated recharge has been observed. This aspect is very important because these points represent the contact of the conduit network with the model surface.

The coherence of the “artificial conduit network” defined by the sequence of steps presented below can be checked by the investigation of its role in the definition of the regional flow pattern using a discrete continuum model. Therefore, the four steps proposed for the definition of the “artificial conduit network” can be considered as a strategy for model calibration.

1 – Definition of an “artificial conduit network” controlling flow at aquifer scale

The definition of an “artificial conduit network” started by mapping of points where the occurrence of dissolution channels with active circulation had been reported. These points were tracked down by the identification of features such as karstic landforms associated with the presence of swallow holes and the identification of conduits in boreholes. A primary “artificial conduit network” was defined by the connection of the points in which dissolution channels were known to exist. That task was accomplished by the definition of regional conduits (parallel to major structural alignments identified in the aquifer) interconnected by transversal conduits (linked to the aquifer surface in points where concentrated recharge is known to take place). A conduit network defined in this way assumes that channels are controlling flow at the scale of the entire aquifer.

At this point it is very important to remember that, conductive parameters characterising conduits present in carbonate aquifers often differ by 6 to 9 (or more) orders of magnitude from the hydraulic conductivity values of "low permeability rock volumes". Therefore it must be accepted that the propagation of any excitation affecting hydraulic head must be almost instantaneous within the channel network, when compared to slow changes in hydraulic head occurring within a more or less fractured rock matrix. Under these circumstances any "artificial conduit network", defined by the above described process, will be responsible for a general flow pattern characterised by the existence of a smooth equipotential surface with a gentle slope toward the aquifer discharge areas. Obviously, such hydraulic behaviour does not reflect the observations made in all real carbonate aquifers were diffusive and conduit flow exists.

Based on these considerations we assumed that different branches in a conduit network, with different degrees of connectivity with the aquifer discharge areas could be detected by the identification of regional trends affecting the spatial distribution of regional hydraulic head gradients in the "real aquifer". In other words, it is assumed that changes in hydraulic head gradients, with expression at the aquifer scale, are related to the efficiency of the conduit network in establishing hydraulic connection between different parts of the aquifer.

> 2 – Identification of sectors in the conduit network based on the interpretation of regional trends affecting the distribution of gradients in hydraulic head in the "real aquifer"

For the above reasons it is assumed that the detected trends in regional hydraulic head gradients are related to the efficiency of the conduit network in establishing hydraulic connection between different parts of the aquifer. That assumption is supported by the analysis of the spatial distribution and temporal variability of hydraulic head in the Castelo de Vide aquifer, where some restrictions on the connectivity of different branches of the conduit network with the aquifer discharge areas were established on the basis of both experimental evidence and theoretical considerations. In fact, taking into account: (1) the observed distribution of gradients in hydraulic head; (2) the order of magnitude for the conductive parameter of conduits with metric width in the saturated zone (which were identified in all aquifer sectors) and (3) the outflow volumes in the aquifer discharge areas, it can be shown that the channels identified in some aquifer sectors cannot be part of a conduit network controlling flow at the aquifer scale.

It is important to remark that the definition of limits for the capacity of the conduits in establish an efficient hydraulic connectivity between adjacent parts of the aquifer is not necessarily based in the assumption of spatial discontinuity of dissolutions channels. Factors as changes in diameter shape and/ or filling of dissolution channels can induce losses in head high enough to justify the deficient hydraulic connexion in a spatially continuous conduit.

In practice, the identification of zones where gradients are systematically steeper in the aquifer were associated with the presence of factors limiting the capacity of the conduits in establishing an efficient hydraulic connectivity between adjacent parts of the aquifer.

> 3 – Definition of sectors in the initial "artificial conduit network"

After the identification of sectors in the "real conduit network", based on the detection of positive "regional anomalies in hydraulic head gradients" the conductive parameters characterising the initial "artificial conduit network" can be changed in order to take into account the presence of such sectors.

> 4 – Assessment of the role of the "artificial conduit network" in the definition of the aquifer regional flow pattern

Finally the investigation of the impact of the sectors defined in the "artificial conduit network" in the regional flow pattern is performed using the discrete continuum model. This is part of the model calibration process and is done by comparing the model predictions with field data.

Using the method outlined in the above four points, the regional discrete continuum model was used to assess the impact of conduit networks with different configurations in the definition of the hydraulic behaviour observed in the aquifer. Therefore, in addition to using it to assess the coherence of information obtained with other techniques, the implemented discrete continuum model could be used in itself as a tool contributing to the characterisation of the system.

### 6.3 – Finite element mesh

A schematic general framework for the use of numerical models implemented at aquifer scale was presented in chapter 2 focussing on the relations between the model and the programs used to perform pre-processing and pos-processing tasks. In the following sections the technical description of the discrete continuum model is done on the level of the geometry and structure, including the definition of the initial geometry defined for the "artificial conduit network".

Pre-processing tools are computer programs used to manage geo-referenced information in order to translate the geological data in computer files expressing the geometry of the system, boundary conditions and material characteristics (as hydraulic parameters) in a format compatible with the input files required by the model. In modern commercial finite element models these tools as well as post-processing programs are available in the same software package. However, as such facilities are not available for the implementation of discrete continuum models, the aspects related to the generation of the finite element mesh, allowing the use of this method for the Castelo de Vide carbonate aquifer, are discussed in detail.

#### 6.3.1 – Geometry and structure

Mesh generators available for standard single continuum finite element models cannot be used to generate a finite element mesh with the characteristics required to use the discrete continuum approach. This is due to the fact that these mesh generators are not designed to handle elements with 1-D, 2-D and 3-D in the same grid. The mesh constructed for the model presented in this chapter includes: (1) 3-D elements to simulate the low permeability rock volumes containing lower order fractures or channels; (2) 1-D elements to simulate the role of the higher order dissolution conduits, which define the "artificial conduit network" and (3) 2-D elements to simulate diffuse discharge at the top of the aquifer. The actual absence of software generating such meshes is one of the limiting factors in the use of the discrete continuum approach in applied hydrogeology.

##### 6.3.1.1 – Definition of the model geometry

As observed in drilled wells near the aquifer limits the contact of the carbonate rocks with the adjacent lithologies can be reasonably described by vertical no-flow boundaries. Taking the aquifer thickness into account the lateral limits of the model are represented by vertical surfaces about 200m high. The shape representing the top of the aquifer is the average 2-D equipotential surface defined in Section 3.5.2.1 and represented in Figure 3.14. A somewhat different criteria was used in the definition of the 2-D cross-sectional model used in Chapter 4. At this time, taking into account that the distance between the ground surface and water level in the aquifer is always very short (less than 25m), the top of the aquifer was defined by a ground surface profile, which was slightly smoothed. However, using the same method to define the 2-D surface of the top of the 3-D model lead to a shape with slope ruptures, depressions and small hills. As the constructed model is used to simulate a fully saturated flow domain such a wiggly surface is less realistic than the one defined on the basis of average equipotential surface of the aquifer.

The initial step for the construction of the finite–element mesh was the generation of linear quadrilateral elements with four nodes respecting the shape of a polygon defining the lateral limits of the aquifer. That task was performed using the mesh generator available in the finite element simulation package FEFLOW (Diersch, 1998). The 2-D finite element mesh represented in Figure 6.1 was generated with this software. An additional node was defined later on each side of every linear element in order to define quadrilateral quadratic elements with eight nodes.

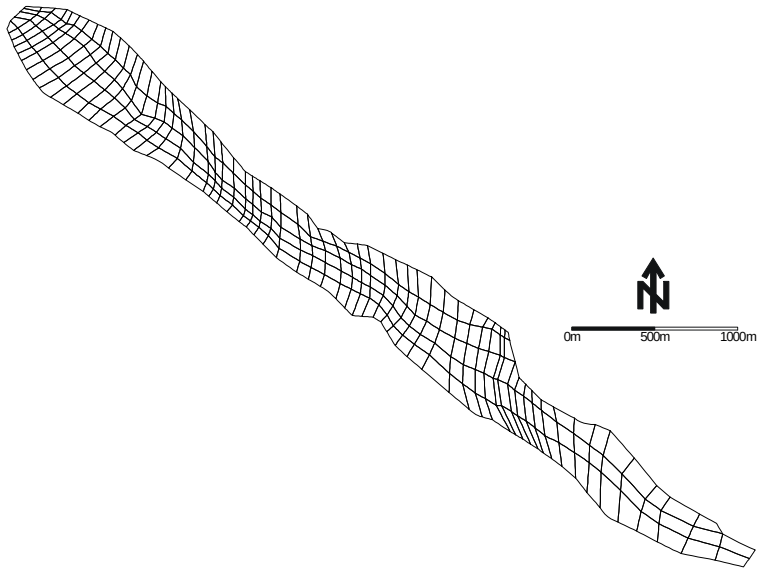


Fig. 6.1 - First step of the finite element mesh generation corresponding to a coarse discretization of the 2-D top of the aquifer.

The finite element mesh defined in this way corresponds to a coarse discretization of the plane geometry of the aquifer top with 978 nodes and 281 quadratic elements with 8 nodes each. The discretization of this mesh is not sufficient to assure the numerical stability of the calculations, required to perform the flow simulations that will be presented later. However, the subdivision of this mesh was performed only after the generation of a coarse 3-D mesh, which top surface correspond to Figure 6.1. This is related to the need of defining the 1-D geometry to be embedded in the 3-D elements representing the “artificial conduit network”. As no available mesh generators exist, which allow the automatic construction of 1-D elements in a 3-D grid, the 1-D elements simulating the conduit network were defined in an input file read by the model, describing the connectivity of the nodes. Therefore, the refinement of the mesh was performed after the introduction of the 1-D elements in the mesh in order to reduce the size of the files registry manipulation.

According to its topology the mesh is an “unstructured mesh” because the position of the nodes does not obey to a regular spatial pattern in space. That kind of mesh can take full advantage of the possibilities in simulating flow domains with complex geometry allowed by the finite element method. Unstructured grids are defined in opposed to structured grids, where an array of points with a well-defined and regular relationship of each point with its neighbour can be defined. Structured grids are easy to generate but cannot be used to define complex irregular geometries.

The second step in the process of mesh construction consists in automatically extending the mesh in Figure 6.1 “downward”. This was done by the generation of four slices of hexahedral finite elements with 20 nodes having the top geometry defined by the 2-D elements shown in Figure 6.1. This operation was performed using a pre-processing tool available for the FEN codes allowing the extension of 2-D structured or unstructured grids in to 3-D grids. However that operation is performed in a “structured way”, leading to newly generated slices having the same plan geometry as the 2-D original surface. The 3-D finite element mesh represented in Figure 6.2 was constructed in this way.

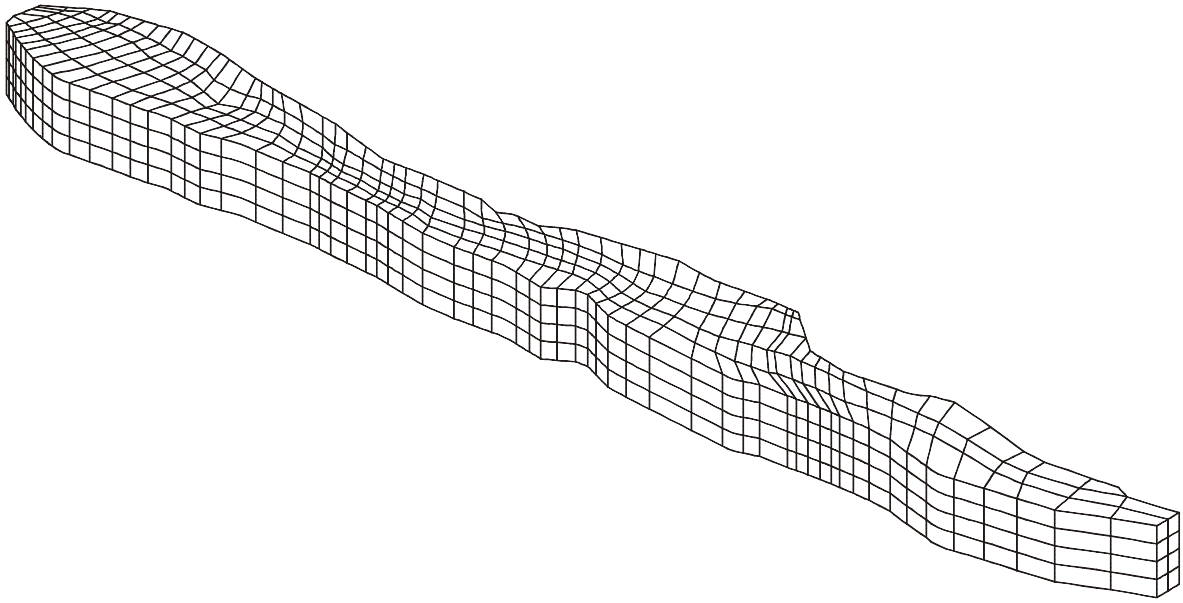

Fig. 6.2 – 3-D finite element mesh with four slices of hexahedral quadratic elements with 20 nodes constructed by extending of the 2-D finite element mesh shown in Figure 6.1. The maximum length of the model along its axis is 8,951m. The aquifer is represented with a 3 times vertical exaggeration.

At the stage represented in Figure 6.2 the 3-D mesh still has the 2-D elements shown in figure 6.1 on the top surface of the model. In addition to these elements there are 1124 3-D hexahedral quadratic elements with 20 nodes. Note that the number of nodes does not increase by the fact that a 2-D element exists at the top of the 3-D elements. This is due the fact that eight nodes of each 2-D element define simultaneously the top surface of the subjacent 3-D element.

**6.3.1.2 – Definition of the initial "artificial conduit network" controlling flow at the aquifer scale**

After the generation of the 3-D geometry shown in Figure 6.2, 1-D elements defining a conduit network where introduced in the grid. The justification for the structure defined for the initial "artificial conduit network" presented here is explained in detail in section 6.2. At that time the structure was defined prior to any previous consideration about the channel network density. As the 1-D elements can be "active" or "not active" in a given simulation, the initial criteria was to define the entire channel network with a high density in order to avoid the need in introducing additional conduits in later phases of the calibration process. The initial conduit network was continuous over the entire flow domain. Practically this means that all the present branches were connected in some point to the total structure. Therefore, in simulations performed using that initial "artificial conduit network" the hydraulic head propagation is very rapid throughout the entire model.

An important aspect to keep in mind is the fact that the "artificial conduit network" has 15 nodes coinciding with points at the top of the aquifer located where swallow holes were identified in the field. These points allow the simulation of concentrated recharge directly into the "artificial conduit network" as opposed to the diffuse infiltration simulated on the surface of the model throughout the 2-D elements on the top of the mesh. The location of these points can be seen in Figure 3.5 (Section 3.3) and corresponds to the location of the intersection of sinking streams with the carbonate aquifer limits. This aspect is particularly important because the points where concentrated recharge is simulated are points known to exhibit such phenomena in the real system.

In Figure 6.3 the finite element mesh is shown with the 1-D elements representing the "artificial conduit network". At this stage the grid has 281 2-D quadratic elements with 8 nodes each, 1124 hexahedral elements with 20 nodes each and 243 1-D elements with 3 nodes each. Note that the total number of nodes of the entire grid counts 6286. Again, the introduction of 1-D elements does not increase the total number of nodes because the 3 nodes defining each 1-D element simultaneously define corners of 3-D hexahedral finite elements (see Figure 2.1 in Section 2.3.2).

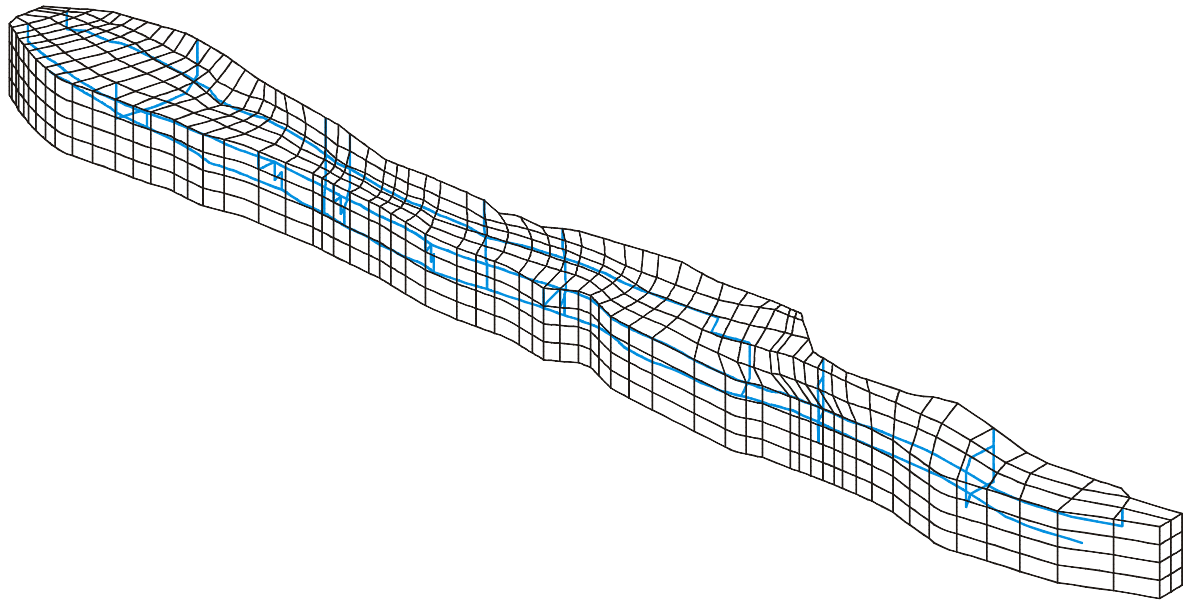

Fig. 6.3 – 3-D finite element mesh with four slices of hexahedral quadratic elements with 20 nodes and with 1-D elements representing the “artificial conduit network” embedded in the 3-D elements. The maximum dimension of the model along its axis is of 8,951m. The aquifer is represented with a 3 times vertical exaggeration.

Three major branches sub-parallel to the long axis of the aquifer compose the basis of the conduit network. Two of these branches where introduced between the first and the second slices of 3-D elements. A third major conduit was placed between the third and fourth slices of 3-D elements. These main branches are connected to the surface in 15 points corresponding to swallow holes identified in the real system close the aquifer limits. Finally, there are transversal conduits linking the major branches in different regions of the “artificial conduit network”, connected with the model surface. The structure of the defined “artificial conduit network” is difficult to perceive in a single graphical representation. In order to better visualise the channel geometry, different perspectives of the 3-D grid are presented in this chapter. Transversal sections will be shown at the time of the presentation of equipotentials and flux vectors, allowing an additional way to perceive the shape of the “artificial conduit network” (figure 6.14 in section 6.5.1.2). After the introduction of the 1-D elements simulations of flow at the regional scale could be done, incorporating the impact of the entire “artificial conduit network”. Moreover each of the mesh branches can be active, inactive and connected or disconnected from other branches.

The refinement of the mesh was done after the definition of the conduit geometry. This operation was performed using a pre-processing tool available with FEN that subdivides the grid maintaining the original geometry but producing a more discretized mesh. Each 3-D and 2-D elements of the mesh was subdivided in to four elements and each 1-D element into two elements in such a manner that the typology of the mesh did not change, except for the degree of discretization. Figure 6.4 shows the result of the refinement of the mesh presented in Figure 6.3. According to the way the operation of refinement was performed the two meshes are strictly equivalent, but with a larger element density.

After the refinement the mesh shown in figure 6.4 had 8 slices of 3-D elements instead of 4 as prior to the refinement. As consequence there are 8992 3-D hexahedral quadratic elements with 20 nodes each, 1124 2-D quadratic elements with 8 nodes each and 486 1-D elements with 3 nodes each. The total number of nodes is 42,841.

At this point the finite element grid shown in Figure 6.4 is not complete, because each of the 17 layers of nodes defining the 8 element slices are still defining plane surfaces. As referred in Section 6.2.1 the top surface of the model was defined based on the shape of the 2-D equipotential surface defined in Section 3.5.2.1 and represented in Figure 3.14. In order to define a shape for the top layer of the model corresponding to that equipotential surface it was necessary to assign an elevation to each node on the top surface of the model. This could easily be done using standard software and resulted in a piecewise representation of the surface of the model. After the assignment of an elevation value to each node of the 2-D surface the same configuration was applied to the base layer (nodes representing the aquifer bottom), respecting an average of 200m of aquifer thickness. This layer was smoothed by a factor of about 3. Finally the nodes between the top and the base of the model, were placed at regular intervals defining the 8 3-D element slices. In that way each of the 17 node layers, defining the 8 element slices, vary in shape from a surface equivalent to the equipotential surface at the top of the model to an almost plane surface at the bottom of the model. The finite element

mesh is shown in Figure 6.5 after the definition of these surfaces. The shape of the top and bottom surfaces defining the aquifer geometry is shown in figure 6.6.

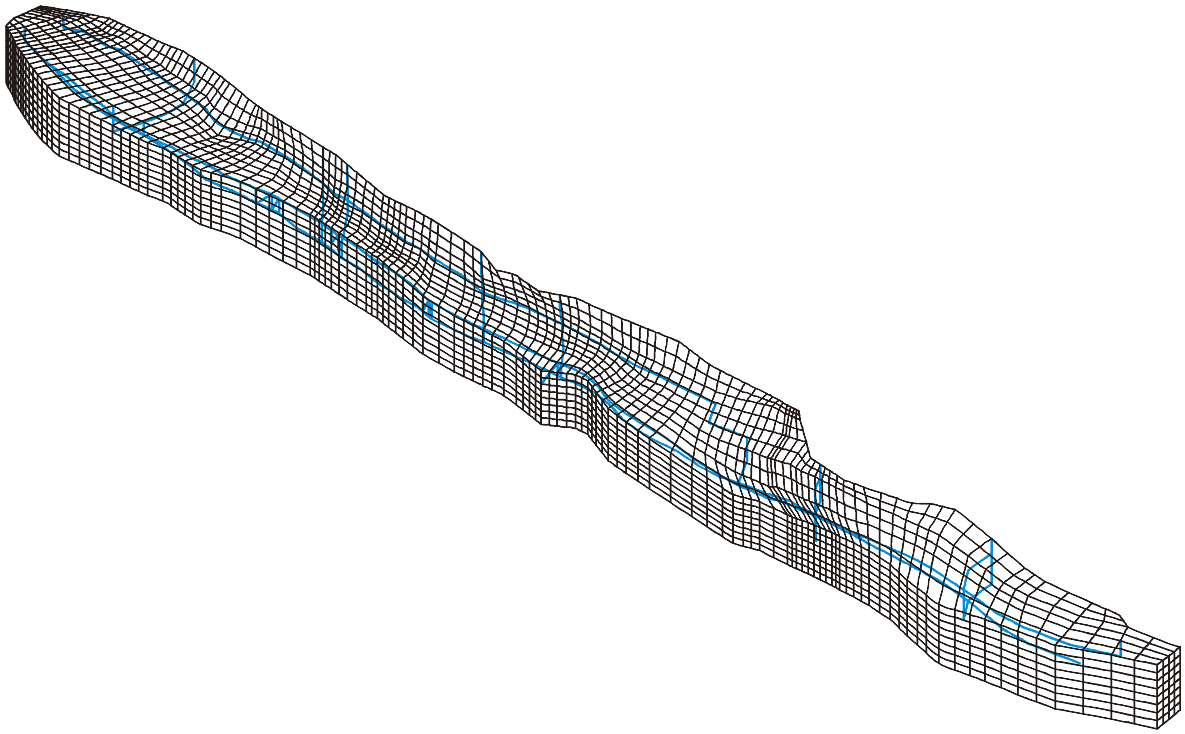

Fig. 6.4 – 3-D finite element mesh with eight slices of hexahedral quadratic elements with 20 nodes each and with 1-D elements representing the "artificial conduit network" embedded in the 3-D elements. The maximum length of the structure along its axis is 8,951m. The aquifer is represented with a 3 times vertical exaggeration.

The final general aspect of the 3-D finite element mesh, including the 1-D structure of the initial "artificial conduit network" and the 2-D top layer of the aquifer is shown in fig 6.7. From this point on the mesh is ready to start preliminary flow simulations.

As discussed in section 6.2 the typology of the conduit network as defined in this section suffered subsequent modifications. However, the evolution of this initial conduit network is better explained during the description of the model calibration process.

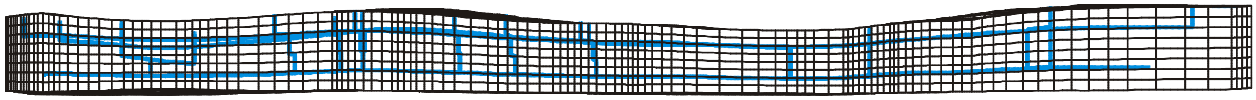

Fig. 6.5 – 3-D finite element mesh, after the definition of altitude for each node.

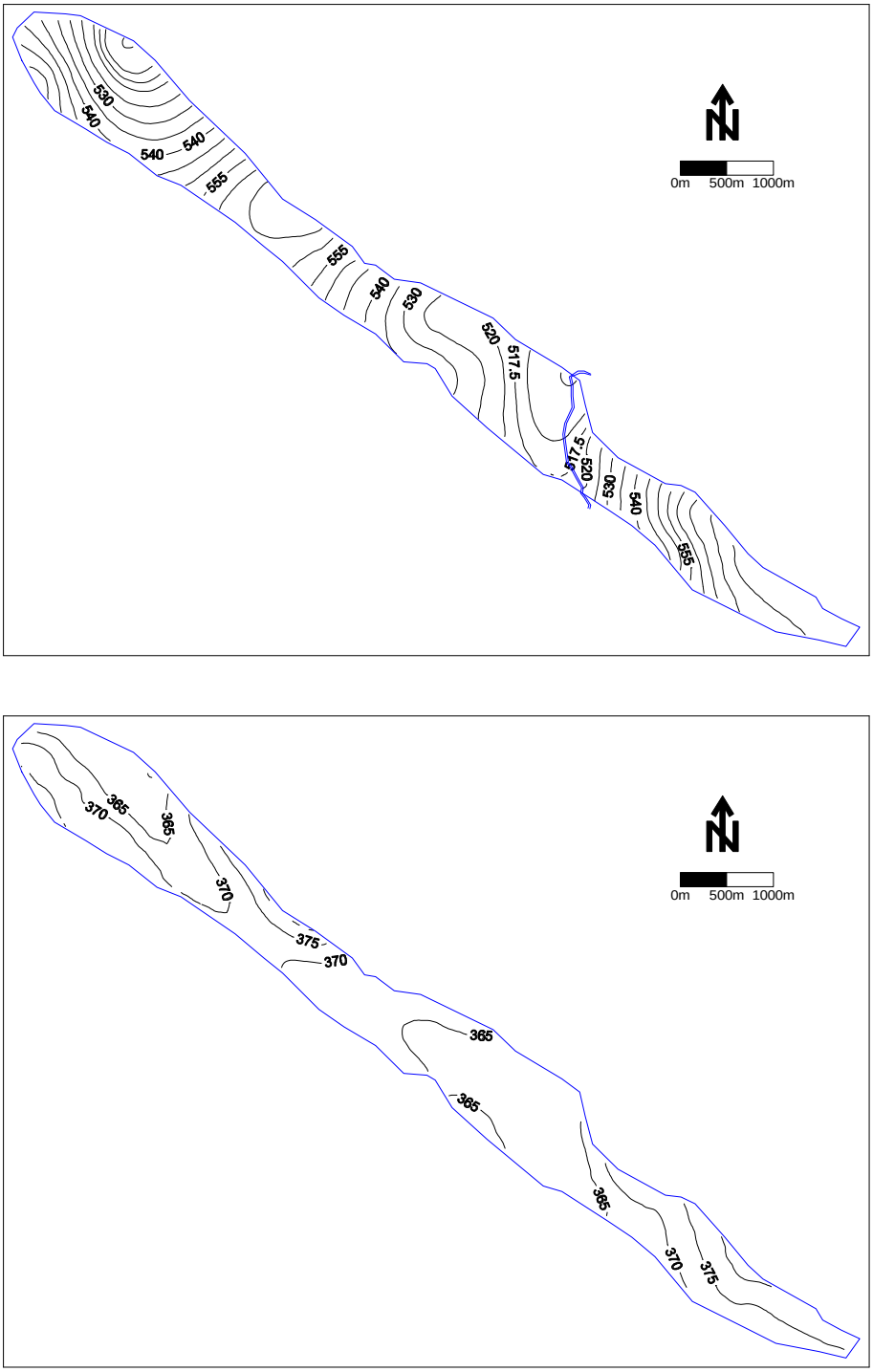

Fig. 6.6 - Shape of the top and bottom surfaces defining the aquifer geometry.

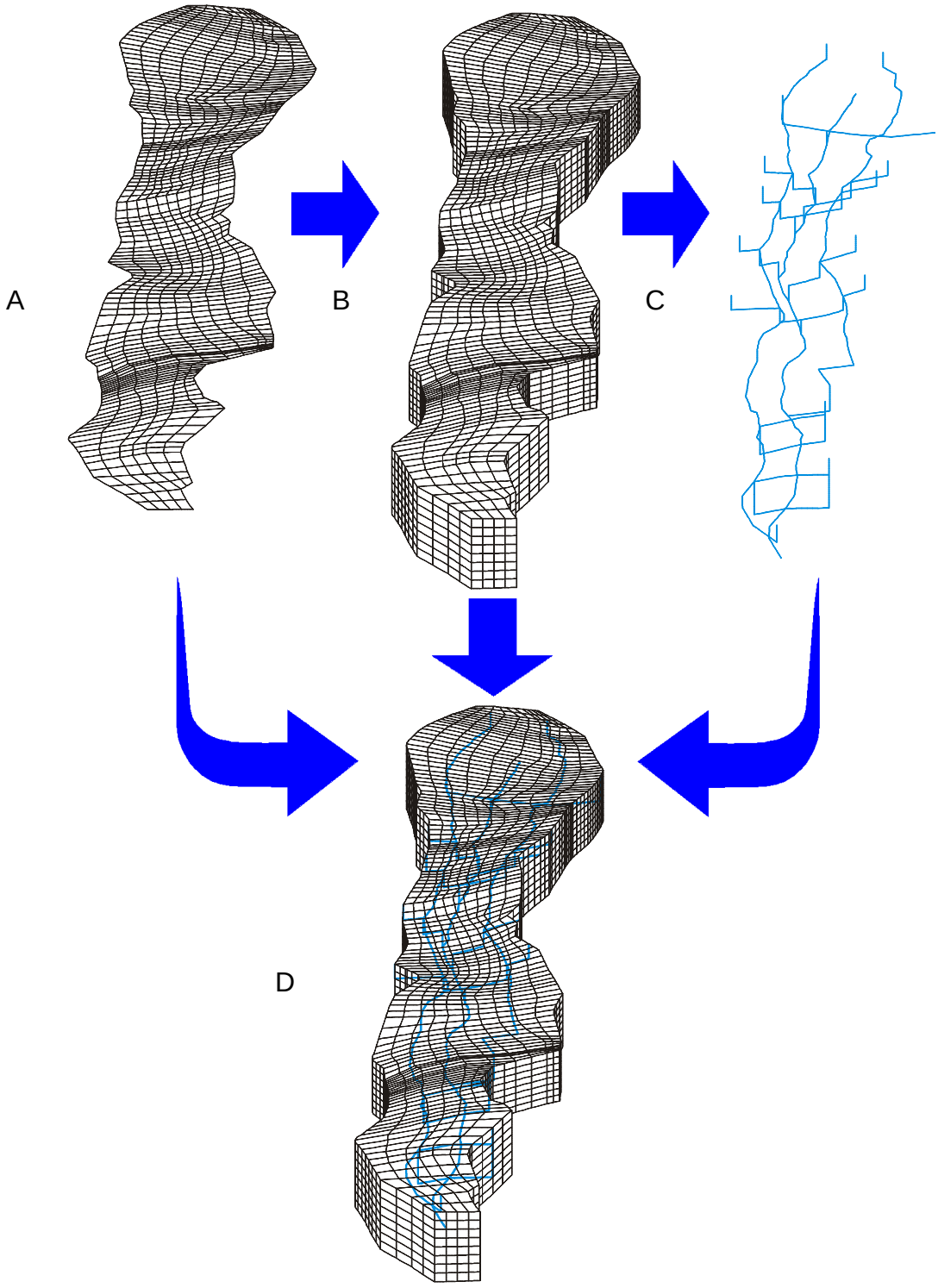


Fig. 6.7 - The global finite element mesh includes: (A) a 2-D top surface where diffuse infiltration is simulated, build with quadrilateral quadratic elements with 8 nodes each; (B) 3-D elements representing the capacitive low hydraulic conductivity rock volumes, built with quadratic hexahedral elements with 20 nodes each and (C) Quadratic 1-D elements with 3 nodes used to define the “artificial conduit network”. The 1-D elements are used to simulate the high hydraulic conductivity dissolution channels connected to the surface where temporary sinking streams disappear into the subsurface, close to the aquifer limits. Finally in (D) all the components of the mesh are assembled. There are 42,841 nodes in the mesh. The maximum dimension of the model along its axis is 8,951m. The aquifer is represented with a 3 times vertical exaggeration.

**6.4 – Boundary conditions**

Two kinds of boundary conditions were used in order to express the relations of the aquifer with its surrounding environment: prescribed head values (Dirichlet conditions) and prescribed flux values (Neumann conditions). No flow boundaries are a particular case where flux through the aquifer boundaries equals zero. As prescribed head or specified flux conditions can be used to define equivalent aquifer conceptualisations the change of boundary conditions using both conditions for the same model variant was often performed, in order to check the consistency of the simulations (de Marsily, 1986).

As the aquifer is limited in almost all its extension by "impermeable lithologies" the bottom and lateral limits of the model are represented by horizontal and vertical no-flow boundaries. The only exception was made in the case of the secondary outflow area of the aquifer on the northwest boundary of the carbonate rocks near Castelo de Vide. In that area the aquifer is in contact with granites and metamorphic rocks, which hydraulic conductivity is higher than the "impermeable schist's" limiting the aquifer in almost all its extension.

The boundary conditions defined to simulate the hydraulic behaviour of the aquifer using the 3-D model are essentially the same defined for the cross-sectional 2-D model presented in Chapter 4. However, some differences exist regarding both definition of discharge areas and the aquifer recharge. Instead of using the average altitude of discharge areas, as in the 2-D model, more detailed values were used in the 3-D model in order to define the prescribed head values. As in the cross-sectional 2-D model, recharge in the 3-D model is simulated by an input value distributed on the surface of the aquifer. However, in the 3-D model water input in the aquifer resulting from allogenic diffuse recharge is also simulated. Additionally concentrated recharge in swallow holes can be also taken into consideration in transient simulations but is ignored in steady state conditions. Discharge areas and a zone of allogenic recharge in the Escusa sector are represented in figure 6.8.

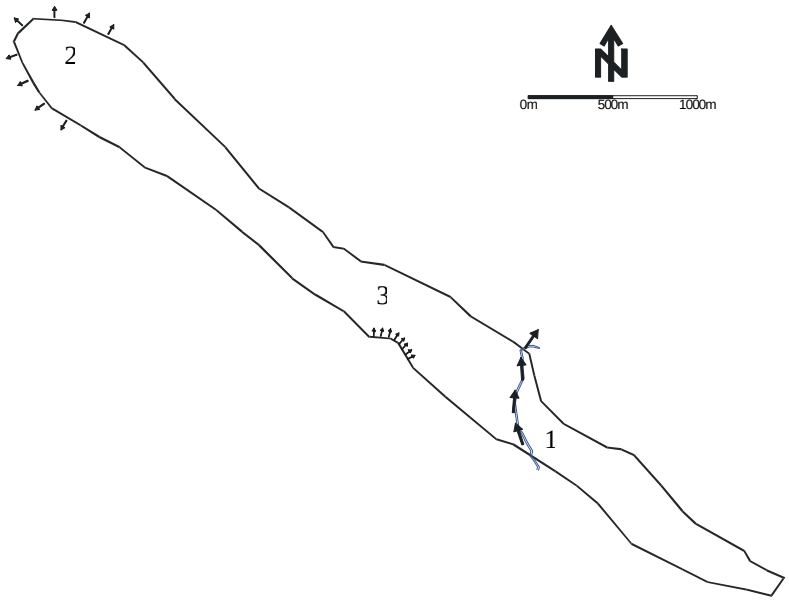


Fig. 6.8 – Outflow and lateral allogenic recharge area. The arrows represent the areas where (1) water is transferred from the aquifer toward the Sever River, (2) from the aquifer toward the lithologies in contact with the NW limits of the aquifer and (3) from the deposits covering carbonate rocks and adjacent lithologies toward the aquifer corresponding to the allogenic recharge in the Escusa sector.

Sever River is the main discharge area in the aquifer and is included in the model as a constant head boundary. Water discharge throughout the riverbed is governed by the difference between the hydraulic head in the aquifer and the water surface elevation of the river. The sum of the outflow in the nodes where the prescribed head values are defined, along a line representing the position of the river at the surface of the model, correspond to the calculated water discharge from the aquifer to the river. As long as the groundwater table does not drop below the river altitude these transferences will be negative (the river is effluent, and thus water is transferred towards the river). In global terms it is known that the common conditions present in the aquifer corresponds to transferences from the aquifer toward the river. However, in reality, the only way to quantify the discharge is to install hydrometric stations upstream and downstream of the aquifer. This problem was discussed in Section 3.5 and it is possible that during extreme drought periods some water transference takes place from the river toward the aquifer. The analysis of this particular problem will only be made

possible by the collection of detailed data about river discharge upstream and downstream of the aquifer. However, the possible existence of such conditions is certainly of little importance at the scale of aquifer balance.

The prescribed head values in the NW secondary discharge area were more difficult to define because the knowledge of the geometry of the discharge area, being a hidden surface constituting the contact between the carbonate rocks and adjacent lithologies in Castelo de Vide region, is far more difficult to describe in a precise way.

As can be seen the in figure 3.15 (section 3.5.2.2) hydraulic head values in the aquifer close its limits in the Castelo de Vide area vary between 507m and 523m. The essential question arising from the characteristics of that discharge area is the determination of the depth to which the water is transferred from the aquifer to the adjacent fractured rocks. In the defined model it was considered that the discharge area lies between the ground surface and 50m beneath the ground level.

The occurrence of lateral recharge is known in the aquifer and is especially important in transient simulations during recharge events. However, in parts of the Escusa sector, even in steady state simulations, the results are improved by the consideration of small values of allogenic diffuse recharge simulated in the segment of the aquifer boundary shown in figure 6.8. Despite the volume of recharge simulated in that area being only about 2 l/s, better results were obtained when such infiltration was taken into account. This is related to the larger extension of deposits covering the carbonate rocks in that area and is supported by field data. In fact, wells 33 and 35, drilled along the aquifer limits (see figure 3.12 in section 3.5.1) show that hydraulic head in that area of the aquifer limit is always higher than in the adjacent points in the Escusa sector, indicating water input throughout this aquifer limit.

## 6.5 – Model calibration

### 6.5.1 – Steady state simulations

The steady state calibration of the regional flow model was done by the analysis of numerous variants which will not all be extensively described. In practice many of the revisions of the model characteristics were related to the efforts in understanding the role of the conduit network in the regional flow pattern of the aquifer. The first phase of the calibration process (steady state simulations) was based on the investigation of three groups of variants, each very different from the another: (1) preliminary variants in which the flow domain was treated as a homogeneous single continuum; (2) simulations in which an “artificial conduit network” control flow pattern at aquifer scale and (3) simulations in which sectors of the “artificial conduit network” with different degrees of connectivity with the aquifer discharge areas were defined.

The preliminary variants of the 3-D model, where the flow domain was treated as a homogeneous single continuum, will not be described here. These model variants are equivalent to the aquifer simulation using a cross-sectional 2-D model presented in Chapter 4. Different values for hydraulic conductivity were used in this kind of simulations. For example, an equivalent hydraulic conductivity determined at aquifer scale and harmonic and geometric means of values for this parameter obtained from the interpretation of pumping tests were used. These simulations based on the representation of the aquifer as a single continuum equivalent media were done in order to check the mesh for errors and interpret the model sensitivity to changes in hydraulic conductivity. In spite of the considerable errors for the prevision of hydraulic head in observation points, it must be noted that the presence of aquifer sectors, identified in section 3.5.2.1 and simulated in section 4.2.1, is respected in that group of simulations (Castelo de Vide, Escusa and P. Espada Sectors), simultaneously with infiltration values estimated based on long-term water balance calculations. After these preliminary simulations the discrete continuum model was used in order to investigate the possibilities in defining some restrictions regarding the role and impact of conduit flow on the regional flow pattern. The models for the second and third type of variants, defined in the above paragraph, illustrate the calibration method proposed in section 6.2.

For all the steady state simulations the calculated water balance was controlled by a uniformly distributed 450mm/year recharge on the top of the aquifer, which corresponds to the average annual recharge estimated in Section 3.4.5. In addition to this value, allogenic recharge is also considered in the Escusa sector. However the volume evolved in these lateral inputs is only about 2% of the total recharge. Steady state simulations also consider extractions in three groups of wells used for water supply and one well used for irrigation of food crops. Further details about criteria used for simulation of wells are discussed at the time of the presentation of the transient simulations, in which an additional group of 11 wells is active during irrigation periods. The pumping rate of these wells is of little importance at the scale of the global water balance. However the impact of these wells during recession periods of the aquifer is very important, as they are used during the long periods of the hydrologic cycle, characterised by the absence of recharge.

#### 6.5.1.1 – Simulations considering the presence of an "artificial conduit network" controlling flow at the aquifer scale

The present simulation corresponds to the first step of the method applied in the calibration process of the discrete continuum model proposed in section 6.2. At this point an "artificial conduit network" controlling flow at aquifer scale was introduced in the model. We remind that the initial "artificial conduit network" structure was defined by regional conduits (parallel to major structural alignments identified in the aquifer) interconnected by transversal conduits (linked with the aquifer surface in points where concentrated recharge is known to occur). Therefore, a conduit network defined in this way assumes that channels are controlling flow at the entire aquifer scale. The "artificial conduit network" used in the presented simulation in this section corresponds to the initial version of the model shown in figure 6.7 (section 6.3.1.2), prior to any model calibration.

One single model variant is presented for this phase of model calibration. In this case the used parameters correspond to a hydraulic conductivity of $10^{-6}$ m/s for the 3-D elements and 10 $m^3$/s for the 1-D elements. It is somewhat unexpected that, despite the presence of frequent predominant conduit flow conditions identified in all Castelo de Vide aquifer sectors by field evidence, a simulation based on the existence of a conduit network controlling flow at aquifer scale produces worse results than an as basic conceptualisation of the system as the one represented in section 4.2.1 (based on the simulation of the aquifer as an homogeneous equivalent single continuum). In the present simulation (see figure 6.9) all the flow systems, allowing the detection of the aquifer sectors identified on the basis of experimental evidence, are absent in the model. The spatial distribution of the hydraulic head in these conditions is strongly affected by the initial "artificial conduit network" controlling flow at aquifer scale, which induces a general flow pattern characterised by the existence of a smooth equipotential surface with a gentle slope towards the aquifer discharge areas.

As in all model variants the root mean square error is used in order to quantify the simulation errors. Root mean square error (*RMSE*) is defined by the expression (Belitz et al., 1993).

$$RMSE = \sqrt{\sum_{i=1}^{n} \frac{\left(h_{meas} - h_{sim}\right)_i^2}{n}} \qquad 6.1$$

Where $h_{meas}$ is hydraulic head registered in observation points, $h_{sim}$ is hydraulic head simulated with the model and $n$ is the number of measurements. The value for the root mean square error is 18.9m for this simulation.

Different variants for a configuration based on an "artificial conduit network" allowing an efficient connection between all aquifer sectors were performed. Providing that conduits present a high contrast to the low permeability rock volumes the results are always similar: The groundwater divides between the Castelo de Vide and Escusa sectors is always absent as a result of the smooth equipotential surface characterising the regional flow pattern. In spite of the presence of variations of hydraulic head with depth in the vicinity of conduits (as observed in the aquifer) the rapid propagation of hydraulic head in the horizontal direction are responsible for the elimination of any spatial variability as observed in the real system.

The outflow in discharge areas predicted by the model for the present variant, taking into account natural discharge areas and water use in pumping wells, is registered in table 6.1. A calculated recharge/ discharge balance, used as an indicator of model accuracy, shows a very low value (4.76 l/year), showing the excellent quality of the results provided by the program FEN.

| Outflow | Volume (m3/year) | (%) | Inflow | Volume (m3/year) | (%) |
|---|---|---|---|---|---|
| Sever River | $1.14\times10^{6}$ | 31.38 | Autogenic recharge | $3.57\times10^{6}$ | 97.97 |
| Castelo de Vide | $8.35\times10^{5}$ | 22.93 | Allogenic recharge | $7.40\times10^{4}$ | 2.03 |
| Pumping wells | $1.66\times10^{6}$ | 45.69 | | | |
| Total | $3.64\times10^{6}$ | 100.00 | | $3.64\times10^{6}$ | 100.00 |

Table 6.1 – Water balance calculated by the discrete continuum model for the model variant in this section. Autogenic recharge corresponds to infiltration on the top of the aquifer. Allogenic recharge corresponds to infiltration originated from deposits covering the aquifer in Escusa sector (see figure 6.8 in section 6.4).

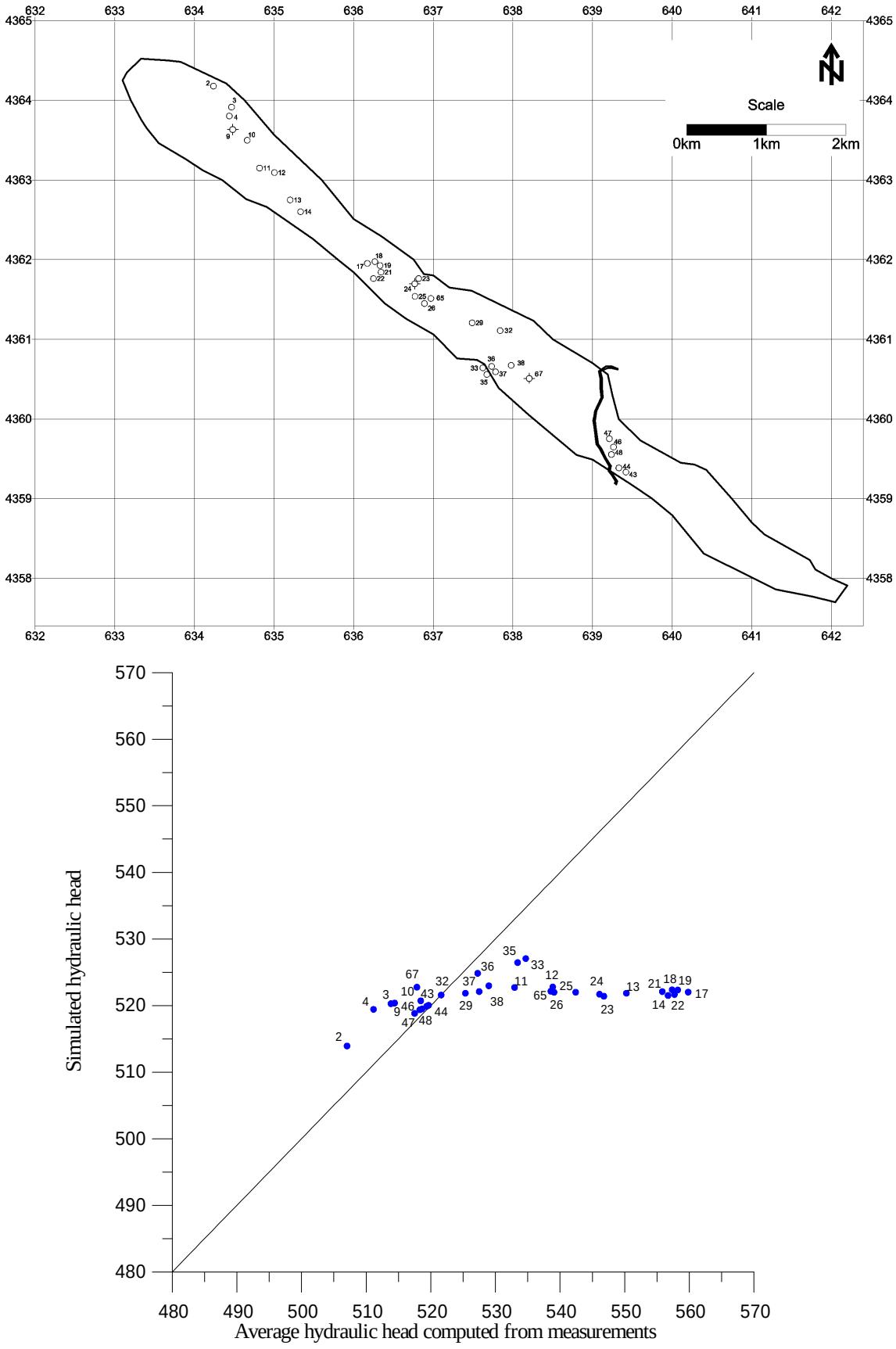


Fig 6.9 – Relation between hydraulic head computed from measurements in observation points and simulated using the discrete continuum model, considering the existence of an "artificial conduit network" controlling groundwater flow at the aquifer scale. Measured values are the average of observations between 1991 and 1999. Hydraulic conductivity is $10^{-6}$ m/s for 3-D elements and the conductive parameter for 1-D elements is 10 $m^3$/s.

### 6.5.1.2 – Simulations based on the definition of sectors in the "artificial conduit network"

Results obtained with model variants where a conduit network controls flow at aquifer scale clearly suggests that the "real conduit network" present in the aquifer cannot be establishing an efficient enough connexion throughout the entire aquifer. Furthermore, the analysis of results obtained from the investigation of synthetic discrete continuum flow models, in which conduit networks with different densities control flow at aquifer scale, shows that, despite of important variations in hydraulic head in the vertical direction near conduits, the general flow pattern is characterised by the absence of distinguishable trends for hydraulic head variation in the horizontal direction (see, for example, Kiraly 1995 and Cornaton 1999). In fact, the existence of a conduit network with such characteristics in the Castelo de Vide aquifer would lead to a spatial distribution of hydraulic head at aquifer scale completely different to the one inferred based in field observations.

At that point we remember that, according to the method proposed for model calibration (section 6.2), it is assumed that the detected large scale trends in hydraulic head gradients are related to the efficiency of the conduit network in establishing hydraulic connection between the different parts of the aquifer. According to the second step established for the model calibration process it is now time to identify the zones where positive anomalies in hydraulic head gradients (corresponding to the trends of systematic steeper gradients) are present in the aquifer. After the identification of these zones it is assumed that they correspond to areas where the conduit network exhibits a low efficiency in terms of hydraulic connexion with adjacent areas of the aquifer. Therefore, low conductivity values are assigned to the parameters of the 1-D elements representing dissolution channels in the corresponding part of the "artificial conduit network" introduced in the discrete continuum model. In this case the conductivity assigned to these 1-D segments are similar to the values used for the 3-D blocks. This corresponds to step 3 of the methodology defined in section 6.2.

Finally, as established for the fourth step in the defined method for model calibration, these changes in the "artificial conduit network" can be investigated in terms of their impact on the spatial distribution of hydraulic head using the discrete continuum model. The general procedure used for definition of sectors in the "artificial conduit network" is illustrated in figure 6.10

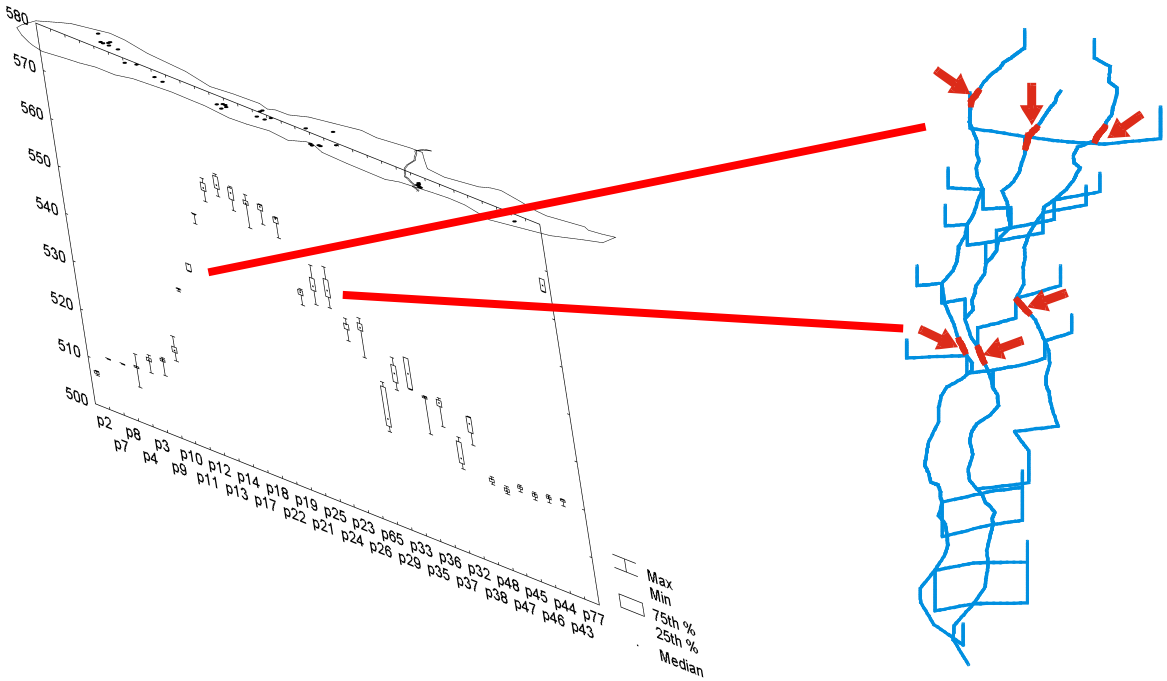


Fig. 6.10- Schematic representation of steps 2 and 3 of the method used for model calibration described in section 6.2. The arrows in the "artificial conduit network" mark the areas where it is assumed that channels present a deficient hydraulic connexion with adjacent sectors of the network. These points were located according the identified areas where the large scale gradient in hydraulic head tends to increase in the real aquifer. Spatial distribution and temporal variability of hydraulic head in the aquifer is represented in boxplots at left, along the axis of the aquifer.

General parameters used in this variant of the model are $10^{-6}$ m/s for hydraulic conductivity of the low permeability rock volumes, and 10 $m^3$/s for the conductive parameter characterising conduits (corresponding to an equivalent circular conduit with 8 cm in diameter). Thus the only difference between simulations presented in section 6.5.1.1 and the present one is the definition of sectors in the conduit network. The definition of these sectors allowed a conciliation of the presence of conduit flow, affecting in an important way the general flow pattern, with the simultaneous existence of regional trends of hydraulic head as detected in the Castelo de Vide aquifer. As shown before, these trends are clearly revealed by field observations, and are not compatible with the existence of a conduit network controlling flow at aquifer scale. Therefore, the proposed definition of sectors in the "artificial conduit network" could be interpreted as an evolution in the understanding of the role of the "real conduit network" in the definition of the observed aquifer hydraulic behaviour.

In fact, the calibration of the model in the phase corresponding to the definition of sectors in the "artificial conduit network" was easier than the investigation of older variants, in which the conduit network control flow at aquifer scale. In fact, the only efforts needed to adapt the initial conduit network to the definition of sectors consisted in deciding what value had to be assigned to the conductive parameter in the areas where systematic increase in gradients is detected in the real system. The solution for this problem is not unique and depends on the length of the conduit affected by the change in the conductive parameter value. For example, in this case the value assigned to conduits corresponds to the same value characterising the low permeability rock volumes. The length of conduits with low conductive values are expressed in table 6.2 and the position of the segments is shown in figure 6.11.

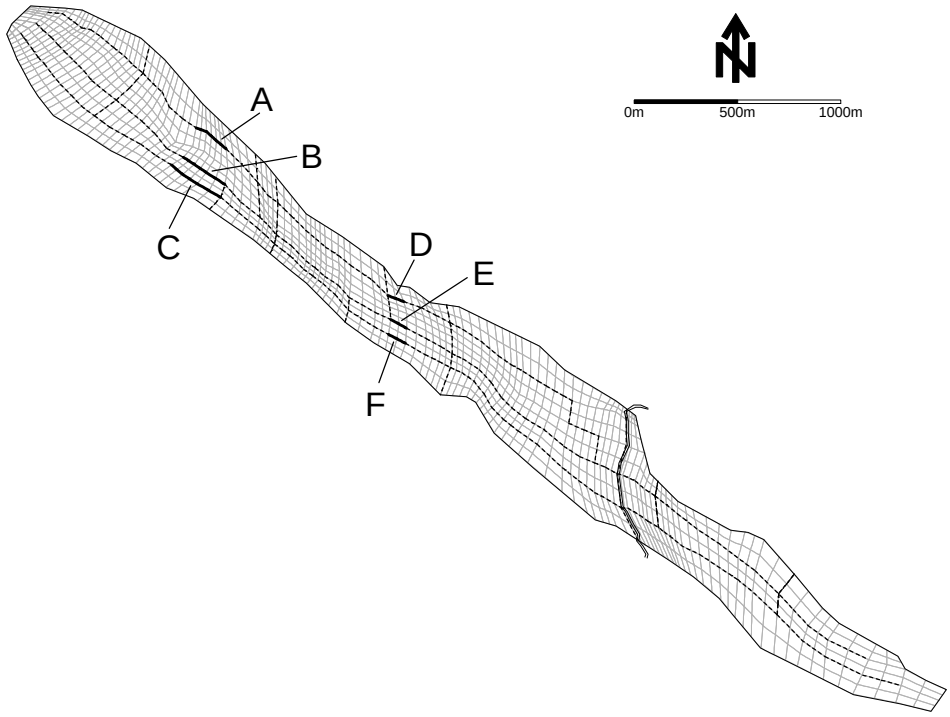


Fig. 6.11 – Location of the segments of the conduit network presenting a conductive parameter similar to the hydraulic conductivity of the low permeability rock volumes. The dashed lines represent the general conduit network and the areas with changed parameters are marked in bold. Note that the 3-D conduit network is represented by a 2-D projection at the aquifer top.

| Segment | $L_c$ (m) |
|---|---|
| A | 382 |
| B | 499 |
| C | 581 |
| D | 185 |
| E | 202 |
| F | 207 |

Table 6.2 – Length of the segments ($L_c$) where the conductive parameter for conduits was changed to $10^{-6}m^3$/s

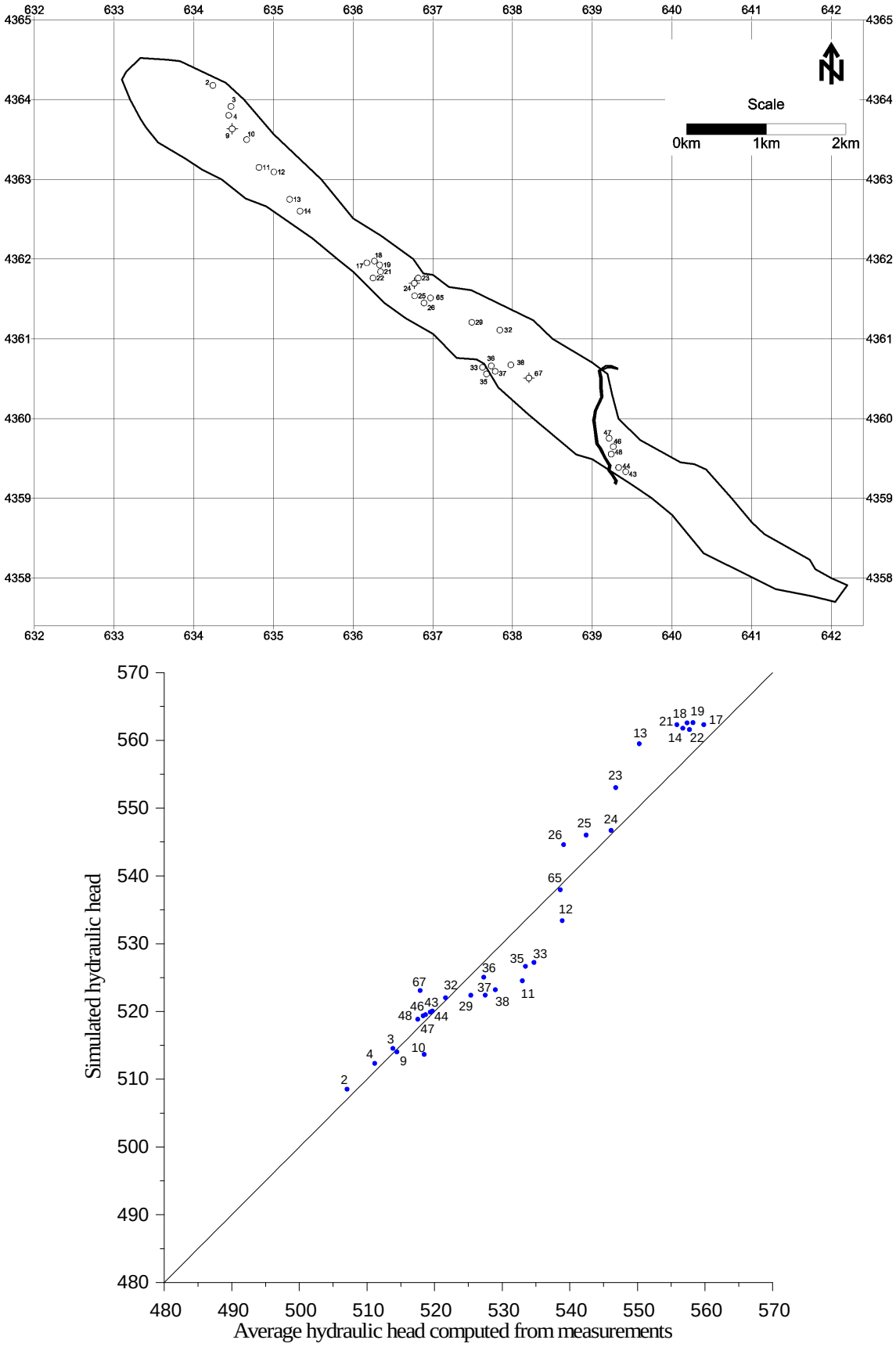


Fig 6.12 – Relation between hydraulic head computed from measurements in observation points and simulated using the discrete continuum model, considering the existence groundwater flow controlled at the regional scale by sectors of an "artificial conduit network" with different degrees of connectivity with the aquifer discharge areas. Hydraulic conductivity is $10^{-6}$m/s for 3-D elements and the conductive parameter for 1-D elements is $10m^3/s$. Measured values are the average of observations between 1991 and 1999.

As can be seen in figure 6.12 the definition of sectors in the conduit network was responsible for a substantial improvement in the simulation of the spatial distribution of hydraulic heads in the aquifer. In the present model variant the calculated value for root mean square error is only 4.5m (see equation 6.1).

The distribution of hydraulic head for the present model variant is complex and the results, calculated for the entire 3-D flow domain, are difficult to perceive in a single graphic representation. 2-D projections, showing equipotentials and flux vectors, defined along sections of the model are represented in figures 6.13 and 6.14.

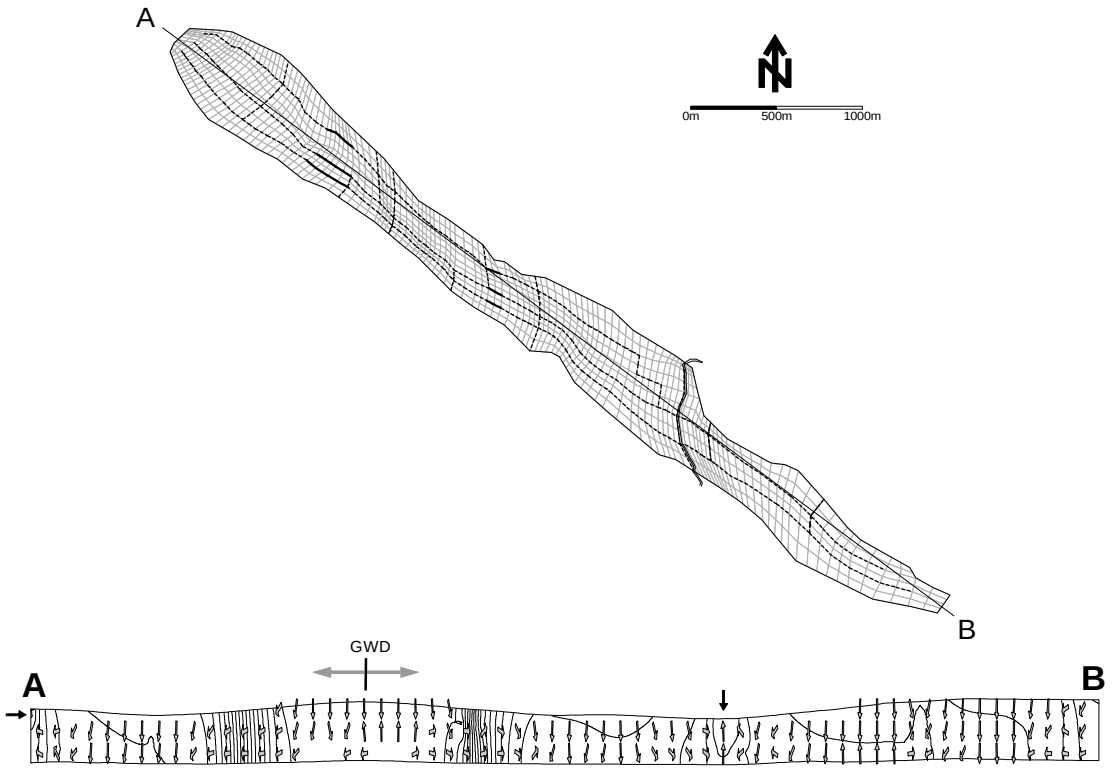


Fig. 6.13 – Top 2-D projection of the finite element mesh top showing the location of the 2-D cross-section AB, defined along the aquifer axis. The dashed lines represents the "artificial conduit network". The areas with changed parameters are marked in bold. Black arrows pointing to aquifer limits in the cross-section indicate the position of discharge areas. GWD – groundwater divides between Castelo de Vide and Escusa sectors. Equidistance of potential lines is 2.5m. Vertical exaggeration is 3 times.

It is interesting to compare figure 6.13 with figure 4.2 in section 4.2.1, where equipotentials and flux vectors of a 2-D cross-sectional finite element model characterising the entire flow domain are represented. In figure 6.13 the variations of hydraulic head in vertical direction are far more complex, resulting from the presence of conduit flow. The zones with systematic anomalies in hydraulic head gradients within the Castelo de Vide and Escusa sectors are now clearly visible. As discussed in section 5.6 these anomalies must be related to extreme development of karstic processes in conduits, provoking the filling and plugging of dissolution channels, resulting in a substantial reduction of conductivity in these areas.

It must be noted that the identification of sectors of a given conduit network is independent of aquifer sectors defined by the presence of regional or local flow systems, which boundaries can be identified by the presence of features as no-flow boundaries, groundwater divides and aquifer discharge areas. In the present case study the sectors defined for the aquifer do not spatially coincide with the sectors considered for the conduit network. In fact, the areas where deficient connexion between adjacent sectors of the conduit network were defined are somewhere inside the Castelo de Vide and Escusa sectors. Observation wells for the determination of hydraulic heads in P. Espada sector are not sufficient to achieve a detailed characterisation of the spatial distribution of hydraulic head. Therefore, it is possible that sectors for the conduit network could also be defined in the P. Espada sector, if more data were available.

The calculated water balance for the present model variant, taking recharge, natural discharge processes and water use in pumping wells into account, is registered in table 6.3. This time the calculated recharge/ discharge balance (2.79 l/year) is again very low, proving once again that the quality of results obtained by the discrete continuum model. It must be

remarked that changes provoked by the definition of sectors in the conduit network does not dramatically change the total water balance. If the global water balance presented in this section is compared to the values obtained using the model variant discussed in section 6.5.1.1 (see table 6.1), it can be seen that changes are almost negligible. On the other hand, the spatial distribution of hydraulic head, and therefore the flow field, is dramatically different for each of these typologies defined for the “artificial conduit network”.

| Outflow | Volume (m3/year) | (%) | Inflow | Volume (m3/year) | (%) |
|---|---|---|---|---|---|
| Sever River | $1.27\times10^{6}$ | 34.84 | Autogenic recharge | $3.57\times10^{6}$ | 98.02 |
| Castelo de Vide | $7.07\times10^{5}$ | 19.44 | Allogenic recharge | $7.22\times10^{4}$ | 1.98 |
| Pumping wells | $1.67\times10^{6}$ | 45.72 | | | |
| Total | $3.64\times10^{6}$ | 100.00 | | $3.64\times10^{6}$ | 100.00 |

Table 6.3 – Water balance calculated by the discrete continuum model for the model variant in the present section. Autogenic recharge corresponds to infiltration at the top of the aquifer. Allogenic recharge corresponds to infiltration originated from deposits covering the aquifer in Escusa sector (see figure 6.8 in section 6.4).

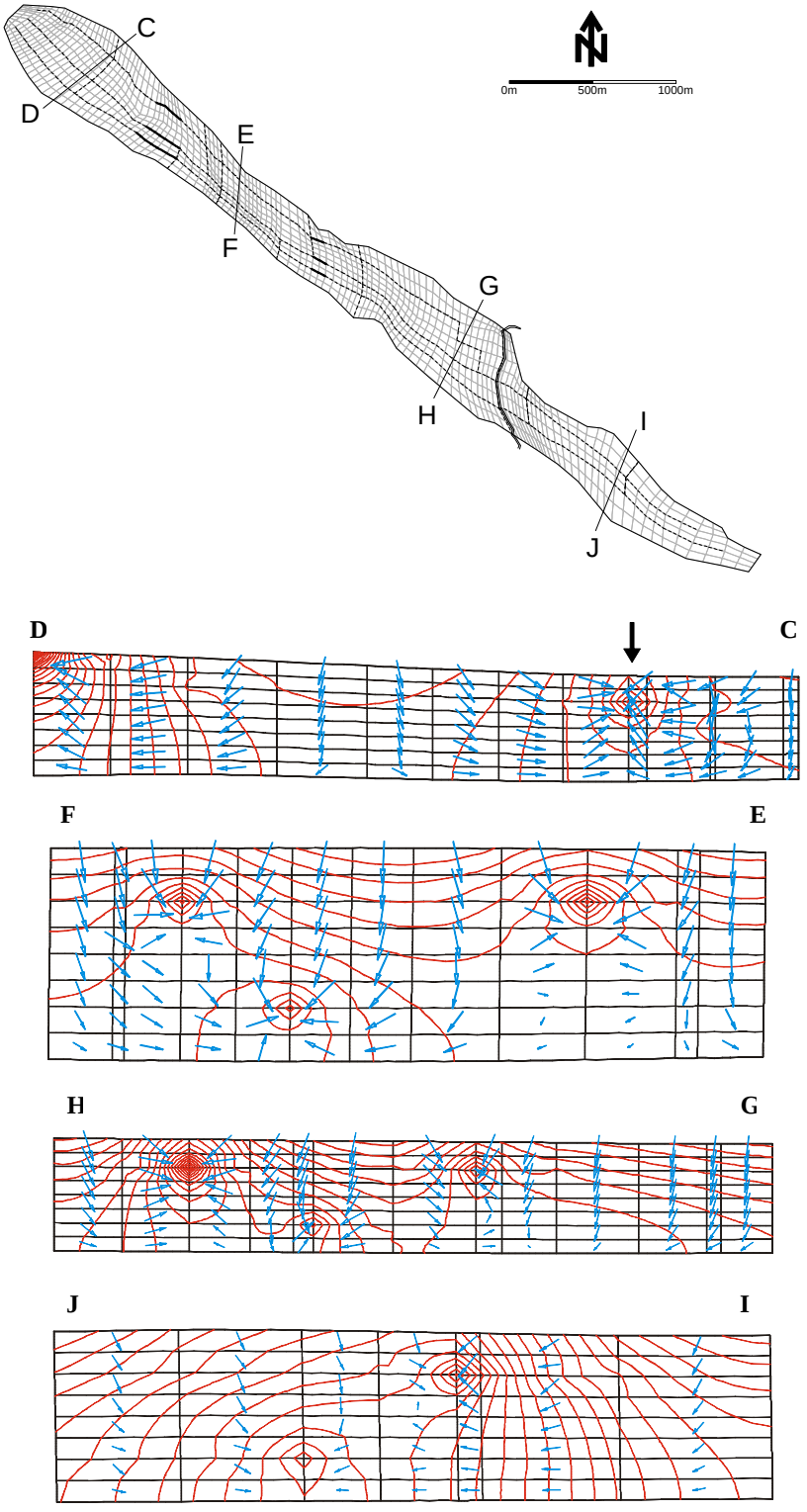


Fig. 6.14 – 2-D vertical cross-sections of the 3-D model showing equipotentials and flux vectors. Cross-sections: C-D (1104m), equidistance of equipotentials-1.0m; E-F (645m) equidistance 0.2m; G-H (1007m) equidistance 0.2m; I-J (810m) equidistance 0.3m. Aquifer thickness is always approximately 200m. The arrow outside the aquifer limits in profile C-D shows the perturbation produced by the pumping well used for Castelo de Vide Water Supply, directly implanted in a conduit with a pumping rate of 15 l/s.

#### 6.5.1.2.1 – Remarks on parameter distribution and conduit network structure and density

The parameters used in the simulation presented in section 6.5.1.2 correspond to a high simplification of reality. In fact all the 3-D elements representing the low permeability rock volumes are characterised by a single hydraulic conductivity value, which corresponds to $10^{-6}$ m/s. The conductive parameter defined for the conduit network is $10m^3/s$, except for the segments where deficient connectivity was defined (in areas identified by regional anomalies in hydraulic head gradients). As referred before, the value assigned to the conduits conductive parameter corresponds to a n equivalent circular conduit with 8 cm in diameter. Despite of its simplicity this representation of the aquifer allows an accurate simulation of the spatial distribution of hydraulic head, simultaneously with the values of the global water balance determined as described in section 3.4.5.

The possibilities of describing the real system with so a simple model is related to the fact that the low permeability rock volumes seem to be adequately described with a homogeneous value. Hydraulic conductivity values characterising the unaltered rock matrix obtained from the interpretation of pumping tests, in wells drilled without interception of fractures or dissolution voids, are very close the value used to characterise the 3-D elements in the discrete continuum model ($10^{-6}$ m/s) - see section 5.3.1. The values obtained at well scale vary over four orders of magnitude. However, the interpretation of these tests have shown that values in the two highest orders of magnitude are related to the proximity of conduits. Thus, it was expected that a value of one order of magnitude superior to the one used ($10^{-6}$ m/s) in the best model variant (see last section), was more adequate to characterise the 3-D elements. In fact, according to the conceptualisation defined for the model, it was said that the 3-D elements were used to simulate the fractured rock matrix and low order dissolution channels present in the carbonate rocks. However, a variant of the model similar to the one presented in the last section, with the exception of the use of a $10^{-5}$ m/s value for hydraulic conductivity characterising the 3-D elements, describe the system behaviour less accurately (figure 6.15 shows the results of a model variant with these characteristics). Two different factors are probably in the origin of these results. Firstly, wells which were considered unproductive from the economical point of view were not submitted to pumping tests. Therefore, it is probable that the estimations of the hydraulic conductivity are biased. As showed in section 5.3.1 near 50% of the values of hydraulic conductivity determined in pumping tests were between $10^{-5}$m/s and $10^{-4}$m/s against only 20% of the values between$10^{-6}$m/s and $10^{-5}$m/s. If the wells considered unproductive were submitted to pumping tests too, probably the parameter distribution could have been inverted. A second factor affecting the global parameter distribution is the "artificial conduit network" density; because its value also affects the global parameters distribution.

The density of an "artificial conduit network" introduced into a discrete continuum model is restricted by technical limitations related to the simultaneous presence of 1-D and 3-D elements characterised by parameters differing by many orders of magnitude (see section 2.2.2). In addition to limitations on this level it must be assumed that the density of the "real conduit network" is totally unknown. The impact of conduit network density in the carbonate aquifers hydraulic behaviour using discrete continuum models was pioneered by Cornaton (1999) and Cornaton and Perrochet (2000). The variables evolved in this problem are the length of conduits ($L_c$), volume ($V_t$) and area ($A$) of the aquifer. Two alternative ways of defining network density are discussed in Cornaton (*op. cit.*): (1) $d' = L_c/V_t$ (km.km$^{-3}$) and (2) $d = L_c/A$ (km.km$^{-2}$). The "artificial conduit network" density defined for the Castelo de Vide aquifer is presented in table 6.4.

| | $L_c$ (km) | $V_t$ (km$^3$) | $A$ (km²) | $d' = L_c/V_t$ (km.km$^{-3}$) | $d = L_c/A$ (km.km$^{-2}$) |
|---|---|---|---|---|---|
| NA | 38.23 | 1.362 | 7.92 | 28.064 | 4.825 |
| NB | 36.18 | 1.362 | 7.92 | 26.555 | 4.566 |

Table 6.4 – Conduit network density. NA – conduit network controlling flow at aquifer scale, used in the model variant presented in section 6.5.1.1; NB-conduit network used in the model variant presented in section 6.5.1.2, based on the definition of sectors in the conduit network.

The "artificial conduit network" in a discrete continuum model is not defined with basis in the "real conduit network" geometry but with basis in its role in the definition of the regional flow pattern. The "artificial network density" is certainly inferior to the real one. Estimates presented by Worthington (1991 *in* Cornaton 1999) point to values superior to 100 km.km$^{-3}$ for the network density in real karst aquifers.

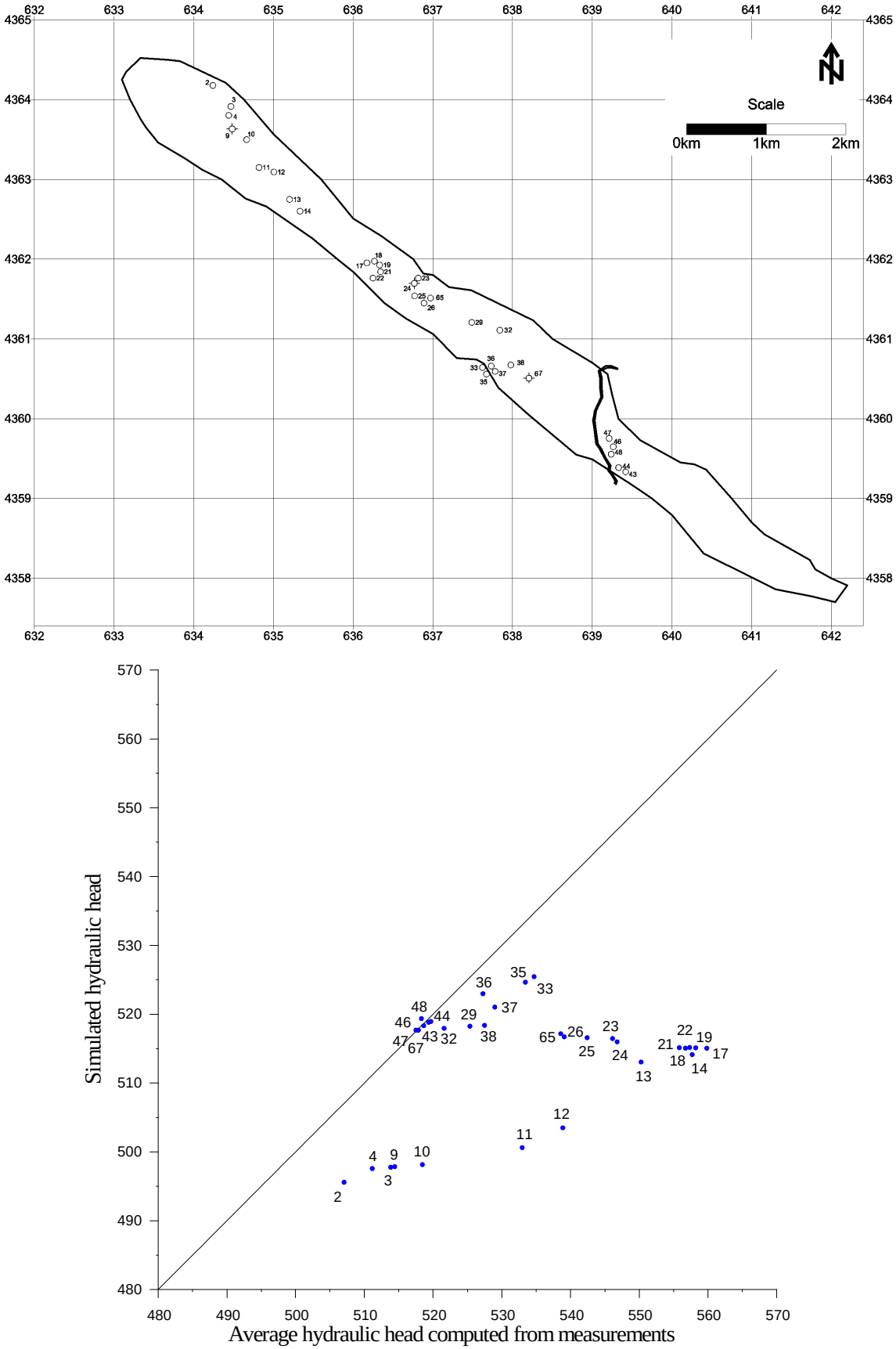


Fig. 6.15 – Relation between hydraulic head computed from measurements in observation points and simulated using the discrete continuum flow model, considering the existence groundwater flow controlled at the regional scale by sectors of an "artificial conduit network" with different degrees of connectivity with discharge areas. Hydraulic conductivity is $10^{-5}$m/s for 3-D elements and the conductive parameter for 1-D elements is $10m^3/s$. Measured values are the average of observations between 1991 and 1999.

According to the results Cornaton (1999) obtained the network density plays an important role in the hydraulic behaviour of karst aquifers when conduit flow establishes an efficient connectivity throughout the entire flow domain. In this work a relation was found between network density and the hydraulic behaviour of synthetic karst aquifers during emptying periods of the system. That relation was put in evidence by the existence of a correlation between network density and the recession coefficient of spring hydrographs obtained using Maillet equation. However it must be considered that the validity of such a correlation is constrained to the analysis of conduit networks directly connected with the aquifer discharge areas. In the cases where different sectors of the network have different hydraulic connectivity with the discharge areas the problem is more complicated. Hence global responses cannot give information about the global network density.

As shown in table 6.4, the density of conduit networks is very similar for the variants of the discrete continuum model presented in section 6.5.1.1 (considering the presence of a conduit network controlling flow at aquifer scale) and in section 6.5.1.2 (based on the definition of sectors in the conduit network). However, despite the similarity in structure and network density the simulation of the aquifer hydraulic behaviour is dramatically different. These results seem to show that the identification of sectors in the conduit network is more important and less subjective than the investigation of hypothetical different network densities to characterise carbonate aquifers on the levels required for the use of discrete continuum models.

### 6.5.2 – Transient simulations

#### 6.5.2.1 – Introduction

After the introduction of the transient term in the groundwater flow two parameters are required for the characterisation of the aquifer: (1) hydraulic conductivity and (2) specific storage. The hydraulic conductivity values used for calibration of the model in transient conditions are the same as the ones used in the steady state model presented in section 6.5.1.2.

Water in carbonate rocks is mainly stored in the capacitive rock volumes, as opposed to the highly conductive dissolution channels having low storage capacity. In the present case study storativity values for conduits were established taking the conductivity value used at the time of steady state model calibration into account. The coherence between these values was established based on the physical principles expressed in equations 5.16 and 5.18 in section 5.5. Considering the value for the conductive parameter of conduits as used in section 6.5.1.3 ($T_d$=10 $m^3/s$), the corresponding value for storativity ($S_d$) is $2.5\times10^{-8}$ m. These values for conductivity and storativity of conduits correspond to an equivalent circular section conduit with 0.08m in diameter. The physical coherence between $S_d$ and $T_d$, taking an equivalent diameter into account, corresponds to a strong simplification of the real system. The choice of these values is once again related to the evaluation of the role of the "artificial conduit network" in the definition of the regional flow pattern, instead to search for values characterising any particular point in the "real conduit network". Karstic voids with large dimensions, without direct connection to discharge areas, can play an important role in water storage. By consequence the capacitive role of conduits is assimilated to specific capacity assigned to 3-D elements in the model, which include the water storage corresponding to conduits without direct connection to the aquifer discharge areas.

Specific storage values, for 3-D elements were estimated by trial and error considering the aquifer hydraulic behaviour during emptying periods of the system. Emptying periods are particularly well suited for transient calibration of the model, because during these periods the aquifer is in continuous outflow without disturbances caused by recent recharge events.

Practical limitations related to the available data in the Castelo de Vide aquifer are also responsible for the use of recession periods to calibrate the model in transient conditions. The characterisation of the aquifer on the level of the temporal variability of state variables was presented in sections 3.5.2.2 and 3.5.3. Available data registrations characterising the time variability of piezometric data and spring discharge are mainly based on monthly observations. In some points data collection was done on a weekly basis. Under these conditions the characterisation of the aquifer consist of the analysis of the seasonal fluctuations in hydraulic head characterising the aquifer behaviour at an annual time scale. As the climatic conditions in that region are characterised by a long period of the year without recharge (six months or more), the emptying period of the aquifer can be well described by monthly data. On the other hand, recharge episodes are typically defined by infiltration processes being responsible for aquifer responses acting at a daily time scale. Therefore, a second type of aquifer response, with a short frequency, is present around the annual cycle of fluctuations related to annual climatic variability. Under these high frequency events conditions, prevailing during recharge periods, monthly measurements cannot capture the aquifer responses resulting from individual recharge events. Therefore, the validity of recharge simulations can only be done taking the annual variability of state variables into account.

### 6.5.2.2 – A practical classification of wells based on specific capacity

Water use in the Castelo de Vide aquifer was taken into account for steady state simulations considering the existence of wells with pumping rates affecting the general water balance. These wells are continuously active and are used for water supply of Portalegre, Castelo de Vide and Marvão towns (see section 3.4.5). The remaining pumping wells, mainly used for irrigation of food crops, are of minor importance when the respective pumping rates are compared to the aquifer long-term water balance. However, the analysis of state variables, during emptying periods of the system, shows that a realistic transient simulation cannot be done without the inclusion of irrigation wells, as their influence is very strong in the regional flow field during recession periods.

The simulation of pumping wells in a discrete continuum model (as well as points for analysis of hydraulic head variation) must take into account the relation between hydraulic behaviour of the considered point and the hydraulic properties of conduits and low permeability rock volumes. The definition of such relations cannot be generalised and consist in a quite qualitative choice of the location of the pumping wells (and observation points), taking into account the relation with the presence of dissolution channels in the "artificial conduit network", necessarily present in a regional discrete continuum flow model.

A quite practical analysis of drawdown in wells as response to pumping in carbonate aquifers shows that two kinds of typical situations exist: "pumping wells with high discharge rates and remarkably small drawdown" and, conversely, "pumping wells with low discharge rates and remarkably high drawdown". These typical situations, known to any practicing hydrogeologist, are common place in carbonate rocks. A less qualitative way to classify wells can be done by the calculation of the specific capacity. Specific capacity $C_s$, is defined as $C_s=Q/\Delta h_w$, where Q is the pumping rate and $\Delta h_w$ is the drawdown in hydraulic head produced as response to pumping (Freeze and Cherry 1979).

Specific capacity values are usually referred to a period of time, after which, a steady state is attained for a given pumping rate. However, the detection of the period, after which drawdown is negligible for a given pumping rate is difficult to determine in practice. In the case of the Castelo de Vide wells with known drawdown, after one hour of pumping, were selected in order to compare the results obtained for the classification of wells as an alternative to the more detailed procedures applied to estimate transmissivity values in chapter 5. The wells where such records exists are shown in figure 6.16.

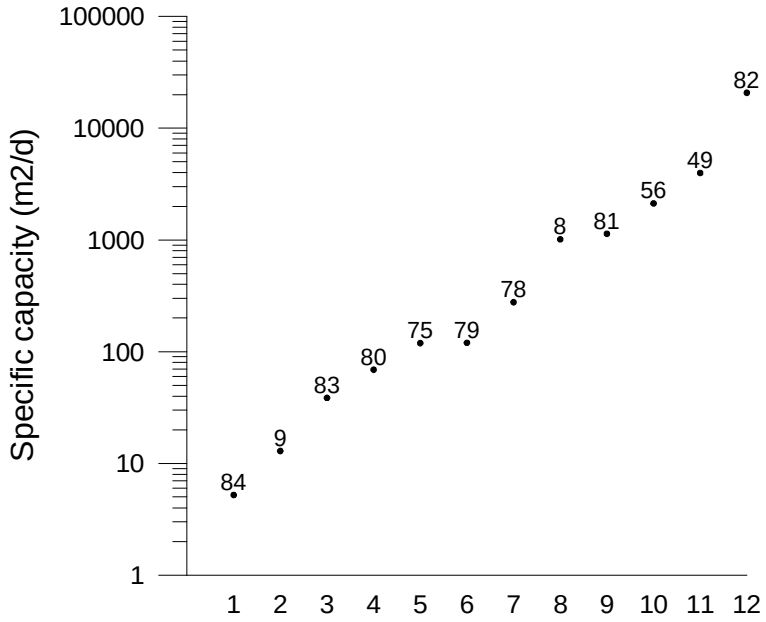


Fig. 6.16 – Classification of pumping wells according to Specific capacity ($C_s$), for drawdown registered after one hour of pumping.

By using the values of specific capacity it is possible to define the wells that must simulated as points extracting water directly from conduits in the "artificial conduit network" (characterised by high specific capacity values) or, alternatively, from the low permeability rock volumes (corresponding to points with low specific capacity values). It is interesting to note that the definition of these points based on detailed time/drawdown values as presented in chapter 5 conduces to the same classification of wells as obtained based on the determination of the specific capacity. According to these results, prescribed discharge rates of wells 82, 49 and 56 were simulated in highly conductive 1-D elements. The remaining pumping wells presented in table 6.5 were not submitted to pumping tests. However the observation of

these points shows that drawdown is important during few hours of pumping per day. Therefore they were simulated by prescribed discharge values in nodes at the corner of 3-D elements.

The extraction rates and volumes in the wells during a long emptying period of the aquifer (February 1997-October 1997) are presented in table 6.5. During 241 days precipitation was negligible and therefore recharge is near zero during this period. Pumping rates are values calculated by the multiplication of instantaneous pumping rates, in each well, by the average number of extraction hours. The results of the transient simulations of this period will be subject of the next section 6.5.2.3.

| Stress period | 1 | 2 | 3 | 4 | 5 | 6 | 7 | 8 | 9 |
|---|---|---|---|---|---|---|---|---|---|
| Time (h) | 0-1320 | 1320-1728 | 1728-2136 | 2136-2688 | 2688-3696 | 3696- 4656 | 4656- 4752 | 4752-5160 | 5160-5784 |
| Pumping well | Pumping rate (l/s) | Pumping rate (l/s) | Pumping rate (l/s) | Pumping rate (l/s) | Pumping rate (l/s) | Pumping rate (l/s) | Pumping rate (l/s) | Pumping rate (l/s) | Pumping rate (l/s) |
| 82 | 15.00 | 15.00 | 15.00 | 15.00 | 15.00 | 25.00 | 25.00 | 25.00 | 15.00 |
| 79 | 5.00 | 5.00 | 5.00 | 5.00 | 5.00 | 5.00 | 5.00 | 5.00 | 5.00 |
| 49 | 30.00 | 30.00 | 30.00 | 30.00 | 30.00 | 30.00 | 30.00 | 30.00 | 30.00 |
| 56 | 2.74 | 2.74 | 2.74 | 2.74 | 2.74 | 2.74 | 2.74 | 2.74 | 2.74 |
| 33 | | 1.00 | 1.00 | 1.00 | 1.00 | 1.00 | 1.00 | 1.00 | 0.00 |
| 17 | | | | 0.40 | 0.40 | 0.60 | 0.60 | 0.00 | 0.00 |
| 18 | | | | 0.25 | 0.35 | 0.35 | 0.35 | 0.35 | 0.35 |
| 19 | | | | | 0.50 | 0.50 | 0.50 | 0.50 | 0.50 |
| 21 | | | | | 0.40 | 0.40 | 0.40 | 0.40 | 0.00 |
| 22 | | | | | 1.50 | 1.50 | 0.70 | 0.70 | 0.00 |
| 36 | | | | | 1.00 | 1.00 | 1.00 | 0.50 | 0.00 |
| 37 | | | | | 0.50 | 0.50 | 0.50 | 0.20 | 0.00 |
| 38 | | | | | 0.15 | 0.30 | 0.30 | 0.30 | 0.30 |
| 65 | | | | | | 1.00 | 1.00 | 1.00 | 1.00 |
| 23 | | | | | | 0.20 | 0.20 | 0.20 | 0.20 |
| TPR (l/s) | 52.74 | 53.74 | 53.74 | 54.39 | 58.54 | 70.09 | 69.29 | 67.89 | 55.09 |
| TPV ($m^3/s$) | $2.51\times10^5$ | $7.89\times10^4$ | $7.89\times10^4$ | $1.08\times10^5$ | $2.12\times10^5$ | $2.42\times10^5$ | $2.39\times10^4$ | $9.97\times10^4$ | $1.24\times10^5$ |

Table 6.5 – Extractions in wells during a 5784 hours (241 days) emptying period of the aquifer corresponding to a drought period. Then stress periods were defined between February 1997 and October 1997. Pumping rates are values calculated by the multiplication of instantaneous pumping rates, in each well, by the average number of extraction hours. TPR – total pumping rate for each stress period; TPV – total pumped volume during each stress period. Total value of extractions during the entire period is $1.22\times10^6 m^3$.

#### 6.5.2.3 – Simulation of an eight-month emptying period of the aquifer

The long-term climatic conditions prevailing in the area of Castelo de Vide aquifer are responsible for the existence of a recharge period usually comprised between November and April (see table 3.5 in section 3.4.2). However, these average conditions are of little significance as revealed by the extreme climatic variability characterizing the region (see figure 3.7 in section 3.4). The occurrence of extreme seasonal conditions often occurs in the entire Alentejo region. These periods are mainly characterised by the occurrence of precipitation during only part of the period between November and April. On the other hand precipitation between May and October rarely induce recharge events. A good example of a long period without precipitation, with the consequent absence of relevant water input into the aquifer was detected during the measurement of state variables between February and October of 1997. Taking these climatic conditions into account it must be considered that recharge events are of very short duration, when compared to the long recession periods observed in the aquifer. Intensification of water exploitation during recession periods is added to these natural conditions, giving a special relevance to the study of the aquifer hydraulic behaviour during long depletion periods.

As discussed earlier, the value for the conduit storativity ($S_d$) used in the transient simulations is $2.5\times10^{-8}$m and is thus in agreement with the conductive parameter ($T_d$=10 $m^3/s$) used to characterise the conduits in steady state conditions. Coherence between these values is defined by the physical principles expressed in equations 5.16 and 5.18 in section 5.5. On the other hand the simulation of this emptying period of the aquifer showed that the specific storage ($S_s$) values around $1\times10^{-3}$ $m^{-1}$ provide an acceptable description of the system. Despite the reserves for the accuracy of storativity values determined in chapter 5 (in single well pumping tests) it must be remarked that the obtained results point at that the values for this parameter are high. Simulations performed using specific storage values between $1\times10^{-6}$ $m^{-1}$ and $1\times10^{-5}$ $m^{-1}$ are responsible for a less realistic representation of the aquifer than simulations based on values between $1\times10^{-4}$ $m^{-1}$ and $1\times10^{-3}$ $m^{-1}$. Reliable values of specific storage are very difficult to determine at the well scale. Therefore the values for this parameter were chosen taking the definition of regional values into account, which probably encompass the more frequent "real" values at lower scale levels. Despite the best results obtained when a value for specific storage of $1\times10^{-3}$ $m^{-1}$ was used in the model, lower values were better suited for part of the Escusa sector. Observation points in this aquifer sector are characterised by a general trend corresponding to the presence of the highest amplitudes in hydraulic head observed in the aquifer. That trend is clearly identified in figure 6.17. A possible explanation for this hydraulic behaviour could be the highest karstification of the aquifer in the proximity of its main discharge area. The best results obtained for the simulation of the studied aquifer recession period show that an important part of Escusa sector is better characterised by a $1\times10^{-4}$ $m^{-1}$ for the specific storage. The complete set of parameters used for that model variant is shown in table 6.6. Parameter distribution used for 3-D elements is presented in figure 6.18.

| Parameter | Kind of elements | Value |
|---|---|---|
| $T_d$ ($m^3/s$) | 1-D | 10 |
| $K$ (m/s) | 3-D | $10^{-6}$ |
| $S_d$ (m) | 1-D | $2.5\times10^{-8}$ |
| $Ss$ ($m^{-1}$) – General value | 3-D | $10^{-3}$ |
| $Ss$ ($m^{-1}$) – Part of Escusa sector | 3-D | $10^{-4}$ |

Table 6.6 – parameters used in the model for the more realistic transient simulation of the eight-month recession period.

Figures 6.19 to 6.21 show hydraulic head values measured in the field and calculated using the discrete continuum model using the parameter values shown in table 6.6. In order to made the figures 6.19 to 6.21 legible the errors found during steady state simulations were eliminated. The magnitude of these changes is illustrated in figure 6.17.

In steady state simulations the water balance was controlled by a uniformly distributed 450mm/year recharge at the top of the aquifer model, which corresponds to the average annual infiltration estimated in Section 3.4.5. In order to define more realistic initial conditions needed to perform transient simulations, a recharge period of 31 days was simulated in order to produce an excitation of the system prior to the simulation of the long emptying period of the aquifer. This was done taking a recharge period into account, which preceded the subsequent period without precipitation. According recharge estimations for this period a value of 120mm was considered for the month prior to the simulations of the recession period.

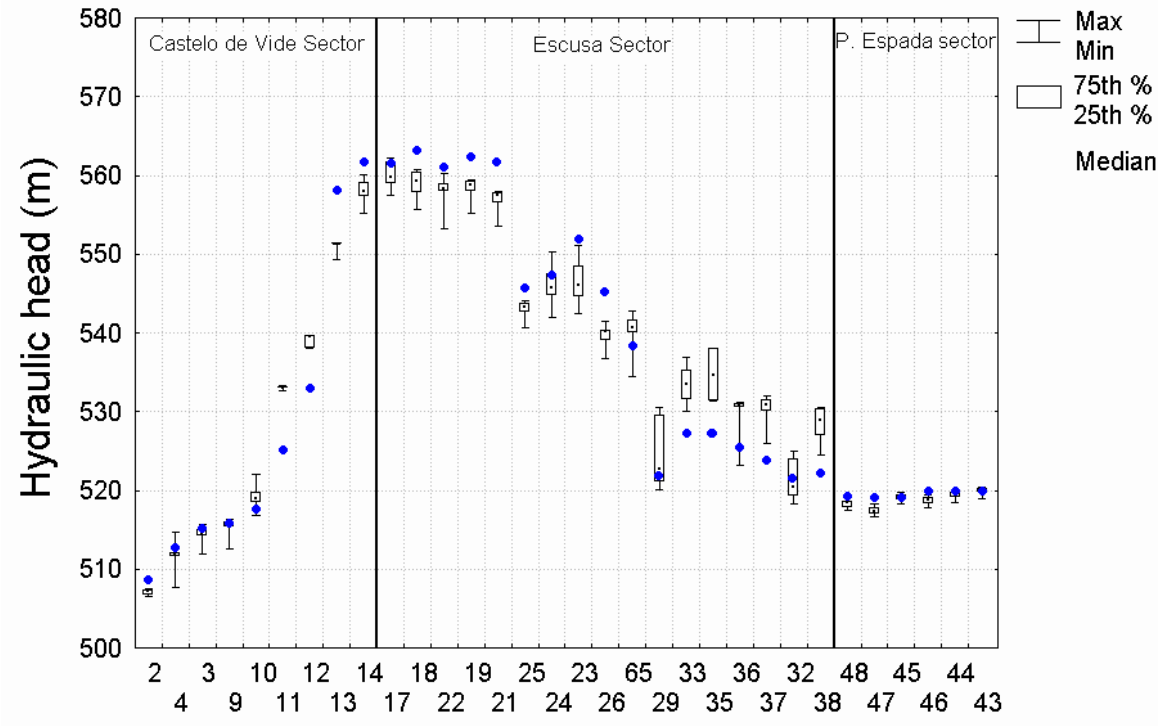


Fig. 6.17 – Boxplots representing hydraulic head variability registered between 1991 and 1999. Dots marked in bold correspond to hydraulic head values calculated by the steady state simulation presented in section 6.5.1.2. The simultaneous transient representation of hydraulic head values determined by field measurements and the ones calculated using the discrete continuum model in figures 6.19 to 6.21 is done after the elimination of residuals encountered in steady state simulations. In practice this is done by the displacement of the steady state calculated values of each observation point (points marked in bold) for positions near the median of values obtained from field measurements. Therefore, the transient graphical analysis of differences between observed and calculated values is based on the representation of hydraulic head variability and not in the absolute values calculated using the model.

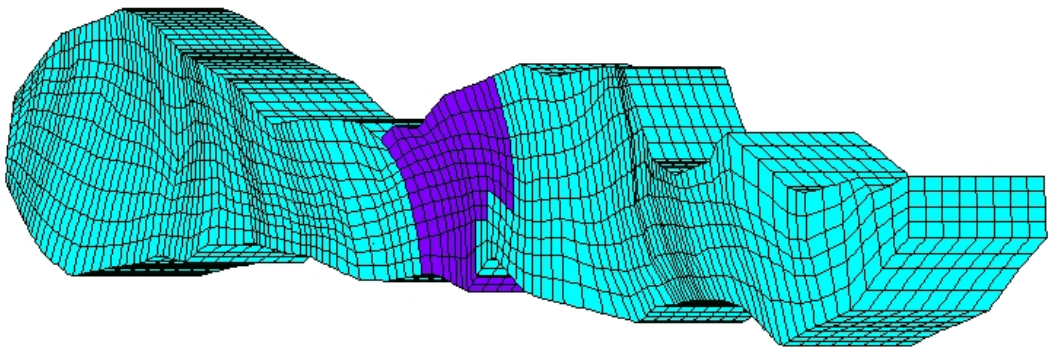

Fig. 6.18 – Specific storage distribution for 3-D elements, used in the discrete continuum model for the variant with best results for an eight-month aquifer recession period. General value used in most of the aquifer corresponds to $10^{-3}$ $m^{-1}$. The assigned value for shaded elements, in part of the Escusa sector, was $10^{-4}$ $m^{-1}$. This value was defined for all the eight element slices between the surface and the model bottom. As can be seen in figure 6.17, observation points in this aquifer sector are characterised by a general trend of increased amplitudes in hydraulic heads. These oscillations are better reproduced when a lower specific storage is assigned to the shaded elements. The maximum dimension of the model along its axis is 8,951m. The aquifer is represented with a vertical exaggeration of 3.

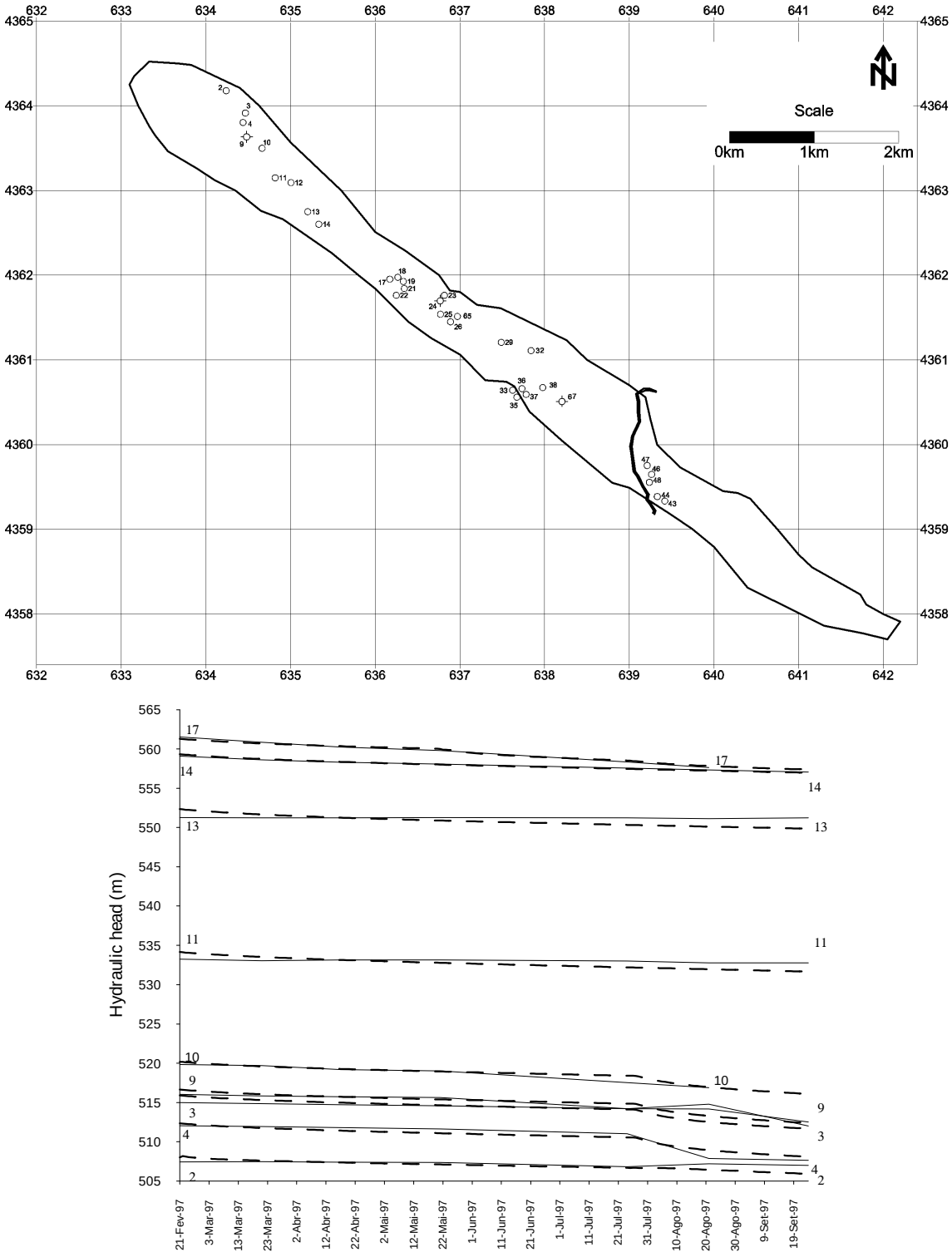


Fig. 6.19 – Hydraulic head values determined in the aquifer (solid lines) and calculated using the discrete continuum model (dashed lines) for the Castelo de Vide sector. Note that observation point 17 shown here belongs to Escusa sector and is only represented here in order to illustrate the behaviour of wells close the groundwater divides located between observation points 17 and 14. Hydraulic head values calculated for some of the points were displaced along the *y*-axis, in order to keep the figure readable. The magnitude of these changes is shown in figure 6.17.

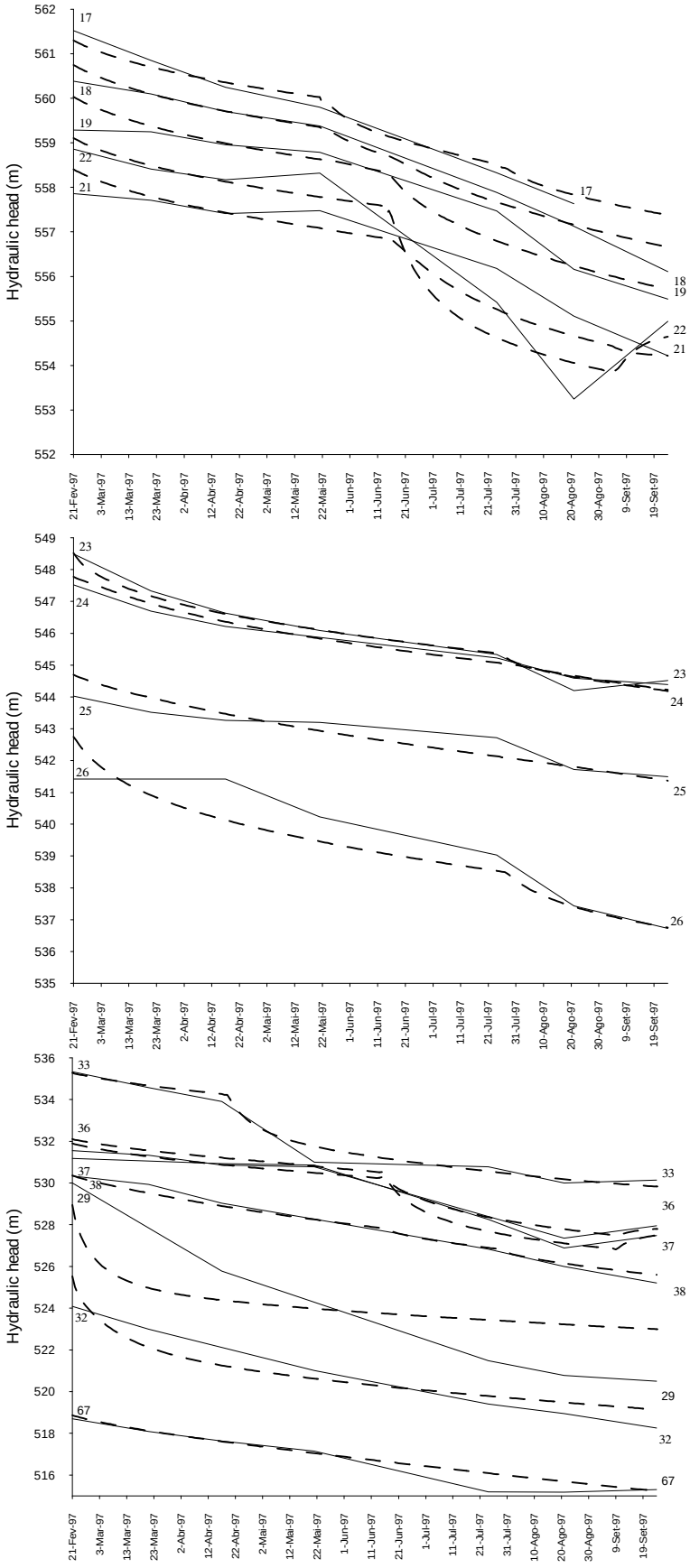


Fig. 6.20 – Hydraulic head values determined in the aquifer (solid lines) and calculated using the discrete continuum model (dashed lines) for the Escusa sector. Location of observation points can be seen in figure 6.19. Hydraulic head values calculated for some points were displaced along the *y*-axis, in order to keep the figure readable. The magnitude of these changes is shown in figure 6.17.

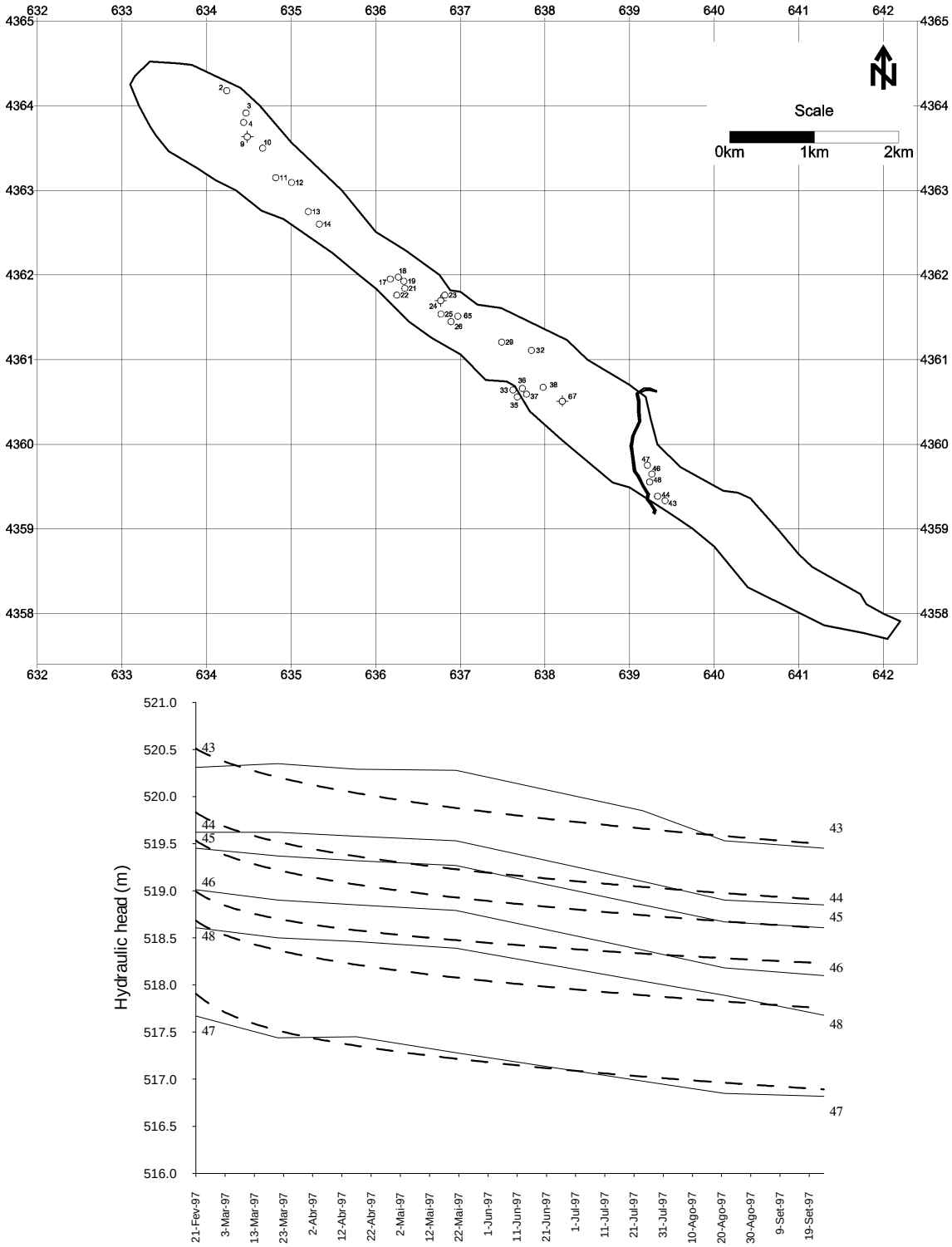


Fig. 6.21 – Hydraulic head values determined in the aquifer (solid lines) and calculated using the discrete continuum model (dashed lines) for the P. Espada sector. Hydraulic head values calculated for some points were displaced along the *y*-axis, in order to keep the figure readable. The magnitude of these changes is shown in figure 6.17.

The assignment of a specific storage value of $1\times10^{-4}$ $m^{-1}$, characterising parts of the Escusa sector, instead of the general value of $1\times10^{-3}$ $m^{-1}$ in the remaining aquifer volume, introduced changes in the simulated temporal hydraulic head variability in that part of the aquifer. The impact introduced by such a change could be evaluated in figure 6.24. Results presented in this figure correspond to a simulation equivalent to the model variant presented throughout figures 6.19 to 6.21. The only difference is the assignment of a specific storage value uniform for the entire aquifer ($1\times10^{-3}$ $m^{-1}$). The results of those calculations are only compared to hydraulic head values in the Escusa sector. The differences produced by this change in the other aquifer sectors are negligible and are not distinguishable in the graphical representations. In fact, even for observation points 17 to 21, in the Escusa sector, the results are practically the same in both model versions.

Analysis of figures 6.20 and 6.24 show that some improvement is gained in terms of predictability of the hydraulic head variability when specific storage is changed to a lower value in parts of the Escusa sector. This is related to the higher values of drawdown simulated during recession periods observed in that part of the aquifer.

Another interesting aspect resulting from the analysis of the transient simulations of the period February 1997 to October 1997 is the difference between observed and calculated drop in hydraulic head in P. Espada sector, shown figure 6.21. That figure shows the determined and calculated hydraulic head values in observation points 43 to 48, located close the Sever river, which acts as the main discharge area of the aquifer. The shape of the curves representing the variation of the observed hydraulic heads seems to show that in long recession periods the usual transferences from the aquifer toward the river might be inverted. Water transference through the riverbed is governed by the difference between the hydraulic head in the aquifer and the water surface elevation of the river. As long as the groundwater table does not drop below the river level this transferences will be negative (the river is effluent, and thus water is transferred towards the river). In general terms it is known that the most common situation present in the aquifer corresponds to transferences from the aquifer towards the river. However, it is possible that in extreme drought periods some water transference takes place from the river towards the aquifer, thus converting the river to a temporal recharge area.

As referred to in section 3.5, the only way to determine the volumes of transferences throughout the riverbed consists of installing two gauges, monitoring the river discharges in two points immediately upstream and downstream of the carbonate aquifer limits. The difference between discharge values measured in these points corresponds to the aquifer discharge or, conversely, as experimental conditions seem to show in some low water periods, to water transference from the river toward the aquifer. The installation of these gauges is one of the recommendations proposed in this work in order to improve knowledge about the Castelo de Vide aquifer.

Figure 6.22 shows the variation of water transference from the aquifer toward discharge areas (Sever River and the aquifer limit near the Castelo de Vide zone) during the simulated recession period. The analysis of this figure shows the relative importance of the aquifer discharge areas. As expected, water transference toward crystalline rocks in the Castelo de Vide area is less important than outflow toward the river. Moreover, transient phenomena is also much more important for water transferences toward the river. Another important aspect distinguishable in the transient analysis of outflow in the discharge areas is the fact that the intensification of the aquifer exploitation affects water transferences in a sensitive way in the Castelo de Vide Sector. This can be seen in figure 6.23 where only the outflow in the Castelo de Vide area is plotted. The slope increase detected after July is mainly related to the seasonal increase in the pumping rate of well 82 used for water supply in the Castelo de Vide town.

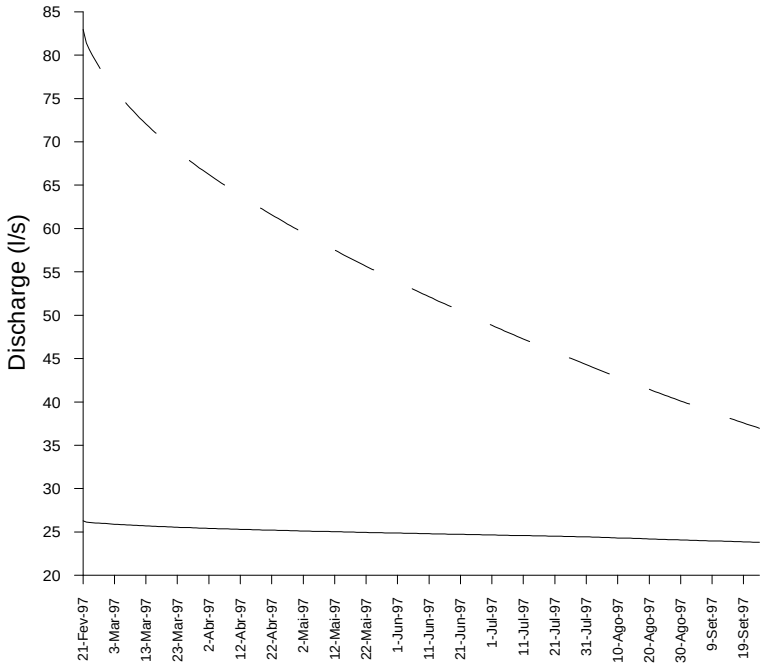


Fig. 6.22 – Calculated water transference from the aquifer towards discharge areas during the simulated recession period. Sever River is represented by the dashed line. The solid line represents transferences towards crystalline rocks in contact with the aquifer close the Castelo de Vide area.

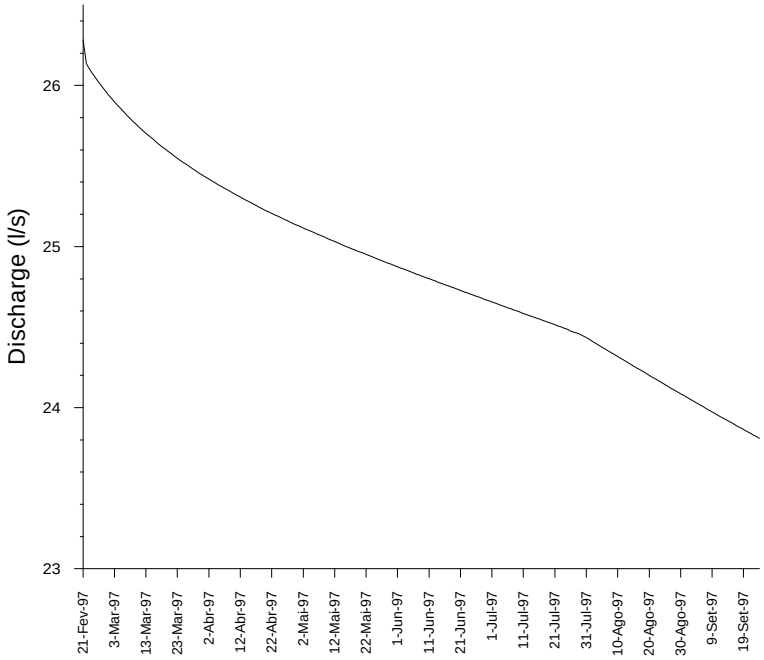


Fig. 6.23 – Calculated water transference from the aquifer toward the crystalline rocks in contact with the aquifer close to the Castelo de Vide area during the simulated recession period, showing the effect of seasonal pumping increase after July.

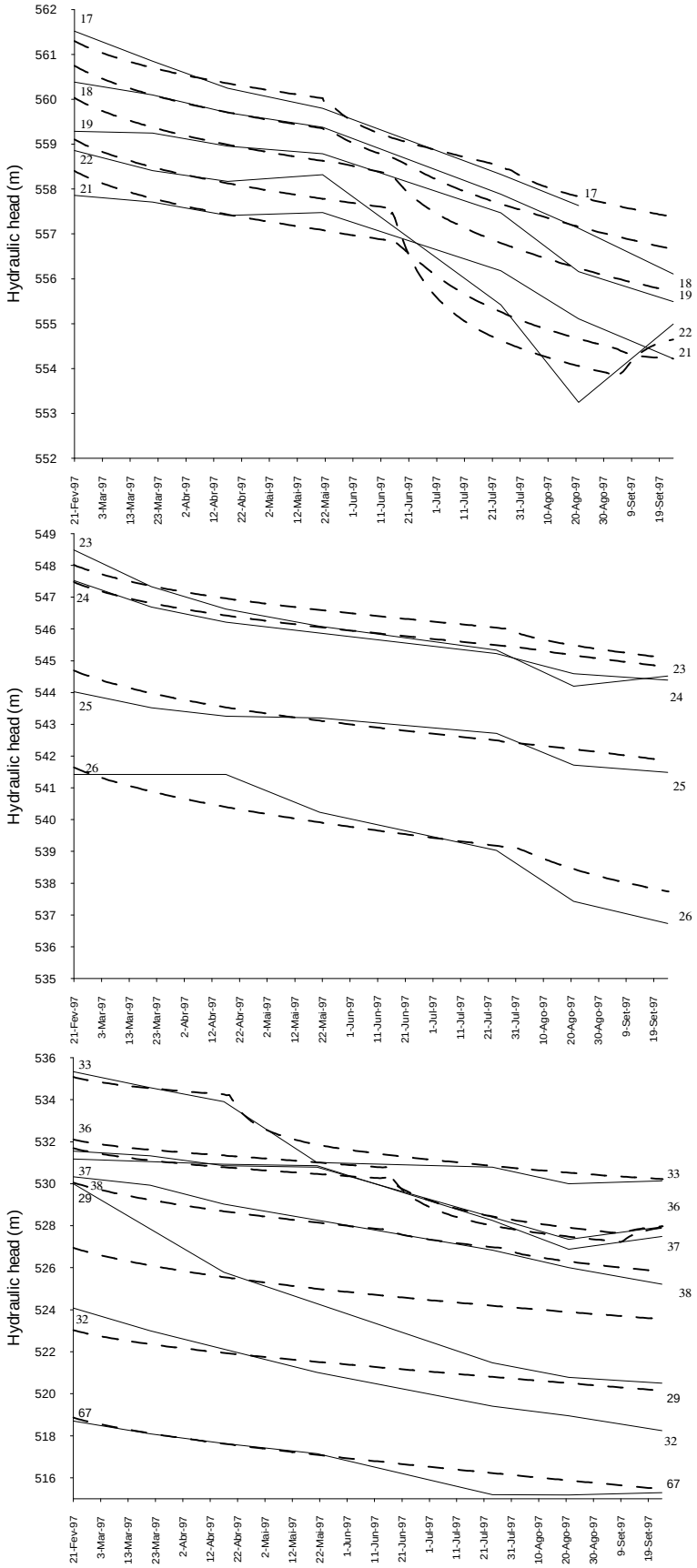


Fig. 6.24 – Hydraulic head values determined in the aquifer (solid lines) and calculated using the discrete continuum model (dashed lines) for the Escusa sector. Location of observation points can be seen in figure 6.19. Hydraulic head values calculated for some points were displaced along the *y*-axis, in order to make the figure readable. The magnitude of these changes is shown in figure 6.17. This time using a uniform value for specific storage characterising 3-D elements.

#### 6.5.2.4 – Remarks on the problems in characterising recharge events in real carbonate aquifers

As referred to in section 3.5.2.2 the available data registry characterising the time variability of state variables is mainly based on monthly observations. Under such conditions the characterisation of these variables is based on the analysis of the seasonal fluctuations in hydraulic heads characterising the aquifer at the annual time scale. As shown in the previous section these data sets allow an adequate characterisation of the aquifer during recession periods, because climatic conditions in that region are characterised by long periods without recharge. Therefore, after the steady state calibration of the model it was possible to obtain a reasonable simulation of the aquifer hydraulic behaviour during a long recession period. Under these circumstances there are good reasons to expect that the actual state of development of the model allows the simulation of the aquifer hydraulic behaviour during recharge periods as well. However recharge episodes are characterised by infiltration processes leading to aquifer responses on a smallest time scale. Thus, a second kind of aquifer response having a short frequency, during recharge periods, is present and superimposed on the fluctuations related to annual climatic variability. The aquifer responses to these short recharge episodes cannot be captured with monthly measurements of state variables.

As discussed in section 3.4.3 recharge in the Castelo de Vide carbonate aquifer takes place trough processes including autogenic diffuse and concentrated recharge (originating from precipitation occurring directly in the aquifer area) and allogenic diffuse and concentrated recharge (derived from lateral water inputs). It was shown that allogenic recharge seems to be important enough (in parts of the Escusa Sector) to justify improvements in simulations, even in steady state simulations.

However, some basic questions need to be answered prior to characterisation of the recharge processes in order to obtain reliable simulations of the aquifer behaviour. Three levels of decisions are required to characterise processes linked to the infiltration processes, in order to simulate recharge events:

1 - Definition of the fraction of precipitation that escapes from the evapotranspiration and reaches the saturated zone of the aquifer;

2 - The determination of the relative fractions of diffuse and concentrated recharge;

3 – Distribution of the fraction of the overall value of concentrated recharge to the different swallow holes.

The first problem is not difficult to solve because the density of the stream network tends to zero in the Castelo de Vide aquifer (as often occurs in karst aquifers). Under these conditions a reliable value for evapotranspiration is sufficient to define the fraction of precipitation corresponding to recharge.

The second problem is crucial and, in the present case study, there are no means providing estimations of the relative fractions of concentrated and diffuse recharge. In the cases where a global response is identified in karst aquifers it is possible to make inferences about the relative importance of these processes (even if theoretical studies and experimental evidence seem to show that such inferences are not very consistent, as discussed in section 3.5.3.3). However, in the present case study, due to the prevailing natural conditions it is very difficult to characterise the global responses of the aquifer. Thus, the use of these methods cannot be done with the presently available data sets.

Results presented by Kiraly *et al.* (1995), based on the investigation of a synthetic karst aquifer, seem to show that the typical global responses, often detected in well developed karst aquifers are only possible when an important fraction of concentrated recharge occurs. According to these theoretical considerations more than 40% of the infiltration should occur as concentrated recharge to provide a typical storm hydrograph in a karstic spring. Similar results were obtained by Cornaton (1999) using another synthetic karst aquifer, where only concentrated infiltration superior to 60% provoked typical karstic spring hydrographs and the occurrence of other transient phenomena typical in karst aquifers (as gradient inversions between the conduits and the low permeability rock volumes after storm events).

The main problem in translating these theoretical results to real carbonate aquifers lies in the determination of the relative importance of each swallow hole, in which concentrated recharge occurs. In other words, for each defined hypothetical scenario (for example 40%, 50% or 60% of concentrated recharge) the relative contribution of each swallow hole to the global concentrated recharge has to be determined. In the “artificial karst aquifers” used in theoretical studies the distribution of these values is not important because the interpretation of the results is mainly based on the analysis of global responses. However, in real case studies this is very important because the propagation of potentials and, consequently, the aquifer hydraulic behaviour is dramatically affected by the relative fraction of the total concentrated recharge occurring in each sink-hole.

The simulation of recharge events in model variants characterised by the absence of concentrated recharge (100% of diffuse infiltration) show that simulated hydraulic heads are almost always superior to values determined in observation points. However, when concentrated recharge is 50% many of the observation points present more important responses than the simulated ones. For 80% of concentrated recharge the amplitude of "real responses" is higher than the simulated ones. The problem in accurately simulate the aquifer responses in different sectors is related to the distribution of the global value of concentrated recharge to the different swallow holes. The evaluation of the impact of different values characterising the total amount of concentrated recharge can easily be approached by a strategy of trial and error with few simulations. On the other hand, the decision of the amount of concentrate infiltration that must be attributed to each model swallow hole can vary among thousands of plausible possibilities, even for a relatively simple case. In the case of the Castelo de Vide aquifer it is clear that concentrated infiltration cannot be uniformly distributed in the 15 swallow holes identified in the field and defined in the model. The absence of methods to deal with this problem is among the more important drawbacks regarding the possibilities of characterising carbonate aquifers on the different levels required for the use of discrete continuum models. The identification of this problem is, in our opinion, one of the aspects deserving more attention in the future developments as derived for the present work. As the method for calibration of the discrete continuum model presented in this work shows good results (in steady state and recession periods), there are good reasons to believe that good results could also be obtained for simulations of recharge events. As a "trial and error" calibration technique cannot be applied to deal with this problem we suggest that, after the calibration of a model in steady state and recession periods, an automatic calibration of the model for recharge periods could be a good strategy to approach this problem.

### 6.5.3 – Concluding remarks on the obtained results

The present state of knowledge about the Castelo de Vide hydrogeology and the present state of development of the discrete continuum flow model allows the identification of some aspects needing further research in order to improve the possibilities in simulating the aquifer hydraulic behaviour.

Regarding the aspects related to the aquifer characterisation, the essential problem to solve consists of obtaining more detailed data for state variables in transient conditions. As previously referred, data collection of Sever river discharge upstream and downstream the aquifer is essential to evaluate the global water balance and recharge estimations. On the other hand, it is also essential to obtain daily data registries for hydraulic heads in observation points in order to assess the impact of individual recharge events.

As the central objectives of the present work are related to the aquifer characterisation on the different levels required for the implementation of a discrete continuum model the technical description of the model, presented throughout this chapter is far from being exhaustive. Therefore some complementary aspects about the model characteristics need to be presented in more detail in order to create a basis for the discussion of the technical aspects concerning model improvements. However, these improvements also depend on the need of obtaining more detailed data sets for state variables as referred to in the previous paragraph and, additionally, conduce complementary hydrogeologic studies in the crystalline rocks in contact with the aquifer in the Castelo de Vide area. The first of these aspects is related to the need in define a finer discretization of the finite element mesh in the area of the Sever River. In fact, the control points in that area are very close to each other and therefore its representation in the model needs a more accurate spatial representation. Also the gradients in hydraulic head in that area are very low and the future investigation of the probable inversions of gradient between the River and the aquifer needs a very accurate representation of the aquifer geometry there. However, the effort in improving the model on this level can only be justifiable if a detailed topographic survey is made available for this zone. On the other hand the discharge of the river must be monitored during a reasonable period in order to allow to approach this problem in a more consistent basis. The second aspect related to this problem is the definition of boundary conditions in the aquifer discharge area near the Castelo de Vide town. In fact, the prescribed heads along the aquifer boundary were defined only in the nodes on the model surface. It would be preferable, however, to impose heads also along the lateral no-flow boundary and not only on the surface. In that sense the 2-D cross sectional flow model presented in section 4.2.1 is more realistic than the present 3-D model, because in that case, the prescribed heads in the Castelo de Vide discharge area were defined on the top 50m of the aquifer boundary. However, in the 2-D model this corresponds to three nodal values. In the case of the 3-D model the definition of such conditions corresponds to the introduction of hundreds of points in a file, in which the nodal conditions are defined. In that sense, the second problem is related to the absence of pre-processing tools with the characteristics needed to manipulate finite elements meshes with 1-D, 2-D and 3-D elements. In this case such efforts can be only justified if a more detailed hydrogeological characterisation for that zone is make available. It must be noted that the research needed to solve this problem is more related to the study of the granitic and metamorphic rocks in contact with the aquifer in that zone than with the study of the carbonate aquifer itself. However, if such a studies are conducted, a more realistic approach could be done including of the neighbouring hydrogeological units in lateral contact with the actual model and seeking better no flow boundaries at a reasonable distance of the carbonate rocks.

Despite the described efforts needed to improve the model accuracy the obtained results suggest that the absence of these improvements does not affect the general conclusions regarding the potential and the limits of the use of the discrete continuum approach in carbonate aquifers as analysed in the present case study. On the other hand, as discussed in the last paragraphs, the time required to implement these improvements in the model can only be justifiable if an improvement of the actual data set is made available for the state variables. In fact the evaluation of the improvements predicted by the implementation of the discussed changes is difficult (or even impossible, in the case of the simulation of individual recharge events) with the actual weekly and monthly data sets.

# Chapter 7

## GENERAL CONCLUSIONS AND FURTHER PERSPECTIVES

Contents

## 7.1 – General overview

The main objectives of this work were expressed in chapter 1 as the search for the answer to two questions:

- Do the actual possibilities to investigate the characteristics of a particular carbonate aquifer allow the definition of a simplified symbolic representation of the system, compatible with the information needed to implement a discrete continuum model?

- Does the actual state of development of discrete continuum models allow the simulation of the hydraulic behaviour in carbonate aquifers, where conduit and diffuse flow are superimposed in the same flow domain?

Despite the lack of standard methods allowing the characterisation of carbonate aquifers on the different levels required for the use of discrete continuum flow models, the results presented in this work seem to show that, at least in some cases, the answer to the first question is positive. The main difficulties in characterising the real system are related to the difficulties in interpreting the role of the "real conduit network" present in carbonate aquifers and to reproduce its hydraulic characteristics in a strongly simplified "artificial conduit network". The "artificial conduit network" introduced in the model implemented in this work was defined assuming that different branches in a conduit network, with different hydraulic connectivity with the aquifer discharge areas, could be detected by the identification of trends characteristic of spatial distribution of the regional gradients in hydraulic heads in the "real aquifer". The obtained results following this strategy yielded good results in the present case-study. Therefore, it is tempting to suggest that the steps defined for the calibration of the model, followed in this work, are valid for the characterisation of other carbonate aquifers. However, it must be taken into account that, without detailed field studies focused in the same objectives in other aquifers, it is not possible to assess to which extent the results obtained in the present case study can be generalised, or are related to the particular natural conditions prevailing in the Castelo de Vide aquifer.

The second question is partially answered in the last paragraph. As referred before it must be considered that the discrete continuum approach is a more adequate basis to simulate the flow processes acting in carbonate aquifers than standard single continuum flow models. However the results obtained in this work using both single continuum and discrete continuum flow models show that the starting point for a meaningful use of discrete continuum models is not necessarily there, where the single continuum approach attains its limit of applicability. As a matter of fact, single continuum models were used in this work in order to estimate hydraulic parameters at the single well scale and to obtain equivalent hydraulic conductivity at the entire aquifer scale. Without the use of a regional single continuum flow model it would have been very difficult to validate the conceptual flow model conceived for the Castelo de Vide aquifer, prior to the implementation of a discrete continuum flow model. On the other hand, the current use of regional discrete continuum flow models cannot be easily generalised before integrated software packages exist, including the discrete continuum model itself and, additionally, a complete environment allowing an efficient set of pre-processing and post-processing tools. Otherwise, the time spent defining the typology of "artificial conduit networks" is prohibitive when dealing with the usual requirements of applied hydrogeologic problems.

Despite the positive results obtained in this work it must be remarked that the prevailing natural conditions usually present in carbonate aquifers conduit flow is very often turbulent. Therefore, the parameters assigned to characterise the "artificial conduit network" introduced in the discrete continuum model lead to a quite unrealistic representation of the dissolution channels present in the "real conduit network". In fact the parameters used to characterise these conduits correspond to equivalent parameters of pipes with circular cross-section with only 8 cm in diameter. This is in contradiction with the presence of conduits with metric dimensions often encountered in all the aquifer sectors. However, taking into account the fact that the computer programs available for this work simulate flow in laminar conditions, this is the only way to simulate flow at the aquifer scale in real conditions. It must be emphasized that this is the major drawback associated to the modelling technique employed in this work.

Prior to the elaboration of the aspects deserving special attention in future developments, as derived from the present work, a synopsis of the obtained results is presented in the next section regarding: (1) the actual knowledge about the hydrogeology of the Castelo de Vide carbonate aquifer and (2) the actual development of the implemented regional discrete continuum flow model. The development on these levels show that the reliability of the simulations allowed by the actual version of the discrete continuum regional flow model can be improved by the technical evolution of the model itself and by complementary hydrogeologic studies, mainly related to the collection of detailed data sets characterising the state variables. On the other hand, it must be considered that the improvement of the knowledge regarding the hydrogeology of carbonate rocks depends also on the characterisation of the crystalline rocks in contact with the carbonate aquifer in the Castelo de Vide area. The hydrogeologic characterisation of these lithologies, hydraulically connected with the carbonate aquifer, will contribute to the definition of more accurate boundary conditions in the Castelo de Vide aquifer sector.

**7.2 – Summary of the actual hydrogeologic knowledge of the Castelo de Vide carbonate aquifer and development of the regional discrete continuum model**

The principal conclusions summarised in this section are related to the improvement of the hydrogeologic knowledge of the Castelo de Vide carbonate aquifer discussed throughout chapters 3 to 5. The summary of the actual development of the regional discrete continuum model is mainly related to the results presented in chapter 6. The synthesis of these aspects will be focused in the discussion of the perspectives for further development of the present work.

The 7.9Km$^2$ Castelo de Vide carbonate aquifer has an annual recharge volume varying between approximately $1.5\times10^6$ m$^3$ and $7.7\times10^6$ m$^3$, corresponding to an average of $3.6\times10^6$ m$^3$/year for a 30 years long-term water balance. Therefore, the annual water volume actually extracted in pumping wells ($1.88\times10^6$ m$^3$/ year) is superior to the recharge rates estimated for some years during the period between 1960 and 1998. Considering the actual extracted volumes, such situations occurred in 1981 and 1992. Despite the identification of years characterised by recharge volumes inferior to well extractions, the recovery of water levels seems to be immediate in a single year characterised by recharge values around average conditions. This is related to the fact that almost the entire flow domain is immersed within the low permeability lithologies below the altitude of the recharge areas. With these particular boundary conditions, when water levels drop below the discharge areas, all the recharge volume (autogenic and allogenic recharge) contributes to a very effective recovery of the water reserves, until the level of the discharge areas is reached again.

The coupled analysis of the long-term water balance, geometry of the flow domain, position of discharge areas and the spatial distribution and time variability of hydraulic head allowed the definition of a conceptual flow model characterised by the existence of three sub-regional flow systems within the aquifer. The defined conceptual flow model was used to formulate a problem, which solution allow the estimation of equivalent hydraulic conductivity at the regional scale. The solution of this problem consists in determine the position of a groundwater divides between Castelo de Vide and Escusa sectors of the aquifer, which depends on equivalent hydraulic conductivity and recharge at the aquifer scale. The solution for this problem was found by two different methods: using a single continuum finite-element flow model and an analytical model based on Dupuit-Forcheimer simplifications. Equivalent hydraulic conductivity estimated for the entire flow domain using the numerical flow model is $7\times10^{-4}$ m/s. When the equivalent hydraulic conductivity was determined by the use of the analytical solution, a different value was obtained for each of the three flow systems (sectors) separately. In this case equivalent hydraulic conductivity is $2.1\times10^{-4}$ m/s (Castelo de Vide sector), $1.5\times10^{-4}$ m/s (Escusa sector) and $2.9\times10^{-4}$ m/s (P. Espada sector).

Hydraulic conductivity values were also determined at the well scale by the interpretation of pumping tests using single continuum and double continuum analytical models. The obtained values showed that the hydraulic conductivity values characterising the carbonate rocks at the well scale take on values over four orders of magnitude, between $2.5\times10^{-6}$ m/s and $1.3\times10^{-3}$ m/s. These values, together with equivalent hydraulic conductivity determined at the aquifer scale reflect the change of this parameter with scale, often detected when diffuse and conduit flow processes are present within the same flow domain.

Parameters determined with pumping tests allowed an accurate simulation of drawdown and recovery observed in wells as response to pumping. At the same time, equivalent hydraulic conductivity values, determined at the aquifer scale allowed a reliable steady-state description of the aquifer, compatible with the observed spatial distribution of hydraulic head and the long-term water balance calculated by different methods. These results show that it is possible to obtain reliable estimates of the hydraulic conductivity at the well and the aquifer scales. However the values obtained at these different scales cannot be linked in order to define a global representation of the aquifer. This limitation is related to the presence of a conduit network, which influence in parameters distribution cannot be captured by pumping tests or by methods allowing the determination of equivalent parameters determined at the scale of the aquifer.

As the characterisation of geometry and hydraulic parameters of a conduit network is always fragmentary and incomplete, its role in the definition of the observed regional flow pattern in a carbonate aquifer is very difficult to establish. However, due to the natural conditions present in the Castelo de Vide aquifer, it was possible to define some restrictions with respect to the role of the conduit network on the definition of the regional flow pattern. These restrictions are based in the detection of regional trends characterising the spatial distribution of hydraulic head gradients in the aquifer, leading to the definition of sectors in a regional conduit network. The presence of dissolution channels, with efficient hydraulic connection between some parts of the aquifer and the aquifer discharge areas, was found to be entirely incompatible with the observed hydraulic head gradients and the outflow volumes in the discharge areas. Therefore, an "artificial conduit network" with different degrees of connectivity to the discharge areas was constructed, using the observed regional hydraulic head gradients as main argument. This lead to remarkable positive results in the simulation of the aquifer hydraulic behaviour in both steady state and transient simulations. Furthermore,

the structure of the "artificial conduit network", defined on the basis of the results from the steady state model calibration was successfully used without any further modifications in transient simulations.

It must be noted that the identification of sectors in the "artificial conduit network" is entirely independent of the aquifer sectors, defined by the presence of regional or local flow systems, which are identified by the presence of no-flow boundaries, groundwater divides and aquifer discharge areas. In the present case study the sectors defined for the aquifer (sub-regional flow systems) do not coincide with the sectors defined for the conduit network. In fact, the areas where deficient connexion between adjacent sectors of the conduit network were defined are somewhere within the Castelo de Vide and Escusa sectors. Measuring points for the determination of the hydraulic head available in P. Espada sector are not sufficient to obtain a detailed characterisation of the spatial distribution of the hydraulic head. Therefore, it is possible that even more sectors for the "artificial conduit network" could be defined in the aquifer if more data were available.

At the present state of development, the implemented discrete continuum flow model allowed an acceptable simulation of the hydraulic behaviour of the Castelo de Vide aquifer, under steady state conditions and during emptying periods of the system. Therefore, despite the highly simplified representation of the aquifer, it seems that the simulated processes encompass the essential features needed to obtain a realistic image of the real system.

The steady state simulations of the aquifer were based on the long term water balance, which corresponds to a uniformly distributed recharge of 450mm/year. In addition to this value allogenic recharge is also considered in the Escusa sector. However the volume involved in these lateral inputs is only about 2% of the total recharge.

Steady state simulations also consider extractions in three groups of wells used for water supply and one well used for irrigation of food crops. In transient simulations an additional group of 11 wells is active during irrigation periods. The pumping rate of these wells is of little importance at the scale of the global water balance. However, the impact of these wells in recession periods cannot be neglected during long periods without recharge. As the extractions during recession periods affect the water levels at the regional scale, the model allows to evaluate the impact of well extractions on different aquifer sectors. Under these conditions the actual knowledge of the parameters at the well scale (determined in pumping tests) and the parameters defined at the aquifer scale, used in the discrete continuum model, allowed an adequate basis to support the management of the aquifer under natural conditions and for different scenarios of water use. On the other hand, despite the results obtained on these levels, it must be considered that, with the present knowledge of the temporal evolution of the state variables, the efficiency of the model for simulation of recharge events cannot be validated.

### 7.3 – Perspectives for further research

The present state of development of the discrete continuum model shows that some modifications must be introduced in the model in order to improve the quality of the description of the hydraulic behaviour of the aquifer in transient simulations. The results obtained with the implemented model contribute to the definition of a more objective planning for future field work conducted in order to improve the knowledge of the hydrogeology of the Castelo de Vide Carbonate aquifer.

A basic problem to solve regarding the aspects related to the carbonate aquifer characterisation consists in obtaining more detailed data for state variables in transient conditions. The time scale of the flow processes involved in individual recharge events is in the order of few hours. Therefore the monthly and weekly data sets available for this work cannot seize the time variability of hydraulic head and spring discharge during recharge periods. The efficiency of the present version of the regional flow model for simulation of recharge events cannot be validated without prior acquisition of daily datasets. On the other hand, data collection of Sever river discharge upstream and downstream of the aquifer is essential to check the global water balance and recharge estimates.

The interpretation of field data as well as the results from flow simulations show that there are probably short periods where Sever river behaves as an influent river, thus contributing for aquifer recharge. These conditions are certainly of little importance at the scale of the aquifer water balance. However the occurrence of such conditions could be important for the evaluation of major problems such as the possibility of contamination of the aquifer from the river. The detailed analysis of this problem cannot be done with the present mesh density in the river area. On the other hand, as the gradients in that area are very low the increase of the finite element mesh density would have to be anticipated by a detailed topographic survey, in order to adequately characterise the river and aquifer geometry with detail enough to approach this problem.

Boundary conditions for the discharge area of the aquifer near Castelo de Vide town can be defined in a more accurate way by including the crystalline rocks adjacent to the carbonate aquifer in the regional flow model. However the introduction of these units into the model must be preceded by the hydrogeological characterisation of these units.

Further evolution of the model and a more detailed hydrogeological characterisation, as proposed in the last paragraphs, are required for the improvement of the predictive capability of the model. Despite the different aspects identified as needing further investigations, the results obtained with the different model variants used in this work suggest that the absence of these improvements does not affect the general conclusions in the present case study about the potentials and the limits for the use of the discrete continuum approach to treat such problems.

The main objectives referred in the last paragraphs for further investigations are related to the implementation of a more detailed version of the model presently available. On the other hand, it must be considered that some of the identified problems related to the possibilities of improving the aquifer characterisation and the model characteristics cannot be approached by the use alone of the methods applied during this work. The more important aspect on this level is related to the simulation of individual recharge events. As in many other carbonate aquifers recharge in the Castelo de Vide aquifer occurs as diffuse infiltration and partially as concentrated infiltration. The definition of the proportion for each of these kinds of water inputs is only one of the aspects of a very complex problem. In fact, after the definition of a hypothetical scenario on this level (for example, 60% of concentrated infiltration and thus 40% of diffuse infiltration), based on some experimental criteria, or simply on use of a model on a trial and error basis, one more difficult problem remains: the definition of the contribution of each swallow hole relative to one another. The definition of such values can vary from among thousands of plausible possibilities, even for a relatively simple case. In the present case study it is clear that concentrated infiltration cannot be uniformly distributed in the 15 swallow holes identified in the field and introduced in the model. The lack of methods dealing with this problem is among the most important drawbacks with respect to the actual possibilities in characterising carbonate aquifers on the levels required for the use of a discrete continuum model. The identification of this problem is, in our opinion, one of the aspects deserving more attention in future development of the present work. As the method for calibration of the discrete continuum model, as presented in this work, shows good results in steady state and recession periods, there are reasons to expect that positive results could also be obtained for the simulation of recharge periods. As a "trial and error" calibration technique cannot be used to solve this problem we suggest that, once the calibration of a model for steady state and recession periods has been done, an automatic calibration of the model for recharge periods could be a good strategy to approach this problem. Due the fact that the present model of the Castelo de Vide carbonate aquifer allows an essentially correct simulation of the hydraulic behaviour of the system in steady state conditions and during long emptying periods, the next step will be to test inverse modelling techniques to investigate recharge patterns in the aquifer. This work is planned to follow just after the installation of devices for daily data collection, which will be installed in the aquifer in the next months.

Finally, the use of regional scale discrete continuum flow models in current applied hydrogeologic studies is strongly conditioned by the lack of computer programs allowing the use of such an approach. The last words regarding the identified fields, in which further research (or simply hard work of adequately skilled engineers and scientist) is needed to apply large scale continuum discrete models on real aquifers, are dedicated to the identification of the basic tools lacking on this level.

First of all the development of pre-processors and post processors able to deal with 1-D, 2-D and 3-D elements in the same finite element mesh is essential in order to make the implementation of that kind of models economically interesting in current hydrogeological studies. These kind of programs, including mesh generators and graphical software, is more difficult to develop than the finite element codes used to perform the flow calculations. Despite the very efficient direct solver available in the finite element code used throughout the present work (FEN), the dimension of the problems which can be treated are relatively small. At the present time this is not a severe limiting factor due the lack of automatic mesh generators. This limits the size of the meshes limit the size of the meshes, which can be defined to solve a given problem. However, if in the near future pre-processors ant post-processors are make available to generate and deal with more complex and discretized meshes, the use of direct solvers will be a serious limitation to the range of problems that can be approached. Therefore, the use of iterative solvers will be a basic requirement for a more efficient implementation of discrete continuum models.

Another kind of methodology that presents a large field of possibilities in the development of discrete continuum models is the use of stochastic methods that could be used to generate "artificial conduit networks". At the time of writing the present dissertation we noticed that a stochastic mesh generator, which allows the incorporation of conditioning information on the levels of general flow directions, surface karstic manifestations, presence of major faults and other direct or indirect features allowing the identification of dissolution channels was recently presented by Jaquet et al. (2001).

**REFERENCES**


Adamczyk, A.F.; Motyka, J.; Zbigniew, W.; Witczak, S. (1988) – Mining drainage of a Karstic aquifer and the related protection problems (Olkusz Mining district, Poland). Karst hydrogeology and karst environment protection. 21st IAH congress. Vol. XXI, part II. Guilin. China. pp 1097-1104.

Almeida, C.C. (1985) - Hidrogeologia Algarve Central. Diss. para obt. do grau de Doutor em Geologia, Dep. Geol. Fac. Ciênc. Univ. de Lisboa. 333 pp.

Almeida, C.C., Ribeiro, T., Oliveira, M. (1992) - Interpretação automática de ensaios de bombagem. Geonovas. A informática na Geologia. Assoc. Port. Geol. N3. pp 64-82.

Almeida, C.C.; Oliveira, M.M. (1990) - Caracterização hidráulica de aquíferos fracturados. Livro de Homenagem a Carlos Romariz. Fac.Cienc. Univ. Lisboa. pp 30-64.

Angelini P., Dragoni, W. (1996) – The problem of modeling limestone springs: the case of Bagnara (North Apennines, Italy). Groundwater, Vol. 35, No. 4. pp 612-618.

Appelo, A.; Postma, D. (1996) – Geochemistry groundwater and pollution. Ed. Balkema. Rotterdam. 536pp.

Baedke, S.J.; Krothe (2001) – Derivation of effective hydraulic parameters of a karst aquifer from discharge hydrograph analysis. Water resources research. Vol. 37. NO.1. pp13-19.

Barenblatt , G. E.; Zheltov, I.P.; Kochina, I.N. (1960) – Basic concepts in the theory of seepage of homogeneous liquids in fissured rocks (strata). Journ. Appl. Math. Mech. (transl.) USSR, V.24, n.1 pp 1286-1303.

Barret, M.E.; Charbeneu. R.J. (1996) - A Parsimonious Model for Simulation of Flow and Transport in a Karst Aquifer. Center for Research in Water Resources. Univ. of Texas (Austin). 149pp.

Bear, B.; Verruijt, A. (1987) - Modeling Groundwater Flow and Pollution. D. Reydel Publishing Company. Dordrecht. 414pp.

Beck B.F. (1988) – Environmental and engineering effects of sinkholes - the processes behind the problem. Karst hydrogeology and karst environment protection. 21st IAH congress. Vol. XXI, part I. Guilin. China. pp17-29.

Boulton N.S.; Streltsova T.D. (1977) Unsteady Flow to a Pumped Well in a Fissured Water-Bearing Formation. Journ. Hydrol., 35. pp. 93-103.

Cornaton F. (1999) – Utilisation de modèles continu discrete et à double continuum pour l'analyse des réponses globales de l'aquifère karstique. Essai d'identification des paramètres. Travail de diplôme du Cycle postgrade interuniversitaire. CHYN. Neuchâtel. Switzerland. 83p.

Cornaton F.; Perrochet, P. (*in press*) – Analytical 1-D dual-porosity equivalent solutions to 3-D discrete single-continuum models. Application to a karstic spring hydrograph modeling. Journal of Hydrology.

Custódio, E.; Llamas, M.R. (1976) - Hidrología subterrânea. Ed. Omega. Barcelona, Vol I and II, 2359 pp.

Dassarges A., Brouyère S., (1997) – Are deterministic numerical models helpful to delineate groundwater protection zones in kastic aquifers? Karst Waters & Environmental impacts. Gunay & Johnson (eds). Balkema, Rotterdam. pp 109-116.

de Marsily, G. (1986) – Quantitative Hydrogeology. Academic press. San Diego. USA. 440 pp.

Diersch, H.J. (1998) – Feflow. Version 4.7. Interactive, Graphics-Based Finite-Element Simulation System for Modeling Groundwater Flow, Contaminant Mass and Heat Transport Process. Reference manual. Wasy. Institute for Water Resources Planning and Systems Research ltd. 294pp.

Eisenlohr L., (1995) – Variabilité des responses naturelles des aquifères karstiques. De l'identification de la réponse globale vers la connaissance de la structure de l'aquifèere. Thèse de Doctorat, Université de Neuchâtel, Centre d'Hydrogéologie. 121p.

Eisenlohr L., Bouzelboudjen M., Király L., Rossier Y., (1997a) - Numerical versus statistical modelling of natural response of a karst hydrogeological system. Journal of Hydrology, 202, p. 244-262.

Eisenlohr L., Bouzelboudjen M., Király L., Rossier Y., (1997b) - Numerical simulation as a tool for checking the interpretation of karst spring hydrographs. Journal of Hydrology, 193, pp. 306-315

Eriksson, E. (1983) Guidebook on nuclear techniques in hydrology. Chapter 2 – Stable Isotopes and Tritium in Precipitation. International Atomic Energy Agency - IAEA. Technical reports series. N.91. Vienna. 439 pp.

Estrela T.,Sahuquillo A. (1997) - Modeling the response of a karstic spring at Arteta Aquifer in Spain. Groundwater, Vol. 35, No. 1. pp 18-24.

Fernandes, A.P.; Perdigão, J.C.; Peres, A.M. (1973) - Notícia explicativa da folha 28-D (Castelo de Vide) Carta Geológica de Portugal 1/50000. Serv. Geol. Port., Lisboa, 44 pp.

Field M.S. (1999) – A lexicon of cave and karst terminology with special reference to environmental karst hydrology. Environmental Protection Agency. National Center for Environmental Assessment. USA. Washington, D.C. 201pp.

Freeze, A.; Cherry, J. (1979) - Groundwater. Prentice-Hall. New Jersey U.S.A., 604 pp.

Gable, C.W.; Trease, H.; Cherry, T. (1996) - Geological applications of automatic arid generation tools for Finite Elements Applied to Porous Flow Modeling. Numerical Grid Generation in Computational Fluid Dynamics and Related Fields, edited by B. K. Soni, J. F. Thompson, H. Hausser and P. R. Eiseman. Engineering Research Center, Mississippi State Univ. Press, 9 pp.

Gonçalves F.; Perdigão, J.C.; Coelho, A.V.P.; Munhá, J.M. (1978) - Notícia explicativa da folha 33-A (Assumar) Carta Geológia de Portugal 1/50000. Serv. Geol. Port. 37 pp.

Irons, B.M. (1970) – A frontal solution program for finite element analysis. International Journ. Num. Methods in engineering. Vol. 2, 5. 32. pp 5-32.

Jaquet, O.; Siegel, P.; Klubertanz, G.; Benabderrhamane, H. (2001) – The combined stochastic discrete conduit and continuum approach for groundwater management and protection in karst areas. 3rd International Conference on Future Groundwater resources at risk. UNESCO. Lisboa. 8pp.

Jeannin, P.Y.; Grasso, A. (1997) – Permeability and hydrodynamic behaviour of a karstic environment. Karst Waters & Environmental impacts, Günay & Johnson (eds). Balkema. Rotterdam. pp335-342.

Huyakorn, P.S.; Pinder, G.F. (1983) - Computational methods in subsurface flow. Academic Press, New York, 473 pp.

Kazemi H. (1969) - Pressure transient analysis of naturally fractured reservoirs with uniform fracture distribution. Society of Petroleum Engineers Journal, AIME 246, p. 451-462.

Kessler, H. (1965) – Water balance investigations in the karstic regions of Hungary. Act. Congress AIHS- UNESCO. Vol. 73. pp 91-105.

Kinzelbach, W. (1986) – Groundwater modelling. An introduction with sample programs in Basic. Developments in Water Science nº25. Elsevier. 333pp.

Kiraly, L., (1975) - Rapport sur l'état actuel des connaissances dans le domaine des caractères physiques des roches karstiques. Hydrogeology of karstic terrains. Union Geol. Sciences, (eds. Burger & Dubertret), Series B, 3 pp 53-67.

Kiraly L., Morel G. (1976a) - Etude de la régularisation de l'Areuse par modèle mathématique. Bull. Centre d'Hydrogéologie.Univ. Neuchâtel. N1. pp 19-35.

Kiraly L., Morel G. (1976b) - Remarques sur l'hydrogramme des sources karstiques simulées par modèles mathématiques. Bull. Centre d'Hydrogéologie, N°1, p. 37-60, Université de Neuchâtel.

Kiraly L. (1979) - Remarques sur la simulation des failles et du réseau karstique par éléments finis dans les modèles d'écoulement. Bull. Centre Hydrogéol. Neuchâtel n°3, p. 155-167.

Kiraly L. (1985) - FEM301, A three dimentional model for groundwater flow simulation. NAGRA Technical report 84-89, 96p.

Kiraly L., Perrochet P., Rossier Y. (1995) - Effect of epikarst on the hydrograph of karst springs : a numerical approach. Bull. Centre Hydrogéol. Neuchâtel n°14, p. 199-220.

Kiraly L. (1998) - Modeling karst aquifers by combined discrete channel and continuum approach. Bull. Centre Hydrogéol. Neuchâtel n°16, p. 77-98.

Kresic, N. (1997) – Quantitative Solutions in Hydrogeology and Groundwater Modeling. Crc press. Lewis publishers. New York. 459 pp.

Larocque M. O., Banton O., Ackerer P., Razack M. (1999) - Determining karst transmissivities with inverse modeling and an equivalent porous media. Groundwater, Vol. 37, No. 6 . pp 897-903.

Linsley, R.K.; Kohler, M.A.; Paulhus, J.L.H. (1975) - Hidrology for Engineers. Ed.2, Mcgraw-Hill, Tokio 482 pp.

Mangin, A. (1997) – Structure et fonctionnement des aquifers karstiques les conzepts et les approches. Proceedings of the 12 international congress of speleology. La Chaux de Fonds, Switzerland. pp 3-9.

Mavor, M.J., Cinco L. (1979) – Transient pressure behaviour of naturally fractured reservoirs. Pap. SPE 7977, soc. of Petrol. Engineers of AIME.

Mercer, J.W.; Faust, C.R. (1980) Ground-Water Modeling: An overview. Groundwater. Vol. 18. N. 2. pp108-115.

Moench A.F., 1984 - Double porosity models for a fissured groundwater reservoir with fracture skin. Water Resour. Res., 20(7), p. 831-846.

Monteiro, J.P.; Silva, M.L. (1992a) - Estudo hidrogeológico dos calcários dolomíticos de escusa (Portalegre). A.P.R.H. Rev. Assoc. Port. Rec. Hídr. Lisboa. pp 13-19.

Monteiro, J.P.; Silva, M.L. (1992b) - Aspectos da hidrogeologia e qualidade das águas associadas à formação Carbonatada de Escusa (Castelo de Vide). Geolis, Vol. VI, fasc. 1 e 2. Lisboa pp 19-32.

Monteiro, J.P. (1993) - Hidrogeologia da formação carbonatada de escusa (Castelo de vide). Dissertação Apresentada à Faculdade de Ciências da Universidade de Lisboa para a obtenção do grau de Mestre em Geologia Aplicada. Lisboa. 170pp.

Monteiro, J.P.; Silva, M.L. (1994) - Influência da actividade antrópica na qualidade das águas da formação carbonatada de Escusa (Castelo de Vide). Actas del congresso celebrado en Alcalá de Henares (Madrid, España de 7 al 10 de Febrero de 1994) sobre Análisis y Evolución de la Contaminación de las Aguas Subterráneas. Dep. de Geologia de La Universidad de Alcalá. Madrid. Tomo II.pp 455-467.

Monteiro, J.P.; Silva, M.L.; Carreira, P.M.; Soares, A.M. (1997) – Aplicação de Métodos Geoquímicos Isotópicos à Interpretação da Hidrodinâmica do Aquífero Carbonatado da Serra de S. Mamede (Castelo de Vide). VII Congresso de Espanha de Geoquímica, Ed. Cedex, pp. 544-551.

Monteiro (2001) - Calculation of equivalent hydraulic conductivity as unknown variable of a boundary value problem in a carbonate aquifer (Castelo de Vide, Portugal). 3rd International Conference on Future Groundwater resources at risk. UNESCO. Lisboa. 8pp.

Oliveira, M.M. (1993) - Modelação de escoamento e determinação de parâmetros hidráulicos em aquíferos fracturados. Diss. para obt. do grau de Mestre em Geologia Económica e Aplicada, Dep. Geol. Fac. Ciênc. Univ. de Lisboa, Lisboa, 194 pp.

Oliveira, J.T.; Pereira, E.; Piçarra, J.M.; Young, T.; Romano, M. (1992) - Paleozoico inferior de Ibero-America, contribuciones regionales Ibéricas. O Paleozóico Inferior de Portugal: Síntese da estratigrafia e da evolução paleogeográfica. Ed. G. Marco, J. Saavedra, I. Rábano. Univ. de Extremadura. pp 359-373.

Payne, B.R. (1983) - Guidebook on nuclear techniques in hydrology. Chapter 1 – Introduction. International Atomic Energy Agency - IAEA. Technical reports series. N.91. Vienna. 439 pp.

Perdigão, J.C. (1967a) - Os Graptolitos e fauna associada da região de portalegre. Com. Serv. geol. Portugal. Vol. LII. Lisboa pp 65-77.

Perdigão, J.C. (1967b) - Descoberta de Mesodevónico em Portugal (Portalegre). Com. Serv. geol. Portugal. Vol. LII. Lisboa pp 27-48.

Perdigão, J.C. (1972) - A fauna dos grés e quartzitos Silúrico-Devónicos de Portalegre. Com. Serv. geol. Portugal. Vol. LVI. Lisboa pp 5-25.

Perdigão, J.C.; Fernandes, A.P. (1976) - Notícia explicativa da folha 29-C (Marvão) Carta Geológica de Portugal 1/50000. Serv. Geol. Port., Lisboa, 18 pp.

Pulido-Bosh A., Padilha, A. (1988) – Some considerations about the simulation of karstic aquifers. Proc. Of the I.A.H. XXI Congress Karst Hydrogeology and Karst Environment Protection. Guilin, China, pp. 538-588.

Perrochet, P. (1995) – Finite hyperelements: a 4D geometrical framework using covariant bases and metric tensors. Comm. In numerical methods in engeneering. Vol. 11. pp. 525-534.

Perrochet, P. (2000) - "Hydrodynamique souterraine" Lecture notes. Hydrogeological Center, Univ. Neuchâtel, Switzerland CHYN. (Unpublished).

Quijano, L.; Dray, M. (1983) - Guidebook on nuclear techniques in hydrology. Chapter 18 – Origin of Groundwater. International Atomic Energy Agency - IAEA. Technical reports series. N91. Vienna. 439 pp.

Renard, P.; de Marsily, G. (1997) - Calculating equivalent permeability: a review. Advances in Water Resources, 20 (5-6) pp. 253-278

Ribeiro, A.; Antunes, M.T.; Ferreira, M.P.; Rocha, R.B.; Soares, A.F.; Zbyszewski, G.; Almeida, F.M.; Carvalho, D.; Monteiro, J.H. (1979) - Introduction à la Géologie Générale du Portugal. Serv. Geol. Port., Lisboa, 114 pp.

Ribeiro, A. (1990) - Pre-Mesozoic geology of Iberia, central-iberian zone, Introduction. Ed. R.D. Dallmeyer, E. Martínez Garcia. Springer-Verlag, UNESCO pp 143-144.

Silva, J.M.; Camarinhas, M.V.F. (1961) - Estudo económico dos calcários de marvão. Est.Not. e Trab. do Serv. Fom. Min., Vol. XV, pp 315-430.

Silva, M.L. (1988) - Hidrogeologia do Miocénico do Algarve (Portugal). Diss. para obt. do grau de Doutor em Geologia, Dep.Geol.Fac.Ciênc.Univ. de Lisboa, Lisboa, 496 pp.

Silva, M.L.; Monteiro, J.P. (1999) - "Aplicação de Métodos Geoquímicos Isotópicos e Modelos de Escoamento ao Aquífero Carbonatado de Castelo de Vide (Serra de S. Mamede)". Final report of a groundwater research project. Financed by FCT (PEAM/SEL/557/95). Dep. de Geologia da Faculdade de Ciências (Lisboa), Instituto Tecnológico e Nuclear. Lisboa. 48 pp (Unpublished).

Teixeira, C. (1981) - Geologia de Portugal, Vol.1, Precâmbrico, Paleozóico. Fund. Calouste Gulbenkian, Lisboa, 629 pp.

Wang H.F., Anderson M.P., 1982 - Introduction to groundwater modelling. finite difference and finite element Methods. Freeman, New-York, 237 pp.

Warren J.E, Root P.J., 1963 - The behavior of naturally fractured aquifers. Society of Petroleum Engineers, Fall meeting, L.A., USA, Oct. 1962.